Modeling and robust control of biological systems : example of lactic acid production in industrial fermenter

Karen Vanessa Gonzalez

▶ **To cite this version:**

Karen Vanessa Gonzalez. Modeling and robust control of biological systems : example of lactic acid production in industrial fermenter. Other. Ecole Centrale Paris, 2015. English. <NNT : 2015ECAP0044>. <tel-01247311>

HAL Id: tel-01247311
https://tel.archives-ouvertes.fr/tel-01247311

Submitted on 4 Jan 2016

THÈSE

Pour l'obtention du grade de

Docteur de CentraleSupélec

Spécialité : Génie des Procédés

**Modélisation et commande robuste des systèmes biologiques :
Exemple de la production d'acide lactique en fermenteur industriel**

Présentée par : Karen Vanessa Gonzalez
Directeur de thèse : Dominique Pareau
Encadrants : Didier Dumur, Filipa Lopes, Sihem Tebbani

Soutenue le 25 septembre 2015 devant les membres du jury:

M. Francis Courtois	Professeur (AgroParisTech)	Rapporteur
M. Francis Duchiron	Professeur (Université de Reims Champagne-Ardenne)	Rapporteur
M. Didier Dumur	Professeur (CentraleSupélec)	Co-encadrant
M. Michel Fick	Professeur (ENSAIA)	Examinateur
M. Sébastien Givry	Chef de projet fermentation (Groupe Soufflet)	Invité
Mme Filipa Lopes	Enseignant –chercheur (CentraleSupélec)	Co-encadrante
Mme Dominique Pareau	Professeur (CentraleSupélec)	Directrice
M. Dan Selişteanu	Professeur (Université de Craiova)	Examinateur
Mme Sihem Tebbani	Enseignant –chercheur (CentraleSupélec)	Co-encadrante

A mis Padres

A mi Familia

A la familia Busson

A Thibaut

ACKNOWLEDGEMENTS

The completion of my dissertation and Ph.D. has been a long journey. I could not have succeeded without the invaluable support of many people I would like to thanks at this time.

First of all, I would like to express the deepest appreciation to my supervisor Professor Dominique Pareau, she has been a great mentor for me. I would like to thank her for encouraging me and for helping me to grow as engineer and as scientific. Her advice in this multidisciplinary work has been precious. I am also thankful for the excellent example she gave me as successful woman, engineer and professor in the chemical engineer field, my passion.

I would also like to thank deeply my supervisor Dr. Sihem Tebbani who dedicated a lot of her time to ensure the progress of this PhD work. She helped me enormously to make my first steps in the bioprocess control field. Thanks for the scientific discussions and advices that guided my research.

I would specially like to thank my supervisor, Dr. Filipa Lopes. At the beginning of this PhD, I was not familiar with the bioprocesses, but she guided me with precious and numerous advices in this field.

Special thanks to Pr. Didier Dumur for his continuous encouragement and helpful discussions during these years which were a great contribution in this research work.

I would also like to thank my industrial supervisor Dr. Sébastien Givry for hosting me in the CRIS (Centre de recherché et d'innovation Soufflet) laboratory and allowing me to validate experimentally my research work.

I wish to express my gratitude to my industrial supervisor Dr. Aurore Thorigné for helping me during my experimental work. Thanks for the valuable discussions that were a tremendous contribution when experiments did not work so well.

I would specially like to thank the committee members for accepting to evaluate my work. Special thanks to Francis Courtois and Francis Duchiron for accepting to review this work, for the time they spent reading this manuscript and for their valuable advice. I would also like to thank Michel Fick and Dan Seişteanu for agreeing to be part of my thesis committee.

I am grateful to Patrick Perré for hosting me in the laboratory LGPM. Special thanks to the staff of the laboratory, especially Cyril, Thierry, Touhami, Annie and Sylvie for helping and offering me the resources for my experiments.

I would also like to thank my office colleagues, "the Lilianas", Ligia and Maria who already left the laboratory. It was very nice to share more than an office with you. Best wishes for Pierre and Angela in their PhD project. Finally, I would like to thank deeply Hela, she always gave me good advices in personal and professional levels. I hope the special friendship we created will last with time.

I would also like to thank all the liquid fermentation team at Soufflet. Special thanks to Jonathan Mazaudon who helped me enormously during my experimental validation.

I would like to express my gratitude to the automatic control department staff, especially to the "PhD students control the world" team, Sophie, Miassa, Nicolò, Kate, Iris, Guillaume and Marjorie. Thanks for making me laugh so much during my last and most critical year of PhD. I lived great moments with you. Best wishes for Seif and his research project.

On a personal level, I would like to thank:

A mis padres, mi motor para seguir adelante y luchar por mis sueños. Gracias de todo corazón por ser el mejor ejemplo, por darme tanto cariño y estar siempre ahí. No sería nada de lo que soy ahora sin su amor y apoyo incondicional, todo se lo debo a ustedes. Gracias también a toda mi familia por su apoyo y motivación, a pesar de la distancia los llevo a todos en mi corazón.

Je voudrais aussi remercier la Famille Busson, pour m'avoir si bien accueilli en France. Cela fait vraiment plaisir de se sentir supportée, aimée et intégrée dans une nouvelle famille. Ces trois années ont été beaucoup plus heureuses en sachant que vous étiez là.

Finalement je voudrais remercier Thibaut, merci d'être mon partenaire, mon ami, mon complice, mon moteur, mon tout. Je n'aurais pas pu faire cette thèse sans ton support, ta patience, tes beaux mots d'encouragement et ton amour inconditionnel. Merci de m'avoir accompagnée dans cette aventure et de continuer à le faire pour les prochaines à venir.

PREFACE

The results presented in this thesis led to the publication of a number of articles during various international conferences with and without proceedings and to the submission of one article for an international journal.

International conferences with proceedings

- Gonzalez, K., Tebbani, S., Dumur, D., Pareau, D., Lopes, F., Givry, S., Entzmann, F. 2013. Modeling and parameter identification of the batch lactic acid production process from wheat flour. *In Proceedings of 17th International Conference on System Theory, Control and Computing* - ICSTCC 2013, Romania, pp. 238-243.
- Gonzalez, K., Tebbani, S., Dumur, D., Pareau, D., Lopes, F., Givry, S., Entzmann, F. 2014. Control strategy for continuous lactic acid production from wheat flour. *In Proceedings of 2nd International Conference on Control, Decision and InformationTechnologies* - CoDIT'14, Metz, France, pp. 465-470.
- Gonzalez,K., Tebbani, S., Dumur, D., Pareau, D., Lopes, F., Givry, S., Thorigné, A. 2014. Adaptive Control of lactic acid production from wheat flour. *In Proceedings of International Symposium on Advances Control of Chemical Processes*- ADCHEM 2015, Whistler, British Columbia, Canada.
- Gonzalez, K., Tebbani, S., Dumur, D., Pareau, D., Lopes, F., Givry, S., Thorigné, A. 2015. Feedback linearizing controller coupled to an Unscented Kalman filter for lactic acid regulation. ICSTCC 2015, Romania.

International conferences without proceedings

- Gonzalez, K., Lopes, F., Tebbani, S., Givry, S., Entzmann, F., Dumur, D., Pareau, D., 2014. Optimization of lactic acid production from wheat flour: hydrolysis of starch proteins in batch fermentation, ESBES-IFIBIOP Symposium, Lille, France.

International journal article

- Gonzalez, K., Tebbani, S., Lopes, F., Givry, S., Thorigné A., Dumur, D., Pareau, D. 2015. Modelling the continuous lactic acid production process from wheat flour. *Applied Microbiology and Biotechnology*. DOI: 10.1007/s00253-015-6949-7.
- Gonzalez, K., Tebbani, S., Lopes, F., Givry, S., Thorigné A., Dumur, D., Pareau, D. 2015. Regulation of lactic acid concentration in its bioproduction from wheat flour: An adaptive control approach. *Journal of Biotechnology* (*submitted* in october 2015).

Other publications

- Modeling and control of biological systems: example of lactic acid production in industrial fermenter. PhD students-enterprises meeting (Rencontres entreprises doctorants, RED) 2014. Ecole CentraleSupélec, Châtenay-Malabry, France. October 2014.

RESUME

L'acide lactique est un produit largement utilisé dans l'industrie alimentaire, pharmaceutique et des solvants. Il connait depuis peu un engouement certain en tant que monomère pour la production d'acide poly lactique (PLA, poly lactic acid), un polymère biodégradable. L'acide lactique peut être produit par voie chimique ou par voie biotechnologique. Cette dernière offre plusieurs avantages par rapport à la synthèse chimique, en particulier le faible coût des substrats et une spécificité élevée par rapport aux stéréo-isomères produits (John, et al., 2007).

La production d'acide lactique par des microorganismes est très répandue depuis plus de deux décennies, mais généralement, les procédés proposés utilisent dans ce cas des substrats relativement coûteux (glucose, lactose, extrait de levure, etc). Cet acide peut être produit à partir de plusieurs microorganismes : bactéries lactiques, champignons, levures, micro algues, et cyanobactéries. Les microorganismes les plus largement utilisés pour la production d'acide lactique sont les bactéries lactiques (LAB). Etant un produit relativement peu cher, l'un des principaux défis dans la production d'acide lactique par fermentation à grande échelle est le coût de la matière première. Le potentiel des procédés biotechnologiques utilisant des matières premières peu coûteuses peut être dès lors exploité afin de rendre le procédé économiquement rentable. Actuellement différentes matières premières sont utilisées comme source de carbone : la mélasse, le lactosérum, l'amidon et les hydrolysats.

La farine de blé a été largement étudiée pour la production industrielle d'acide lactique. Ce substrat contient presque tous les nutriments nécessaires pour les différentes souches de bactéries lactiques. Néanmoins, des réactions enzymatiques sont nécessaires pour hydrolyser l'amidon de blé et permettre son utilisation par les bactéries. De façon classique, le procédé de production d'acide lactique à partir d'amidon considère trois étapes : un prétraitement de l'amidon par gélatinisation et liquéfaction produisant principalement du maltose ; une saccharification enzymatique pour obtenir du glucose et une dernière étape de fermentation qui transforme le glucose en acide lactique.

Le procédé développé par Soufflet, qui est à la base de ces travaux de thèse, consiste également en trois étapes principales, la liquéfaction de l'amidon, la saccharification partielle du maltose en glucose dans une étape de pré saccharification, et la transformation du maltose restant en glucose en même temps que la fermentation dans une étape dite de saccharification et fermentation simultanées ou SSF (Simultaneous saccharification and fermentation).

Par ailleurs, les bactéries lactiques ont des besoins en source d'azote qui doivent être satisfaits. Généralement, des nutriments tels que l'extrait de levure et la peptone sont ajoutés pour fournir ces besoins. Néanmoins, la farine de blé contient des protéines (gluten) qui peuvent être hydrolysées en acides aminés nécessaires pour la croissance bactérienne. Afin de profiter de ces sources d'azote, des études enzymatiques de l'hydrolyse des protéines du blé sont nécessaires. De même, ce procédé peut être amélioré par couplage des réactions enzymatiques dans le même bioréacteur. Cependant, l'optimisation de la production d'acide lactique dans ce type de bioréacteur est difficile en raison des diverses réactions enzymatiques ayant lieu simultanément.

D'autre part, des stratégies de commande qui permettent la régulation des composants clés dans le bioréacteur peuvent être utilisées pour optimiser la production d'acide lactique. Pour ce faire, des modèles dynamiques doivent être développés. Ces modèles sont des outils importants pour l'optimisation du procédé biotechnologiques car ils permettent de prédire la performance du bioréacteur et peuvent être ensuite utilisés pour le développement d'une stratégie de commande. Néanmoins, les modèles décrivant des procédés biotechnologiques sont complexes et présentent un caractère très fortement non linéaire, rendant d'autant plus difficile la synthèse des stratégies de commande.

Dans ce contexte, l'objectif de cette thèse est d'optimiser le procédé biotechnologique de production d'acide lactique à partir de farines de blé pour en maximiser la productivité. Trois étapes principales sont considérées pour atteindre cet objectif. Tout d'abord, le milieu de culture est optimisé afin d'améliorer la productivité en acide lactique. Deuxièmement, une modélisation macroscopique du procédé est développée. Le modèle considère les différentes cinétiques (croissance bactérienne, consommation du glucose, production d'acide lactique et hydrolyse enzymatique du maltose) qui se déroulent dans le bioréacteur. Finalement, des stratégies de commande optimisant la productivité d'acide lactique sont proposées. Ce travail couple ainsi deux grands domaines : les bioprocédés et l'automatique.

Les différentes étapes considérées dans ces travaux de thèse pour atteindre l'objectif principal sont récapitulées ci-dessous.

Optimisation du procédé
Tout d'abord, l'optimisation du milieu de culture a été réalisée en s'appuyant sur des essais expérimentaux. La souche utilisée dans ce bioprocédé est *Lactobacillus coryniformis*subsp. *torquens* DMS 20004. Des études enzymatiques ont été effectuées afin d'améliorer la composition du milieu de culture et d'optimiser le procédé de production d'acide lactique. Les résultats obtenus lors de cette phase ont permis de proposer un nouveau procédé de production qui comporte trois étapes. La première étape est la liquéfaction et est suivie d'une étape de saccharification et hydrolyse des protéines simultanées (SSPH, simultaneous saccharification and proteins hydrolysis) qui permet l'hydrolyse d'une partie du maltose en glucose et du gluten en acides aminés. La dernière étape consiste en la saccharification, l'hydrolyse des protéines et la fermentation simultanées (SSPHF, simultaneous saccharification, proteins hydrolysis and fermentation). Dans cette dernière phase, le maltose et le gluten restants sont hydrolysés simultanément à la fermentation. Le bioréacteur dédié à l'étape SSPHF doit fonctionner en mode continu car cela permet d'obtenir une productivité maximale. Deux chapitres sont consacrés à cette première étape d'optimisation : Les chapitres 1 et 2.

Modélisation
La deuxième étape consiste à développer un modèle représentatif des phénomènes biologiques et enzymatiques dans le bioréacteur. Les cinétiques (croissance bactérienne, production d'acide lactique, réactions enzymatiques) des réactions mises en jeu dans le bioréacteur dédié à l'étape SSPHF sont alors prises en compte. Les évolutions des variables clés du procédé (qui seront par la suite prises en compte lors de la synthèse de la commande : les concentrations en biomasse, glucose, maltose et acide lactique) ont été modélisées en considérant une approche macroscopique. Les paramètres du modèle ont finalement été identifiés et validés en utilisant les

résultats des essais continus dans un bioréacteur de 5 L lors de l'étape SSPHF. Le chapitre 3 est consacré à toute la partie de modélisation.

Suivi et commande

Le développement de stratégies de commande permettant d'optimiser la productivité en acide lactique dans le bioréacteur dédié à l'étape SSPHF représente la troisième étape de la méthode d'optimisation globale. En premier lieu, les estimateurs des variables nécessaires au suivi du procédé et à la conception de la commande ont été développés. La synthèse de la commande a ensuite été effectuée en considérant les variables mesurées, les grandeurs issues des estimateurs développés et le logiciel implanté sur site pour piloter le bioréacteur. Deux chapitres sont consacrés à cette étape : les chapitres 4 et 5.

CHAPITRE 1 : PRODUCTION D'ACIDE LACTIQUE

La forte demande énergétique et les problèmes environnementaux associés aux procédés industriels conventionnels encouragent le développement de procédés novateurs assurant la réduction de la consommation énergétique et minimisant les impacts environnementaux. L'acide lactique a attiré l'attention des industriels et des chercheurs en raison de ses nombreux domaines d'application, et sa demande toujours croissante, en particulier pour la production d'acide poly lactique (PLA). Ce chapitre propose une description générale de la production d'acide lactique ciblée à la production de PLA.

1.1. Acide lactique

L'acide lactique est la principale composante de tous les produits laitiers acidifiés. Sa production industrielle a commencé en 1881 aux Etats-Unis. De nos jours, 90% de la production d'acide lactique est fourni par fermentation microbienne (Hofvendahl & Hahn-Hligerdal, 1997). Le marché mondial de l'acide lactique a été estimé à 714 200 tonnes en 2013 et devrait atteindre 1 960 100 tonnes en 2020 (Hofvendahl & Hahn-Hligerdal, 1997).

L'acide lactique est principalement utilisé dans les produits alimentaires, cosmétiques, pharmaceutiques et pour des applications chimiques. Il est classé comme GRAS (GenerallyRecognize As Safe) pour son utilisation comme additif alimentaire par la FDA (Food and Drug Administration). Comme mentionné précédemment, il est particulièrement recherché en tant que monomère matière première pour la production de PLA. Dès lors, la production biotechnologique d'acide lactique s'avère depuis quelques années de plus en plus intéressante car elle offre une alternative à deux préoccupations environnementales : la pollution causée par les produits pétrochimiques et la limitation en carbone fossile.

1.2. Production d'acide lactique

1.2.1. Voie Chimique

La synthèse chimique d'acide lactique est fondée sur la réaction du lactonitrile. Du cyanure d'hydrogène est ajouté à de l'acétaldéhyde en présence d'une base pour produire du lactonitrile. Ce dernier est ensuite récupéré et purifié par distillation. Il est ensuite hydrolysé avec de l'acide chlorhydrique ou sulfurique pour produire le sel d'ammonium correspondant et de l'acide lactique. L'acide lactique est ensuite estérifié avec du méthanol pour produire du lactate de

méthyle, que l'on purifie par distillation. Ultérieurement le lactate de méthyle est ré-hydrolysé par de l'eau dans une réaction acide catalytique pour produire de l'acide lactique à nouveau ainsi que du méthanol. Cette synthèse chimique produit un mélange racémique d'acide lactique D et L (Narayanan, et al., 2004).

1.2.2. Voie fermentative

La plupart de l'acide lactique disponible sur le marché est produit par fermentation. Au cours de la fermentation lactique, un hydrate de carbone est converti en acide lactique par les microorganismes. Seuls quelques-uns d'entre eux ont besoin d'oxygène pour croître. De ce fait, la conversion des sucres est réalisée sans oxygène car dans des conditions aérobies, l'oxydation complète des sucres est favorisée énergiquement, obtenant dioxyde de carbone comme produit de fermentation au lieu d'acide lactique. De plus, la plupart de microorganismes producteurs d'acide lactique sont inactivés en présence de concentrations élevées d'oxygène, de sorte que l'acide lactique est principalement formé dans des conditions anaérobies.

L'acide lactique peut être produit par divers micro-organismes tels que les champignons, les cyanobactéries, les levures, les algues et les bactéries.

1.2.3. Les bactéries lactiques

Une bactérie lactique typique cultivée dans des conditions « standard » (non limitées en glucose, nutriments de croissance ou oxygène) est une bactérie à Gram-positif, non sporulée, catalase négative, aérotolérante, tolérante à l'acide, chemoorganotrophe et qui produit de l'acide lactique comme produit final de la glycolyse. Les cellules sont typiquement immobiles. Elles ont besoin d'éléments nutritifs de croissance complexes tels que des vitamines et des acides aminés. Les conditions de croissance optimales dépendent de la souche; les bactéries peuvent se développer pour une large gamme de pH (3,5 à 10) et à des températures comprises entre 5 et 45 ° C (Abdel-Rahman, et al., 2013).

1.2.4. Le genre Lactobacillus

Les Lactobacillus sont classifiés en trois groupes en fonction de leur métabolisme du sucre :

- Groupe I : Ces bactéries donnent l'acide lactique à partir des hexoses par un métabolisme strictement homofermentaire, elles ne peuvent pas fermenter les pentoses.
- Groupe II : Ce groupe comprend les espèces ayant un métabolisme optionnellement homofermentatif. Les hexoses sont fermentés dans de l'acide lactique par la voie d'Embden-Meyerhof. Dans le cas contraire, les pentoses peuvent être dégradés par la voie hétérofermentaires avec production d'acides lactique et acétique.
- Groupe III : Ces espèces ont un métabolisme strictement hétérofermentaire. Elles fermentent les gluconates et les pentoses. Elles produisent de l'acide lactique, de l'acide acétique, du dioxyde de carbone et de l'éthanol.

1.2.5. Fermentation : conditions opératoires et paramètres

Plusieurs paramètres affectent la production optimale d'acide lactique. L'un des paramètres ayant une forte influence sur la performance du procédé de production d'acide lactique est la souche

microbienne utilisée. Parmi les caractéristiques souhaitées pour la souche productrice on note la production d'acide lactique à des rendements et des productivités élevés et la capacité à utiliser des matières premières peu coûteuses. La sélection des souches se fait généralement de manière empirique. La souche utilisée dans ce travail de thèse est *Lactobacillus coryniformis* subsp. *torquens* DSM 20004. Cette souche a été choisie pour sa production d'acide lactique élevée ainsi que ses conditions d'opération satisfaisantes (température optimale basse, pH 6). Les bactéries de cette souche appartiennent au groupe II de la classification des lactobacilles ; cela signifie qu'elles effectuent un métabolisme optionnellement homofermentatif.

Les bactéries lactiques, comme tous les micro-organismes, ont un métabolisme soumis à des réglementations imposées par les contraintes environnementales. Il est nécessaire de distinguer les différents types de stress qui impactent fortement le comportement des bactéries. Un effet d'inhibition est caractérisé par la limitation de l'activité microbienne due à l'accumulation de produits de fermentation inhibiteurs (acides organiques, bactériocines) et, dans le cas de procédés industriels, de l'acidification du milieu de culture. Ce stress augmente tout au long de la fermentation, ayant différents effets sur le métabolisme. L'accumulation de l'acide lactique, par exemple, provoque un effet d'inhibition sur la croissance. La température est l'un des facteurs environnementaux le plus important affectant la production d'acide lactique. *Lactobacillus coryniformis* subsp. *Torquens* est une bactérie mésophile et sa température optimale pour la production d'acide lactique est comprise entre 30 et 38 ° C.

En ce qui concerne l'acidification du milieu, le pH de la culture est non inhibiteur parce que les cellules sont capables de maintenir leur pH intracellulaire proche de la neutralité. Cependant, cela nécessite une dépense d'énergie qui impose un régime métabolique pour lequel l'énergie utilisée pour la croissance est limitée (Garrigues, et al., 1998).

Un stress environnemental qui a un rôle important dans le développement des bactéries lactiques est lié à la disponibilité des nutriments dans le milieu de culture. Comme mentionné précédemment, les bactéries lactiques ont besoin des sels et des vitamines pour se développer. Or les principales contraintes sur le métabolisme de croissance sont imposées par l'absence d'azote organique (peptides, acides aminés, bases, etc) et des substrats carbonés. En ce qui concerne la source d'azote, six acides aminés sont essentiels à la croissance des bactéries d'acide lactique : l'acide glutamique, la valine, la méthionine, l'isoleucine, la leucine et l'histidine (Marshal et droit, 1984). Les nutriments peuvent être ajoutés sous forme de malt, extrait de viande, extrait de levure et de peptone. Concernant la source de carbone, différentes sources ont été utilisées pour la production d'acide lactique par fermentation utilisant des bactéries lactiques. L'acide lactique de pureté la plus élevée est obtenu quand un seul sucre est fermenté, entraînant des coûts de purification inférieurs (Rashid, 2008). Cependant, cela n'est pas économiquement favorable, parce que les sucres purs sont des matières premières coûteuses et l'acide lactique est un produit bon marché. De façon alternative, différentes matières premières ont été étudiées.

1.3. Matières premières

L'acide lactique produit dans cette étude est destiné à être transformé en PLA. Comme la production de ce polymère nécessite de grandes quantités d'acide lactique (produit relativement peu cher), l'un des principaux défis dans sa production à grande échelle est le coût de la matière première. Par conséquent, l'utilisation de matières premières bon marché est requise pour rendre le procédé industriellement viable. Les caractéristiques souhaitées pour les matières premières

sont un prix bas, de faibles niveaux de contaminants, des taux de production rapides, des rendements élevés pour le produit, une réduction de la formation de sous-produits et une bonne capacité à être fermentées sans prétraitements lourds (Wee, et al., 2006). Des procédés de production d'acide lactique utilisant des matières premières peu coûteuses ont été largement étudiés. Parmi les substrats étudiés, on peut citer l'amidon à base de biomasse non convertie, la biomasse lignocellulosique non transformée, et des déchets (John, et al., 2007). Dans cette étude, la matière première utilisée pour la production d'acide lactique est l'amidon de farine de blé.

1.6. Conclusions

L'intérêt de la production d'acide lactique s'est accru depuis peu grâce à son application dans la production de PLA. Il y a deux façons de produire de l'acide lactique, la voie chimique et la voie biotechnologique. Cette dernière est préférée car elle s'avère plus respectueuse de l'environnement. Bien que différents micro-organismes puissent être utilisés pour la production d'acide lactique, les bactéries lactiques sont les plus largement utilisées. Ces bactéries ont besoin de nutriments complexes pour croître et produire de l'acide lactique. En effet, il est important de garantir les besoins nutritionnels pour la croissance des bactéries lors de la fermentation. Afin de garantir ces besoins et de réduire le coût des matières premières, divers substrats ont été proposés dans la littérature. Dans ce travail, nous nous concentrons sur l'utilisation de la farine de blé comme seul substrat (source de carbone et d'azote) pour la production d'acide lactique. Le développement du procédé de production d'acide lactique en utilisant ce substrat est décrit dans le chapitre suivant.

CHAPITRE 2: PRESENTATION DU SYSTEME ETUDIE

Comme mentionné précédemment, ce projet vise à améliorer la performance du procédé de production d'acide lactique. Une des solutions proposée par le CRIS (Centre de Recherche et d'Innovation Soufflet) et également décrite dans la littérature pour réduire le coût de production est d'utiliser la farine de blé comme matière première. Ainsi la production d'acide lactique peut être effectuée sans aucune addition de nutriments (Hetényi, et al., 2010).

La production mondiale de blé pour les années 2014/2015 a été estimée à 717 millions de tonnes par l'USDA (United States Department of Agriculture). Cette production représente 30% de la production mondiale de céréales. La France est le premier producteur de céréales dans l'Union européenne et occupe la sixième place au niveau mondial. Concernant la production de blé, la France occupe la cinquième place au niveau mondial (Lyddon, 2013).

En tant que constituant principal du blé, l'amidon est un glucide complexe formé de chaînes de molécules de D-glucose. Les molécules de glucose sont liées par des liaisons glycosidiques qui sont stables à un pH élevé mais sont hydrolysées à des valeurs de pH faibles. L'amidon se présente sous forme de granulés et contient deux polymères de glucose, l'amylose et l'amylopectine.

Ce chapitre s'intéresse à l'amélioration du procédé de production d'acide lactique à partir de farine de blé. Les procédés existants pour la production d'acide lactique en utilisant des matériaux à base d'amidon sont tout d'abord décrits. Ensuite, la conception du procédé à étudier est réalisée en partant du procédé proposé par Soufflet. La description de tout le procédé de production est présentée pour conclure.

2.1. Procédés existants

2.1.1. Procédé conventionnel

Le procédé conventionnel de production d'acide lactique à partir d'amidon est composé de trois étapes :

Liquéfaction

L'amidon est transformé en oligosaccharides et du glucose par hydrolyse enzymatique par des enzymes α-amylase. Comme les enzymes ne sont pas capables d'agir directement sur les granulés d'amidon, il est nécessaire d'augmenter la température pour former un amidon gélifié sur lequel les enzymes ont un effet significatif.

Saccharification

Dans cette étape, les oligosaccharides sont transformés en glucose en utilisant l'enzyme amyloglucosidase. La réaction dépend fortement de la longueur de la chaîne et des conditions opératoires telles que le pH et la température.

Fermentation

Cette étape est décrite en détail dans le chapitre 1. Toutefois, plusieurs aspects importants sont rappelés ici. Les bactéries lactiques exigent un niveau élevé de nutriments, notamment en source d'azote, vitamines et oligo-éléments (Hetényi, et al., 2010). Pour répondre à ces besoins, une alternative est d'utiliser la fraction protéique insoluble du blé (représentant 13% de la composition du blé) comme source d'azote. Cette approche sera considérée dans ces travaux de thèse pour améliorer l'étape de fermentation et sera décrite ultérieurement.

2.1.2. Autres procédés

2.1.2.1. Saccharification et fermentation simultanées

La conversion d'amidon en acide lactique peut être effectuée de manière plus efficace par couplage de l'hydrolyse enzymatique des oligosaccharides et de la fermentation en une seule étape, dite « simultaneous saccharification and fermentation » (SSF). Ce procédé offre plusieurs avantages par rapport au procédé conventionnel, tels que l'utilisation d'un seul réacteur, une durée plus courte et une productivité en acide lactique plus élevée. Cependant, les différences en termes de conditions optimales de pH et de température pour la culture bactérienne, l'hydrolyse enzymatique et la production d'acide lactique conduisent à des difficultés opératoires accrues.

#### 2.1.2.2. Production directe d'acide lactique

Des bactéries lactiques amylolytiques ou des champignons tels que les *Rhizopusoryzae* peuvent être utilisés pour la production directe d'acide lactique à partir d'amidon. Cependant, seule une minorité de souches de bactéries lactiques a la capacité de produire des enzymes pour hydrolyser l'amidon (Narita, et al., 2004) (Shibata, et al., 2007).

2.2. Conception du procédé à étudier

Le procédé de production d'acide lactique proposé dans ces travaux de thèse a été conçu en partant du procédé de base effectué par le laboratoire du CRIS. Ce dernier comporte trois étapes : une liquéfaction (comme dans le procédé conventionnel), une pré saccharification (ou seule une partie du maltose et des oligosaccharides sont transformés en glucose) et une étape de saccharification et fermentation simultanées.

Le procédé que nous proposons contient également trois étapes : une liquéfaction, une étape de saccharification et hydrolyse des protéines simultanées (SSPH, simultaneous saccharification and proteins hydrolysis) et une dernière étape de saccharification, hydrolyse des protéines et fermentation simultanées (SSPHF, simultaneous saccharification, proteins hydrolysis and fermentation). La figure 2.1 montre un aperçu des étapes précédemment décrites.
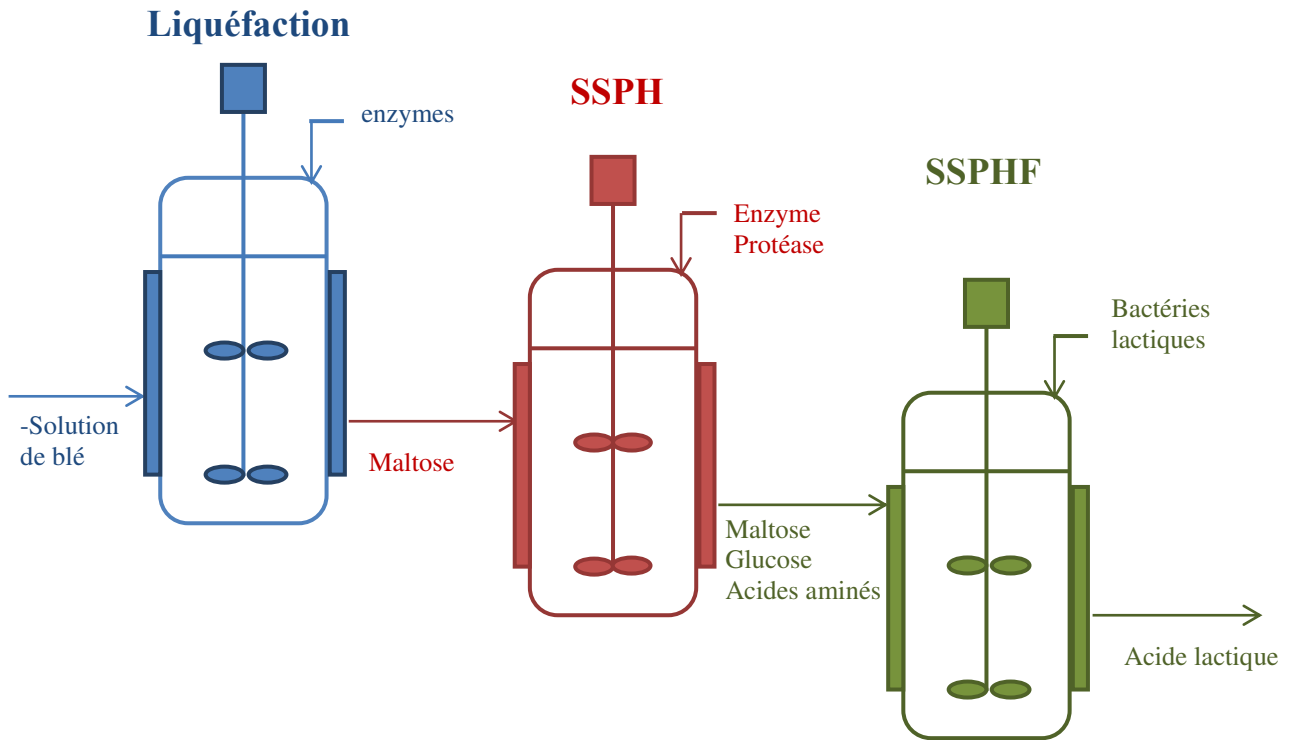
Figure 2.1. Etapes du procédé de production d'acide lactique proposé

La suite décrit la conception du procédé. Tout d'abord, des expériences effectuées pour optimiser le milieu de culture (pour garantir les besoins azotés pour la croissance bactérienne) sont présentées, suivies par le développement d'une étape de saccharification et hydrolyse des protéines simultanées. Le choix du mode de fonctionnement du bioréacteur est exposé à la fin.

2.3.   Etude de l'hydrolyse des protéines

Cette étude a été effectuée afin d'optimiser le milieu de culture et augmenter la productivité en acide lactique, notamment pour satisfaire les besoins azotés des bactéries lactiques. La fraction protéique de blé (gluten) est donc utilisée comme source d'azote. Pour ce faire, des protéases différentes (enzymes qui effectuent l'hydrolyse des protéines) ont été testées. L'objectif est de trouver la protéase conduisant à la productivité en acide lactique la plus élevée. Les essais effectués dans cette étude sont réalisés au cours de l'étape SSF (saccharification et fermentation simultanées), la troisième étape dans le procédé de Soufflet. Considérant que l'hydrolyse des protéines est réalisée simultanément avec le SSF, cette étape a été renommée: saccharification, hydrolyse des protéines et fermentation simultanées (SSPHF).

2.3.1. Description de l'essai

Quatre protéases à deux concentrations différentes ont été utilisées afin de choisir la plus appropriée pour l'étape de SSPHF dans des essais batch (en fiole). Il s'est avéré que la concentration de la protéase n'a pas eu d'effet significatif sur la productivité en acide lactique donc seuls les résultats concernant la concentration la plus faible (200 mg kg^{-1}) seront présentés.

Pour la préparation de la solution de blé, de la farine de blé a été mise en suspension dans de l'eau à une concentration de 260 g L^{-1}. Pour l'étape de liquéfaction, deux enzymes ont été ajoutées : Lyvanoldevisco plus et Lyquozyme SDCS (Lyven, Colombelles, France) et la réaction s'est déroulée à 85 °C et à un pH de 5,5. Ensuite, un litre de la solution d'amidon liquéfié a été dilué avec de l'eau distillée pour obtenir une concentration finale de blé de 130 g L^{-1}. Du sulfate de manganèse a été ajouté à 0,05 g L^{-1} et le pH a été ajusté à 5,7. Du carbonate de calcium a été ajouté à une concentration de 30 g L^{-1} de façon à tamponner la solution de blé et à réduire l'effet de diminution du pH avec la production d'acide lactique pendant l'essai. Avant la SSPHF, l'enzyme amyloglucosidase (AMG) (Lyvanol GA, Lyven, Colombelles, France), a été ajoutée afin de commencer la saccharification à 50 °C. Une fois l'étape de pré-saccharification terminée, la température dans l'étuve a été réduite à 30 °C. Chaque protéase a été ajoutée à deux concentrations différentes : 200 et 1400 mg d'enzyme kg^{-1} de blé. Au total, 8 conditions différentes ont été testées : 4 protéases différentes, chacune à 2 concentrations. Ensuite, la biomasse a été ajoutée à une concentration initiale égale à 10^9 cellules mL^{-1}. Cette étape de SSPHF a été effectuée pendant 48 h à 30 °C et à pH 5,7.

2.3.2. Suivi des variables

Pour tous les essais présentés tout au long de ce manuscrit, les analyses pour suivre le comportement des variables sont celles décrites ci-après. Des échantillons ont été prélevés à des intervalles de temps différents. La concentration cellulaire a été suivie par des comptages effectués dans une chambre de comptage de cellule de Thoma.

Pour le suivi des concentrations en glucose, maltose et acide lactique, les échantillons ont d'abord été chauffés à 95 °C pendant 15 minutes puis filtrés à travers des filtres de 0,2 µm de cellulose. Les concentrations ont été ensuite mesurées sur un système par HPLC.

Les concentrations des acides aminés ont été mesurées en utilisant une méthode colorimétrique (Friedman, 2004). La concentration de free amino nitrogen (FAN), un mesure de la concentration des acides aminés individuels et des petits peptides, a été déterminée par spectrophotométrie comme un équivalent de la glycine, cette substance étant utilisée comme référence.

2.3.3. Résultats de l'étude d'hydrolyse des protéines

La figure 2.2 montre les résultats obtenus avec cette étude. La plus forte concentration (FAN) a été obtenue avec l'enzyme P4, Prolyve NP à 48h. Une concentration plus élevée d'acide lactique a été obtenue aussi avec Prolyve NP. A 24 h de fermentation, la productivité obtenue avec la protéase Prolyve NP était de 1,45 g L^{-1}.h^{-1}. A la fin de la fermentation (à 48 h) la productivité était de 1,04 g. L^{-1}h^{-1}, ce qui prouve une réduction du taux de production d'acide lactique au cours des dernières 24 heures.
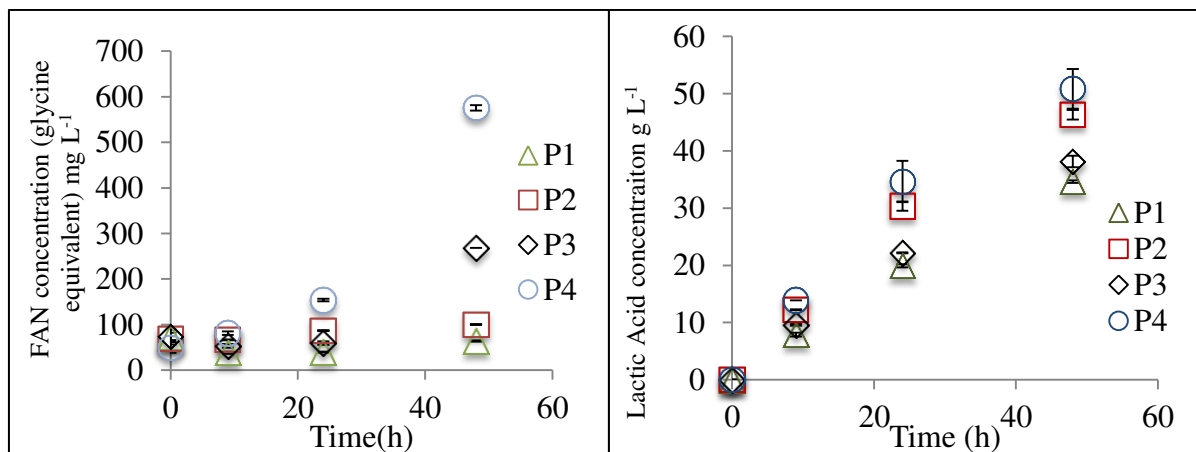
Figure 0.2 A gauche concentration de Free Acid Nitrogen (FAN), à droite concentration d'acide lactique pendant l'étape de SSPHF. P1= Prolyve PAC, P2= Prolyve BS, P3= Prolyve 4000 and P4= Prolyve NP. Conditions de fermentation: 30°C et pH 5,7 sans régulation du pH.

Certains auteurs utilisant la farine de blé comme matière première dans la fermentation de l'acide lactique ont obtenu des productivités comparables à celles obtenues dans cet essai. Une productivité de 2,1 g L^{-1} h^{-1} a été obtenue par Akerberg, et al (1998) en utilisant *Lactococcuslactis*ssp. *lactis* ATCC 19435. Une productivité d'acide lactique de 0,8 g L^{-1} h^{-1} en utilisant *Lactobacillus*sp. MKT-878 NCAIM B02375 a été obtenue par Hetényi et al. (2010). Cela prouve que les valeurs des productivités obtenues dans ce travail sont en accord avec la littérature. A partir de ces résultats, Prolyve NP à une concentration de 200 mg kg^{-1} a été choisie pour les études suivantes.

2.4. *Saccharification et hydrolyse des protéines simultanées (SSPH)*

Après avoir choisi la protéase, des expériences visant à améliorer l'ensemble du procédé ont été réalisées. En considérant que les températures optimales pour l'hydrolyse des protéines en utilisant Prolyve NP et la saccharification sont de 50°C et 55°C, respectivement, nous avons décidé de coupler ces deux réactions enzymatiques en une seule étape avec les conditions suivantes : température 50°C et à pH 5,7. La valeur du pH reste la même que celle choisie pour l'étude des protéases et seule la température a été modifiée (pour l'étude du choix de la protéase elle était de 30 °C). L'enzyme Prolyve NP est donc ajoutée au début de l'étape de saccharification, cette étape devient donc une étape de saccharification et hydrolyse des protéines simultanées (SSPH pour le sigle en anglais). Cette démarche permet d'améliorer l'ensemble du procédé car la température de la SSPH est proche de la valeur optimale de l'activité enzymatique de chaque enzyme, à la différence de l'étape de SSPHF qui est effectuée à 30° C. Des essais ont permis de montrer que cette étape de SSPH doit se dérouler pendant 6 h avant le début de l'étape de SSPHF afin de garantir les meilleures conditions de production.

2.5. *Choix du mode d'opération*

Sachant que les paramètres tels que le type et la nature des substrats, les micro-organismes et les caractéristiques du milieu de fermentation (viscosité, composition, présence de particules solides, etc.) doivent être considérés lors de la conception du procédé de fermentation, le mode de fonctionnement du bioréacteur est également un facteur important lorsque des améliorations de la

18

performance du procédé sont recherchées. Le tableau 2.1 résume les principaux avantages et inconvénients d'une partie des modes d'opération utilisés dans la production d'acide lactique par fermentation.

En plus de l'optimisation de la souche et de l'utilisation d'autres matières premières, le passage du procédé batch traditionnel vers un procédé fed-batch, continu ou avec recyclage cellulaire pourrait conduire à une meilleure performance du procédé de production d'acide lactique. Il est également important de considérer le traitement down stream associé (Kamm, 2015).

Tableau0.1 Avantages et inconvénients d'une partie des procédés de production d'acide lactique par fermentation (Abdel-Rahman, et al., 2013).

Mode opératoire	Avantages	Inconvénients
Fermentation batch	- Opération simple - Concentration du produit élevée - Risque de contamination réduit	- faible productivité - Inhibition par le produit et par le substrat
Fermentation fed-batch	- Inhibition par le produit évitée - Concentration du produit élevée	- Inhibition par le produit
Fermentation répétée	- Gain de temps - Omission du temps de préparation de l'inoculum	- Exigence de dispositifs spéciaux pour la concentration cellulaire -Difficile à utiliser avec des milieux complexes
Fermentation continue	- productivité élevée - possibilité de contrôler le taux de croissance - fréquence d'arrêt du procédé plus faible	- Utilisation incomplète de la source de carbone - Produit dilué

Le but de l'optimisation du procédé étudié dans ce travail est de maximiser la productivité en acide lactique, d'une part en optimisant les conditions de fonctionnement et d'autre part en utilisant une stratégie de commande pour maintenir le bioprocédé dans les conditions optimales de fonctionnement.

Afin d'être en mesure de construire une stratégie de commande pilotant le débit d'entrée du substrat (paramètre considéré comme commande dans la plupart des stratégies de commande), le procédé doit être opéré soit en fed-batch, soit en mode continu. En outre, la fermentation répétée n'a pas été considérée dans ce travail car des dispositifs spéciaux sont nécessaires pour la filtration et le recyclage cellulaire. Ceci sort du domaine de ce travail. En outre, comme le bouillon de culture utilisé pour la production d'acide lactique est un mélange de farine de blé et d'eau à 25% p / p, la filtration d'un bouillon si complexe pourrait être difficile.

En comparant les fermentations fed-batch et continues, des valeurs de productivité plus élevées

sont obtenues avec la fermentation en mode continu. De plus, la fermentation fed-batch empêche les inhibitions par les substrats, mais pas par les produits de fermentation. Pour ces raisons, la fermentation en mode continu a été retenue pour l'étude et l'implantation d'une loi de commande pour le procédé.

2.6. Conclusions

La matière première pour la production d'acide lactique dans ces travaux de thèse est la farine de blé. Cela se justifie principalement par la grande disponibilité de cette céréale en France, son faible coût et l'expertise de Soufflet quant à son utilisation. Ce chapitre s'est intéressé à la conception du procédé de production de l'acide lactique en partant du procédé proposé par Soufflet. Une étape de saccharification, hydrolyse de protéines et fermentation simultanées (SSPHF) a été conçue afin de garantir les besoins en azote pour la croissance des bactéries. La protéase Prolyve NP a permis d'obtenir des productivités plus élevées en acide lactique et a été choisie pour la suite des travaux. Par ailleurs, les réactions de saccharification et d'hydrolyse des protéines ont été couplées en une même étape (SSPH). Le procédé obtenu consiste alors en trois étapes : l'amidon est d'abord liquéfié, suivi par une étape de SSPH où le maltose et le gluten sont partiellement hydrolysés. La dernière étape de saccharification, hydrolyse des protéines et fermentation simultanées, SSPHF, permet de produire l'acide lactique, le produit d'intérêt. Dans cette dernière étape, le maltose et le gluten restants sont hydrolysés en même temps que la fermentation. Concernant le mode opératoire, le mode continu a été choisi compte tenu des productivités en acide lactique élevées qu'il permet d'obtenir. La modélisation et la commande seront développées pour l'étape SSPHF, l'étape la plus longue du procédé.

CHAPITRE 3 : MODELISATION

Les modèles sont des outils importants pour l'optimisation des procédés biotechnologiques complexes, et pour prédire la performance du bioréacteur. La modélisation mathématique des fermentations permet de représenter par des équations, dont certaines sont des équations différentielles, l'évolution des variables importantes ou fondamentales du procédé. Les variables considérées sont généralement les concentrations des cellules, des substrats et des métabolites. Pour décrire un procédé microbiologique, il existe essentiellement deux types de modèles : structurés et non structurés.

• Les modèles structurés considèrent l'évolution de la composition interne du micro-organisme. Ils décrivent les voies métaboliques et prennent en compte les caractéristiques intracellulaires (Gadjil et Venkatesh, 1997) (Nielsen et al., 1991).
• Les modèles non structurés utilisent les cinétiques microbiennes pour décrire l'évolution des taux de croissance, la consommation du substrat et la production de métabolites. Seule la concentration cellulaire totale est considérée. Pourtant, il a été prouvé que ces modèles peuvent décrire avec précision la fermentation d'acide lactique dans une large gamme de conditions expérimentales (Bouguettoucha, et al., 2011). Ce chapitre est consacré à l'élaboration d'un modèle pour une SSPHF (saccharification, hydrolyse des protéines et fermentation simultanées) dans un bioréacteur continu.

3.1. Modélisation de la fermentation lactique

La modélisation de la croissance bactérienne et de la production de métabolites dans la

fermentation lactique considère généralement le phénomène d'inhibition exercée par le substrat et le produit (acide lactique). Les effets d'autres paramètres importants pour les conditions de culture sont souvent non pris en compte. En effet, certains d'entre eux, y compris le pH et la température, sont généralement fixés. D'autres facteurs tels que l'agitation, la concentration en oxygène dissous, ne sont régulièrement pas pris en compte. Le réacteur utilisé dans l'approche de modélisation est illustré figure 3.1.
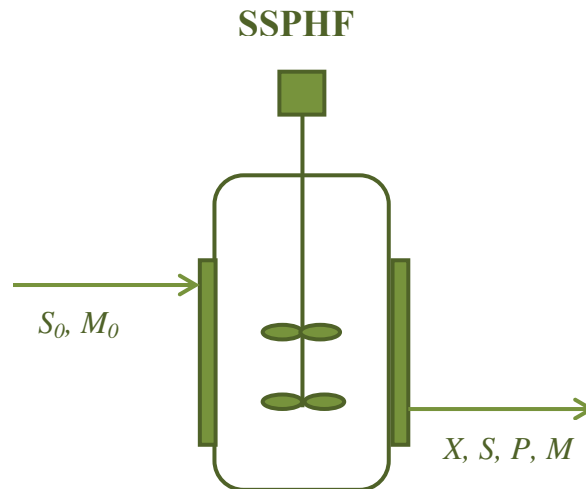
SSPHF

Figure 0.1 SSPHF continue

Les variables d'intérêt sont X (concentration en biomasse en g L^{-1}), S (concentration en glucose en g L^{-1}), P (concentration en acide lactique en g L^{-1}) et M (concentration en maltose en g L^{-1}). Le modèle doit inclure quatre équations dynamiques décrivant leur évolution dans le temps. M_0 et S_0 représentent les concentrations de maltose et de glucose alimentant le réacteur, respectivement. Ces concentrations sont obtenues à partir de la SSPH (saccharification et hydrolyse des protéines simultanées), étape précédente du procédé. Il convient de souligner que la valeur du pH dans le bioréacteur SSPHF est régulée par l'addition de NaOH, par conséquent le bioréacteur comporte en fait deux flux d'entrée. Néanmoins, le débit d'entrée de NaOH est très faible par rapport au débit d'alimentation du bioréacteur (35 fois plus petit). Le débit d'entrée de NaOH peut donc être négligé pour la modélisation.

3.2. Développement d'un modèle de l'étape SSPHF continue

Le procédé de production d'acide lactique à partir de farine de blé proposé dans cet ouvrage est innovant. En effet, la souche, le substrat et les étapes proposées n'ont jamais été utilisés auparavant. En conséquence, il n'y a pas de modèle disponible dans la littérature décrivant ce procédé.

Avant de présenter notre modèle, certaines hypothèses considérées pour son développement doivent être exposées. Tout d'abord, les acides aminés obtenus par l'hydrolyse du blé ne sont pas considérés dans le modèle car leur modélisation est complexe et ils sont supposés être en excès (substrat non limitant). Ainsi, nous considérons le cas général où le glucose, la source de carbone, peut être le substrat limitant. Ce sucre est produit à partir de maltose et consommé par les bactéries simultanément, par conséquent les mécanismes impliqués dans la transformation du

21

maltose et du métabolisme des bactéries lactiques doivent être considérés dans l'approche de modélisation mathématique.

Dans le fonctionnement en continu, toutes les variables, X, S, P et M restent constantes une fois le régime stationnaire atteint. Néanmoins, il est nécessaire de modéliser les phases transitoires au moyen d'équations dynamiques. Les équations de bilan de matière décrivant la dynamique de ces variables sont obtenues pour le bioréacteur parfaitement agité représenté par la figure 3.1. Cependant le mélange dans ces bioréacteurs est souvent non idéal. Par conséquent, l'écart par rapport à la réalité doit être évalué et quantifié. La méthode de distribution du temps de séjour (DTS) est l'une des façons de caractériser le comportement non idéal du réacteur afin d'assurer une bonne représentation des phénomènes. Il a été constaté que le réacteur a un volume mort de 9% qui a été pris en compte dans notre approche de modélisation.

Le modèle proposé dans ces travaux de thèse consiste en quatre équations dynamiques décrivant l'évolution des variables X, P, S et M :

$$\frac{dX}{dt} = \mu X - DX$$

$$\frac{dP}{dt} = \frac{Y_{XS}}{Y_{PS}}\mu X - DP \qquad (0.1)$$

$$\frac{dS}{dt} = -\frac{1}{Y_{PS}}\mu X + k_M M + D(S_0 - S)$$

$$\frac{dM}{dt} = -k_M M + D(M_0 - M)$$

avec :

$$\mu = \mu_{max}\ \frac{S}{k_S + S}\left(1 - \frac{P}{P_{max}}\right)^n$$

Dans ce modèle, X, P, S et M sont les concentrations en biomasse, acide lactique, glucose et maltose (g L^{-1}) respectivement, μ la vitesse de croissance (h^{-1}), D le taux de dilution défini comme le ratio entre le débit et le volume (h^{-1}), μ_{max} le taux de croissance maximal (h^{-1}), k_S la constante de demi-saturation (g L^{-1}), P_{max} la concentration du produit au-dessus de laquelle les bactéries ne croissent plus (g L^{-1}), n le pouvoir toxique du produit, Y_{XS} le rendement en biomasse par rapport au substrat (g cellules g^{-1} substrat), Y_{PS} le rendement en acide lactique par rapport au substrat (g cellule g^{-1} substrat), k_M la constante de dégradation du maltose (h^{-1}) et M_0 et S_0 les concentrations en maltose et en glucose dans le flux d'alimentation (g L^{-1}), respectivement. Les paramètres qui doivent être déterminés pour les conditions de fermentation considérées sont les paramètres intervenant dans la cinétique de croissance (μ_{max}, k_S, P_{max} et n), les rendements Y_{XS} et Y_{PS} et la constante cinétique k_M.

3.3. Vers une stratégie d'identification

Une étude de sensibilité des paramètres du modèle a permis d'établir que le paramètre k_S n'influence aucune des variables (pour la gamme de concentrations de glucose considérée dans ce travail). Son identification ne sera donc pas réalisée car elle conduirait à un résultat ayant une faible précision. Sa valeur est alors fixée à la moyenne des valeurs rapportées dans la littérature, 0,5 g L^{-1}. L'identification du pouvoir toxique de l'acide lactique (n) présent dans la cinétique de croissance semble complexe en raison de la structure de l'équation (voir équations 3.1); sa valeur sera fixée à 3. Cette valeur a été choisie considérant une étude qui a permis de déterminer son impact sur la cinétique de croissance et des valeurs présentées par d'autres auteurs travaillant sur la fermentation de l'acide lactique (Akerberg, et al., 1998) (Kwon, et al., 2001), qui ont trouvé des valeurs du pouvoir toxique de 2,06 et 2,68, respectivement. Avec cette démarche, les paramètres à identifier sont réduits à 5 (μ_{max}, P_{max}, Y_{PS}, Y_{XS} et k_M).

L'estimation de l'ensemble des valeurs des paramètres est effectuée en utilisant des données expérimentales provenant d'essais réalisés en continu décrits plus loin dans ce chapitre. Les paramètres du modèle ont été déterminés par minimisation de la fonction de cout suivante.

$$
\begin{aligned}
RSE = &\sum_{i=1}^{N} w_X \cdot (X_{i,\exp} - X_{i,cal})^2 + \sum_{i=1}^{N} w_P \cdot (P_{i,\exp} - P_{i,cal})^2 \\
&+ \sum_{i=1}^{N} w_S \cdot (S_{i,\exp} - S_{i,cal})^2 + \sum_{i=1}^{N} w_M \cdot (M_{i,\exp} - M_{i,cal})^2
\end{aligned}
\tag{0.2}
$$

Dans l'équation (3.2), RSE est la somme des carrés des erreurs entre les valeurs calculées via le modèle ($X_{i,cal}$, $P_{i,cal}$, $S_{i,cal}$ et $M_{i,cal}$,) et les données expérimentales ($X_{i,exp}$, $P_{i,exp}$, $S_{i,exp}$ et $M_{i,exp}$,). N est le nombre d'observations. w_X, w_P, w_S, w_M sont des facteurs de pondération permettant de normaliser tous les termes de l'équation (3.2), ils ont été fixés à 100, 1, 1 et 1, respectivement en considérant l'ordre de grandeur de chaque variable.

Les équations différentielles (3.1) sont résolues numériquement (par la méthode Runge-Kutta d'ordre quatre). Les données calculées sont ensuite comparées à celles mesurées en calculant la RSE. Les valeurs des paramètres qui minimisent RSE conduisent au meilleur ajustement des données expérimentales. Ceci peut être réalisé considérant une approche d'identification globale de tous les paramètres, en utilisant des algorithmes de moindres carrés non linéaires (par exemple l'algorithme de Levenberg-Marquardt, (Fletcher, 1987)). Le problème d'optimisation présenté dans l'équation (3.2) est toutefois difficile à résoudre, car il existe plusieurs solutions sous-optimales, soit en raison de la précision des mesures soit à cause de l'imprécision du modèle. La solution optimale dépend fortement de l'initialisation des valeurs des paramètres dans l'algorithme d'optimisation. L'initialisation pourrait être faite par des données de la littérature, mais malheureusement très peu des données sont disponibles pour les bactéries considérées. Ainsi, afin de résoudre ce problème d'optimisation, une procédure d'identification spécifique est développée. La procédure d'identification est résumée figure 3.2.
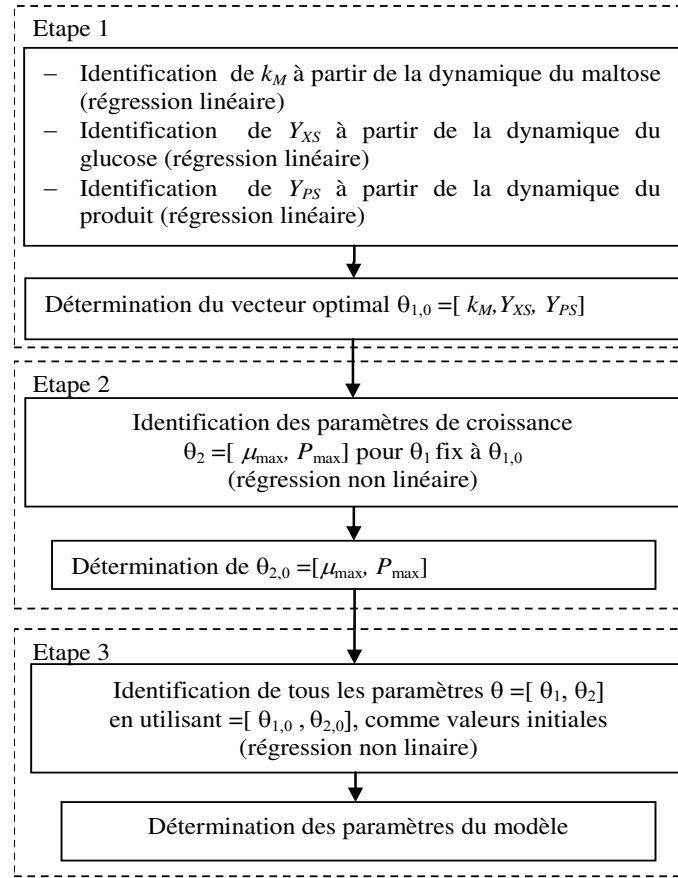
Figure 3.2. Procédure d'identification proposée pour déterminer les paramètres du modèle.

L'idée principale consiste à déterminer la valeur de chaque paramètre indépendamment, en utilisant chaque dynamique séparément. Afin de réduire la complexité de la procédure d'identification, l'approche envisagée est de déterminer les valeurs des paramètres en phase transitoire. En effet, l'identification des paramètres à l'état d'équilibre semble difficile car les dynamiques dans les équations (3.1) seraient annulées. Pour cette raison, l'identification a été effectuée en phase transitoire, notamment ici, pour simplifier, pendant les phases de fonctionnement discontinu où D = 0. Les paramètres intervenant dans les dynamiques du glucose du maltose et de l'acide lactique (k_M, Y_{XS} et Y_{PS}) peuvent être déterminés par des régressions linéaires qui ne nécessitent pas d'initialisation. Seuls les paramètres du taux de croissance doivent être identifiés via un algorithme des moindres carrés non linéaires, conduisant à un problème d'optimisation non convexe. Dans ce cas, les autres paramètres (k_M, Y_{XS} et Y_{PS}) sont fixés aux valeurs obtenues à partir de la régression linéaire. Enfin, le problème global de l'équation (3.2) est résolu en utilisant les valeurs des paramètres obtenus comme valeur initiales.

3.4. Validation expérimentale du modèle

3.4.1. Description de l'essai de validation

Dans ce travail, les étapes de liquéfaction et SSPH ont été effectuées en mode batch, et l'étape de SSPHF a été réalisée en mode continu. Deux types de bioréacteurs sont utilisés, deux

bioréacteurs de 5 L pour les expériences continues et un bioréacteur de 12 L pour produire le stock de solution de blé liquéfiée et pré saccharifiée nécessaire pour alimenter le procédé SSPHF en continu. L'étape de SSPHF a été effectuée dans deux bioréacteurs de 5L en parallèle avec les mêmes conditions pour la duplication. L'étape de SSPHF a démarré en mode batch et le mode continu a été déclenché une fois une concentration en biomasse suffisante atteinte. Deux essais ont été réalisés dans le but d'acquérir des données expérimentales pour l'identification des paramètres. Dans le premier essai, quatre taux de dilution ont été testés : 0,05, 0,1, 0,15 et 0,31 h^{-1}. L'intérêt de tester différents taux de dilution est d'identifier expérimentalement ceux qui permettent d'obtenir les plus fortes productivités. Dans la seconde expérience, la fermentation continue a été effectuée avec deux taux de dilution, 0,15 et 0,2 h^{-1}. La procédure utilisée dans chaque essai est résumée dans le tableau 3.1. Les étapes de liquéfaction et SSPH se sont déroulées comme il a été précédemment décrit dans les sections 2.3.1. et 2.4. Les suivis des concentrations des variables dans le temps a été effectué comme décrit dans la section 2.3.2.

3.4.2. Résultats et analyse

Les données expérimentales correspondant à la phase batch final de l'essai 2, B4 (voir le tableau 3.1) ont été utilisées pour identifier les paramètres du modèle. Les paramètres identifiés sont présentés dans le tableau 3.2.

Tableau 0.1 Taux de dilution testés dans les essais 1 et 2.

	Etape	Désignation	Duration (h)	Taux de dilution (h^{-1})
Essai 1	1	Phase batch 1 = B1	15	0
	2	Phase continue 1 = D1	22	0,1
	3	Phase batch 2 = B2	5	0
	4	Phase continue 2 = D2	21	0,05
	5	Phase continue 3 = D3	3	0,31
	6	Phase continue 4 =D4	4	0,15
Essai 2	1	Phase batch 3 = B3	10	0
	2	Phase continue4 = D4	8	0,15
	3	Phase continue5 = D5	7	0,2
	4	Phase batch 4 = B4	6	0

Le modèle décrit de manière satisfaisante l'évolution des concentrations dans le temps comme montré par la figure 3.3, qui présente la comparaison entre les données expérimentales de l'essai 2 et les valeurs obtenues par le modèle. En ce qui concerne la concentration de glucose, les données expérimentales étaient légèrement plus élevées que les valeurs calculées. Ceci peut s'expliquer par la production de glucose à partir de sucres autres que le maltose, présents dans le blé, qui n'est pas prise en compte dans le modèle. L'équation cinétique du premier ordre est suffisante pour décrire la dynamique du maltose. La prédiction des concentrations d'acide lactique et de biomasse est également satisfaisante.

Tableau 0.2 Paramètres identifiés pour un bioréacteur de 5 L avec un volume mort de 9%.

Paramètre	Valeur identifiée
μ_{max} (h^{-1})	0,28
P_{max} (g L^{-1})	98,6
Y_{XS} (g Cell g^{-1} Glucose)	0,053
Y_{PS} (g Product g^{-1} Cell)	0,8
k_M (h^{-1})	0,035
k_S (g L^{-1})	0,5 (valeur de la littérature)
n	3 (fixé par essai-erreur)
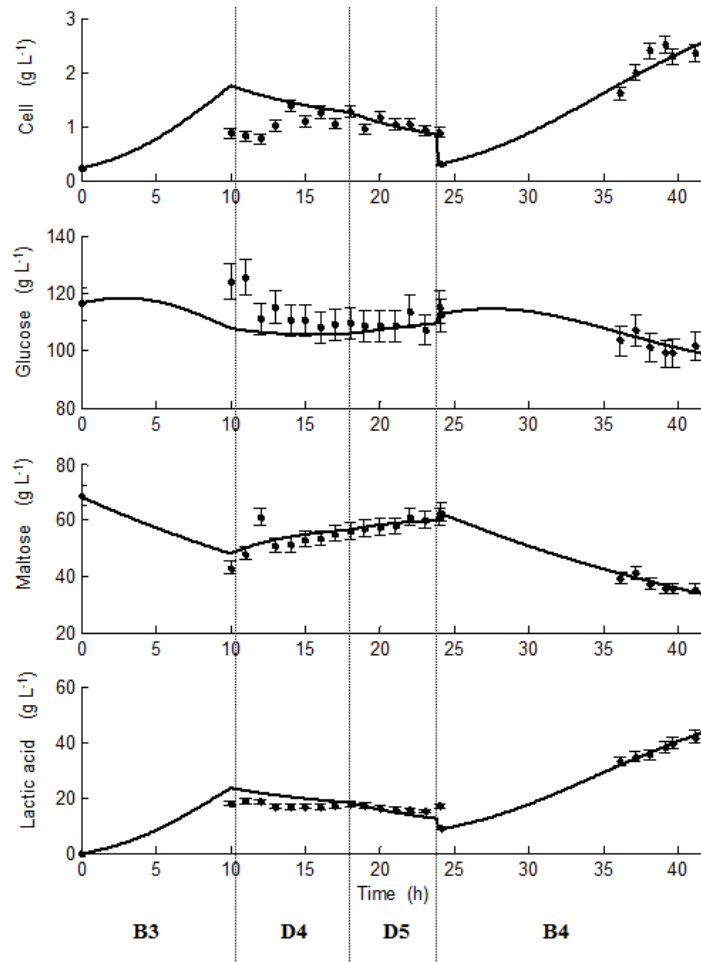
Figure 0.2 Données expérimentales (●) et simulées (———) des concentrations de cellules, glucose, maltose et acide lactiquepour des SSPHF en batch et en continu. Deux taux de dilution testés D4 = 0,15 h^{-1} et D5 = 0,2h^{-1}.

3.5 CONCLUSIONS

Ce chapitre a présenté le développement d'un modèle capable de décrire le comportement des variables dans le bioréacteur de SSPHF. Le modèle proposé est composé de quatre équations dynamiques décrivant la croissance des bactéries, la consommation des substrats et la formation du produit (équations 3.1). Le maltose est le seul sucre pris en compte dans la dynamique du glucose. L'identification et la validation des paramètres du modèle a été effectuée en utilisant des

données expérimentales des essais en batch et continu. Le modèle décrit correctement le comportement des variables au cours de temps. Ce modèle peut maintenant être utilisé pour accomplir le prochain objectif de ce travail, à savoir l'élaboration d'une stratégie de commande pour atteindre un état de fonctionnement optimal.

CHAPITRE 4 : Suivi et surveillance

Après validation du modèle, le principal problème pour la maîtrise des procédés biotechnologiques est le manque de capteurs physiques fiables et peu coûteux permettant de mesurer en ligne les différentes variables d'état. En effet, il est souvent difficile, pour des raisons économiques ou technologiques, de mesurer toutes les variables nécessaires à la commande du bioréacteur. Une solution alternative consiste à estimer les états non mesurés à l'aide d'observateurs qui utilisent le modèle dynamique du système et les mesures disponibles en ligne. Il est également possible d'estimer d'autres variables importantes dans le système, par exemple les taux cinétiques de croissance ou de production. Dans ces travaux de thèse, nous avons tout d'abord développé un capteur logiciel pour reconstruire, en ligne, la concentration en acide lactique. Des observateurs (Extended Kalman filter et Unscented Kalman filter) fondés sur l'approche du filtre de Kalman ont ensuite été étudiés pour estimer les variables d'état du système. Ils ont été validés en simulation. Enfin, considérant l'importance du taux de production d'acide lactique pour évaluer la performance du bioprocédé, des observateurs estimant sa valeur ont aussi été développés. Leur performance a été validée en simulation également.

4.1. Détermination de la concentration d'acide lactique en ligne

Dans ce travail, les variables clés sont les concentrations en biomasse, glucose, acide lactique et maltose. Pour l'élaboration de la loi de commande, il est nécessaire de mesurer en ligne au moins une des variables clés du système. Dans ces travaux de thèse, la concentration en acide lactique est reconstruite en utilisant la masse d'hydroxyde de sodium (disponible en ligne) ajoutée pour réguler le pH du bioréacteur. En effet, la concentration en acide lactique produit lors de l'étape de SSPHF peut être corrélée à la masse de base ajoutée pour maintenir le pH à 5,7. Par conséquent, nous avons développé une expression mathématique corrélant ces deux variables comme présenté ci-dessous. Le bilan de matière de la concentration d'acide lactique est alors celui décrit par l'équation dynamique de *P* (3.1) rappelée ici:

$$\frac{dP}{dt} = \frac{Y_{PS}}{Y_{XS}} \mu X - DP \tag{4.1}$$

L'objectif est alors de considérer ce bilan massique et la neutralisation de l'acide lactique par l'hydroxyde de sodium afin de développer une technique pour la détermination en ligne de la concentration en acide lactique. En sachant que une mole d'acide lactique est neutralisée par une mole de soude, le taux de production d'acide lactique en g L^{-1} h^{-1} peut être alors exprimé en fonction de la quantité de soude ajoutée au bioréacteur par :

$$\gamma = \frac{Y_{PS}}{Y_{XS}} \mu X = \frac{F_{Na} C_{Na} M_{LA}}{V} \tag{0.2}$$

où *V* est le volume du milieu de culture (L), F_{Na} le débit de soude ajoutée dans le bioréacteur pour la neutralisation du lactate (L h^{-1}) à l'instant *t*, C_{Na} la concentration de soude dans son débit

d'entrée (mol L^{-1}) et M_{LA} la masse moléculaire de l'acide lactique (g mol^{-1}). En remplaçant 4.2 dans 4.1 on obtient :

$$\frac{dP}{dt} = F_{Na} \frac{C_{Na} M_{LA}}{V} - DP \tag{0.3}$$

En discrétisant l'équation (4.3), la concentration d'acide lactique à chaque instant k est donnée par :

$$P_{k+1} = \left(F_{Na,k} \frac{C_{Na} M_{LA}}{V} - D_k P_k \right)(t_{k+1} - t_k) + P_k \tag{0.4}$$

L'équation (4.4) permet la détermination de la concentration d'acide lactique dans un bioréacteur en continu à l'instant $k + 1$ à partir du débit d'entrée de soude, du taux de dilution, de la concentration de l'acide lactique à l'instant k et des constantes C_{Na}, M_{LA}, V. La concentration en acide lactique est mise à jour à chaque période d'échantillonnage à partir des variables $F_{Na,k}$ et D_k, mesurées en ligne.

4.2. Estimation des variables d'état

Cette section propose des observateurs pour estimer les variables clés qui ne sont pas mesurées en ligne, à partir de celles disponibles en ligne, à savoir la concentration d'acide lactique. Le système d'équations différentielles (3.1) peut être représenté dans le formalisme d'état de la manière suivante :

$$\begin{aligned} \dot{x}(t) &= \mathbf{F}(x(t), u(t)) \\ y(t) &= \mathbf{H}(x(t)) \end{aligned} \tag{0.5}$$

avec $x = (X, S, M, P)^T$, $u = D$, $y = P$ et $\mathbf{F}$ et $\mathbf{H}$ définies par les équations (4.6) et (4.7).

$$\mathbf{F} = \begin{bmatrix} \mu_{\max} \dfrac{S}{k_S + S} X \left(1 - \dfrac{P}{P_{\max}}\right)^n - DX \\[2ex] -\dfrac{1}{Y_{XS}} \mu_{\max} \dfrac{S}{k_S + S} X \left(1 - \dfrac{P}{P_{\max}}\right)^n + k_M M + D(S_0 - S) \\[2ex] -k_M M + D(M_0 - M) \\[2ex] \dfrac{Y_{PS}}{Y_{XS}} \mu_{\max} \dfrac{S}{k_S + S} X \left(1 - \dfrac{P}{P_{\max}}\right)^n - DP \end{bmatrix} \tag{0.6}$$

$$\mathbf{H} = \begin{bmatrix} 0 & 0 & 0 & 1 \end{bmatrix} \tag{0.7}$$

Ce système est observable, par conséquent des observateurs pour estimer les variables d'état peuvent être construits pour le système (4.5).

L'évolution des variables d'état dans le temps est lente, d'où la possibilité d'une discrétisation du système simple par la méthode d'Euler, avec une période d'échantillonnage notée T_s.

4.3. Filtres de Kalman EKF et UKF appliqués au système

Pour l'estimation des états, deux techniques fondées sur le principe du filtre de Kalman sont utilisées. Le filtre de Kalman permet d'obtenir des estimées des états mesurés et non mesurés en utilisant un modèle mathématique du système. L'approche consiste à minimiser la variance de l'erreur d'estimation en utilisant un algorithme récursif :

- Phase de prédiction : le modèle est utilisé pour propager l'estimation initiale des états jusqu'à avoir une nouvelle mesure disponible.
- Phase de correction : les estimées propagées par le modèle sont combinées avec les mesures pour mettre à jour ou corriger ces estimées.

Le filtre de Kalman étendu (EKF, Extended Kalman Filter)

Dans l'EKF, l'estimation est effectuée par linéarisation des équations non linéaires du modèle autour de l'estimation actuelle, puis en appliquant la stratégie du filtre de Kalman pour les équations linéarisées. La technique d'estimation EKF se retrouve dans la littérature pour l'estimation d'état de plusieurs procédés biotechnologiques.

Le filtre de Kalman sans odeur (UKF, Unscented Kalman Filter)

L'observateur UKF utilise une approche similaire à celle de l'EKF, en évitant la procédure de linéarisation et conduisant à une meilleure robustesse et vitesse de convergence (Kandepu et al., 2008). Comme le système étudié a des fortes non linéarités et incertitudes, la méthode UKF évitant la linéarisation semble attractive. Dans ce cas, la distribution de l'état est représentée par un ensemble minimal de points soigneusement choisis, des points dits sigma. Chacun de ces points se propage à travers les non linéarités, et l'estimation de l'état est calculée comme la moyenne de ces points transformés (Julier & Uhlmann, 1997).

Les observateurs EKF et UKF peuvent être appliqués au système (4.5). La structure des observateurs obtenus est représentée figure 4.1.
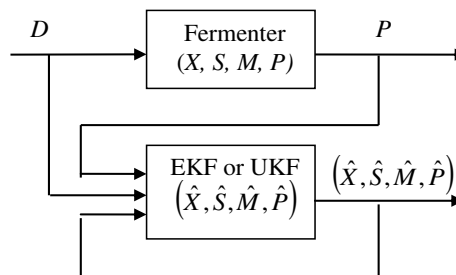

Figure 0.1 Structure des filtres de Kalman étendu et sans odeur

où $\hat{X}$, $\hat{S}$, $\hat{M}$ et $\hat{P}$ sont les valeur estimées des concentrations en biomasse, glucose, maltose et acide lactique, respectivement.

4.4. Validation des estimateurs d'état en simulation

La convergence des observateurs EKF et UKF est analysée pour une erreur d'initialisation des concentrations en biomasse, glucose, maltose et acide lactique. De plus, afin de tester la robustesse des filtres par rapport aux incertitudes du modèle, une erreur non corrélée de 20% des paramètres du modèle est appliquée au système réel (les paramètres du procédé réel sont différents de 20% de ceux utilisés dans le modèle considéré par l'observateur). Les résultats de simulation sont montrés figure 4.2.
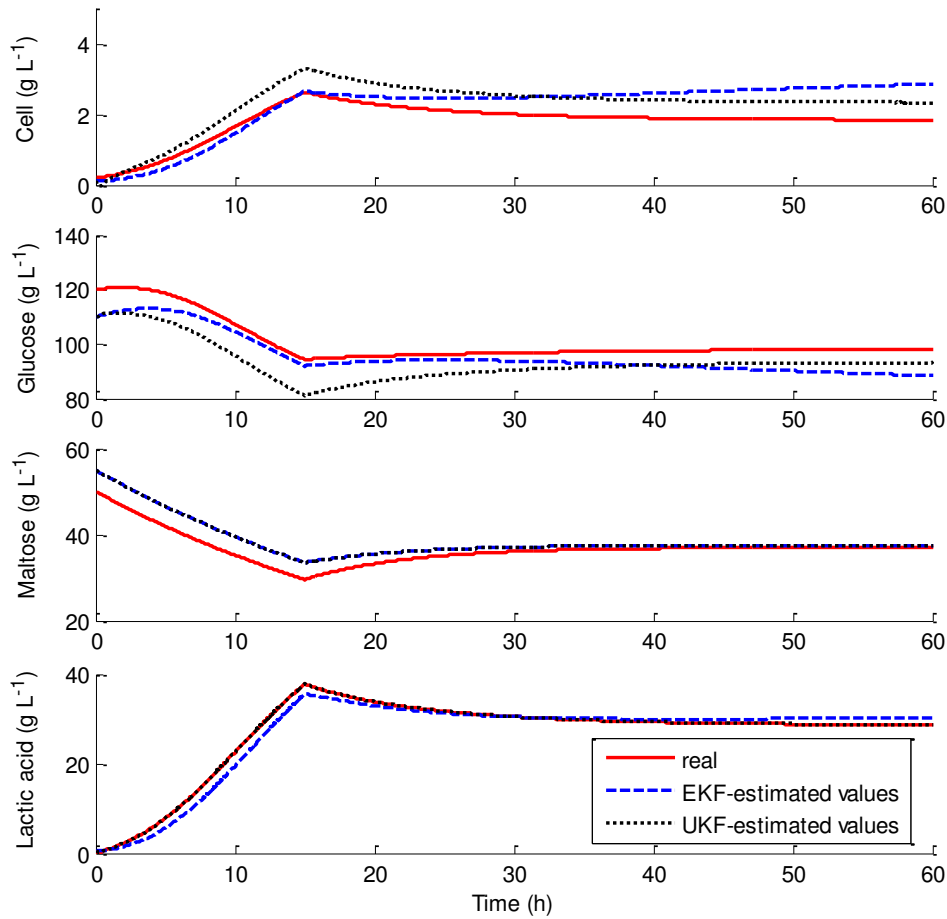
Figure 0.2 Comparaison des observateurs EKF et UKF. Estimation de la concentration en biomasse, glucose, maltose et acide lactique avec une erreur d'initialisation. Une erreur non corrélée de 20% des paramètres du modèle est appliquée au système réel.

Les résultats de simulation montrent que la qualité de l'estimation par les filtres de Kalman dépend fortement de la qualité du modèle. Cette limitation est le principal inconvénient des observateurs exponentiels, et en particulier du filtre de Kalman. On peut remarquer que les estimées obtenues avec le filtre UKF sont plus proches des valeurs réelles que les valeurs obtenues avec l'EKF. Comme la méthode EKF est fondée sur l'approximation linéaire du système à un instant de temps donné, cela peut introduire des erreurs dans l'estimation des états (Figure 4.1). L'UKF montre de meilleures performances que l'EKF, mais l'estimation reste dépendante de la qualité du modèle. Les paramètres du modèle doivent être connus avec précision afin

d'assurer la bonne performance des estimateurs. A partir de cette étude en simulation, on peut conclure que le filtre de Kalman UKF est préférable car sa mise en œuvre est plus simple (pas de nécessité de linéarisation du modèle) et il montre une meilleure performance par rapport au filtre de Kalman étendu (EKF).

4.5. Estimation du taux de production

Cette section est consacrée au développement d'un estimateur du taux de production d'acide lactique. Vu que l'objectif de ce travail de thèse est d'optimiser le procédé de production d'acide lactique, une mesure de l'efficacité du procédé est le taux de production. La méthode d'estimation du taux de production a été choisie en considérant que la concentration d'acide lactique est déterminée en ligne. Le taux de production d'acide lactique (noté γ, en g L^{-1} h^{-1}) est défini comme suit :

$$\gamma = \frac{Y_{PS}}{Y_{XS}} \mu X \qquad (0.1)$$

Dans le modèle du système, le taux de production est lié directement à la concentration du produit par :

$$\frac{dP}{dt} = \gamma - DP \qquad (0.9)$$

Ainsi, la dynamique de la concentration du produit sera utilisée afin de développer une estimation de γ. Trois stratégies d'estimation ont été étudiées. Elles sont présentées ci-dessous.

Différentiation numérique

De l'équation (4.71), une manière simple de calculer une estimée de γ, notée $\hat{\gamma}$, est d'utiliser la concentration d'acide lactique et sa dérivée première :

$$\hat{\gamma} = \dot{P} + DP \qquad (0.10)$$

La dérivée première $\dot{P}$ peut être calculée par une technique de discrétisation standard. Cependant, en cas de mesures bruitées de P, cette approche peut conduire à une très mauvaise estimation. Une approche classique pour éviter ce phénomène consiste à filtrer le signal bruité. Dans ce travail, la technique proposée dans (Fliess, et al., 2008) a été utilisée. La dérivée première de la concentration du produit est calculée par :

$$\hat{\dot{P}} = -\frac{3!}{T^3} \int_0^T (T - 2t)P(t)dt \ . \qquad (0.11)$$

où [0, T] est une fenêtre « courte » de temps.

Filtre de Kalman Linéaire

Le principe du filtre de Kalman linéaire est considéré afin de construire un estimateur linéaire du taux de production. Cette approche est appliquée dans deux cas : pour un modèle avec un taux de production constant dans le temps et pour un modèle avec une évolution linéaire du taux de production.

Modèle avec taux de production constant

Le système à considérer dans ce cas est comme suit :

$$\begin{cases} \dot{P} = \gamma - DP \\ \dot{\gamma} = 0 \end{cases} \qquad (0.2)$$

Modèle avec taux de production linéaire

Cette hypothèse est plus précise dans le cas d'une culture batch ou dans les phases transitoires d'une culture continue. Le modèle est dans ce cas donné par :

$$\begin{cases} \dot{P} = \gamma - DP \\ \ddot{\gamma} = 0 \end{cases} \qquad (0.13)$$

4.6. Validation des estimateurs du taux de production en simulation

Les techniques d'estimation du taux de production ont été validées en simulation. Les résultats obtenus avec l'approche de différentiation numérique, avec le filtre de Kalman avec un modèle constant pour γ (dénommé ci-après Kalman 1) et le filtre de Kalman avec un modèle linéaire pour γ (nommé Kalman 2) sont représentés par la figure 4.3. Un bruit blanc gaussien est appliqué à la concentration de l'acide lactique, P, avec un écart type de 1%. La simulation a commencé en mode batch ($D = 0$) et à partir de 15 h, un taux de dilution de 0,1 h^{-1} a été appliqué.
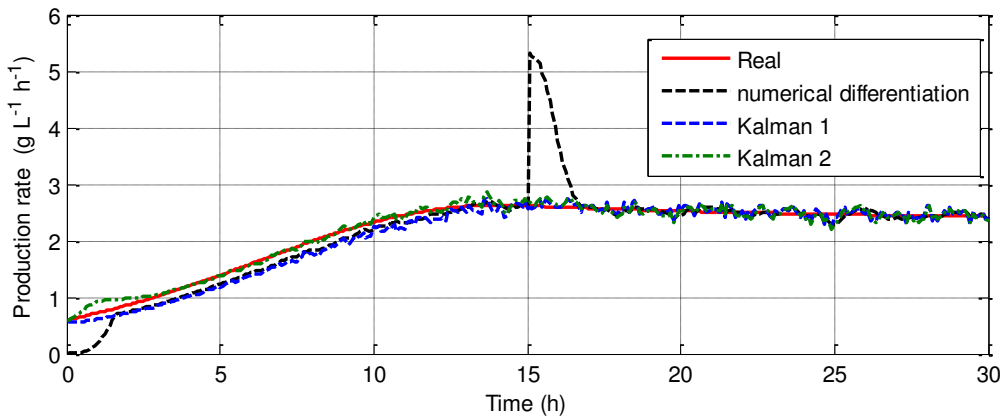
Figure 0.3 Comparaison des estimateurs du taux de production

Avec la méthode de différentiation numérique, une discontinuité est observée lorsque le taux de dilution change. Les deux filtres de Kalman montrent de meilleures performances que la différentiation numérique. Le zoom sur le taux de production (Figure 4.4) montre que le filtre de Kalman 1 estime bien lorsque le taux de dilution n'est pas nul, mais un décalage est présent lorsque $D = 0$. Dans le cas du filtre de Kalman 2, une surestimation de la production du taux de production est présente pendant les 2 premières heures de fermentation. Ensuite, la valeur estimée est très proche de la valeur réelle. Dans l'état d'équilibre, les deux filtres conduisent à des performances assez similaires.
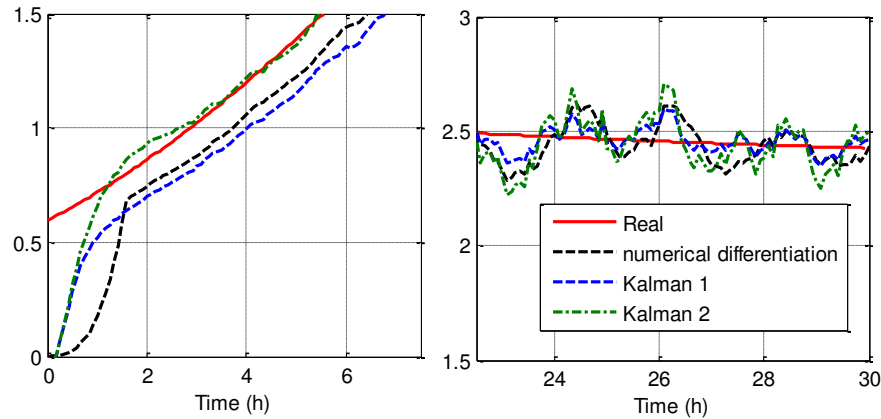
Figure 0.4 Zoom sur l'estimation du taux de production au cours des 5 premières heures (à gauche) et à l'état d'équilibre (à droite).

4.7. Conclusions

La conception de stratégies d'estimation pour reconstruire les variables d'état du bioréacteur SSPHF a été présentée. Le calcul en ligne de la concentration en acide lactique est tout d'abord développé. L'approche considérée exploite la mesure en ligne du débit d'entrée de soude pour obtenir une reconstruction en ligne de la concentration en acide lactique. Pour l'estimation en ligne des autres variables d'état non mesurées, deux observateurs ont été proposés : le filtre de Kalman étendu (EKF) et le filtre de Kalman sans odeur UKF. Ce dernier montre de meilleurs résultats en simulation car il ne nécessite pas une linéarisation du modèle. Néanmoins, les deux estimateurs sont très dépendants de la qualité du modèle. L'estimation du taux de production a ensuite été étudiée. Trois approches différentes ont été examinées : une méthode de différentiation numérique et deux filtres de Kalman, le premier considère un modèle constant pour la dynamique du taux de production et l'autre un modèle linéaire. La méthode de différentiation numérique s'avère peu satisfaisante, tandis que les deux filtres de Kalman ont montré de bonnes performances. Le filtre de Kalman fondé sur un modèle de taux de production constant offre le meilleur compromis entre performance et simplicité de mise en œuvre.

CHAPITRE 5 : Stratégie de commande

La plupart des travaux en termes de stratégies de commande appliquées à la production d'acide lactique n'ont pas été validées expérimentalement en raison du manque de fiabilité des capteurs. Il est alors intéressant d'étudier ces aspects. Ce chapitre se concentre sur le développement de stratégies de commande pour la production d'acide lactique à partir de farine de blé, et leur validation par des essais expérimentaux. En premier lieu, il est important de décrire les différentes composantes du système à contrôler :

• Le bioréacteur SSPHF, représenté par les équations (3.1) est le système que nous voulons contrôler.

• La variable de sortie est la concentration en acide lactique, reconstruite en ligne.

• La variable d'entrée ou commande est le taux de dilution dont la manipulation affecte la variable de sortie.

• L'objectif de commande est de réguler la concentration d'acide lactique à une valeur souhaitée en jouant sur le taux de dilution. L'objectif est d'atteindre les meilleures performances en taux de production d'acide lactique

Dans l'élaboration d'une loi de commande, il est important de déterminer le point de fonctionnement optimal qui conduit à des taux de production d'acide lactique plus élevés.

5.1.   Point optimal de fonctionnement

Le taux de production d'acide lactique expérimental (en g L^{-1} h^{-1}) à l'état d'équilibre, défini comme $\overline{D} \cdot \overline{P}$, a été calculé pour chaque expérience décrite au chapitre 3 pour la gamme des taux de dilution compris entre [0,04 0,24] h^{-1} (Figure 5.1). Le modèle (3.1) prédit que la fonction de la productivité est concave et n'a qu'une seule valeur maximale. L'objectif est de faire fonctionner le procédé autour de cette productivité maximale. En considérant la forme parabolique du taux de production en fonction du taux de dilution, les données expérimentales ont été approchées par une parabole concave afin de faciliter la détermination de la productivité maximale.
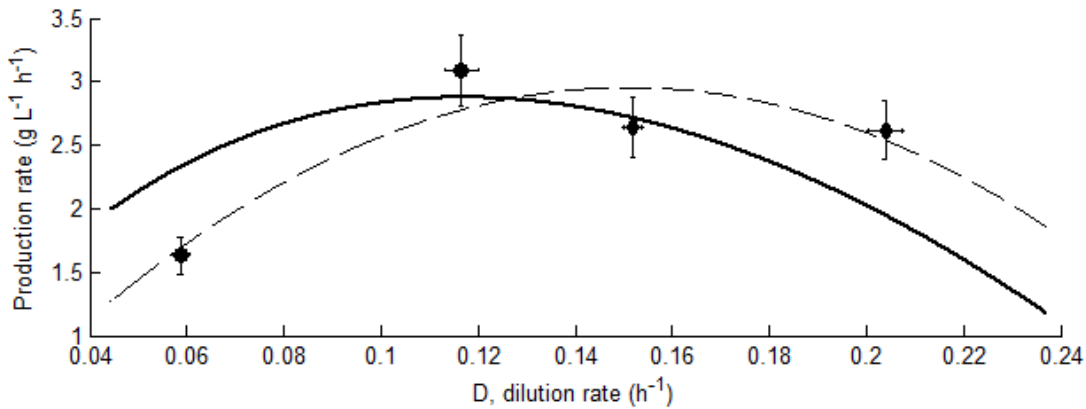
Figure 0.3 Modélisation l'étape SSPHF à l'état stationnaire. Comparaison entre les données experimentales et le modèle pour l'essai 1 (●) et l'essai 2 (◆). (——) Modèle à l'état stationnaire (–––) Approximation polynomiale des données experimentales.

En estimant le maximum de la fonction parabolique utilisée pour approcher les données expérimentales, il est possible de trouver le point optimal de fonctionnement: Les valeurs optimales de taux de dilution et taux de production à l'état stationnaire obtenues en utilisant cette approche sont 0,15 h^{-1} et 2,95 g L^{-1} h^{-1}, respectivement.

A partir du modèle, le point d'équilibre du système (3.1) est déterminé de sorte que la productivité de l'acide lactique soit maximisée. Ce problème est formulé en tant que problème d'optimisation sous contrainte à variable unique comme suit :

$$\overline{D}^{*} = \arg \max \overline{D} \cdot \overline{P}$$
$$\text{s.c. équations (3.1)} \tag{0.1}$$
$$0 \le \overline{D} \le D_{\max}$$

où $D_{\max}$ est le taux de dilution maximal permis par le dispositif expérimental. La solution de ce problème a été déterminée numériquement avec un algorithme de recherche de type section dorée (Fletcher, 1987). La solution obtenue par cette approche est $\overline{D}^* = 0{,}12\,\text{h}^{-1}$ et $\overline{\gamma}^* = 2{,}87\,\text{g L}^{-1}\,\text{h}^{-1}$. En considérant tous ces résultats, l'objectif de commande sera de réguler la concentration d'acide lactique à la valeur optimale, 21 g L^{-1}.

5.2. Développement d'une loi de commande linéarisante par retour d'état

Pour le développement de la commande et sa validation expérimentale, les contraintes liées à la capacité du logiciel du bioréacteur SSPHF ont été prises en compte. Le bioréacteur est équipé d'un logiciel C-BIO (Concept Global Process, La Rochelle, France). Ce logiciel dispose d'une interface de calcul qui peut être utilisée pour la mise en œuvre d'une loi de commande. Néanmoins, en raison de la restriction dans le logiciel (cela fonctionne uniquement avec des algorithmes simples), seule une stratégie de commande simple doit être conçue.

Dans la commande linéarisante par retour d'état, l'idée de base est de simplifier la forme d'un système en choisissant une représentation d'état différente (Hedrick et Girard, 2010). Pour un système affine en la commande représenté par :

$$\dot{x}(t) = f(x) + g\big(x(t)\big)u(t)$$
$$y(t) = h(x(t))$$

(0.3)

où u apparaît linéairement dans l'équation (5.2), une loi de commande linéarisante par retour d'état peut être développée.

Pour le développement de ce type de commande pour le système (4.5), tout d'abord le degré relatif du système doit être déterminé. Le degré relatif, r, de ce système est 1 car il est nécessaire de dériver la sortie, $y = P$, une seule fois par rapport au temps afin d'obtenir l'entrée $u = D$ explicitement. Cela veut dire que seule la dynamique de la concentration du produit, P, peut être linéarisée. La loi de commande obtenue avec cette approche est représentée par :

$$D = -\frac{1}{P}\left[\hat{D} - \frac{Y_{PS}}{Y_{XS}}\mu X\right]$$

(0.4)

Le système linéarisé dans l'équation (5.3) est équivalent à une simple intégrateur $r = 1$. Afin de corriger les erreurs du modèle et de rejeter les perturbations, le signal de commande sera délivré par une boucle extérieure via un régulateur proportionnel :

$$\hat{D} = G(P - P_{ref})$$

(0.5)

où G est le gain du régulateur et P_{ref} est la consigne. Le gain du régulateur est réglé pour fournir une temps de réponse en boucle fermée désiré. La loi de commande obtenue est illustrée figure 5.3.
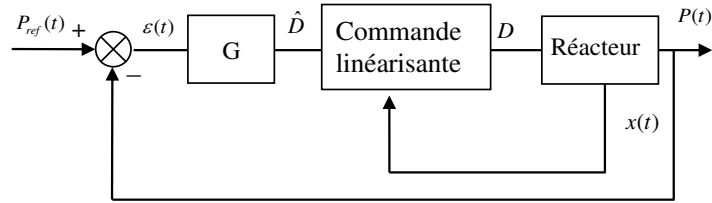
Figure 0.4 Structure de la commande linéarisante par retour d'état

Pour mettre en œuvre la stratégie de commande illustrée figure 5.3, toutes les variables d'état doivent être disponibles en ligne, par leur mesure ou par leur estimation. Les observateurs des variables d'état développés au chapitre 4, EKF et UKF, ont été utilisés pour les estimer.

5.3.   Développement d'une loi de commande adaptative

Afin de réduire la dépendance de la commande de la qualité du modèle, une stratégie de commande adaptative, où seul le taux de production est estimé en ligne, est proposée. En introduisant γ (définie par l'équation (4.8) dans l'équation (5.3), la loi de commande obtenue est :

$$D = -\frac{1}{P}\left[\hat{D} - \hat{\gamma}\right] \qquad (0.6)$$

où $\hat{D}$ est le signal de commande et est encore donné par (5.4), et $\hat{\gamma}$ le taux de production estimé. Pour l'estimation de γ, les filtres de Kalman développés dans le chapitre 4 sont utilisés.

5.4.   Comparaison des stratégies de commande en simulation

Dans cette section, seuls les estimateurs qui ont montré les meilleurs performances pour estimer les états sont retenus pour être implémentés en chaque loi de commande. Ainsi, dans la commande linéarisante par retour d'état, le filtre UKF est utilisé pour estimer les variables d'état. Dans l'approche de commande adaptative, le filtre de Kalman avec le modèle constant pour γ est retenu. Afin de tester la robustesse des lois de commande, une erreur de 30% des paramètres utilisés a été considérée. La figure 5.4 montre la performance des stratégies de commande.

La loi de commande adaptative conduit à un meilleur suivi de la consigne. La valeur de consigne est atteinte avec un bon comportement transitoire et sans erreur statique. Cette commande est robuste par rapport aux erreurs de modèle. La commande linéarisante par retour d'état conduit à un décalage par rapport à la consigne. Compte tenu de la simplicité de la structure de la loi de commande adaptative, et comme elle a montré de meilleures performances, elle a été choisie pour une validation expérimentale dans le bioréacteur.
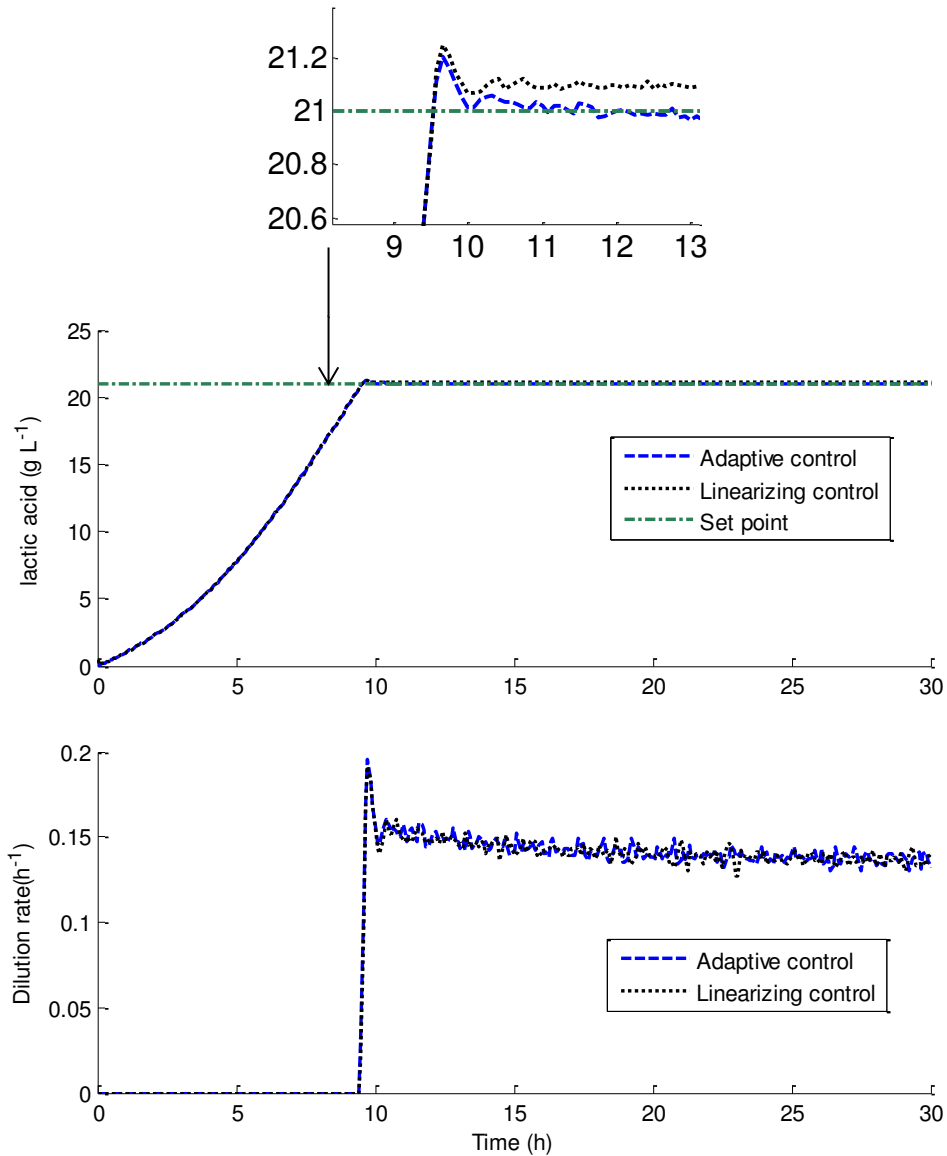
Figure 0.4 Comparaison des performances des lois de commande. Evolution de la concentration d'acide lactique et du taux de dilution avec le temps.

5.5. *Validation expérimentale de la loi de commande*

La validation expérimentale de la stratégie de commande adaptative a été effectuée dans un bioréacteur de 5 L. Les performances et la robustesse de la stratégie de commande sont évaluées dans une expérience SSPHF en mode continu. Après inoculation, la commande est activée afin de réguler la concentration d'acide lactique. Deux consignes de concentration d'acide lactique ont été testées au cours de l'essai. A la fin de l'expérience la robustesse de la loi de commande a été évaluée dans le as d'une perturbation de température.
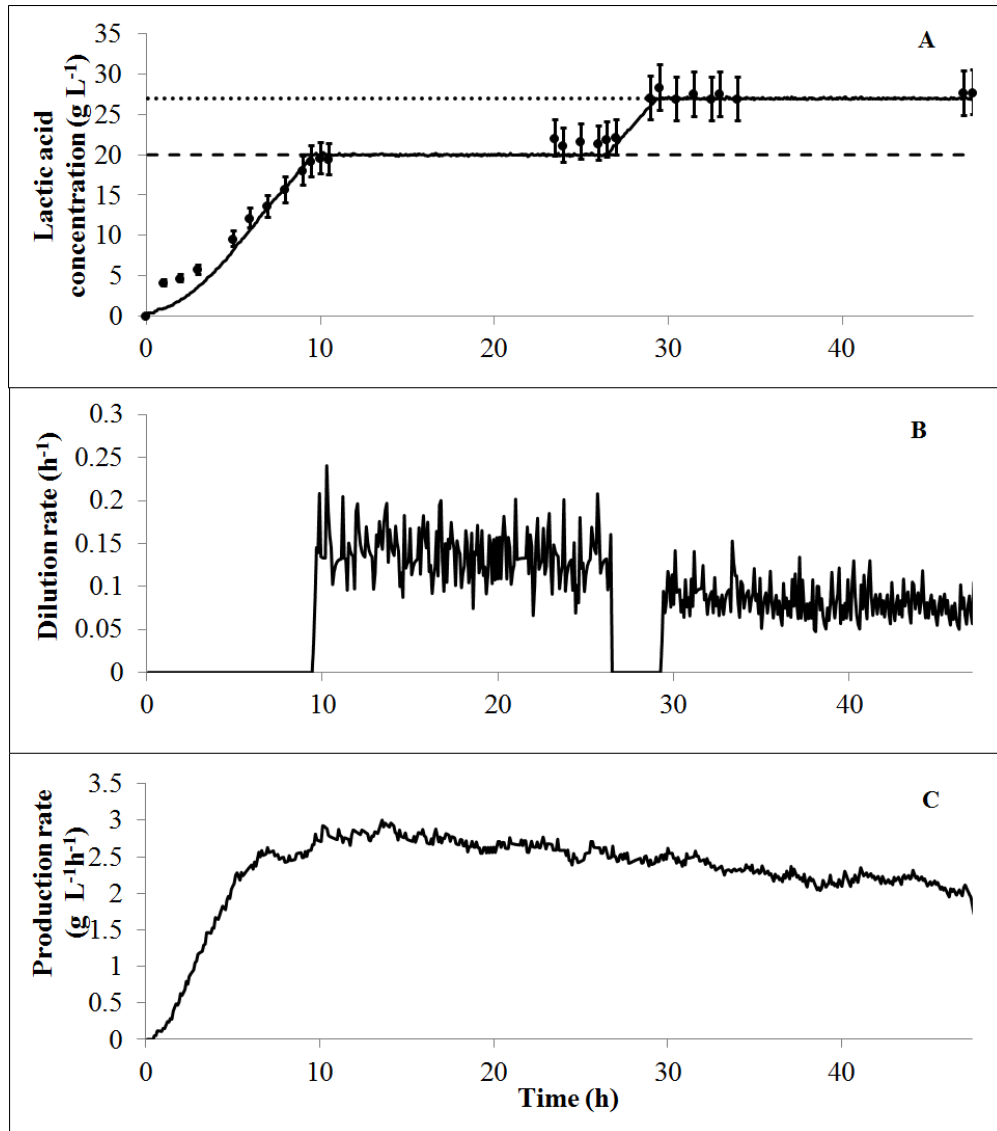
Figure 0.5. Validation expérimentale de la loi de commande. A Evolution de la concentration d'acide lactique en fonction du temps. Pref 1= 20 g L^{-1} (– –), Pref 2= 27 g L^{-1} (·····), concentration d'acide lactique déterminée en ligne (——) concentration d'acide lactique (●). B évolution du taux de dilution. C taux de production estimé.

La première consigne a été fixée à 20 g L^{-1}. Après inoculation, la loi de commande fait fonctionner le bioréacteur en mode batch afin d'augmenter la concentration d'acide lactique. La consigne est atteinte après 10 h, puis le réacteur commence à fonctionner en continu afin de maintenir constante la concentration d'acide lactique égalé à 20 g L^{-1}. Aucun dépassement de la valeur de consigne n'est observé. Les concentrations d'acide lactique mesurées hors ligne sont en accord avec celles calculées en ligne. A 26 h, la valeur de consigne est modifiée de 20 g L^{-1} à 27 g L^{-1}. Les résultats de l'analyse de la robustesse de la loi de commande ont montré également que cette commande est robuste vis-à-vis de perturbations de température.

Conclusions et perspectives

Conclusions

Une démarche a été proposée afin d'optimiser le procédé de production d'acide lactique à partir de farine de blé. Cette démarche comprend : une première étude de l'optimisation des étapes du procédé de production d'acide lactique, la modélisation du bioprocédé, la détermination de la concentration d'acide lactique en temps réel, l'estimation des états et du taux de production et finalement le développement d'une loi de commande adaptative.

Cette démarche a permis d'obtenir des résultats qui contribuent à l'optimisation du procédé tels que : i) La conception d'un procédé innovant de trois étapes : liquéfaction, saccharification et hydrolyse des protéines simultanées (SSPH) et saccharification, hydrolyse des protéines et fermentation simultanées (SSPHF). ii) La validation expérimentale du modèle décrivant les dynamiques des concentrations en biomasse, glucose, maltose et acide lactique. iii) Le développement d'estimateurs des variables d'état et du taux de production à partir de la détermination de P. iv) la validation expérimentale de la loi de commande adaptative permettant la régulation de la concentration d'acide lactique d'une manière précise et robuste vis-à-vis des erreurs de modèle et de perturbations. Ces résultats se traduisent par un gain de productivité d'acide lactique par rapport au procédé batch de Soufflet: 2,6 g L^{-1} h^{-1} en mode continu face à 1.3 g L^{-1} h^{-1}.

Perspectives

Il est possible de proposer de perspectives académiques et d'autres concernant le milieu industriel. Au niveau académique il est possible de proposer : des études d'optimisation du milieu de culture et du procédé (réduire le gaspillage du substrat et le volume mort dans le bioréacteur) ; plus des essais pour perfectionner le modèle mathématique décrivant l'étape de SSPHF et tester le modèle avec d'autres microorganismes et substrats ; le développement d'un modèle décrivant les trois étapes de transformation de l'amidon en acide lactique ; l'amélioration des techniques d'estimation des variables d'état ; une modification du filtre de Kalman sans odeur avec une approche Monte-Carlo ; la conception d'observateurs hybrides afin d'obtenir des meilleures estimations ; la régulation du taux de production en utilisant une stratégie d'optimisation en ligne dans l'algorithme de commande.

Au niveau industriel, différents aspects de la mise en œuvre du procédé doivent être étudiés tels que : L'implémentation de l'étape de SSPHF en continu dans un réacteur industriel ; la modélisation d'un réacteur SSPHF industriel (en incluent la dynamique des fluides) ; l'interconnexion des trois réacteurs pour une exploitation industriel ; le développement d'une stratégie de commande pour le procédé de trois étapes et l'application de la commande adaptative sur un autre procédé de production.

SUMMARY

Summary

INTRODUCTION

Context and motivations

Lactic acid is a traditional chemical product that is widely used in food, pharmaceutical, solvents and leather tanning industries. It has recently received much attention as the monomer for the production of PLA (Poly Lactic Acid) material, a biodegradable polymer. Lactic acid can be produced by biotechnological or chemical processes. The biotechnological production of lactic acid offers several advantages compared to the chemical synthesis: 1) the use of lower cost substrates and 2) the higher product specificity as the former process produces a desired stereoisomer (optically pure L or D lactic acid).(John, et al., 2007).

The lactic acid production by microorganisms has been well developed for over two decades. Lactic acid can be produced by several microorganisms classified into bacteria, yeasts, cyanobacteria and algae. Lactic acid bacteria (LAB) are the most widely used microorganisms. Recently, genetic engineering of various microbial producers has improved the yield and the optical purity of lactic acid.

Although the increasing interest of producing lactic acid by fermentation, this process still uses relatively expensive substrates (glucose, lactose, yeast extract, etc). The use of mixed strains in fermentation allows the utilization of complex raw materials and enhances lactic acid production yield and productivity (or production rate). Indeed, as lactic acid is a relatively cheap product, one of the major challenges in its large-scale fermentative production is the cost of the raw material. Then new biotechnological processes using complex cheap raw materials can make lactic acid production more economical. Currently, different inexpensive raw materials are used as carbon sources for the production of lactic acid: molasses, whey, starch, hydrolysates.

Wheat flour has been reported as suitable for the lactic acid production on a largescale. Indeed, it contains almost all the necessary nutrients for the different strains of lactic acid bacteria. Nevertheless, enzymatic reactions are required to hydrolyze wheat starch for further lactic acid fermentation. The conventional biotechnological production of lactic acid from starch materials requires then three steps: **starch pretreatment** by gelatinisation and liquefaction (starch hydrolysis) which produces mainly maltose; **enzymatic saccharification** (hydrolysis) of maltose to glucose and subsequent conversion of glucose to lactic acid by **fermentation**.

Otherwise, the lactic acid bacteria have nitrogen needs that must be fulfilled. Conventionally nutrients as yeast extract and peptone are added to the medium to provide nitrogen to bacteria.

49

Wheat flour contains proteins (gluten) that can be hydrolyzed into amino acids. Therefore, enzymatic studies are required to optimize this process. In addition, protein hydrolysis from raw materials can be improved by coupling different enzymatic reactions in the same bioreactor, which is very challenging.

On the other hand, control strategies which allow regulating key components in the bioreactor may be used to optimize the overall lactic acid production. To do so, mathematical models have to be developed. They are important tools for optimizing the biotechnological process and to predict bioreactor's performance. Nevertheless, models describing biotechnological processes are complex and exhibit large nonlinearities making the development of control strategies for continuous bioreactors a difficult task.

In this context, the aim of this PhD thesis is to optimize the lactic acid production biotechnological process from wheat flour by maximizing its lactic acid productivity. Three main steps are considered to accomplish this objective. First, the culture broth is optimized in order to improve the lactic acid production rate. Second, a macroscopic modelling of the process is developed. The model takes into account the different kinetics (bacterial growth, lactic acid production and enzymatic maltose hydrolysis) taking place in the bioreactor. Finally, control strategies to maximize the lactic acid productivity are proposed. This work couples two main areas: bioprocess and control.

This PhD is the result of the collaboration between two research teams of CentraleSupélec and one of the Soufflet Group Company who decided to combine their skills and know-how. One of the research team of CentraleSupélec is the bioprocess team from the LGPM Laboratory (Laboratoire de Génie des Procédés et Matériaux). This team couples experimental and modelling approaches to design and improve bioprocesses. The Sydico group (Uncertain Dynamic Systems, Control and Optimization) of the L2S laboratory (Laboratoire des Signaux et Systèmes, Control department of CentraleSupélec) works on bioreactors control and develops software sensors for bioprocesses. The last team is the Soufflet Research and Innovation Center (CRIS, Centre de Recherche et d'Innovation Soufflet) of the Soufflet Group. This company focuses on the collection and production of cereals and is specialized in wheat and barley production. In 2009, the Soufflet Group embarked on four regional biotechnology research programs (the OSIRIS programs), aimed at the development of solutions for different areas; one of these is the improvement of lactic acid production. The purposes of these programs are to increase the value derived from agricultural resources and especially from agro-industrial by-products. The lactic acid production project aims at promoting the incorporation of cereal-based ingredients instead of chemical-based products and optimizing the use of wheat flour in the lactic acid production process.

Work methodology and thesis organization

As previously mentioned, the main objective of the work is the optimization of the lactic acid production process from wheat flour. The different steps considered in this work to reach this objective are described thereafter.

Process optimization

First, the optimization of the culture medium was performed by experimental assays. The bacteria used in the bioprocess is *Lactobacillus Coryniformis* subsp. *torquens* DMS 20004. The choice of the bacteria was done taking into account previous results obtained by the private partner. Enzymatic studies were performed in order to improve the medium composition and optimize the lactic acid production process. The results obtained with this step allowed proposing a new process design which involves **three main steps**. In the first step, starch is converted into maltose and glucose (in a liquefaction step), and then a simultaneous saccharification and proteins hydrolysis (SSPH) step allows hydrolyzing one part of maltose into glucose and wheat proteins into amino acids. The last step consists in the simultaneous saccharification, proteins hydrolysis and fermentation step (SSPHF). In this final phase, the remaining maltose and gluten are hydrolyzed simultaneously while the conversion of glucose into lactic acid (fermentation) takes place.

In order to maximize the whole process productivity, the SSPHF bioreactor should be operated in continuous as this allows obtaining the highest productivity. Two chapters are consecrated to this approach: Chapters 1 and 2.

Chapter 1: *Lactic acid Production*

This first chapter provides an overview of the industrial production of lactic acid. An overview of the different microorganisms able of carrying out lactic acid fermentation as well as their main growth factors is presented. Additionally, the major raw materials commonly used in lactic acid production are described.

Chapter 2 *Design of the studied process*

The second chapter focuses on the description of lactic acid production from wheat flour. First, the state of art of starch transformation processes is presented. Then, the experimental campaigns performed to optimize the culture broth and design an optimal process are described and the results are discussed. Later, the different fermenter operation modes for lactic acid production described in the literature are summarized. This helped the choice of the bioreactor's mode of operation used thereafter in this study. The proposed lactic acid production process is finally detailed.

Modelling

The second step consists in developing a model representing the biological and enzymatic phenomena in the bioreactor. The kinetics (bacteria growth, lactic acid production, enzymatic reactions) of the reactions involved in the SSPHF process are presented. The key variables of the process (those which are considered for the control design, such as biomass, glucose, maltose and lactic acid concentrations) were modeled and identified using a macroscopic approach. Model parameters were finally identified and validated using the results of continuous SSPHF experiments performed in a bioreactor. These subjects are presented in Chapter 3.

Chapter 3 *Modelling*

In chapter 3 the model development of the continuous SSPHF bioreactor for lactic acid production is presented. First, a bibliography survey of the models describing lactic acid fermentation kinetics processes is done. Thereafter, the model of the SSPHF bioreactor is developed. An identification strategy allows finally determining the model parameters that are experimentally validated through continuous SSPHF experiments.

Monitoring and Control

The development of control strategies to maximize the lactic acid productivity in the SSPHF bioreactor represents the third step of the overall methodology. First, estimators required for the control design were developed. The latter was performed considering the measured and control variables, the developed estimators and the software used to control the bioreactor. Two chapters are devoted to this step: Chapter 4 and 5.

Chapter 4 *Monitoring*

In this chapter, the development of estimators necessary for the bioprocess monitoring and control design is considered. First, the construction of a software sensor to determine online the lactic acid concentration is presented. Then, estimators of the biomass, glucose and maltose concentrations are developed from the online available lactic acid concentration. Finally, estimators of the lactic acid production rate (the indicator of the process productivity) are proposed. The performance and robustness of all developed estimators is tested in simulation.

Chapter 5 *Control strategy*

This chapter starts with a short survey of the different control strategies applied to the lactic acid fermentation process. Then the optimal operation point that maximizes the lactic acid production rate is determined through a steady state analysis; the control objective is to operate the bioreactor at this optimal point. Later, two control strategies are proposed: a feedback linearizing controller using biomass, glucose and maltose concentration estimators; and an adaptive controller coupled to an estimator of the lactic acid production rate. These control strategies are

tested and compared with one another by simulations. Finally, the experimental validation of the best control strategy giving the best performance is presented.

Conclusions and Perspectives

This final section presents the results of work performed in this PhD. Similarly, some perspectives are proposed in the continuity of this work, particularly to improve the monitoring and control strategies, as well as to extend the control strategy for the whole process (including the three bioreactors).

Appendixes

This report contains 10 appendixes. Appendix A.1 shows other relevant results of the protease choice study. In the appendix B.1, results of the residence time determination of the bioreactor used for the model and control law validation are presented. Appendix B.2 contains the results of experiments performed to study substrate effects on growth and lactic acid production. Appendix B.3 presents the identification of model parameters for the SSPHF batch process. In appendix C.1 the observability theory is presented. The experimental validation of the lactic acid concentration determination from the sodium hydroxide inlet flow is presented in Appendix C.2. Appendix C.3 shows the influence of the process noise covariance matrix on the state variables estimators. Appendix D.1 presents a detailed description of the control law implementation in the bioreactor software. Results obtained in the study of the effect of the temperature on growth and lactic acid production are summarized in appendix D.2. Finally a glossary of terms used in the biology and biotechnology areas concludes the appendixes section in Appendix D.3.

CHAPTER 1: LACTIC ACID PRODUCTION

1.1. INTRODUCTION

The high energy demand and environmental problems associated with standard industrial processes drive the development of innovative green processes. Thus, processes intensification through the development of new products and processes ensuring reduced material and energy consumption as well as environmental impacts are needed. This is the case of lactic acid which can be produced by biotechnological processes and can participate in a wide variety of chemical reactions. Green solvents (ethyl, propoyl, butyl lactates), oxygenated chemicals (propyleneglycol) and biodegradable thermoplastics (Poly Lactic Acid) are few examples of lactic acid-derived products. This compound has attracted the attention of industrials and researchers due to its widespread applications and its growing market demand especially for Poly Lactic Acid (PLA) production.

In this chapter, a general description of lactic acid production, mainly for PLA production, is presented. The different microbial lactic acid producers are listed. The metabolism of lactic acid bacteria and growth factors that they require are described. Finally the raw materials used for the lactic acid production are discussed.

1.2. LACTIC ACID

Lactic acid is the main component of all acidified milk products giving them their fundamental characteristics. This is a non-toxic natural product. It was first discovered in 1780 by the Swedish chemist, Carl Wilhelm Scheele, who isolated lactic acid from sour milk as impure brown syrup. In 1789 Lavoisier named this milk component "acide lactique", which became the core origin of the current terminology. It was considered as a milk component until 1857, when Pasteur discovered another phenomenon and postulated that lactic acid was a fermentation metabolite generated by microorganisms. Beside Pasteur's discovery, a French scientist, Frémy, produced lactic acid by fermentation (Ghaffar, et al., 2004). Lactic acid production started in 1881 in the USA. Its applications in food, pharmaceutical, cosmetic, and chemical industries are described since the late 19th century (Narayanan, et al., 2004). In 1894 its production, primarily intended for leather and textile industries, reached 5 tons/year. Nowadays 90% of lactic acid production is provided by microbial fermentation and only 10% obtained chemically by the hydrolysis of lactonitrile (Hofvendahl & Hahn-Hligerdal, 1997).

The global lactic acid market was estimated at 714,200 tons in 2013 and is expected to reach 1,960,100 tons by 2020 (Grand-View-Research, 2015). It is dominated by the USA, with 35.8% of the total market in 2010. Europe and Asia-pacific are the second and third largest markets representing 29.9% and 29.2%. Lactic acid is nowadays mainly used in industrial applications (42.4% of the production market in 2010), exceeding food and beverages applications. This was the result of a strong growth of PLA and solvents markets, products for which lactic acid is the main raw material (marketsandmarkets.com, 2015) .

Lactic acid is mainly used in food, cosmetic, pharmaceutical and chemical applications (Figure 1.1). It is classified as GRAS (Generally Recognize As Safe) for use as a food additive by FDA (Food and Drug Administration). It is widely used in almost all segments of the food industry for functions such as flavoring, pH regulation and improvement of the microbial quality. In addition, lactic acid is used commercially in the meat and poultry industries, where it improves flavor and helps controlling food borne pathogens. Because of its slightly acid flavor, it is also used as acidifying agent in salads, sauces, pastries, pickled vegetables and beverages (Wee, et al., 2006). In cosmetic applications, lactic acid is mainly used as lightening agent and pH regulator, but it also has other interesting properties such as antimicrobial activity and skin moisturizing power. Lactic acid is also used in the pharmaceutical industry as an electrolyte in a large number of parenteral / intravenous solutions for reconstruction of body fluids or electrolytes. As for chemical applications, lactic acid is used as descaling agent, pH regulator, neutralizing agent, chiral intermediate, solvent, cleaning agent, complexing agent for metals, antimicrobial and humectant agent. Finally lactic acid is currently considered as the raw material monomer with the biggest potential for chemical conversions, due to its two reactive functional groups, a carboxylic group and a hydroxyl group. Lactic acid can be transformed into potentially useful chemicals such as propylene oxide (by hydrogenation), acetaldehyde (via decarboxylation), acrylic acid (by dehydration), propionic acid (by reduction), 2,3-pentanedione (via condensation) and dilactide (by self-esterification). As previously mentioned, lactic acid has received much attention as a raw material monomer for the production of PLA (Varadarajan & Miller, 1999).

Due to these numerous applications, lactic acid is a very important product and its biotechnological production received more and more interest in recent years as an alternative to chemical processes to overcome environmental concerns: pollution caused by petrochemicals and limitation of fossil carbon.

Food industry
acidulant
antimicrobial agent
flavor enhancer
pH controller
mineral fortification

Cosmetics industry
moisturizer
skin lightening agent
pH controller
anti-acne agent
scale inhibitor

Chemical feedstock
propylene oxide
acetaldehyde
propanoic acid
ethyl lactate
Poly lactic acid

Pharmaceutical Industry
dialysis solution
mineral preparation
encapsulation (Tablets)
biodegradable implants
control drug release

Chemical industry
descaling agent
pH controller
neutralizing
chiral intermediate
complexing agent
cleaning agent

Figure 1.1 Applications of lactic acid in industry (Wee et al., 2006).

1.2.1. Physicochemical properties of lactic acid

Lactic acid is the simplest 2-hydroxy-acid having a chiral center. It exists as two enantiomers. Different names are used in the literature to call them. They can be named by the spatial configuration of the atoms using the D, L nomenclature (named after Latin dexter and laevus, right and left). This system is based on the stereochemistry of glyceraldehyde and defines relative configurations of lactic acid. Another system used to name the lactic acid enantiomers is the R/S system, which does not involve a reference molecule such as glyceraldehyde. In this system each chiral center in a molecule is assigned a prefix (R or S), according to whether its configuration is right or left handed. The lactic acid enantiomers can also be named by the direction in which it rotates the plane of polarized light. If it rotates the light clockwise that enantiomer is labeled (+). Its mirror image is labeled (-). Lactic acid enantiomers are presented on figure 1.2.

The chirality of lactic acid often results in confusion between molecular structures and physical properties (optical rotation). (S) lactic acid (or L-lactic acid) has a slight positive specific optical rotation and is often referred to L (+) lactic acid. However, a concentrated solution of (S) lactic acid in equilibrium with oligomers of lactic acid results in a negative total optical rotation.

Therefore it is recommended to use the structural notation R / S or the former notation L/D and avoid the + /- one (Auras, et al., 2010).

(S) -acid lactic

L - (+) - Lactic acid

(R) -lactic acid
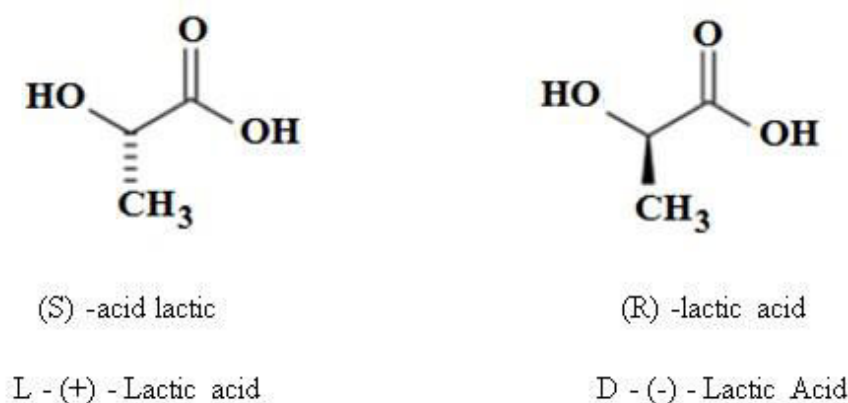
D - (-) - Lactic Acid

Figure 1.2 Enantiomers of lactic acid: (S) - and (R) - 2-hydroxypropionic acid (Auras et al., 2010)

The physical properties of lactic acid are shown in Table 1.1. It can participate either as an organic acid or an organic alcohol in a large number of chemical reactions. It is completely soluble in water and has a low volatility.

Concerning its physiological role in human body, it is necessary to distinguish between the L and D forms. It is known that the L-form is more rapidly metabolized than the D-form and has also superior nutritional qualities(Vick Roy, 1985).

Table 1.1 Physical properties of lactic acid (Vick Roy, 1985)**.**

Property	Value
Molecular weight	90.08 g mol^{-1}
Melting point for D and L enantiomers	D=52.8°C, L=54°C
Boiling point for D and L enantiomers	D=103°C, L= 122°C at 14mmHg
Dissociation constant (K_a at 20°C)	$1.37*10^{-4}$
Heat of Combustion (ΔH_c)	1361 kJ mol^{-1}
Specific heat (Cp at 20°C)	190 mol °C

1.2.2. PLA (Poly Lactic Acid)

Natural polymers, biopolymers and synthetic polymers based on renewable resources are the basis for the ecological plastics portfolio of the XXIst century. These materials are gradually replacing the family of petroleum-based polymers by becoming more and more competitive in terms of performance and cost. Poly Lactic Acid (PLA) is leading in the emerging bioplastics

58

market through its availability and attractive cost. PLA is a thermoplastic material with rigidity and clarity similar to polystyrene (PS) or poly ethylene terephthalate (PET). It is used for rigid or flexible packaging, cutlery, textile fibers, bottles, biomedical materials and other applications (Auras, et al., 2010).

Lactic acid may be polymerized into PLA by polycondensation in series or by polymerization. Its optical purity is a critical factor for the final properties of polylactic acid; the D/L mixture provides an amorphous and optically inactive polymer; in contrast pure L or D isomers provide crystalline and optically active polymers. PLLA (Poly L-Lactic Acid) is limited to medical applications due to its weakness under impact load, which can be attributed to its low melting temperature and low crystallization capacity. In the other hand, a stereocomplex mixture of both polymers PLLA and PDLA (Poly D-Lactic Acid) has new and interesting properties such as a high melting temperature (Zhao, et al., 2010).

1.2.3. Production of PLA from lactic acid

From a chemical point of view, lactic acid may form PLA from the reaction of its hydroxyl and carboxylic acid groups. By removing the water molecules formed during the condensation reaction, it is possible to draw the reaction toward PLA formation (Equation (1.1)):

$$HO-(CH(CH_3))COO)_n-H+HO-(CH(CH_3)COO)_m-H \qquad (1.1)$$
$$\leftrightarrow HO-(CH(CH_3)COO)_{n+m}-H+H_2O$$
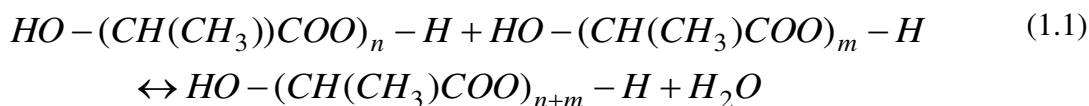
where n and $m \geq 1$. Water removal becomes more and more difficult as the desired molecular weight increases because of the high viscosity of the reaction mixture. To compensate this disadvantage, the application of vacuum can facilitate water removal. However, during polycondensation of lactic acid, other side reactions also occur, such as transesterification, resulting in the formation of cyclic structures of different sizes (Zhang, et al., 2009). These side reactions have a negative influence on the polymer properties.

1.2.4. Lactic acid Production

1.2.4.1.   Chemical synthesis

The commercial process for the chemical synthesis of lactic acid is based on lactonitrile as an intermediate. Hydrogen cyanide is added to acetaldehyde in the presence of a base to produce lactonitrile. This reaction takes place in liquid phase at a high pressure. Lactonitrile is recovered and purified by distillation. It is then hydrolyzed using hydrochloric or sulfuric acid to produce the corresponding ammonium salt and lactic acid. Lactic acid is then esterified with methanol to produce methyl lactate that is purified by distillation (distillation is easier for the ester than for

the organic acid) and re-hydrolyzed by water in an acid catalytic reaction to produce again lactic acid and methanol (Narayanan, et al., 2004). This chemical synthesis produces a racemic mixture of D and L lactic acid.

The process is summarized in equations (1.2) to (1.5):

Addition of Hydrogen Cyanide

$$\underset{acetaldehyde}{CH_3CHO} + \underset{hydrogen\,cyanide}{HCN} \rightarrow \underset{lactonitrle}{CH_3CHOHCN} \tag{1.2}$$

Hydrolysis by H₂SO₄

$$\underset{lactonitrle}{CH_3CHOHCN} + H_2O + \underset{sulphuric\,acid}{H_2SO_4} \rightarrow \underset{lactic\,acid}{CH_3CHOHCOOH} + \underset{ammonium}{\tfrac{1}{2}(NH_4)_2SO_4} \tag{1.3}$$

Esterification

$$\underset{lactic\,acid}{CH_3CHOHCOOH} + \underset{methanol}{CH_3OH} \rightarrow \underset{methyl\,lactate}{CH_3CHOHCOOH_3} + H_2O \tag{1.4}$$

Hydrolysis by H₂O

$$\underset{methyl\,lactate}{CH_3CHOHCOOH_3} + \underset{methanol}{H_2O} \rightarrow \underset{lactic\,acid}{CH_3CHOHCOOH} + \underset{methanol}{CH_3OH} \tag{1.5}$$
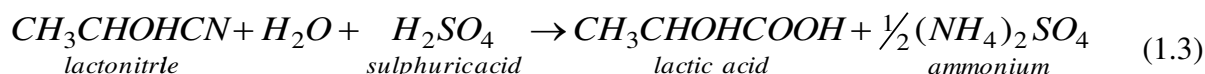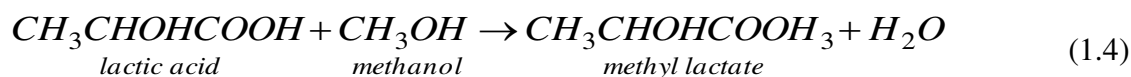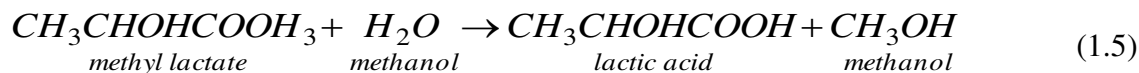
Many other synthesis routes exist: base catalytic degradation of sugars; oxidation of propylene glycol; reaction of acetaldehyde, carbon monoxide and water at high temperature and pressure; hydrolysis of chloropropionic acid and propylene oxidation. However, none of these processes are commercialized due to the growing demand of lactic acid for PLA production needing pure (D or L) isomers of lactic acid.

1.2.4.2.   The fermentation

The major part of lactic acid available in the market is produced by fermentation. During lactic fermentation, a suitable carbohydrate is converted into lactic acid by microorganisms. Only a few of them require oxygen to grow and the conversion of sugars is thus carried out without oxygen. In aerobic conditions, the complete oxidation of sugars to carbon dioxide and water is indeed favored energetically. Moreover, most lactic acid producers are inactivated in the continuous presence of high oxygen concentrations, so lactic acid is mainly formed under anaerobic conditions. In the cell, sugar is first converted to pyruvate by several enzymatic steps; this conversion provides chemical energy in the form of ATP (adenosine triphosphate) and reducing equivalents (NADH, Nicotinamide adenine dinucleotide). To recycle these reducing equivalents,

the cell converts pyruvate to lactic acid (Madigan, et al., 2000). The chemical energy produced is consumed by several mechanisms in the cell, for example cell growth, maintenance, and motility (Auras, et al., 2010). Figure 1.3 shows the reactions previously mentioned.
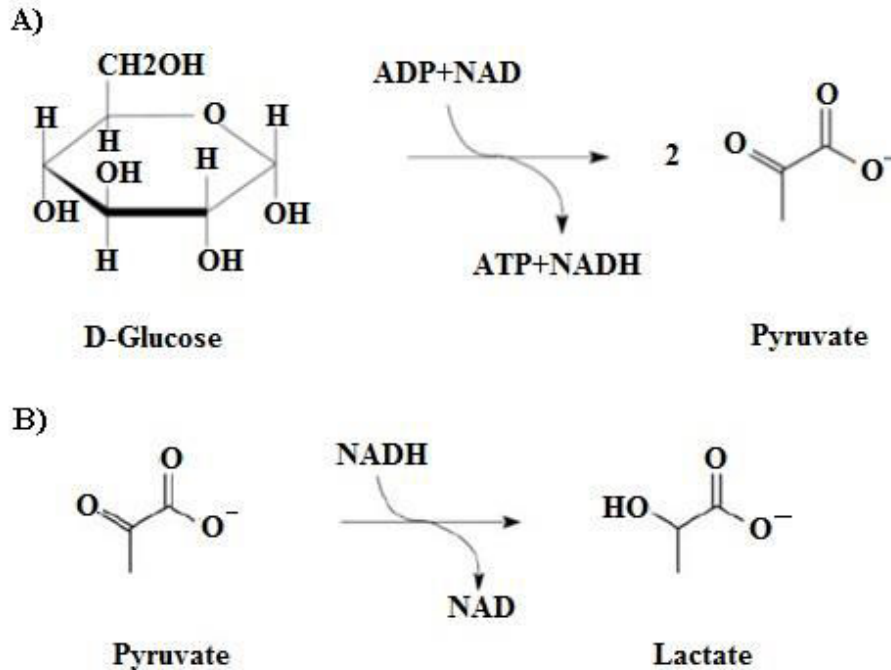
Figure 1.3 A) Conversion of glucose to pyruvate. Generation of chemical energy (ATP), **B)** Lactic acid from pyruvate: The reoxidation of NADH into NAD (the reduced form of NADH) occurs. NAD can be reused in the reaction.

The reactions shown in figure 1.3 occur for homofermentative lactic acid bacteria. These bacteria produce almost exclusively lactic acid as fermentation product. In contrast, heterofermentative lactic acid bacteria produce a mixture of lactic acid, acetate, carbon dioxide and ethanol(Auras, et al., 2010). It will be further discussed in section 1.3.3.

1.2.5. Microorganisms producing lactic acid

Lactic acid maybe produced by different microorganisms such as fungi, cyanobacteria, yeasts, algae and bacteria. In this section, the main characteristics of lactic acid producers are presented as well as their application in the fermentation industrial process.

1.2.5.1. Molds

Several molds as *Rhizopus oryzae*are able to produce lactic acid. *Rhizopus oryzae* uses glucose as a substrate and produces lactate under aerobic conditions. These microorganisms present several advantages: they do not require organic nitrogen sources, are able to use hexoses, pentoses and renewable resources (refined sugar, molasses, starch and crude lignocellulose), especially for genus *Rhizopus*, and are easily separated from the culture medium during the purification of

lactic acid (Miura, et al., 2004). Other advantages compared to bacteria are their amylolytic characteristics, the fungal biomass that can be used in the biosorption process for the purification of the contaminated effluent, and the co-production of fungal chitiosan which can be used as an additive for feed.

However, lactic acid production by molds faces several economic challenges. Their sensitivity to low pH, the need for aeration and agitation and their trend to grow in filaments complicate the process control and increase the production costs. Besides most previous researches with the genus *Rhizopus* exhibited low productivities of lactic acid (Yin, et al., 1997).

1.2.5.2.   Yeasts

Yeasts have won recently significant interest as lactic acid producers because of their ability to tolerate lower pH values, which avoids neutralization of the medium during fermentation. One of their disadvantages is their trend to produce ethanol in the presence of glucose in excess (Ilmén, et al., 2013). Many efforts have been made to develop genetically modified yeasts for lactic acid production, including *Saccharomyces, Zygosacchromyces, Candida, Pichia* and *Kluyveromyces* (Abdel-Rahman, et al., 2013). The development of genetically modified yeasts able to use a variety of sugars other than glucose and xylose is a current field of research. However, more studies on lactic acid production from oligosaccharides and polysaccharides via the integration of specific genes in the genome of yeast strains are required.

1.2.5.3.   Microalgae and cyanobacteria.

Photosynthetic microorganisms which couple CO_2 capture and synthesis of organic products offer an economical alternative approach for lactic acid production as they do not need carbohydrates as feedstock. Several authors have reported lactic acid production by *Scenedesmus D3* (Hirt, et al., 1971) and *Nannochlorum sp. 26A4* (Hirayama & Ueda, 2004). Cyanobacteria have the same advantages, as microalgae: photosynthetic capacity and requirement of simple raw materials (ie, sunlight, CO_2, water, a few mineral elements). Moreover, they can be easily genetically modified (Ducat, et al., 2011).

1.2.5.4.   Bacteria

Bacterial producers of lactic acid can be divided into four main groups: lactic acid bacteria (LAB), *Bacillus* strains, *Escherichia coli* and *Corynebacterium glutamicum*. In general, lactic acid production by bacteria have many limitations including: (i) simultaneous production of D- and L-lactic acid involving enzymatic reactions via two enzymes, L-lactate dehydrogenase (L-LDH) and D-lactate dehydrogenase (D-LDH), respectively; (ii) low lactic acid yield due to the formation of by-products; (iii) nutrient-rich environment (in nitrogen and vitamins) required; (iv) high risk of bacteriophage infection resulting in cell lysis and stopping lactic acid production.

Various studies in metabolic and genetic engineering have been performed to overcome these problems, namely, (i) improving the optical purity in a given isomer of lactic acid by removing the suitable genes; (ii) reducing the by-products by deletion of the genes encoding the suitable enzymes, pyruvate formate lyase (production of formic acid), alcohol dehydrogenase (production of ethanol), acetate kinase (production of acetic acid) and then enhancing lactic acid yield (Zhou, et al., 2003); (iii) developing genetically modified bacterial strains and (iv) improving existing strains by blocking steps in the life cycle of phages (Allison & Klaenhammer, 1998). Additionally, the use of mixed or phage-resistant strains in some cases may be necessary to prevent bacteriophage infection.

1.3.   LACTIC ACID BACTERIA

The first pure culture of lactic acid bacteria (LAB) was obtained by J. Listerin 1873, ten years after the beginning of Pasteur's studies on lactic acid fermentation. The first lactic acid cultures for cheese and curd production were introduced in 1890 (König, et al., 2009). A typical lactic acid bacterium cultured under standard conditions (not limited by glucose, growth nutrients, or oxygen) is a Gram-positive, non-spore forming, catalase negative, aerotolerant, acidtolerant, chemoorganotroph and produces lactic acid. Cells are typically motionless. They need complex growth nutrients such as vitamins and amino acids. The optimal growth conditions depend on the strain; the bacteria can grow for a large pH scale (3.5 to10) and for temperatures between 5and 45 °C (Abdel-Rahman, et al., 2013).

Lactic acid bacteria are generally aerotolerant. However, some species are strict anaerobes. They are unable to carry out oxidative phosphorylation as a result of their inability to synthesize cytochromes and antioxidant enzymes (superoxide dismutases and hydroperoxidases). In the presence of toxic oxygen, some strains use peroxidase enzymes to remove the toxic hydrogen peroxide that is produced by the flavoprotein oxidase system (Djidel, 2007).

Lactic acid bacteria are used for the fermentation of a large variety of products of animal or vegetal origins. The genera *Lactococcus* (milk)*, Lactobacillus* (milk, cereals, meats, vegetables)*, Leuconostoc* (plants,milk)*, Oenococcus* (wine)*, Pediococcus* (meat,vegetables) and *Streptococcus* (milk) are the main members of this group. Due to their recognized beneficial health effects, a significant interest in using lactic acid bacteria to produce "probiotics" for food, drugs or animal feed has increased lately. More recently, lactic acid bacteria are also used in the production of industrial chemicals and biological products including biopolymers, enzymes, ethanol and lactic acid (Hofvendahl & Hahn-Hligerdal, 2000).

1.3.1.   *The genus Lactobacillus*

Lactobacillus species are characterized by cells varying from long and slender, to curved shapes. The motility is not a common feature; a peritrichous flagella is responsible for motility in motile species. No spore formation is reported. These microorganisms belong to the Gram positive

group. They are characterized by an heterogenous composition of their DNA: CG% (Cytosine and Guanine content) varies from 32 to53%. They are considered GRAS (Generally Recognize as Safe) (Vos, et al., 2011).

Lactobacilli have a fermentative metabolism necessarily saccharolytic. At least half of the carbon consumed produces lactate that is not further consumed by the bacteria. Other products can also be synthesized as acetate, ethanol, carbon dioxide, formate and succinate. Although bacteria are aerotolerant, growth on solid surfaces (biofilm based growth) is generally induced by anaerobiosis, reduced oxygen pressure and carbon dioxide concentration of 5-10%. Under strictly aerobic conditions, there is an inhibitory effect on growth.

Their nutritional requirements are complex; they require amino acids, peptides, nucleic acid derivatives, vitamins, salts, fatty acids or fatty acid esters and fermentable carbohydrates. Each species has specific nutritional requirements. The growth temperature ranges between 2 and 50 °C, the optimal interval being 30-40 °C for most strains. The optimal pH is between 5.5 and 6.2 but growth may also occur at lower pH values. The growth rate is generally reduced in neutral or alkaline pH conditions. It is possible to find *lactobacilli* in dairy, grain, meat and fish products, beer, wine, fruit and fruit juices, pickled vegetables, mashed potatoes, sauerkraut, silage, sourdough water, soil and waste waters. These bacteria are an integral part of the normal flora in mouth, intestinal tract and vagina of humans and many animals (Charalampopoulos, et al., 2002).

1.3.2. *Lactobacillus classification*

The *Lactobacillus* microorganisms are classified into three groups according to their sugar metabolism:

Group I: Formerly known Thermobacterium. These bacteria give lactic acid from hexoses by a strictly homofermentative metabolism, they cannot ferment pentoses.

Group II: Formerly known Streptobacterium. This group includes species with an optional homofermentative metabolism. Hexoses are fermented in lactic acid by the Embden-Meyerhof pathway. Otherwise, pentoses can be degraded by the heterofermentative path with production of lactic and acetic acids.

Group III: Previously known as Betabacterium. These species have a strictly heterofermentative metabolism. They ferment gluconate and pentose. They produce lactic acid, acetic acid, carbon dioxide and ethanol.

1.3.3. *The fermentation pathways*

Lactic acid bacteria are also classified as homofermentative or heterofermentative depending on the nature and concentration of the fermentation products of sugars. The metabolic pathways are illustrated in Figure 1.4.
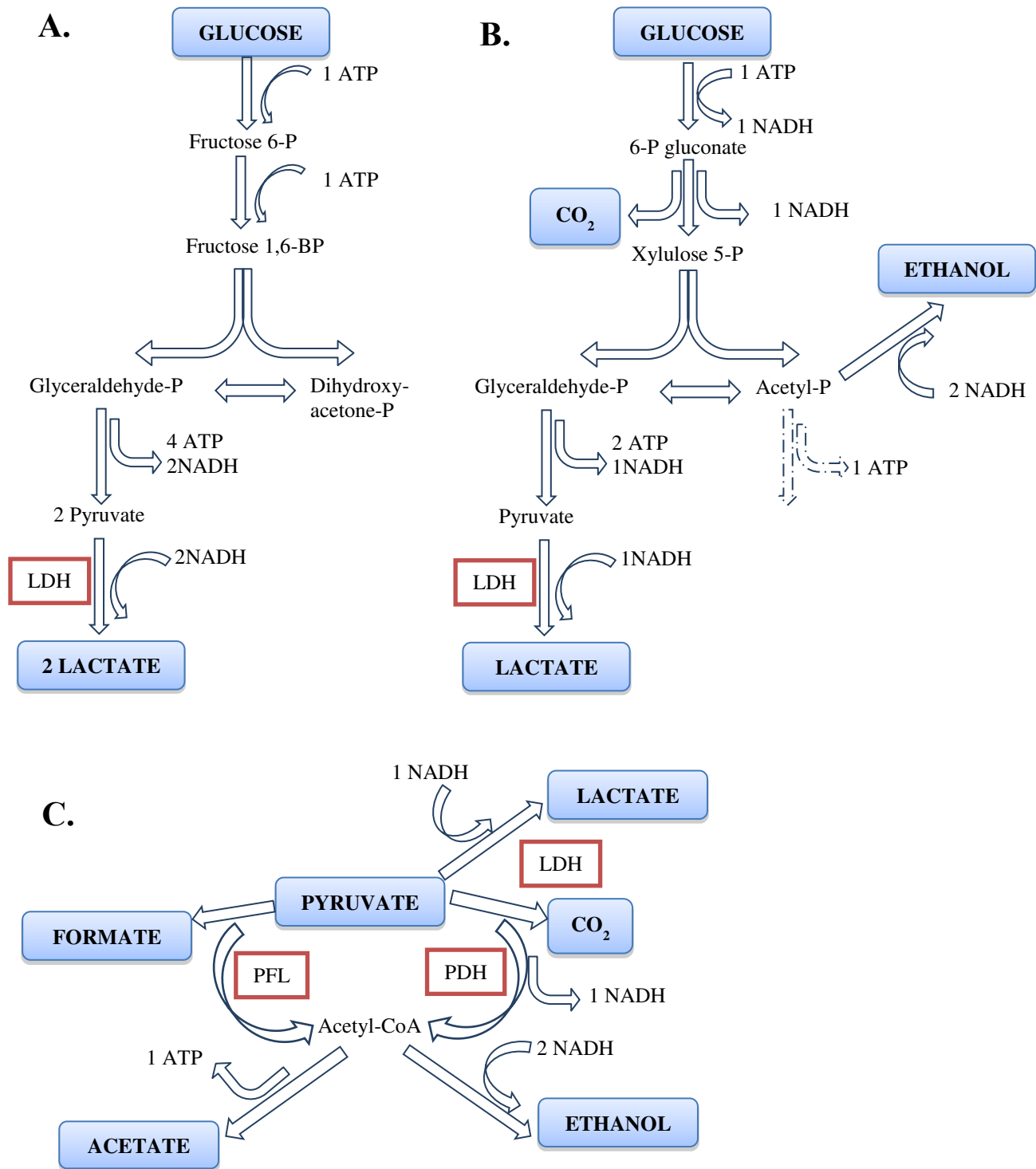
Figure 1.4 Fermentative pathways found in lactic acid bacteria. (A) homofermentative pathway, (B) strict heterofermentative pathway (C) optional heterofermentative pathway. P = phosphate BP biphophate, LDH = lactate dehydrogenase, PFL = pyruvate formate lyase and PDH = pyruvate dehydrogenase(Hofvendahl & Hahn-Hligerdal, 2000).

The homofermentative lactic acid bacteria possess aldolase enzymes and convert almost quantitatively glucose into lactic acid (90-95%). One of the key enzymes of glycolysis is the fructose 1,6 diphosphate aldolase. This enzyme is present in all homofermentative species and can convert fructose biphosphate in triose phosphate (Abdel-Rahman, et al., 2013). Homofermentative bacteria usually contain high concentrations of fructose diphosphate (FDP). This molecule is an activator of enzyme synthesis in the final glycolytic pathway (pyruvate kinase and lactate dehydrogenase).

Besides glucose, the homofermentative bacteria have the ability to ferment other mono or disaccharides that enter into the cell via the phosphotransferase system or in their free form, via a permease system. Nevertheless the main path for phosphorylated derivatives degradation is the Embden-Meyerhof pathway (Djidel, 2007).

1.3.3.2.   The heterofermentative pathway

Heterofermentative bacteria produce ethanol, CO_2, and optionally acetate besides lactate as shown in figure 1.4. Consequently, the maximal yield of lactic acid from glucose reaches 0.5 g of lactic acid per g of glucose (Abdel-Rahman, et al., 2011). They do not contain FDP aldose or triose phosphate isomerase. They are also devoid of a PEP-phosphotransferase system for glucose. Glucose is transferred to the cytoplasm through an active transport, and is phosphorylated by an ATP-dependent glucokinase. The 6P-glucose is converted into 6P-gluconic acid and then decarboxylated in 5P with CO_2 liberation. This pentose-P is metabolized into triose phosphate and acetyl-P. Finally acetyl-P is reduced to ethanol and triose phosphate metabolized to lactic acid by the last reactions of the EMP pathway (Djidel, 2007).

1.4.   FERMENTATION OPERATING CONDITIONS AND PARAMETERS

Lactic acid fermentation has been studied since 1935 using different types of microorganisms and operating conditions such as pH, carbon and nitrogen sources, temperature, inoculum size, initial substrate conditions (Hofvendahl & Hahn-Hligerdal, 1997). The parameters affecting the optimal production of lactic acid will be discussed hereafter.

1.4.1.   Microbial strain

The selection of the production strain is one of the most important points for the process performance. High lactic acid yield and productivities and the ability to use cheap raw materials are among the factors that must be taken into account when choosing the microbial strain. Strain selection is generally done empirically. The strain used in this PhD work is *Lactobacillus corniformis* subsp. *torquens* DSM 20004. This strain was chosen for its high growth and lactic acid production rates as well as its growth operational conditions (low optimal temperature,

pH= 6).Bacteria from this strain belong to the group II of lactobacillus classification; it means that they carry out an optional homofermentative metabolism. The cells are short, often coccoid rods, their size ranges from 0.8 to 3 µm. They produce exclusively D(-) Lactic acid (Wood & Holzapfel, 1995).

1.4.2. Stresses affecting lactic acid bacteria metabolism and lactic acid production

Lactic acid bacteria, like all microorganisms have a metabolism subject to regulations imposed by environmental constraints. It is necessary to distinguish the different types of stress that strongly impact the bacteria behaviour. One inhibition effect is characterized by the limitation in the microbial activity due to accumulation of inhibitory fermentation products (organic acids, bacteriocins) and, in the case of industrial processes, acidification of the culture medium. This stress increases throughout the fermentation, having various effects on metabolism. The accumulation of lactic acid, for example, causes an inhibition effect on growth.

1.4.2.1. Effect of temperature

Temperature is one of the most important environmental factors that affect lactic acid production. Some researchers have studied the temperature effect on lactic acid production. The optimal range of temperature for lactic acid production is between 30°C and 40°C. Lactic acid bacteria can be classified as mesophilic. *Lactobacillus coryniformis* subsp. *Torquens* is a mesophilic bacteria and its optimal temperature for producing lactic acid is comprised between 30 and 38°C.

1.4.2.2. pH effect

Concerning medium acidification, the pH of the culture is not inhibitory because the cells are able to maintain their intracellular pH near to the neutrality. However, this requires expending energy which imposes a metabolic regime where the energy used for growth is limited (Garrigues, et al., 1998). The fermentation pH is then either set at the beginning of the fermentation and then left to decrease with the increasing lactic acid concentration or it can be controlled by different techniques: base addition, elimination of lactic acid by extraction, adsorption or electro dialysis. The pH effects on fermentation have been studied and in all cases pH regulation with base addition resulted in higher or equal lactic acid concentration, yield and productivity than the process without pH control. Removing lactic acid by electro dialysis or extraction, including aqueous two-phase systems, were successful in some studies. The optimal pH for lactic acid production varies between 5.0 and 7.0 (Hofvendahl & Hahn-Hligerdal, 2000).

1.4.2.3. Nutrients and nitrogen sources

An important environmental stress which has a significant role in the development of lactic acid bacteria is related to the nutrients availability in the culture medium. As previously mentioned,

lactic acid bacteria require inorganic salts and vitamins to grow. Nevertheless, the major constraints on the growth metabolism are imposed by the lack of organic nitrogen (peptides, amino acids, bases, etc) and carbon substrates. Concerning the nitrogen source, six amino acids are essential for growth of lactic acid bacteria: glutamic acid, valine, methionine, isoleucine, leucine and histidine (Marshal & Law, 1984). Other amino acids are not essential, but they stimulate bacteria growth. Some investigations have been aimed to study their addition effects (Monnet, et al., 1987). The nutrients can be added in the form of malt, sprout, corn steep liquor, yeast extract and peptone. It has been proved that lactic acid production increases with the concentration of nutrient supplement.

1.4.2.4.   Carbon sources

A number of different carbon sources have been used for lactic acid production by fermentation using lactic acid bacteria. The product with the highest purity is obtained when a pure sugar is fermented, resulting in lower purification costs (Rashid, 2008). However, this is not economically favorable, because pure sugars are expensive raw materials and lactic acid is a cheap product. Instead, waste products from agriculture and forestry are used.

1.5.   RAW MATERIALS

The trend towards environmental sustainability and the development of products from renewable resources have significantly increased the interest on fermentation processes (John, et al., 2007). This is the case of lactic acid produced by fermentation of renewable resources. As mentioned before, lactic acid produced in this study is aimed to be transformed into PLA. As the production of this polymer requires large amounts of lactic acid which is a relatively cheap product, one of the major challenges in its large-scale production is the cost of the raw material. Consequently, the use of cheap raw materials is required when considering the industrial feasibility of the process. The expected characteristics of raw materials are then: low prices, low levels of contaminants, fast production rates and high yields of product, reduced formation of by-products and good ability to be fermented without heavy pretreatments (Wee, et al., 2006). Research studies aiming at improving the efficiency and economics of lactic acid biotechnological production have been conducted. In particular, process development using cheap raw materials at minimal costs have been widely studied. These substrates were biomass-based unconverted starch, lignocellulosic unprocessed biomass, and waste (John, et al., 2007).

1.5.1. Whey

Whey, a by-product of cheese production usually employed for animal feed, is the most commonly used substrate for lactic acid production. It contains proteins, salts, and lactose. Whey can be hydrolyzed to glucose and galactose, deproteinized by ultrafiltration and desalted (Hofvendahl & Hahn-Hligerdal, 1997).

1.5.2. Molasses

Molasses are by-products from sugar manufacturing, generally used as animal feed and for the production of bio-ethanol and yeasts. Moreover, they may be used for the production of lactic acid. Sucrose is the most abundant sugar in their composition, but due to its high concentration, the viscosity of the liquid is important, resulting in an increase of the operating costs. The most common strain to ferment molasses is *Lactobacillus delbrueckii* (Bath & Srivastava, 2008).

1.5.3. Starch

Another common substrate for the production of lactic acid is starch coming from grains or vegetal wastes (wheat, corn, cassava, potato, rye rice, sorghum, barley). It must be hydrolyzed to glucose and maltose to be fermentable by lactic acid bacteria. A detailed description of this raw material will be presented in the next chapter.

1.6. CONCLUSIONS

The interest in lactic acid, closely linked to its application in PLA production, has increased recently. There are two ways to produce lactic acid, the chemical and the biotechnological processes. The latter is preferred as it is more environmentally friendly. Although different microorganisms can be used for lactic acid production, lactic acid bacteria are the most widely used. In this work, we focused on the *lactobacillus* genre. In this chapter, characteristics of these bacteria genre were presented, as well as their different metabolic pathways and the key factors affecting bacterial growth and lactic acid production.

Lactobacillus genre is classified according to its fermentation pathway in three groups: the strictly homofermentative bacteria, the facultative heterofermentative bacteria and the strictly heterofermentative bacteria. These bacteria require complex nutrients to grow and produce lactic acid. It is important to guarantee the nutritional needs for bacteria growth during the fermentation. In order to ensure these needs and to reduce the raw material cost, various cheap substrates have been proposed in the literature. As the nutritional requirements for bacteria are sometimes not ensured by these substrates, nutritional supplement (especially nitrogen sources) has been proposed. In this work, we focus on the use of wheat flour as the sole substrate (source of carbon and nitrogen) for lactic acid production. The development of the lactic acid production process using this substrate is described in the next chapter.

CHAPTER 2: PRESENTATION OF THE STUDIED PROCESS

As mentioned before, this project is aimed at improving the performance of the lactic acid production process. One of the solutions proposed by CRIS (Centre de Recherche et d'Innovation Soufflet) and also described in the literature to reduce the production cost is to use wheat flour as raw material. Enzymatically hydrolyzed wheat flour can indeed provide almost all the necessary nutrients (carbon and nitrogen substrates) for the different strains of lactic acid bacteria, so the production of lactic acid can be performed without any supplementation or with a minimal one (Hetényi, et al., 2010).

Worldwide wheat production is estimated at 717 million tons by the USDA in 2014/2015 (United States Department of Agriculture) while the worldwide consumption is expected to rise up until 713 million tons. This production represents 30% of the whole cereal worldwide production. France is the first producer of cereals in the European Union and ranks sixth in the worldwide producers behind the U.S.A., China, India, Brazil and Russia. France has a total cereal production of 64 million tons; wheat by itself represents 37 million tons. France is the fifth producer of wheat in the world behind China, India, Russia and the U.S.A. (Lyddon, 2013).

As a major compound of wheat, starch is a complex carbohydrate composed by chains of D-glucose molecules. These molecules are linked to one another by *O*-glycosidic bonds which are stable at high pH but hydrolyzed at low pH. An aldehyde group is present at the end of the polymeric chain. Starch exists in the form of granules and contains two glucose polymers, amylose and amylopectin. Cereals generally contain 70% amylopectin and 30% amylose. Amylose is an essential linear molecule in which the glucose units are linked by α 1,4 linkages. This polymer has a crystalline structure with a double helix, containing six molecules of n-glucose per turn. Unlike amylose, amylopectin has a highly branched structure with 4% to 6% α-1,6 bonds on the connection points. The average length of the branch is 20 to 25 glucose units. The amylopectin molecule may have a molecular weight greater than 10^8 g mol^{-1} which makes it the largest molecule in nature (Nigam & Singh, 1995). In the raw state, the granules of starch have round or irregular shapes. Their size ranges from 1 to 100 µm long. While amylopectin is soluble in water, amylose and starch granules themselves are insoluble in cold water.

In solution, with increasing temperature, the structure of the granules changes: they include water, swell and burst forming a starch gel. This gelatinization occurs at different temperatures according to the size of the granules. The smaller the granules, the higher the gelatinization temperature is. During this process, amylose leaches out of the granule and causes an increase in

the viscosity of the slurry. Finally, the granules break apart resulting in a complete viscous colloidal dispersion (Van Maarel et al., 2002).

In this chapter the improvement of the lactic acid production process using wheat flour as raw material is considered. First, the existing lactic acid production process using starch materials are described. Later, the process design is performed starting from the one proposed by Soufflet. Finally, the description of the entire process is presented.

2.1.   EXISTING PROCESSES

2.1.1.   Conventional process

A conventional process for lactic acid production from starch is composed of three steps: a **liquefaction** step in which starch is transformed into glucose and oligosaccharides, a **saccharification** step in which oligosaccharides are transformed into glucose, and a **fermentation** step for the production of lactic acid by bacteria.

2.1.1.1.   Liquefaction step

Starch is transformed into oligosaccharides and glucose by enzymatic hydrolysis. As enzymes are not able to act directly on the solid grains of starch, a relatively high temperature is needed to form gelled starch on which enzymes have a significant effect.

The specific role of each enzyme involved in the hydrolysis of starch is presented in figure 2.1 (Brandam, et al., 2003) . There are basically four groups of enzymes that convert starch into oligosaccharides (Van Maarel et al., 2002): the endoamylases, the exoamylases, the branching enzymes and the transferases.

The endoamylases are able of breaking the 1,4 glycosidic linkages present in any inner part (endo) of the amylose or amylopectin chains. Most enzymes that transform starch belong to a family characterized by the homology of the amino acid sequence: the α-amylase family or family 13 glycosyl hydrolases according to the classification of (Henrissat, 1991). Enzymes of this family act on α-glycosidic bonds and hydrolyze this bond to produce α-anomeric mono or oligosaccharides and form α,1-4 or 1-6 glycosidic linkages. The enzyme α-amylase is present in a wide variety of microorganisms belonging to the Archaea and bacteria domains. Final products obtained with this enzyme are oligosaccharides of variable length with α configuration and with α- dextrins that constitute the branched oligosaccharides (Isomaltose, Branched DP3, Branched DP4, etc).
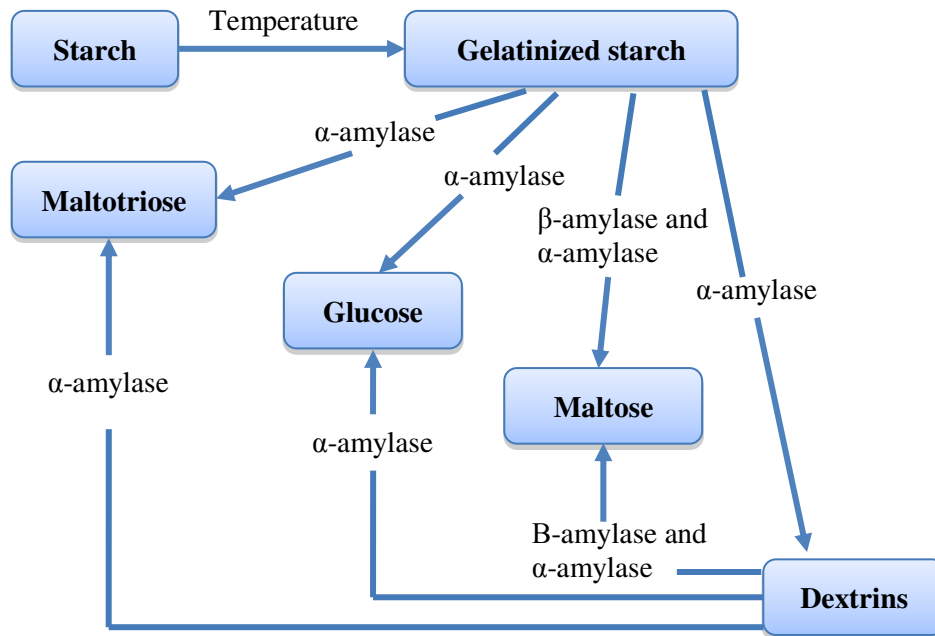
Figure 2.1 Roleofdifferent enzymes in the hydrolysis of starch (Brandam, et al., 2003).

2.1.1.2.   Saccharification step

In the saccharification step, oligosaccharides are transformed into glucose using a specific enzyme, amyloglucosidase. This enzyme belongs to the family of α-amylase. As exoamylase, it is able to hydrolyze exogenously the α (1-4), α (1-6) and α (1-3) glycosidic linkages at the non-reducing end of the oligosaccharide chains to produce glucose. The reaction depends strongly on the chain length and the operating conditions such as pH and temperature.

2.1.1.3.   Fermentation

This step was described in detail in chapter 1. However, several important specific aspects must be reminded here. Lactic acid bacteria require a high level of nutrient supplementation including nitrogen source, vitamins and microelements (Hetényi, et al., 2010). To meet these needs, yeast extract is generally added to the medium as the best nutrient source, but its cost may compromise the process economy. Other alternative nitrogen sources are corn steep liquor, yeast autolysate, peptone and tryptone, but they are expensive too. As an economical alternative, the insoluble protein fraction of wheat (gluten) can also be utilized as nitrogen source for fermentation after a proteolytic digestion step. The wheat proteins hydrolysis will be considered in section 2.2.2 to improve the fermentation step.

2.1.2. Other processes

Figure 2.2, summarizes some of the different processes used for the bioproduction of lactic acid. These processes are further described in the following sections.
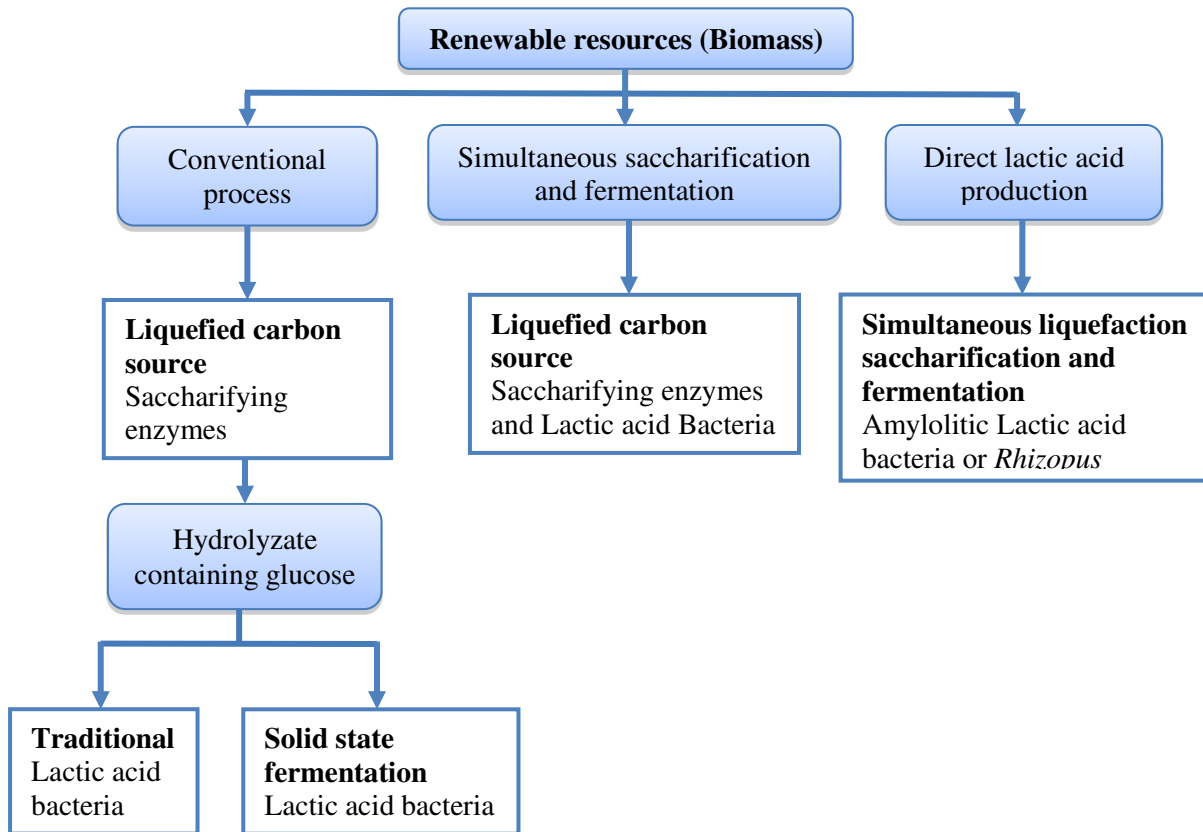
Figure 2.2 Different fermentation processes of agro-industrial waste for the production of lactic acid (John, et al., 2007).

2.1.2.1. Simultaneous saccharification and fermentation

The bioconversion of starch materials into lactic acid can be carried out more efficiently by coupling enzymatic hydrolysis and microbial fermentation of glucose in a single step, known as "Simultaneous Saccharification and Fermentation " (SSF). Figure 2.3 illustrates the comparison of this method with the conventional one.

The SSF method offers several advantages over the conventional process such as the use of a single reactor, short processing time and increased lactic acid productivity. In most cases, the main advantage of SSF is the absence of a separated quantitative saccharification step before fermentation. Enzymatic hydrolysis, bacterial growth and production of lactic acid occur

simultaneously. The potential inhibition of bacteria growth caused by glucose accumulation in the reactor may be avoided when using the SSF process.

Numerous factors such as pH, temperature, substrate and product concentrations can affect the mechanisms of SSF. Nevertheless, the differences in optimal conditions for bacterial culture, enzymatic hydrolysis and lactic acid production in terms of pH and temperature lead to operation difficulties representing the main disadvantage of this fermentation technique. In many cases, a low pH (less than 5), and a high temperature (above 40 ° C), may be favorable for enzymatic hydrolysis, while these conditions are generally not advantageous for growth and lactic acid production (Jin, et al., 1999).
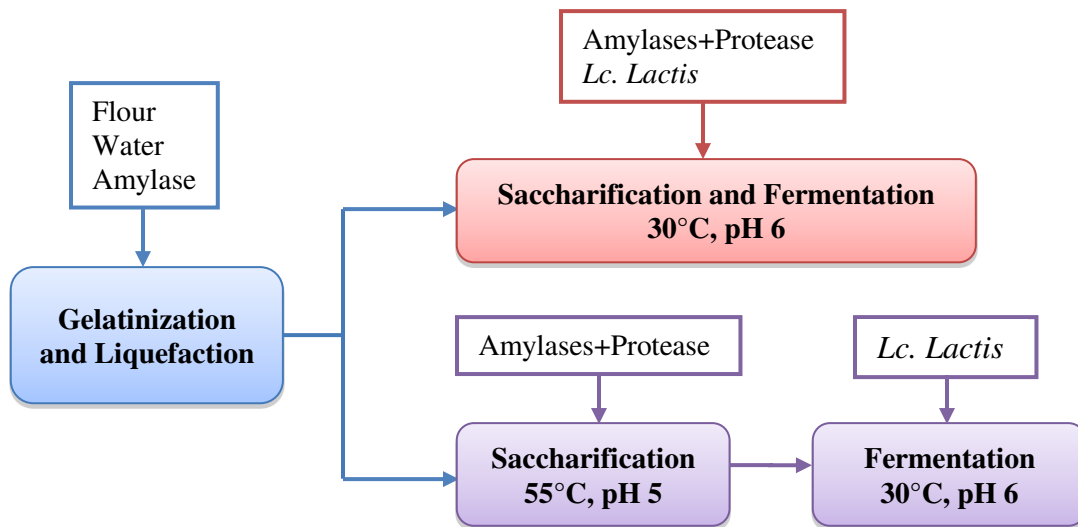
Figure 2.3 Lactic acid production processes fromstarch saccharification with *Lactboacillus Lactis.*(Hofvendahl & Hahn-Hligerdal, 2000).

2.1.2.2.   Direct lactic acid production

Direct lactic acid production with amylolytic lactic acid bacteria or fungi such as *Rhizopus oryzae* is possible but only a minority of lactic acid bacteria has the ability to produce enzymes that hydrolyze the starch. The latest research works aim at isolating amylolytic lactic acid bacteria for direct use on complex substrates such as starch wastes (Narita, et al., 2004) ; (Shibata, et al., 2007).

2.2.   DESIGN OF THE PROPOSED PROCESS

At the beginning of this work, the CRIS laboratory had determined the steps and the process conditions required for the transformation of starch into lactic acid by performing experimental campaigns.

This process consists of three main steps (in batch mode):

- a first liquefaction step, to transform wheat starch mainly into maltose and glucose (besides other oligosaccharides) at 85°C.
- a saccharification step in which maltose is partially hydrolyzed into glucose; this step takes place at a temperature of 55°C and pH 4.7.
- the final step, in which the remaining maltose is transformed into glucose simultaneously with the glucose fermentation (Simultaneous saccharification and fermentation or SSF) at a temperature of 30°C and a pH of 5.7.

This initial state was the basis of the process design studied in this PhD work. The following steps were adopted as a result of the optimization procedure described latter in this chapter (Figure 2.4):

- the first step, liquefaction, was not modified;
- the simultaneous saccharification and proteins hydrolysis (SSPH) represents the second step, here, the nitrogen source is supplied differently from the process proposed by Soufflet (saccharification step). This step was studied and optimized.
- the third step is a simultaneous saccharification, proteins hydrolysis and fermentation step (SSPHF). At this stage, the remaining maltose and wheat proteins coming from the SSPH step are hydrolyzed simultaneously with the fermentation. The hydrolysis products, glucose and amino acids, are consumed by lactic acid bacteria for growth and lactic acid production.

In the following the process design is described. First, experiments performed to optimize the culture broth (to guarantee nitrogen needs for bacteria growth) are described. Then, the development of a simultaneous saccharification and proteins hydrolysis (SSPH) step which may improve lactic acid productivity is presented. Later, the choice of the reactor's operation mode is done keeping in mind the main objective of maximizing lactic acid productivity. Finally the whole process for the transformation of starch into lactic acid is summarized.

All the experiments presented in this section were carried out in batch mode. First, because the process proposed by Soufflet is in batch and secondly, because we want to test many conditions, thus, experiments in batch mode are easier to be carried out. For this reason, in the following, an introduction of important aspects in batch biotechnological processes is presented in order to introduce the reader to the batch fermentation.
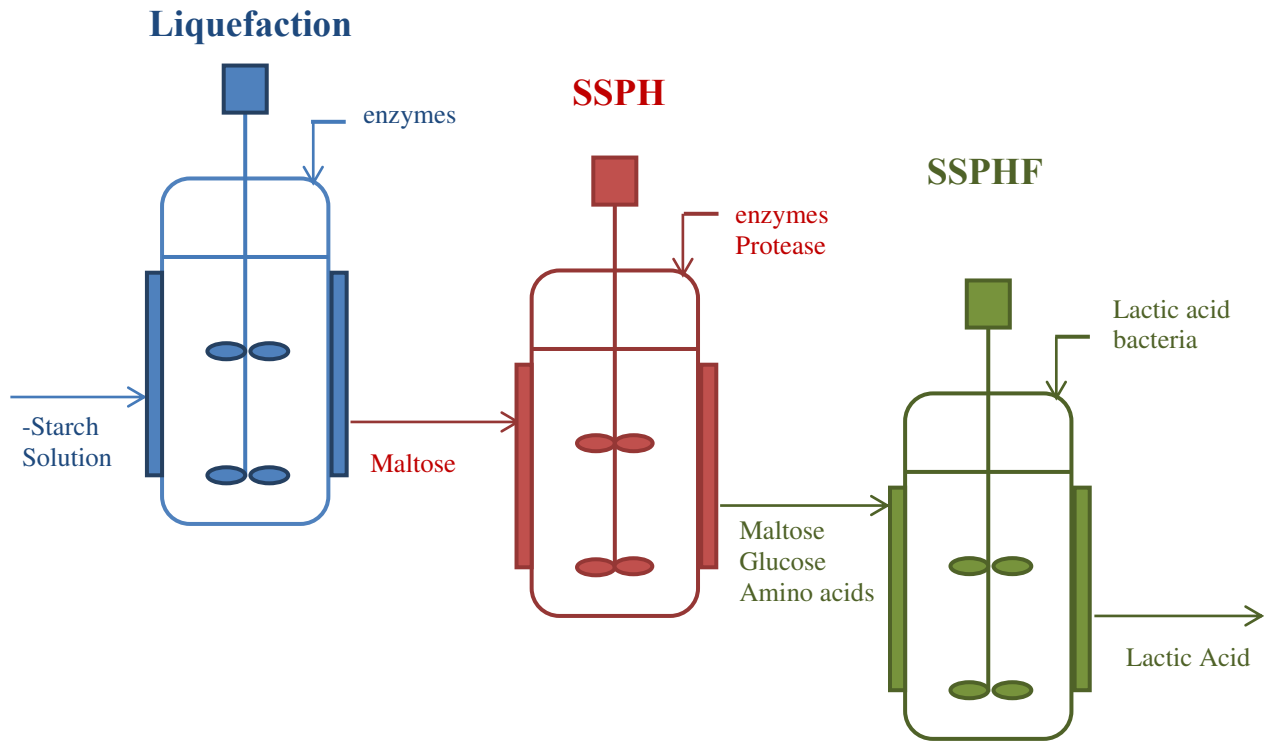
Figure 2.4 Steps involved in the wheat flour transformation in lactic acid for the proposed process.

2.2.1. Batch fermentation

2.2.1.1.   Evolution of the biomass profile in batch mode

Growth is the most essential response of microorganisms to their physiochemical environment. It results of the replication and change in cell size. Microorganisms can grow under different physical and chemical conditions. They require substrates to synthesize new cell material, extracellular products and for energy. For these reasons, growth, substrate consumption, maintenance and product formation are all closely related (Sinclair & Kristiansen, 1987). When a liquid nutrient medium is inoculated using a seed culture, the microorganisms selectively take up the dissolved nutrients from the medium and convert them into cells. In a batch process, the cell concentration changes with time following the phases described hereafter:

a) *Lag phase*: It is the period during which the cells adapt themselves to a new environment, it occurs immediately after inoculation. During this phase, cells synthetize new enzymes and stop the production of others. No growth is observed. In some cases, this stage may be explained by the stress induced by the passage of cells from a concentrated medium to

a diluted one. The duration of this phase depends on the age and size of the inoculum and the nutrient medium. Generally, the lag period increases with the age of the inoculum.

b) *Exponential phase*: Once the cells adjust themselves to their new environment, they start to multiply at full capacity by leveraging the nutrients in the medium. As a result, the cell mass and cell number density increase exponentially with time, cell division follows an exponential function. The growth rate here is maximal and constant over time.

c) *Deceleration growth phase*: In this phase growth decelerates due to either depletion of one or more essential nutrients or to the accumulation of toxic growth by-products.

d) *Stationary growth phase*: This phase starts at the end of the deceleration phase. Here, the growth rate equals the death rate. In this stage, cells are still metabolically active and produce secondary metabolites.

e) *Death phase:* At the end of the stationary phase, because of either nutrient depletion or toxic product accumulation, the death phase begins.

Figure 2.5 summarizes the different phases described previously.
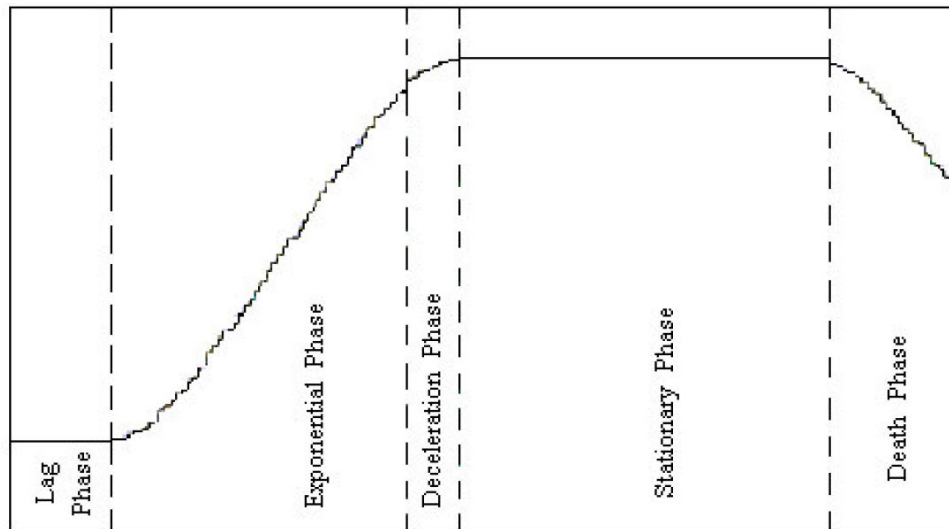
Figure 2.5 Microbial growth curve**.**

2.2.1.2.   Product formation kinetics

In many of the large scale industrial fermentation processes extracellular or intracellular product formation is the main objective, and biomass is only considered as an inevitable waste product. For such types of fermentation processes, the product formation kinetics are as much important as the growth kinetics.

Microbial metabolites produced in a batch system can be classified in three major categories:

(i)   Growth-associated products: produced simultaneously with microbial growth. The specific rate of product formation is proportional to the specific growth rate.

(ii)   Nongrowth-associated product: its formation takes place during the stationary phase. Many secondary metabolites, such as antibiotics (for example, penicillin), are nongrowth-associated products.

(iii) Mixed-growth associated product: its formation takes place during the exponential and the stationary growth phases. Lactic acid fermentation is part of this group.

The relationship between the product formation and microbial growth becomes then a determining factor in the process optimization. Microbial product formation kinetics depends on many factors as pH, temperature, dissolved oxygen, the availability of substrates and the presence of inducers or repressors. Besides that, the metabolic state of the cell, the energy charge, the redox status and the presence of competing metabolic pathways can exert a considerable influence and may affect the product formation rate. The specific growth rate of an organism reflects the metabolic state of the cell. For this reason, the product formation rate is in most of the cases correlated to the specific growth rate.

2.2.2.   *Proteins hydrolysis study-Protease choice*

Considering the process proposed by Soufflet, the first experiments presented here were aimed at optimizing the culture broth in order to increase the lactic acid productivity. Experiments in this section are performed during the simultaneous saccharification and fermentation (SSF) step (the third step in the Soufflet's process).

To meet the lactic acid bacteria nutritional needs, the insoluble protein fraction of wheat (gluten) is used as nitrogen source for fermentation in this work. As a matter of fact, the composition of proteins in wheat is almost 13%. Wheat proteins are classified according to their solubility in various solvents giving the following protein fractions: albumins, globulins, gliadins and glutenins. The latter (gluten) represents 80% of proteins fraction in wheat. The proteolysis (or hydrolysis) of gluten can be carried out either separately or simultaneously with starch hydrolysis (Rojan, et al., 2006).

In order to guarantee a sufficient nitrogen supply (amino acids) during the simultaneous saccharification and fermentation (SSF) process different proteases (enzymes performing the proteins hydrolysis) are tested. The aim of these experiments is to find the protease leading to the highest lactic acid productivity .Considering that proteins hydrolysis is performed simultaneously with the SSF in this work, this step was renamed as: simultaneous saccharification, proteins hydrolysis and fermentation (SSPHF). Different protease enzymes at different concentrations are then tested in order to choose the most appropriate one. The materials and methods of these experiments are presented in the next section.

2.2.2.1. *Materials and methods of protease choice experiments*

2.2.2.1.1. *Experiments description*

Four proteases for proteins hydrolysis were tested: Prolyve PAC (P1), Prolyve BS (P2), Prolyve 4000 (P3) and Prolyve NP (P4). The goal was to determine optimal conditions for the enzymatic reaction in order to obtain the highest lactic acid productivity. The experiments were performed in 200 mL flasks with 100 mL of wheat flour solution. A previous presaccharification of 1.5 h (as proposed by the Soufflet process) was performed followed by a simultaneous saccharification proteins hydrolysis fermentation (SSPHF). Table 2.1shows the tested proteases as well as their optimal operational conditions (Data given by the enzymes supplier, Lyven). All proteases were studied at two different concentrations: 200 and 1400 mg of protease per kg of wheat, both values were chosen taking into account supplier recommendations concerning their optimal concentrations.

Table 2.1 Proteases tested for lactic acid process optimization.

Protease	Optimal pH	stable at pH	Stable until (°C)	Optimal Temperature (°C)
Prolyve PAC	2.5-3.0	2.3-6.0	60	55
Prolyve BS	6.5-7.5	5.5-8.5	80	50
Prolyve 4000	9.0-10.5	6.0-11.0	90	55
Prolyve NP	6.8-7.0	6.0-10.0	60	50

2.2.2.1.2. *Inoculum preparation*

Lactobacillus coryniformis subsp. *torquens* DSM 20004 stored at -80°C, was grown in a medium containing 51 g glucose L^{-1}, 4 g yeast extract L^{-1}, 8 g meat extract L^{-1}, 10 g peptone L^{-1}, 5 g de sodium acetate L^{-1}, 2 g triammonium citrate L^{-1}, 2 g K_2HPO_4 L^{-1}, 0.2 g $MgSO_4$ L^{-1}, 0.05 g $MnSO_4$ L^{-1} and 1 g polysorbate 80 L^{-1}. The strain was cultured in an incubator shaker MAXQ 4000 (Thermo Scientific) in a 100 mL flask at 30°C. This culture was used to inoculate all the flasks of the assays.

2.2.2.1.3. *Preparation of starch solution: Liquefaction*

The liquefaction step was carried out at Soufflet in a 5 L bioreactor equipped with Baie inox controllers (Global Process Concept, La Rochelle, France). For the preparation of the wheat solution, the whole wheat flour was suspended in water at a concentration of 260 g L^{-1}, heated to 50°C and agitated at 200 rpm. The pH was regulated by a PID controller at 5.5, with addition of sodium hydroxide and sulfuric acid. Two enzymes were added: Lyvanol devisco plus and Lyquozyme SDCS (Lyven, Colombelles, France), each at a concentration of 94µLL^{-1}. Afterwards the mixture was heated to 85 °C and maintained at this temperature for about 30 min for

liquefaction. Temperature was then decreased to 25 °C to prepare the resulting mixture for transportation. The final liquefied wheat solution was frozen and transported to the LGPM (Laboratoire de Génie des procédés et matériaux) laboratory of CentraleSupélec.

2.2.2.1.4. Preparation of flasks

One liter of the liquefied starch solution was thawed at 60°C in a water bath during 30 minutes. Then, it was diluted with distilled water to get a final wheat concentration of 130 g L^{-1}. $MnSO_4$ was added at 0.05 g L^{-1} to the wheat solution and the pH was adjusted to 5.7 with NaOH (7N) and H_2SO_4 (2.5 N) addition. This solution was distributed in 15 flasks of 200 mL. The wheat solution volume in each flask was 100 mL. Calcium carbonate was added in each flask at a concentration of 30 g L^{-1} in order to buffer the wheat solution and to reduce the pH decrease with lactic acid production. Flasks were then sterilized for 20 min at 120°C.

2.2.2.1.5. Pre-saccharification step

Before the SSPHF, the amyloglucosidase enzyme (AMG) (Lyvanol GA, Lyven, Colombelles, France), was added to each flask (230 µL L^{-1}) in order to start sugars hydrolysis. The enzymatic saccharification was carried out in an incubator shaker MAXQ 4000 (Thermo Scientific) at 50°C and 150 rpm during 1.5 h.

2.2.2.1.6. Simultaneous saccharification proteins hydrolysis and fermentation (SSPHF)

Once the pre-saccharification step finished, the temperature in the incubator was decreased to 30°C. Each protease was added at two different concentrations: 200 and 1400 mg of enzyme Kg^{-1} of wheat. In total, 8 different conditions were tested: 4 different proteases, each one at 2 concentrations. All experiments were repeated twice (two replicates) in exception of the condition corresponding to prolyve NP at 1400 g Kg^{-1}. All the protease enzymes (Lyven, Colombelles, France) were diluted tenfold in a sodium acetate buffer solution (0.1 M, pH 5.7) and added at the same time with the inoculum to each flask. The initial biomass concentration equaled to 10^9 cells ml^{-1}. This SSPHF step was performed during 48 h at 30°C and 150 rpm.

2.2.2.1.7. Analyses

In order to follow the evolution of cell, substrates (maltose and glucose) and lactic acid concentrations with time, samples were withdrawn from each flask at various time intervals. Cell counting was performed in a Thoma cell counting chamber. Before performing the chemical analysis, samples were first heated at 95°C for 15 minutes in order to inactivate the enzymes and filtered through 0.2 µm cellulose filters.

Glucose, maltose and lactate concentrations were measured on a Waters Alliance HPLC system (Water Corporation, Milford, MA) using a Shodex Sugar column (Shodex, Japan) after separation at 45 °C with 5 mM H_2SO_4 at 0.6 mL min^{-1}, as mobile phase.

Amino acids concentrations were measured using a colorimetric method (Friedman, 2004). The free acid nitrogen concentration (as glycine equivalent, this substance being used as a reference) was determined by spectrophotometry (Varioskan^{TM} Flash Multimode Reader, Thermo Scientific).

In cell counting, the standard deviations of biomass measurements were determined using the technique reported in (Niemelä and Keskus, 2002). Standard deviation of maltose, glucose and lactic acid concentrations were determined considering uncertainties related to the HPLC method and of the sampling treatment.

2.2.2.2. *Results and discussion of the protease choice experiments*

The protease concentration did not have a significant effect on lactic acid productivity (Appendix A.1) for the pH and temperature tested conditions (pH=5.7, temperature= 30°C). Therefore only the results concerning the lowest concentration (200 mg kg^{-1}) are presented in figure 2.6. It should be pointed out that the pH was not regulated and its value decreases during the fermentation due to lactic acid formation. The highest Free Acid Nitrogen (FAN) concentration, indicator for amino acids (see section 2.2.2.1.7), was obtained with the enzyme P4, Prolyve NP (Figure 2.6A) at 48h. A higher lactic acid concentration was obtained in this assay compared to those performed with P1 and P3 enzymes (Figure 2.6 B). At 24 h of fermentation, the productivity obtained with the Prolyve NP protease was 1.45 g.L^{-1}h^{-1}. At the end of the fermentation (at 48 h) the productivity was 1.04 g. L^{-1}.h^{-1}, proving that there was a reduction in the lactic acid production rate during the last 24 hours. Some authors using wheat flour as raw material in the lactic acid fermentation have obtained productivities similar to those obtained here using prolyve NP. In their case they use SAN Super 240 L (a commercial mixture of enzymes glucoamylase and protease) to perform the gluten hydrolysis. A productivity of 2.1 g.L^{-1}h^{-1} was obtained by (Akerberg, et al., 1998) using *Lactococcus lactis* ssp. *lactis* ATCC 19435. Moreover, a lactic acid productivity of 0.8 g L^{-1}h^{-1}using *Lactobacillus* sp. MKT-878 NCAIM B02375 was obtained by (Hetényi, et al., 2010). This proves that the productivities values obtained in this work are consistent with the literature. From these results, ProlyveNP at a concentration of 200 mg kg^{-1} was chosen for the following studies.

2.2.3. *Simultaneous saccharification and proteins hydrolysis.*

After choosing the protease, experiments aiming at improving the whole process were carried out. Taking into account that the optimal temperatures for proteins hydrolysis using Prolyve NP (Table 2.1) and saccharification are 50°C and 55°C, respectively, we decided to couple both

enzymatic reactions (the proteins hydrolysis and the saccharification) in a single step with the following conditions: temperature 50°C and pH 5.7. It should be noticed that the pH value remains the same that the one chosen for the proteases study (previous section) an only the temperature was modified (the one used for the study of the protease choice was 30°C). The enzyme Prolyve NP is thus added at the beginning of the simultaneous saccharification and proteins hydrolysis (SSPH) step. This is expected to improve the whole process as the temperature is close to the optimal of the enzymatic activity unlike the SSPHF step which is performed at 30°C.
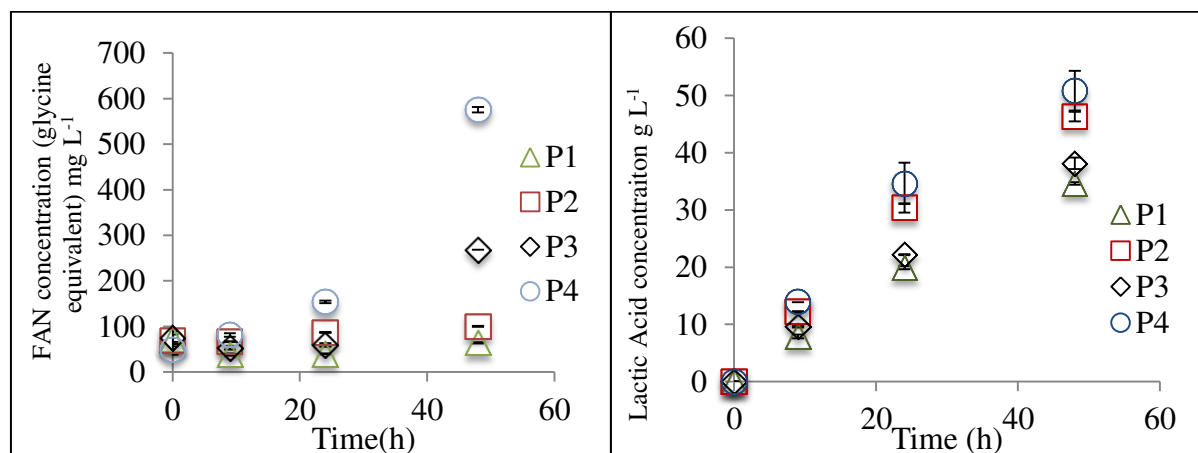
Figure 2.6A) Free Acid Nitrogen (FAN) concentration and **B)** lactic acid concentration during the fermentation. P1= Prolyve PAC, P2= Prolyve BS, P3= Prolyve 4000 and P4= Prolyve NP. Fermentation conditions: 30°C and pH 5.7 without pH regulation. The error bars represents the repetitiveness of the essay.

2.2.4. Effect of SSPH duration

The step of simultaneous saccharification and proteins hydrolysis proposed in this thesis is innovative in lactic acid bioproduction. It was put forward in order to guarantee high substrates concentration of both carbon and nitrogen sources at the beginning of the SSPHF (step which follows the SSPH).

In order to evaluate the effect of the initial concentrations of carbon and nitrogen substrates on lactic acid concentration and productivity, the duration of the SSPH was studied. Four durations were tested. In the following, only results obtained with two durations are presented. The materials and methods of these two experiments are described.

2.2.4.1. Materials and methods

The experiments were performed in a 5 L bioreactor with 2.5 L of wheat flour solution. The pH was regulated at 5.7 (unlike the flasks experiments where the pH was not regulated). The free acid nitrogen, glucose, maltose, lactic acid and biomass concentrations were measured at various time intervals during the SSPH and the SSPHF steps.

2.2.4.1.1. *Experiments description*

The tested SSPH durations were the following: 1.5 h (the hydrolysis time used by Soufflet), referred as experiment A and 6 h, referred as experiment B. Temperature was set at 50°C and pH maintained at 5.7. Once SSPH finished, the bioreactor was set at the SSPHF conditions (pH= 5.7 and temperature=30°C). The experiments were performed in batch operation mode.

2.2.4.1.2. *Inoculum preparationand liquefaction*

Lactobacillus coryniformis subsp. *torquens* DSM 20004 stored at -80°C, was grown in a MRS culture medium. The culture propagations were performed as described in section 2.2.2.1.2. This culture was used to inoculate the bioreactor. The preparation of the starch solution and liquefaction are described in section 2.2.2.1.3.

2.2.4.1.3. *SSPH step*

A 5 L Biostat® B-DCU II bioreactor (Sartorious, Hamburg, Germany) was used to perform the SSPH and SSPHF steps. 2 L of liquefied starch solution were thawed at 60°C in a water bath during 30 minutes and then added to the bioreactor. 0.5 L of distilled water were added to the bioreactor to reach a final wheat concentration of 200 g L^{-1}. $MnSO_4$ was added at a concentration of 0.05 g L^{-1} to the wheat solution and the pH was adjusted to 5.7 and regulated by a PID pH controller with the addition of NaOH (7N) and H_2SO_4 (2.5 N). Then, the Amyloglucosidase enzyme (AMG) (Lyvanol GA, Lyven, Colombelles, France), was added to the reactor (230µL L^{-1}) in order to hydrolyze the sugars produced in the liquefaction step. At the same time, the Prolyve NP enzyme (Lyven, Colombelles, France) was diluted tenfold in a sodium acetate buffer solution (0.1 M, pH 5.7) and added (560 µL L^{-1}) to hydrolyze wheat flour proteins. The temperature in the bioreactor was adjusted to 50°C and the agitation to 150 rpm during the SSPH.

2.2.4.1.4. *SSPHF step*

Once the SSPH step finished, the temperature in the bioreactor was decreased to 30°C. Then the inoculum was added to get an initial biomass concentration of 10^9 cells ml^{-1}. The SSPHF step was performed during 74 h at 30°C and 150 rpm.

2.2.4.1.5. *Analyses*

The analyses performed to determine the FAN, biomass, glucose, lactic acid and maltose concentrations are described in 2.2.2.1.7.

2.2.4.2. *Results and discussion of the SSPH duration experiments*

The evolution of FAN concentration with time during the SSPH and SSPHF steps is presented in figure 2.7. The negative x axis in this figure represents the SSPH step. For SSPH lasting 6 h (experiment B), a higher concentration in FAN was obtained compared to the experiment with SSPH of 1.5 h (Experiment A). Even at the end of the fermentation, the FAN concentration remained higher for the greater SSPH duration.

Concentrations of glucose, maltose, lactic acid and biomass were monitored over time for both experiments (Figure 2.8). Glucose was exhausted after 23 h for experiment A (Figure 2.8A). The consumption of glucose by bacteria is then quicker than its production catalyzed by the amyloglucosidase enzyme. Moreover, no growth is reported after 23h and a stationary growth phase is reached.

An increase of lactic acid concentration is observed even in the absence of glucose. This trend is expected as this *lactobacillus* genre has amylolytic properties. It means, bacteria are able to consume maltose, but this represents energy expenditure as they must synthetize the enzymes necessary for maltose hydrolysis. A higher initial glucose concentration is observed when the duration of the SSPH step increases, as expected (Figure 2.8.B). In this last case, glucose exhaustion occurs only after 72 h of fermentation.

Only the exponential and stationary growth phases were perceived in the experiments (Figure 2.8). For both assays, bacteria growth stops approximately after 21h, corresponding to a lactic acid concentration of about 40 gL^{-1}. This suggests an inhibition effect of growth linked to lactic acid accumulation. This will be further discussed in the next chapter.

In both experiments, lactic acid was produced during the stationary growth phase as lactic acid is a mixed growth associated product, produced both in exponential and stationary growth phases. Nevertheless, the lactic acid production rate in the stationary growth phase is higher in experiment B (0.93 g L^{-1} h^{-1}) compared to the experiment A (0.54 g L^{-1} h^{-1}). The production rate is higher when the glucose is not exhausted of the medium, as expected. The reaction time for the SSPH step was then fixed to 6 h for the next experiments in order to guarantee high initial glucose concentrations at the beginning of the SSPHF. Furthermore, the lactic acid productivity of the whole process (SSPH+SSPHF) remains similar. With SSPH of 6 h the productivity at 72 h of fermentation is 1.1 g L^{-1} h^{-1}, while with a SSPH of 1.5 h the productivity is 1.0 g L^{-1} h^{-1}.

The hydrolysis rate of maltose was similar for both experiments (1.0g L^{-1} h^{-1} and 1.2 g L^{-1} h^{-1} for experiments A and B respectively). In experiment A the initial maltose concentration was higher than in experiment B but it does not have an effect on the maltose hydrolysis. In conclusion, in order to guarantee high substrates concentration at the beginning of the culture, the SSPHF must be performed during 6 h.
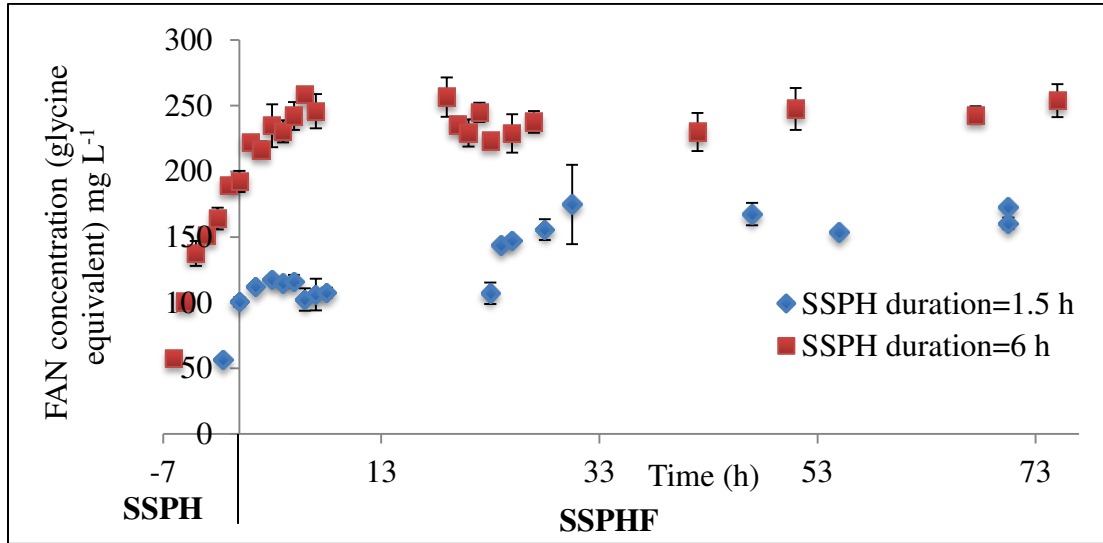
Figure 2.7 Free acid nitrogen concentration during the SSPH and SSPHF steps. SSPH conditions=50°C and pH=5.7. SSPHF conditions: 30°C and pH 5.7.
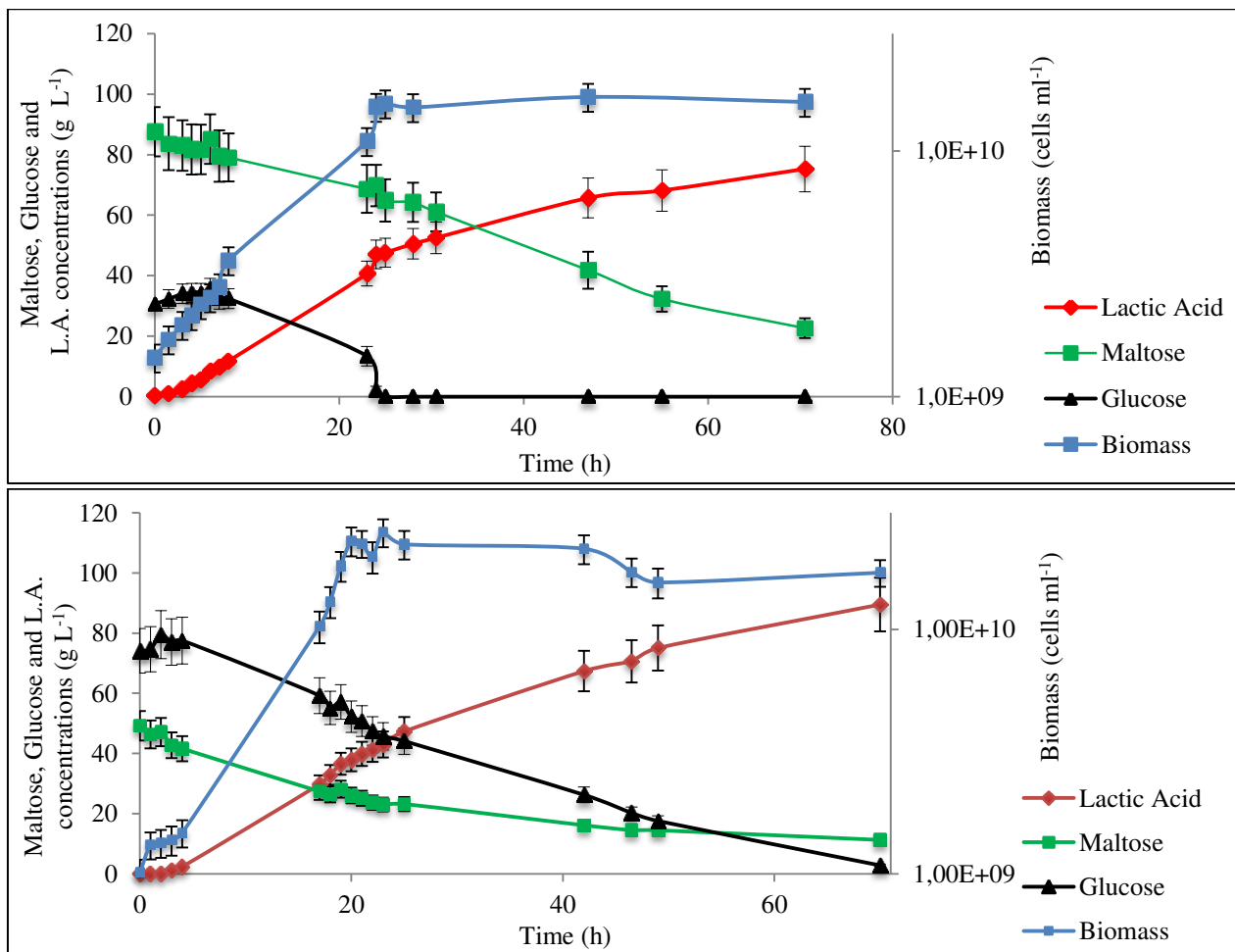
Figure 2.8 Concentration of the species during the fermentation. A) Fermentation with a previous SSPH step of 1.5 h. B) Fermentation with a previous SSPH step of 6 h. Fermentation conditions: 30°C and pH 5.7.

2.2.5. Simultaneous saccharification, proteins hydrolysis and fermentation

The results previously presented were useful to establish the conditions of the different process steps allowing process optimization. The simultaneous saccharification and fermentation step proposed by Soufflet in a first approach was modified to include the proteins hydrolysis resulting in a simultaneous saccharification, proteins hydrolysis and fermentation step. This SSPHF step is the longest step and then, the critical one.

All experiments presented in the previous sections were performed in batch mode of operation. Nevertheless, the productivity obtained in these conditions is known to be low compared with other bioreactor's operation modes. Moreover, the development of a control strategy, one of the main objectives of this PhD, for a process operating in batch is difficult.

For this reason, the different operation modes used in lactic acid fermentation processes were investigated in order to choose the most appropriate one. These operation modes are summarized in the following sections.

2.3. PROCESS OPERATION CHOICE

Although parameters such as the type and nature of substrates, and microorganisms and the fermentation broth characteristics (viscosity, composition, presence of solid particules, etc) must be taken into account when designing the fermentation process, the bioreactor operation mode is also an important factor when process performance improvements are considered. In the following section, the main operation modes used for lactic acid fermentation are presented.

2.3.1. Batch Fermentation

Batch is the simplest and most common mode of operation for fermentation. At the beginning of the fermentation, the reactor is filled with the culture medium; all carbon substrates and other components are added at the same time, except neutralizing agents for pH control, which are added during fermentation. After microbial inoculation, a lag phase is generally observed until the biological reaction begins. The main advantages of this mode are the reduction of the contamination risks (the bioreactor is closed) and the high lactic acid concentrations obtained in comparison to other processes (Hofvendahl & Hahn-Hligerdal, 2000). For lactic acid industrial production, the processes are mainly implemented in batch mode. However, batch fermentation suffers from low productivities, due to either substrate and/or product inhibitions.

Different methods were developed in batch fermentation from starch materials in order to improve the process performance. The methods tested include the SSF (simultaneous saccharification and fermentation) process and the separate hydrolysis and fermentation process (SHF). In most of the cases the starch based culture medium is not sterilized, but various authors have reported fermentation processes from lignocellulosic or waste materials, using sterile

medium. Nevertheless, side-reactions such as Maillard reactions (between amino acids and reducing sugars) or formation of inhibitory furfural compounds may occur when complex carbohydrates are sterilized. Moreover, without sterilization step, a decrease in the energy consumption and equipment needs is reported (Zhang, et al., 2008).

2.3.2. Fed-batch Fermentation

This operation mode is used when high substrate concentrations cause microbial inhibitions, such as cell lysis and/or long lag phases. This kind of inhibition results in the decrease of growth, production and sugar consumption rates (Ding & Tan, 2006). Thus, low substrate concentrations can be maintained in the reactor using a fed-batch process. In this case, the substrate is fed continuously or intermittently to the fermenter. There is no output flow, so the broth volume in the reactor gradually increases during the fermentation. Nevertheless, this operation mode does not prevent inhibition resulting from the lactic acid accumulation. The factors to consider in fed-batch fermentation are the time of the substrate feeding, the feeding procedures and the substrate concentration to be maintained in the fermenter. Intermittent, constant and exponential feeding methods have been reported for production of lactic acid (Abdel-Rahman, et al., 2013).

2.3.3. Repeated Fermentation

This kind of operation involves repeated batch cycles of fermentation by inoculating a part or all of the cells from a previous batch into the next one. In comparison with batch culture, repeated batch operation requires less time for washing, sterilization and culture due to the high initial inoculation volumes that allow reduction of washing and sterilization for the intermediate batches (Ho, et al., 1997). In the repeated batch fermentation, the fermented broth is withdrawn at time intervals, and the residual part of the broth (the biomass) is used as an inoculum for the next batch. Among the methods used for the separation of the culture broth and the biomass, centrifugation and filtration methods may be applied. Repeated fermentation minimizes the fermentation time and increases the productivity. Thus, this process has gained a lot of attention recently. However, this operation mode seems difficult to be developed with a complex medium as wheat flourdue to the presence of wheat solid particles in the broth.

2.3.4. Continuous Fermentation

In a continuous fermentation, fresh medium is fed into the reactor with the same rate as the product exits from the fermenter. In the continuous operation a steady state is then established. Product inhibition occurring in batch or fed-batch fermentation may be avoided in this case. At steady state, the cells are maintained at constant physiological state and growth rate. The latter can be adjusted by changing the feed flowrate because the specific growth rate equals the dilution rate at steady-state (ratio between the feed flowrate and the reactor effective volume). Thus, the dilution rate is an important parameter that allows maximizing the process productivity. Indeed,

as the productivity is defined as the product of the dilution rate by the product concentration, high dilution rates increase the process productivity. Nevertheless, this is true only for a range of dilution rates lower than the maximal specific growth rate. For dilution rates values close or higher to the maximal specific growth rate, the washing out phenomena is observed.

The concentrations of cells, products and substrates in the fermenter can be maintained constant during long periods (Bustos, et al., 2007). Therefore, this mode of operation is much easier to manage than a batch operation in which the fermenter must be emptied, cleaned, sterilized and refilled, after each campaign. One of its disadvantages is that the carbon substrates and the cells leaving the fermenter are wasted, unless recycled. Moreover, there is a decline in lactic acid concentration with an increase in the dilution rate; it could be a problem when considering the downstream processes as product is at low concentrations (diluted) (Abdel-Rahman, et al., 2013). These problems can be solved by using high cell density fermentations.

2.3.5. Cells recycling

In this operation mode the high cell density in the reactor is maintained by recycling the harvested cells from the culture broth. Membrane filtration techniques such as ultrafiltration microfiltration and cross-flow membrane may be used for recycling purposes. The membrane bioreactors are very efficient as they allow achieving complete cell recycling and *in situ* production and separation of the fermentation product. Nevertheless, the main inconvenient related to this fermentation technique is the membranes fragility and the fouling phenomenon (Djidel, 2007).

2.3.6. Cell immobilization

Cell immobilization techniques became one of the most used methods for increasing cell density in fermenters, which should result in higher lactic acid productivity. Moreover, this technique can be run in continuous mode, it reduces downstream processing by avoiding the cell separation step and reduces the risk of contamination due to the high cell concentration (Panesar, et al., 2007). Nevertheless, significant mass-transfer limitations are known as one of the disadvantages of the process (Kosseva, et al., 2009).

The immobilization techniques are classified in four groups: surface attachment followed by bacterial growth, entrapment, containment and self-aggregation. The most used method is the formation of biofilms on surfaces due to its simplicity. Research works dealing with lactic acid production with immobilized cells were carried out in all operating modes (batch, fed-batch and continuous). Different bioreactors have been studied such as packed-bed reactors, continuous stirred-tank reactors, fibrous-bed reactors and fluidized-bed reactors (Abdel-Rahman, et al., 2013).

2.3.7. Comparison between the different fermentation modes

Besides the strain optimization and the use of alternative raw materials, the transition from traditional batch or fed-batch to continuous fermentation, conventional or with cell recycling, could lead to a better performance of the lactic acid production process. It is also important to consider associated downstream processing (Kamm, 2015). Table 2.2 summarizes the advantages and disadvantages of the main processes found in the literature. In order to compare the productivity and the lactic acid concentrations obtained by different fermentation modes, some experimental data reported in the literature are also compared in table 2.3.

Table 2.2 Advantages and disadvantages of some fermentation processes (Abdel-Rahman, et al., 2013).

Operation Mode	Advantages	Disadvantages
Batch Fermentation	-Simple operation -High product concentration -Reduced risk of contamination	-Low Productivity -Substrate and/or product inhibition
Fed-Batch Fermentation	-Overcome substrate inhibition problem -High product concentration	- Product inhibition
Repeated Fermentation	-Time-saving process -Labor-saving -Omission of seed preparation time	-Requirement of special devices (e.g. hollow fiber-module) or special connection lines used for cell concentration -Difficult to use with complex broth
Continuous Fermentation	-High productivity -Control of the growth rates -Less frequency shut down process	-Incomplete utilization of the carbon source -Diluted product

It should be reminded that the aim of the process optimization performed in this work is to maximize the lactic acid productivity, first by optimizing the operation conditions and secondly, by using a control strategy to maintain the bioprocess at the determined optimal operating conditions.

Table 2.3 Comparison between some different fermentation modes reported in the literature.

Operation Mode	carbon source	Micro-organism	Reported data		Fermentation method	Reference
			L.A. concentration (g L^{-1})	Productivity (g L^{-1}h^{-1})		
Batch	Broken rice	*Lb. delbrueckii*	79	3.58	•SSF with glucoamylase, 5 L fermenter with 2.5 L of broth at 40°C, 150 rpm, pH=6, purity D= 96,1 %	Nakano et al. (2012)
	Corn starch	*Lb. Plantarum*	73.2	3.86	•Performed in a 2 L bioreactor with 0,7 L of broth at 37°C, 100 rpm, pH control at 5.5, purity D=99.6 %	Okano et al. (2009)
	Wheat flour	*Lb. delbrueckii*	106	1.6	•SSF with 1 L fermenter with 500 mL of broth at 37°C, 100 rpm, pH control at 5.5, purity D=99.7 %	Hofvendahl et al. (1997)
	White rice bran hydroly-sate	*Lb. Rhamnosus*	82	3.73	•SHF with glucoamylase and amylase, 5 L fermenter with 2 L of broth at 42°C, pH control at 6.2. (L-Lactate)	Li et al. (2012)
Fed-Batch	Peanut and glucose	*Sporolactobacillus Sp strain CASD*	207/226	3.8/4.4	• Pulse / multi pulse feeding. Reactor of 30 L, 24 L of broth at 42 ° C, pH = 5.5, D = 99.3%	Wang et al. (2011)
	Glucose	*Lactobacillus rhamnosus*	170	2.6	Glucose feeding using a controler. 5 L fermenter at 42°C and pH=5.5	Li et al. (2010)
	Starch	*Lactobacillus amylophilus*	43.7	0.75	•5L Fermenter with an initial broth volume of 1L at 30°C, pH= 5.3	Yen and Kang (2010)
	Glucose	*Lb. Lactis*	210	2.2	•5 L Fermenter at 37°C, pH= 6.2. continuous feeding of the substrate	Bai et al. (2003)
	Glucose	*Lb. Casei*	180	2.14	• 5 L Fermenter with 2.2 L broth at 42°C, pH= 6.2. Continuous feeding of the substrate. Exponential feeding	Ding and Tan (2006)
Repeated batch fermentation	Sago starch	*Enterococcus faecium*	36.3	1.96	•3 L Fermenter at 30°C, 200 rpm, pH=6.5.At the end of each fermentation cycle the broth is centrifuged and recycled	Nolasco-Hipolito et al. (2012)
	Glucose	*Enterococcus faecalis*	94	6.2	•2 L Fermenter with 1L broth at 38°C,200 rpm and pH= 7. Cell recycling using a Hollow-fiber filtration unit	Oh et al. (2003)
	Glucose	*Sporolactobacillus Sp strain CASD*	87.3	1.81	• two reactor system in 500 mL flasks, 200mL of broth at 42 ° C, 50 rpm, pH = 5.7. Recycling only a part of the culture	Zhao et al. (2010)
	Corn starch	*Rhizopus oryzae*	91	2.02	• 3 L Fermenter, 2 L of broth at 35 ° C, 300 rpm. Small mycelial pellets of *R. oryzae* were produced after batch. Pellets were precipitated and used for the next batch.	Yin et al. (1998)
Continuous fermentation	Sago starch	*Enterococcus faecium*	11.7	3.04	• Cell recycling via a polymer hollow fiber dilution rate D = 0.26 h^{-1}	Shibata et al. (2007)
	Glucose	*Lb. delbrueckii*	40	12	• Cell recycling via a polymer hollow fiber dilution rate D = 0.3 h^{-1}, operating time 220 h	Major and Bull (1989)
	Glucose	*Lb. delbrueckii*	20.7	18	•A hollow fiber microfiltration module was used for cell recycling. D=0.87 h^{-1}, operating time 36 h	Tashiro et al. (2011)
	Glucose	*Lb. Lactis IO-1*	8.91	4.46	The cells were immobilized in a fixed bed reactor. Process continues dilution rate D = 0.5 h^{-1}	Sirisansaneeyakul et al. (2007)

In order to be able to build a control strategy based on the substrate inlet flow (parameter usually considered as control factor in most of the control strategies) the process must be operated either in fed-batch or continuous modes. Moreover, repeated fermentation was not considered in this work as special devices are required (hollow fiber modules) for filtration and cell recycling. This is out of the scope of this work. Furthermore, as the culture broth used for lactic acid production is a mixture of wheat flour and water at 25% w/w, the filtration of such a complex broth could be difficult.

Comparing fed-batch and continuous processes, it is clear that higher productivity values are found with continuous fermentation (see table 2.3). Furthermore, the use of fed-batch fermentation prevents inhibitions by substrates, but not by fermentation products. For these reasons, the fermentation in continuous mode was chosen for the following control implementation purpose. The high cell density methods were not taken into account as the studies of this kind of techniques are out of the scope of this work. Indeed, the wheat solution used as culture broth hinders the implementation of this type of methods. In the next section, the description of the whole process is presented.

2.4. COMPLETE PROCESS

In this section a detailed description of the whole process is summarized. Taking into account the results obtained from the experiments previously presented (protease choice: type and concentration, and hydrolysis time, see sections 2.2.2 and 2.2.4) and the theoretical considerations concerning reactor operation modes, a process comprising three steps is proposed:

- In the first step, starch is converted into maltose by the enzyme alpha-amylase. This step is performed at 85°C and a pH value of 5.5.
- The second step is a simultaneous saccharification and proteins hydrolysis (SSPH) step allowing in the same time the partial conversion of maltose into glucose (using the enzyme amyloglucosydase AMG) and the partial hydrolysis of wheat proteins into amino acids (by the protease Prolyve NP). This step operates at the optimal operation conditions for both enzymes: 50°C and pH=5.7.
- The simultaneous saccharification, proteins hydrolysis and fermentation (SSPHF) step occurs in the last step. It should be pointed out that at this stage, the remaining maltose and wheat proteins are hydrolyzed simultaneously into glucose and amino acids which are consumed by lactic acid bacteria for growth and lactic acid production.

The reactions taking place in each step of the processand the bioreactors configuration are represented on figures 2.9 and 2.10, respectively.
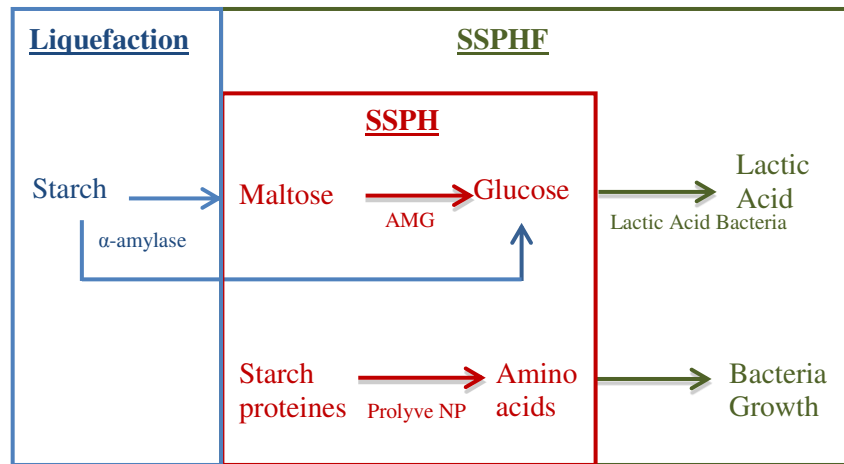
Figure 2.9 Process mechanisms. Liquefaction, Simultaneous saccharification and proteins hydrolysis (SSPH) and simultaneous saccharification, proteins hydrolysis and fermentation (SSPHF).
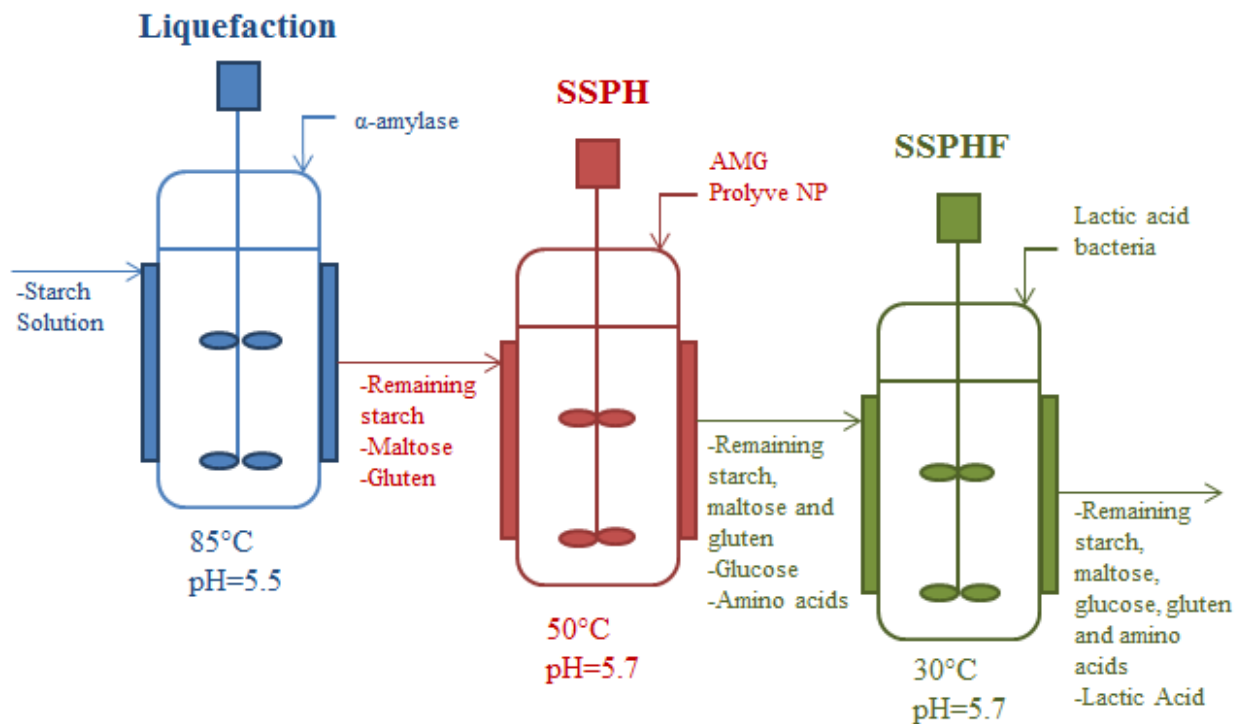
Figure 2.10 Bioreactors configuration for lactic acid production from wheat flour. Continuous process.

93

In order to maximize the productivity of the system, the complete process should be carried out in continuous mode and controlled. Nevertheless, this was not possible in the frame of this PhD, due to time and experimental constraints. SSPHF being the lengthiest step and thus the limiting one, we decided to focus our work on it, by performing it in continuous mode and controlling it. This strategy will certainly have a significant impact on lactic acid productivity of the whole process. It should be pointed out that the other steps are then carried out in batch mode.

2.5. CONCLUSIONS

Wheat flour was chosen as the raw material for lactic acid production in this work. This is mainly justified by the large wheat flour availability in France, its low cost and Soufflet's expertise in the utilization of this cereal. The use of starch from wheat flour for lactic acid production involves enzymatic reactions prior to fermentation. Starch is thus transformed into maltose in a liquefaction step followed by hydrolysis where the maltose is transformed into glucose. The glucose is finally fermented to lactic acid.

In this chapter the process design of the lactic acid production process was performed. A study of the hydrolyze of insoluble protein fraction of wheat (gluten) allowed us to choose Prolyve NP for the process. Moreover, a simultaneous saccharification, proteins hydrolysis and fermentation step (SSPHF) was developed.

The process designed differs from the process initially proposed by Soufflet. Here, first, starch is liquefied followed by a simultaneous saccharification and proteins hydrolysis (SSPH) step where maltose and gluten are partially hydrolyzed. The final part of the SSPH is combined with the fermentation (Simultaneous Saccharification Proteins Hydrolysis and Fermentation, SSPHF). This means that maltose and gluten are partially hydrolyzed in the SSPH step and then the remaining maltose and gluten are hydrolyzed simultaneously with the fermentation.

The choice of the bioprocess operation mode was done after literature survey; the continuous operation mode was chosen due to its advantages: an expected improvement in lactic acid productivity, the possibility of controlling the growth rate and the control the product inhibition problem. It was decided to focus on the modelling and control of the SSPHF step, the limiting step in the process, which will be presented in the next chapters.

CHAPTER 3: PROCESS MODELLING

3.1. INTRODUCTION

Models are important tools for optimizing complex biotechnological processes, and to predict bioreactor performance. A better understanding of the system behavior is assessed using mathematical models, together with carefully designed experiments. A model is a set of relationships between the variables of interest in the system being studied. The mathematical modelling of fermentation processes allows representing by equations, some of which are differential equations, the evolution of important or fundamental variables of the process. The variables considered are first and most generally cell, substrate and metabolites concentrations.

A model represents a simplified reality. One of its purposes is to design large-scale fermentation processes using data obtained at small-scale (McNeil & Harvey, 1990). To describe a microbiological process, there are basically two types of models, structured and unstructured.

- Structured or physiological models take into account the evolution of the internal composition of the microorganism. They describe the metabolic pathways and take into account the intracellular characteristics as the cell structure and their function and composition. Moreover, they have been reported to accurately describe lactic acid fermentation (Gadjil & Venkatesh, 1997)(Nielsen , et al., 1991).
- The unstructured models use microbial kinetics to describe the evolution of growth rates, substrate utilization and metabolites production. Only the total cellular concentration is considered, and hence they do not involve any physiological characterization of the cells. Nevertheless, it has been proved that these models can accurately describe lactic acid fermentation in a wide range of experimental conditions and media (Bouguettoucha, et al., 2011).

This chapter is devoted to the development of a model for a SSPHF (simultaneous saccharification proteins hydrolysis and fermentation) in a continuous bioreactor (see section 2.2.2.1.6). First, a state-of-the-art of kinetic models representing growth, lactic acid production and substrate consumption rates is presented. This literature survey mainly contains models describing batch fermenters (as most works in modelling deals with this operation mode) and only some describing continuous fermenters. In the second part, a description of the model development for the SSPHF continuous bioreactor is discussed. Later, the strategy used for

parameters identification is described. The developed model is finally experimentally validated through fermentation experiments.

3.2. STATE-OF-THE-ARTON LACTIC ACID FERMENTATION MODELLING

The modelling of bacterial growth and metabolites production in lactic fermentation operations generally considers the inhibition phenomenon exerted by the substrate and the product (lactic acid). The effects of other key parameters in the culture conditions are frequently not taken into account. Indeed, some of them, including pH and temperature, are often regulated and set constant. Other factors as agitation, dissolved oxygen concentration are generally not considered.

The reactor used in the modelling approach is illustrated on figure 3.1. The variables of interest are X (biomass concentration in gL^{-1}), S (glucose concentration in gL^{-1}), P (lactic acid concentration in gL^{-1}) and M (maltose concentration in gL^{-1}). The model must include four dynamical equations describing their evolution with time. M_0 and S_0 represent the inlet maltose and glucose concentrations feeding the reactor, respectively. These concentrations are obtained from the SSPH (simultaneous saccharification and proteins hydrolysis) step (the previous one). It should be pointed out that the pH value in the SSPHF bioreactor is regulated by NaOH addition, thus, the bioreactor has in fact two inlet flows. Nevertheless, the NaOH inlet flow is very low compared to the flow rate feeding the bioreactor in glucose and maltose (35 times smaller). Consequently, the NaOH inlet flow is neglected for modelling. It is further discussed in section 4.4.
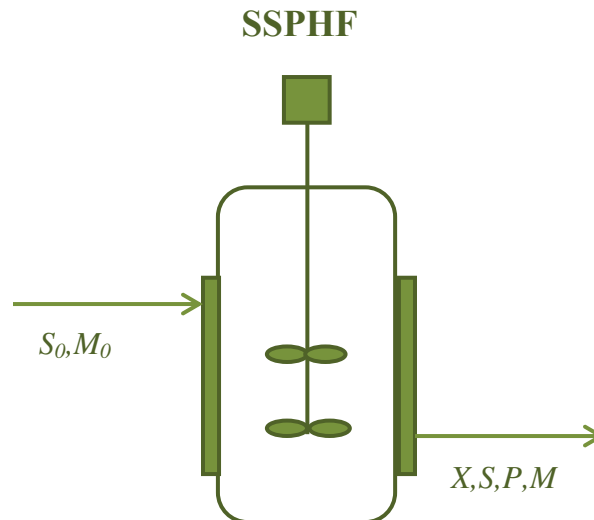
Figure 3.1 SSPHF continuous bioreactor

In the following, a literature survey of the kinetics models representing bacteria growth, product formation and substrate consumption are presented.

3.2.1.   *Kinetics of microbial growth*

In a well-stirred continuous fermentation, the mass balance of biomass in the bioreactor between time t and time $t + dt$, leads to:

$$\frac{dX}{dt} = \mu X - DX \tag{3.1}$$

Where X is the biomass concentration at t (g L^{-1}), μ the specific growth rate (h^{-1}), t the time (h) and D the dilution rate (h^{-1}) (defined as the ratio between the outlet flowrate and the culture broth volume). The first term in equation (3.1) μX represents the biomass production in the reactor corresponding to cell growth and the second term DX, the cell quantity withdrawn with the outlet flow per time.

Some authors also take into account cell death considering an exponential decay for the decline phase:

$$\frac{dX}{dt} = \mu X - DX - k_d X \tag{3.2}$$

With k_d the specific death rate (h^{-1}).

As previously mentioned, in the continuous operation the specific growth rate, μ, can be adjusted by changing the dilution rate. Nevertheless, μ can also be significantly affected during fermentation due to different phenomena as carbon and nutrients limitation, product inhibition, etc. It is then important to identify these limitations and inhibitions to obtain a model describing accurately the growth rate kinetics. In a continuous bioreactor, when the steady state is achieved, the dynamic term in equation (3.1) is cancelled and the growth rate equals the dilution rate making the parameters identification associated to the limitation and inhibition effects on growth impossible to determine.

In order to determine these effects, it is then easier to study the bioreactor behaviour in batch mode, with $D = 0$. This approach allows then to determine the growth and production parameters kinetics of the SSPHF bioreactor. In the following, a literature survey of kinetics growth models considering the main limitation and inhibition effects observed for different lactic acid production processes is presented.

3.2.1.1.   *Carbon limitation*

Substrate limitation by the carbon substrate is usually described by the model proposed by Monod in 1942 (equation (3.3)):

$$\mu = \mu_{max} \frac{S}{k_S + S} \tag{3.3}$$

where S is the substrate concentration (gL^{-1}), k_S is known as the saturation constant or half-velocity constant and is equal to the concentration of the rate-limiting substrate when the specific growth rate is equal to one half of its maximum (Bailey & Ollis , 1986) and μ_{max} is the maximum achievable growth rate (h^{-1}) when S is much greater than k_S.

Some authors added a term for inhibition by the carbon substrate to the Monod model (Haldane model):

$$\mu = \mu_{max} \frac{S}{k_S + S + S^2/k_i}$$ (3.4)

where k_i is the substrate inhibition constant (gL^{-1}). However, this substrate inhibition term was not relevant to describe the experimental data published by some authors(Altiok, et al., 2006).

A growth kinetics depending on several limiting substrates was also described by some authors. The effect of both glucose (G) and fructose (F) concentrations during batch fermentations of *Lactobacillus casei* ssp. *Rhamnosus* on date juice was also examined (Nancib, 2007)and the following model was proposed:

$$\mu X_{total} = \left[\mu_{max\,G} \frac{G}{k_G + G} - k_{dG} \right] X_G + \left[\mu_{max\,F} \frac{F}{k_F + F} - k_{dF} \right] X_F$$ (3.5)

This model can be used when bacteria use more than one sugar substrate for growth and metabolite production. Growth parameters for glucose are referred with the subscript G and those for fructose are referred with subscript F.

3.2.1.2.   *Product inhibition*

As mentioned previously, lactic acid has an inhibitory effect on bacteria growth (see section 2.2.4.2). In order to take into account this inhibition effect, Luedeking and Piret proposed a linear relation between the specific growth rate and the product concentration (Luedeking & Piret, 1959):

$$\mu = \mu_{max} - \delta \cdot P$$ (3.6)

where δ is a constant and P is the lactic acid concentration. Belhocine (1987) showed that this model leads to good results. Otherwise, several authors assumed a non-competitive inhibition by the product, so they added in their model an inhibition term to Monod equation (Ohara, et al., 1992)(Pinelli, et al., 1997):

:

$$\mu = \mu_{max} \frac{S}{k_s + S} \frac{k_P}{k_p + P} \quad (3.7)$$

where k_P is the product inhibition constant.

The non-competitive inhibition equation (3.7) was also modified by adding a term taking into account a critical lactic acid concentration (P_{max}) representing the product concentration above which bacteria do not grow (Ben Youssef, et al., 2005):

$$\mu = \mu_{max} \frac{S}{k_s + S} \frac{k_P}{k_p + P} \left(1 - \frac{P}{P_{max}}\right) \quad (3.8)$$

Other authors added only the term of product inhibition to the Monod relation (Monteagudo, et al., 1997):

$$\mu = \mu_{max} \frac{S}{k_s + S} \left(1 - \frac{P}{P_{max}}\right) \quad (3.9)$$

Some authors modified equation (3.9) by the addition of a toxic power by the product (denoted n)(Kwon, et al., 2001) (Akerberg, et al., 1998)(Kumar Dutta, et al., 1996):

$$\mu = \mu_{max} \frac{S}{k_s + S} \left(1 - \frac{P}{P_{max}}\right)^n \quad (3.10)$$

It is also possible to consider an exponential term to describe the product inhibition (Nandasana & Kumar, 2008):

$$\mu = \mu_{max} \left(\frac{S}{k_s + S}\right)\left(\frac{k_i}{k_i + S}\right) \exp\left(-\frac{P}{k_P}\right) \quad (3.11)$$

In order to consider only the inhibitory effect by lactic acid, equation (3.10) can be modified (Peeva & Peev, 1997)

$$\mu = \mu_{max} \left(1 - k_P P^\alpha\right) - k_d$$
$$\alpha = 6.13 \cdot P_C - 0.056 \quad (3.12)$$

whit k_d as the cell death rate, k_P as the product inhibition coefficient and P_C the theoretical lactic acid concentration obtained after total substrate consumption.

3.2.1.3. *Other growth kinetics*

The models presented in the previous sections take only into account the carbon substrate limitation (mainly using the Monod relation) and the product inhibition effect. Nevertheless, other limitation effects on growth have been observed during lactic acid fermentation, in particular due to nitrogen. As complex substrates (such as yeast extract) that contain nitrogen and other growth nutrients are expensive and only added in small amounts to the culture medium, nitrogen limitations may be observed instead of carbon limitations.

Nevertheless it seems difficult to include these limitations in a growth model. Models involving these nutritional limitations are then rare. The following equation considers both carbon and nitrogen limitations (Leh & Charles, 1989):

$$\mu = \mu_{max} \frac{1}{1 + \dfrac{k_{pr}}{pr} + \dfrac{k_S}{S} + \dfrac{k_S}{S}\dfrac{k_{pr}}{pr}} \tag{3.13}$$

were pr and k_{pr} are respectively the concentration and the saturation constant of 'usable proteins'. The problem with this kind of expression is the definition of 'usable protein'. This model can only be applicable if a clear definition and a method for the determination of the really 'usable proteins' by bacteria is given (Bouguettoucha, et al., 2011):

Some authors have proposed models to describe their experimental data. However, some of them were not completely satisfactory from a cognitive point of view; indeed, some growth parameters did not have a biological meaning (Bouguettoucha, et al., 2011). As an example, the following equation was proposed by Amrane and Prigent (1994) to describe bacteria growth:

$$\mu = \mu_{max} \frac{1}{1 + \dfrac{c \cdot \exp(d \cdot t)}{\mu_{max} - c}} \tag{3.14}$$

where c and d are constants.
The Verlhust model was also proposed to describe experimental data(Amrane & Prigent, 1994)(Diaz, et al., 1999)(Bouguettoucha, et al., 2008)

$$\mu = \mu_{max} \left(1 - \frac{X}{X_{max}}\right) \tag{3.15}$$

where X_{max} is the maximum biomass concentration obtained from nitrogen exhaustion.

In conclusion, the effects of nutritional limitations (by the carbon source) and the product inhibition are the main factors taken into account to describe the growth rate deceleration.

Summarizing, many models have been proposed for describing the carbon limitation effect and most of them are modified versions of the Monod model. Concerning other limitation effects (as those observed by nitrogen), more research is needed to develop models describing correctly bacteria growth and having a real biological meaning. Indeed, most models found in the literature matched well with experimental data without having a clear biological meaning and they generally cannot be extended to other studies. The product inhibition effect has been observed in many studies, but authors have not agreed on the factor that leads to growth inhibition. The role of the bulk pH has been highlighted in some cases. According to some of them (Bouguettoucha, et al., 2011) this effect is only observed for processes without pH control, whereas for others a product inhibition effect could be observed even in fermentations with pH control (Kumar Dutta, et al., 1996)(Boonmee, et al., 2003).

3.2.2. Production Kinetics

The mass balance of lactic acid in a well-stirred continuous bioreactor leads to:

$$\frac{dP}{dt} = \gamma - DP \tag{3.16}$$

where the first term, γ (in g L^{-1} h^{-1}) represents the production rate and the second one refers to the dilution effect.

Different models have been proposed in the literature to describe the production kinetics in the lactic acid fermentation process. The Luedeking and Piret model is the most widely used. This model describes both growth associated and non-associated lactic acid productions (Luedeking & Piret, 1959):

$$\gamma = \alpha\mu X + \beta X \tag{3.17}$$

where α is the growth associated production coefficient and β is the non-growth associated coefficient. Some authors (Keller & Gerhardt, 1975), (Akerberg, et al., 1998), (Kumar Dutta, et al., 1996) and (Boonmee, et al., 2003) successfully used this model.

When lactic acid production is mainly non-growth associated (for stationary growth phase in batch fermentation), the following model was proposed by Peeva and Peev (1997):

$$\gamma = \beta X (1 - k_i P^\alpha)$$

(3.18)

where, k_i is the coefficient of inhibition by the product and α is an exponent.

A logistic model to describe product dynamics in batch fermentation was also proposed in (Moldes, et al., 1999):

$$\gamma = P_0 \left(1 - \frac{P}{P_m} \right) PX$$

(3.19)

where P_0 is the initial product concentration (gL^{-1}) and P_m the maximal product concentration (gL^{-1}).

Most of the production kinetic models found in the literature consider the lactic acid production both in the exponential and stationary phases of growth for batch fermentations. Nevertheless, as in the continuous fermentation bacteria are continuously growing, the lactic acid production can be directly linked to the growth rate (the non-associated lactic acid production is inexistent). The obtained expression to describe the lactic acid production rate is then defined by (Lombardi, 1996), (Bouguettoucha, et al., 2009)(Nancib, 2007):

$$\gamma = \frac{Y_{PS}}{Y_{XS}} \mu X$$

(3.20)

where Y_{PS} (g lactic acid g^{-1} glucose) and Y_{XS} (g biomass g^{-1} glucose) are the yields of product and biomass on glucose, respectively. In equation (3.20) the production rate is directly associated to the growth rate by means of the yields. It means that when bacteria do not grow, lactic acid production stops.

3.2.3. Substrate utilization

Most works in lactic acid fermentation assume carbon as the limiting substrate, so they model its consumption. In continuous fermentation, the mass balance of the carbon substrate in the bioreactor leads to:

$$\frac{dS}{dt} = r_S + D(S_0 - S)$$

(3.21)

where r_S is the substrate consumption rate (g L^{-1} h^{-1}), S the substrate concentration and S_0 the substrate concentration in the inlet flow. The first term represents the glucose consumption for both bacteria growth and lactic acid production, the second term the difference between glucose input and output with inlet and outlet flows.

To describe the consumption rate, some authors used a model which considers its conversion to biomass and product and substrate consumption for cell maintenance (Aborhey & Williamson, 1997), (Monteagudo, et al., 1997)and (Akerberg, et al., 1998).

$$r_S = -\frac{1}{Y_{XS}}\mu X - \frac{1}{Y_{PS}}\gamma - mX \qquad (3.22)$$

where Y_{XS} and Y_{PS} are defined as in (3.20) In this equation r_S is related stoichiometrically to the rates of biomass growth and lactic acid production. The first term describes the substrate consumption for bacteria growth and the second term for lactic acid production; they are considered as independent. The substrate used for energy maintenance is represented by the term mX and is usually assumed as negligible. This model is suitable for the stationary growth phase in which the first term is cancelled but it is redundant when bacteria are in the exponential growth phase. Indeed, the production rate γ already depends on the growth rate, so glucose consumption for bacteria growth and lactic acid production is normally already taken into account implicitly by the model.

Other models have also been proposed (Ben Youssef, et al., 2005)(Trontel, et al., 2010):

$$r_S = -\frac{1}{Y_{XS}}\mu X - mX \qquad (3.23)$$

However the equation (3.23) can only be used when there is not lactic acid production during the stationary growth phase. This expression relates the glucose consumption directly to bacteria growth but states that when the growth rate is zero, there is no glucose consumption anymore. A model which links glucose consumption directly to the production rate has been proposed (Kumar Dutta, et al., 1996)(Altiok, et al., 2006):

$$r_S = -\frac{1}{Y_{PS}}\gamma - mX \qquad (3.24)$$

This expression depends on the model used to describe the production rate. Table 3.1 summarizes some of the growth, lactic acid production and substrate consumption kinetics presented in this section. In the next section, we will focus on the development of a continuous model to represent the dynamical behaviour of variables of our system.

Table 3.1 Models found in the literature to describe the lactic acid fermentation with lactic acid inhibition.

Strain	Substrate	Biomass growth	Lactic acid production rate	Substrate utilization rate	Reference
Streptococcus	Lactose	$\mu = \mu_{\max}\left(\dfrac{S}{k_S + S}\right)\left(\dfrac{k_P}{k_P + P}\right)$	$\gamma = \alpha\mu X + \beta X$	$r_S = -\dfrac{1}{Y_{XS}}\mu X - \dfrac{1}{Y_{PS}}\gamma - mX$	Aborhey and Williamson (1976)
L. Lactis	Glucose from wheat flour	$\mu = \mu_{\max}\dfrac{S}{k_s + S + S^2/k_i}\left(1 - \dfrac{P}{P_{\max}}\right)^n$	$\gamma = \alpha\mu X + \beta X$	$r_S = -\dfrac{1}{Y_{XS}}\mu X - \dfrac{1}{Y_{PS}}\gamma - mX$	Akerberg et al. (1998)
L. casei	Whey	$\mu = \mu_{\max}\left(1 - \dfrac{X}{X_{\max}}\right)^h\left(1 - \dfrac{P}{P_{\max}}\right)^n$	$\gamma = \alpha\mu X + \beta X$	$r_S = -\dfrac{1}{Y_{PS}}\gamma - mX$	Atiok et al (2006)
L. casei	Glucose	$\mu = \mu_{\max}\left(\dfrac{k_P}{k_P + P}\right)\left(\dfrac{S}{k_S + S}\right)\left(1 - \dfrac{P}{P_{\max}}\right)$	$\gamma = \alpha\mu X + \beta X\left(\dfrac{S}{k_S^c + S}\right)$	$r_S = -\dfrac{1}{Y_{PS}}\gamma - mX$	Ben Youssef et al. (2005)
L. delbureckii	Glucose	$\mu = \mu_{\max}\dfrac{S}{k_s + S}\left(1 - \dfrac{P}{P_{\max}}\right)^n$	$\gamma = \alpha\mu X + \beta X$	$r_S = -\dfrac{1}{Y_{PS}}\gamma - mX$	Kumar Dutta et al. (1996)
L. delbureckii	Glucose	$\mu = \mu_{\max}\dfrac{S}{k_s + S}e^{-k_p P}$	$\gamma = \dfrac{Y_{PS}}{Y_{XS}}\mu X$	$r_S = -\dfrac{1}{Y_{XS}}\mu X - mX$	Lombardi (1996)
L. amylovorus	Starch	$\mu = \mu_{\max}\left(\dfrac{S}{k_S + S}\right)\left(\dfrac{k_P}{k_P + P}\right)$	$\gamma = \alpha\mu X + \beta X$	$r_S = -\dfrac{1}{Y_{XS}}\mu X - mX$	Trontel et al. (2010)

X= Biomass concentration (g L^{-1}), S= Substrate concentration (g L^{-1}), P= Product concentration (g L^{-1}), μ=growth rate(h^{-1}), γ= production rate(g L^{-1} h^{-1}), r_S= consumption rate (g L^{-1} h^{-1}), μ_{max}= maximum specific growth rate (h^{-1}), k_S = half-saturation constant (g L^{-1}), k_i= substrate inhibition constant (g L^{-1}), k_P= Product inhibition constant (g L^{-1}), P_{max}= Product concentration above which bacteria do not grow (g L^{-1}), X_{max} = maximum biomass concentration (g L^{-1}), h=toxic power for biomass, n= toxic power of product, α= growth associated production coefficient (g Product g $cell^{-1}$), β= non-growth associated production coefficient (g Product g $cell^{-1}h^{-1}$), Y_{XS}= biomass on carbon substrate Yield (g cell g^{-1} substrate), Y_{PS}= product on carbon substrate Yield (g cell g^{-1} substrate), m= maintenance energy coefficient (h^{-1}).

3.3.   CONTINUOUS MODEL DEVELOPMENT

The process of lactic acid production from wheat flour proposed in this work is innovative. Indeed, the type of microorganism, the substrate and the steps proposed have never been used before. In consequence, there is no model available in the literature.

As it was mentioned before, our modelling approach focuses on the SSPHF (simultaneous saccharification, proteins hydrolysis and fermentation) step of the process.

Before introducing our model, some hypotheses taken into account on its development must be presented. Amino acids from wheat flour are not considered in the model as their modelling is complex and they were assumed to be in excess (non limiting substrate). Thus, we consider the general case where glucose maybe the limiting substrate (the carbon source). It is simultaneously produced from maltose and consumed by the bacteria, thus mechanisms involved in maltose transformation and in lactic bacteria metabolism must be taken into account in the mathematical modelling approach.

In the continuous operation, all variables, *X, S, P* and *M* remain constant once the steady state regime is reached. Nevertheless it is necessary to model the transition phases by means of dynamical equations. The mass balance equations describing the dynamics of these variables are performed for the well-stirred bioreactor presented in figure 3.1. However mixing is often not ideal in bioreactors. Therefore, the deviation from the ideal state must be assessed and quantified. The residence time distribution (RTD) method is one of the ways of characterizing the non-ideal behaviour of the reactor, ensuring a good representation of the phenomena occurring in it. The study of the resident time distribution was performed for the studied system and is presented in appendix B.1. It was found that the reactor has a dead volume of 9% that was taken into account in our modelling approach. The actual dilution rate (ratio between the flow rate and the net volume of the reactor) was calculated considering that the effective volume is 0.91 times the total volume of culture broth. In the following the development of the dynamic equations to describe the *X, P, S* and *M* variations is presented.

3.3.1.   *Growth model for Lactobacillus coryniformis subsp. torquens*

3.3.1.1.   *Substrate effects*

The mass balance to the biomass (bacteria) is represented by equation (3.1). In order to formulate the growth kinetic model, it was necessary to study the system's behaviour experimentally to identify possible limitation or inhibition effects on bacteria growth. Substrate limitation and inhibition effects were the first studied. Batch experiments at different initial glucose concentrations ranging from 10 to 80 g L^{-1} were performed as it facilitates the identification of the growth rate kinetics. The results are presented in appendix B.2.

No substrate limitation or inhibition was detected in the range of concentrations tested. Therefore, as no inhibition effect was observed, we used a simplified Monod kinetics taking only into account the substrate limitation effect, so that it can be used in a broader set of conditions than those of this work. This kinetics is reminded hereafter:

$$\mu = \mu_{max} \frac{S}{k_S + S}$$

Generally k_S has very low values, thus relatively low concentrations of glucose are sufficient for μ to reach its maximal value μ_{max}. Some values of k_S reported in the literature are presented in table 3.2 for different lactic acid bacteria strains. For the same strain in Pinelli's work (Pinelli, et al., 1997), the glucose concentration must be lower than 0.016 gL^{-1} to reduce the growth rate at a half of its maximal value. It proves that bacteria need very low glucose concentrations to grow.

Lactobacillus coryniformis subsp. *torquens* DMS 20004 having a significant amylolyitic activity, is capable of producing enzymes that transform sugar starch into glucose. As a result, even when there is no glucose directly available in the bioreactor, the bacteria can still grow and produce lactic acid but at smaller rates.

It was then impossible to determine the value of k_S with our experimental results. The impact of this parameter on the model will be evaluated later in this chapter (see section 3.4.1.1.).

Table 3.2 Half-saturation constant values reported in the literature for the Monod kinetic.

Reference	Microorganism	μ_{max} (h^{-1})	k_S(gL^{-1})
Boonme et al. (2003)	*Lactococcus lactis*	1.1	1.32
Schepers et al. (2002)	*Lactobacillus helviticus*	0.7	0.22
Akerberg et al. (1998)	*Lactococcus lactis*	0.403	0.79
Pinelli et al. (1997)	*Lactobacillus coryniformis* subsp *torquens*	0.737	0.0160
Dutta et al. (1996)	*lactobacillus delbrueckii*	0.0694	0.0967

3.3.1.2. *Product inhibition effect*

As presented in section 3.2.1.2, many authors reported a product inhibition effect on growth in lactic acid fermentation. Most of them identified this effect in fermentation performed without pH control but some studies showed that this inhibition can also exist in fermentations in which the pH is maintained constant at values higher than lactic acid pKa. In these cases, the inhibitor molecule is the dissociated form of lactic acid, the lactate.

The batch experiments performed with pH control at 5.7 presented in chapter 2 (section 2.2.4), showed that the bacteria growth stopped at 23 h when the glucose concentration in the reactor was still high (about 40-45 gL^{-1}) and the concentration of lactate was about 40 gL^{-1}. It is illustrated on figure 3.2.
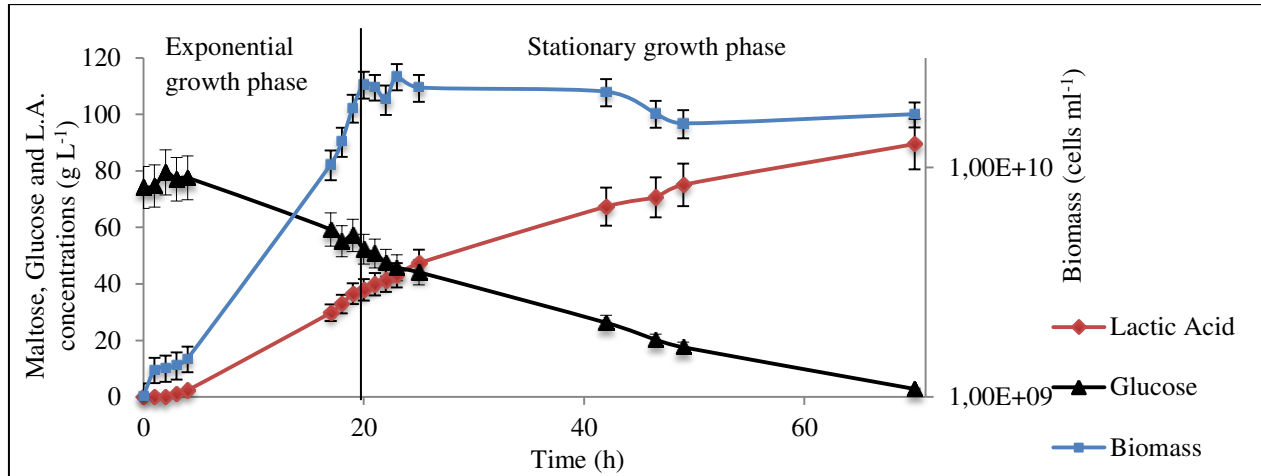
Figure 3.2 Evolution ofBiomass, glucose and lactic acid concentrations with time for a SSPHF in a 5 L reactor with pH regulated at 5.7. Inhibition effect by the lactate.

Many growth rate models were considered for describing this inhibition effect in our work. Indeed, several kinetic models were tested by comparing experimental data to model results. The model proposed by (Monteagudo, et al., 1997) matched at best the experimental data obtained during the transition between exponential and stationary growth phases in our experiments (equation (3.9)).

In contrast in all our experiments, a significant stationary phase with a small decline in cell concentration afterwards was observed after 72 h of fermentation, while bacteria continued to produce lactic acid at high rates. When applying the model proposed in equation (3.9), it did not match well our experimental data in the deceleration phase (after the stationary phase of growth). Therefore, we used the model proposed by (Kumar Dutta, et al., 1996), in which an exponent n, representing the toxic power of lactic acid was added:

$$\mu = \mu_{max} \frac{S}{k_s + S} \left(1 - \frac{P}{P_{max}}\right)^n \qquad (3.10)$$

The n value should be chosen carefully as it has an important impact on the product inhibition term. For this reason, the impact of the n value on the inhibition term ($1-P/P_{max}$) was studied.

Figure 3.3 illustrates the inhibition term as a function of the product concentration for different n integer values. To trace this figure, the P_{max} value was fixed to 45 g L^{-1}(the mean lactic acid concentration value above which bacteria did not grow in a set of experiments).

The n value must be odd in order to model the bacteria growth deceleration after the stationary phase. The higher the n odd value, the later the deceleration phase occurs. It is more consistent with experimental results obtained in this work. The choice of this parameter will be discussed in the parameter identification section (3.4).
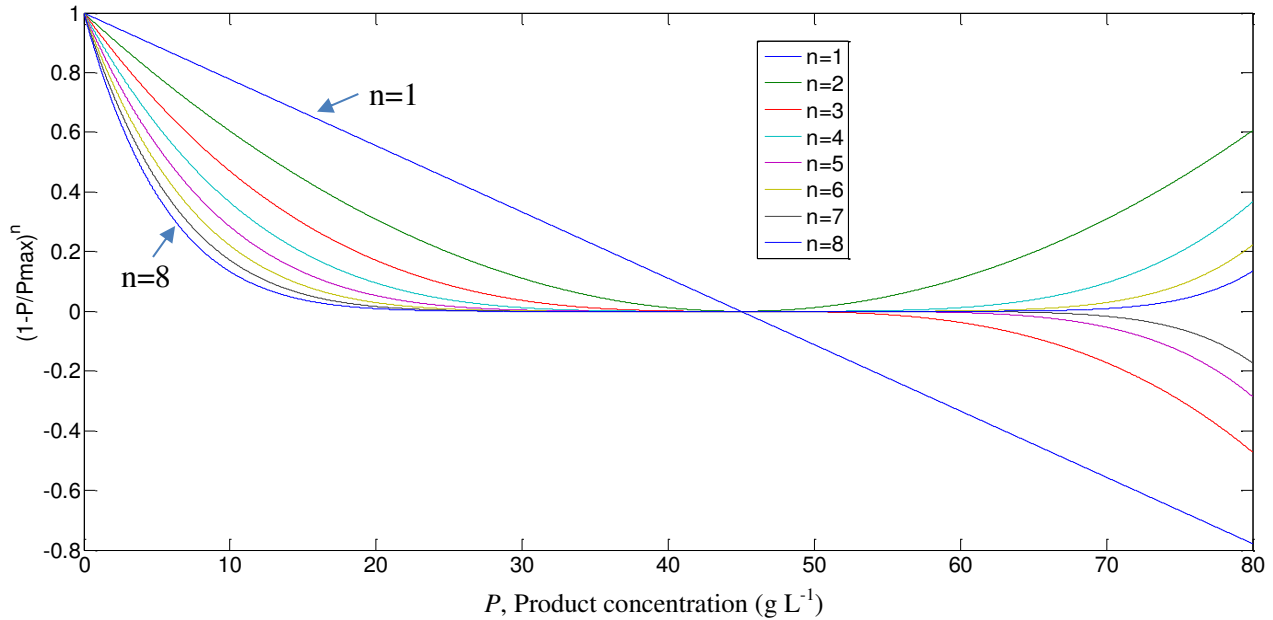
Figure 3.3 Effect of the value of n on the inhibiton term.

In this study, the considered mass balance of the biomass concentration was the one illustrated in equation (3.1) with μ represented by equation (3.10).

3.3.2.   *Product formation model*

Experimental data from different batch experiments (Figure 3.2) showed that lactic acid is also produced in the stationary growth phase. Nevertheless, as the latter phase does not occur in continuous operation (bacteria are continuously growing), modelling the lactic acid production in the stationary growth phase is not considered.

The model developed for the batch SSPHF fermenter is presented in appendix B.3. This model considers the lactic acid production in the stationary growth phase.

The model used to describe the production rate in the continuous SSPHF bioreactor is the one presented in equation (3.20). The mass balance of the product concentration is then, the following:

$$\frac{dP}{dt} = \frac{Y_{XS}}{Y_{PS}} \mu X - DX \qquad (3.25)$$

Equation (3.25) describes the lactic acid dynamics; the first term represents the production of lactic acid associated to bacteria growth and the second one refers to the dilution effect. It should be noticed that the production rate (the first term in the equation) is directly associated to the growth rate by means of the yields.

3.3.3. Substrates utilization

The development of the model describing the substrate consumption received particular attention as there are two kinetics to consider: maltose hydrolysis and fermentation. In fact, after the liquefaction and SSPH steps, besides maltose and glucose there are other sugars with longer chains that can be hydrolyzed to produce glucose. Nevertheless, as they are in low concentrations (compared to maltose and glucose), they were neglected. Consequently, only maltose and glucose dynamics were considered.

3.3.3.1. Maltose dynamics

A first order law was chosen to describe the maltose hydrolysis kinetics, similar to the proposed by (Akerberg, et al., 1998) who described the starch degradation kinetics. The obtained expression is the following:

$$r_M = -k_M M \qquad (3.26)$$

where r_M is the maltose degradation rate (g L^{-1} h^{-1}), k_M (h^{-1}) is an empirical parameter defined as the maltose degradation constant (that depends mainly on the temperature) and M is the maltose concentration. Since temperature is maintained constant in this study (regulated to 30°C in all experimental assays), the kinetic parameter k_M is then constant. The mass balance of maltose in the continuous bioreactor leads to:

$$\frac{dM}{dt} = -k_M M + D(M_0 - M) \qquad (3.27)$$

where M_0 represents the maltose concentration in the feed of the bioreactor. The first term represents the first order maltose hydrolysis kinetics, the second term the difference between maltose input and output with inlet and outlet flows, respectively.

3.3.3.2. Glucose dynamics

Glucose is simultaneously produced from maltose and consumed by the bacteria. Various substrate utilization models have been presented in the previous section. We consider a consumption growth-associated model (equation (3.23)) neglecting the maintenance term and introducing a term of production from maltose. The glucose mass balance in the SSPHF bioreactor leads to:

$$\frac{dS}{dt} = -\frac{1}{Y_{PS}} \mu X + k_M M + D(S_0 - S) \tag{3.28}$$

The first term represents the glucose consumption by bacteria, the second term considers the glucose formation from maltose hydrolysis and the final ones represent the glucose input and output with inlet and outlet flows, respectively.

3.3.4. *Continuous model overview*

To summarize all previous developments, the model developed to describe the variations of the concentrations of biomass, glucose, maltose and lactic acid in the continuous SSPHF reactor is described by the following four differential equations:

$$\frac{dX}{dt} = \mu X - DX$$

$$\frac{dP}{dt} = \frac{Y_{XS}}{Y_{PS}} \mu X - DP \tag{3.29}$$

$$\frac{dS}{dt} = -\frac{1}{Y_{PS}} \mu X + k_M M + D(S_0 - S)$$

$$\frac{dM}{dt} = -k_M M + D(M_0 - M)$$

with

$$\mu = \mu_{\max} \frac{S}{k_S + S} \left(1 - \frac{P}{P_{\max}}\right)^n$$

where *X, P, S* and *M* are the biomass, lactic acid, glucose and maltose concentrations (g L^{-1}), μ the growth rate (h^{-1}), γ the production rate (g L^{-1} h^{-1}), μ_{max} the maximum specific growth rate (h^{-1}), k_S the half-saturation constant (g L^{-1}), P_{max} the product concentration above which bacteria do not grow (g L^{-1}), *n* the toxic power of product, Y_{XS} the biomass on carbon substrate yield (g cell g^{-1} substrate), Y_{PS} the product on carbon substrate yield (g cell g^{-1} substrate), k_M the maltose degradation constant (h^{-1}) and M_0 and S_0 the maltose and glucose concentrations feeding the bioreactor (g L^{-1}) , respectively.

The following parameters must then be determined for the considered fermentation conditions: parameters involved in the growth rate kinetics (μ_{max}, k_S, P_{max} and n), yields Y_{XS}, and Y_{PS} and the kinetic constant k_M.

3.4. PARAMETERS IDENTIFICATION

Once the model is defined, it is necessary to assign a numerical value to the parameters. These values can be based on *a priori* knowledge (values proposed in the literature) or derived from experimental data. As the process is complex and new, there are few parameter values available in the literature. Given the existence of nonlinearities in the model, the parameter identification is a difficult task.

In order to determine the model parameters, a dedicated identification strategy was proposed. In a first step, this strategy is based on the study of the parametric sensitivity of the model. This study identifies the most influential parameters, depending on the scenario used. This method also provides a temporal profile of the sensitivity of the model with respect to its parameters. This simplifies the parameter identification procedure by fixing the values of some parameters (less influent ones) to those found in the literature. In a second step, the set of parameters considered as the most influent is identified by a nonlinear least squares procedure considering the simultaneous estimation of all remaining parameters. This approach was developed by Rocha (2003) for the identification of a culture model of *E.coli* and is further described in the following sections.

3.4.1. Identification strategy

3.4.1.1. Sensitivity analysis

The sensitivity analysis is a rigorous approach which allows a better characterization of the model used. Moreover, this analysis also helps to guide the choice of identification protocols, focusing the identification experiments on the determination of the most influential parameters (Hafidi, 2008).

3.4.1.2. Sensitivity functions

Let $x_i, i = \overline{1, n}$ the n state variables of the considered model and $\theta_j, j = \overline{1, p}$ the p model parameters. The sensitivity functions of the model with respect to the parameters are defined by: $\partial x_i / \partial \theta_j$. These functions can be obtained after integration of the equations $\dfrac{d}{dt}\left(\dfrac{\partial x_i}{\partial \theta_j}\right)$ using the following equality:

$$\frac{d}{dt}\left(\frac{\partial x_i}{\partial \theta_j}\right) = \frac{\partial}{\partial \theta_j}\left(\frac{dx_i}{dt}\right) \qquad (3.30)$$

The states dynamics are given by:

$$\frac{dx_i}{dt} = f_i(x,u,\theta) \qquad (3.31)$$

where f_i are nonlinear functions and represent the n differential dynamics of the state variables x_i. Thus, from equations (3.30) and (3.31), it comes:

$$\frac{d}{dt}\left(\frac{\partial x_i}{\partial \theta_j}\right) = \frac{\partial f_i}{\partial \theta_j} + \sum_{k=1}^{n}\frac{\partial f_i}{\partial x_k}\frac{\partial x_k}{\partial \theta_j} \qquad (3.32)$$

Therefore, the determination of the sensitivity functions is equivalent to solving an ordinary differential equations system of dimension n x p. However, the model parameters can have quite different magnitude orders, generating numerical difficulties during the sensitivity analysis. To solve this problem, it is better to normalize the sensitivity functions by considering $\theta_j\left(\partial x_i / \partial \theta_j\right)$ (Huang, 2007). The latter expression is referred to as normalized sensitivity function.

The calculation of the normalized sensitivity functions classifies the parameters according to their influence on the variables states, and thus determining the most influential parameters. Only the latter are identified according to the identification strategy proposed. This provides an easier parametric identification procedure.

3.4.1.3.   Determination of parameters to identify

Expressions of sensitivity functions of the continuous model presented in the set of equations (3.29) are obtained from equations (3.30) to (3.32) leading to:

$$\frac{d}{dt}\left(\frac{\partial x_i}{\partial \theta_j}\right) = \frac{\partial f_i}{\partial \theta_j} + \frac{\partial f_i}{\partial X}\frac{\partial X}{\partial \theta_j} + \frac{\partial f_i}{\partial S}\frac{\partial S}{\partial \theta_j} + \frac{\partial f_i}{\partial P}\frac{\partial P}{\partial \theta_j} + \frac{\partial f_i}{\partial M}\frac{\partial M}{\partial \theta_j} \qquad (3.33)$$

where $\theta_j = \left[\mu_{max}, k_S, P_{max}, n, Y_{XS}, Y_{PS}, k_M\right]$ is the parameters vector, $j = \overline{1,7}$. The state variables x_i, $i = \overline{1,4}$ represent the states *X, S, P* and *M*. As mentioned before, we focus on the determination of the normalized sensitivity functions in order to easily classify the parameters according to their influence. As the analytical determination of equation (3.33) is very complex, they are calculated numerically using the program CVodes (Serban & Hindmarsh, 2005) in the Matlab[TM] environment.

3.4.1.4.   *Sensitivity analysis for the continuous bioreactor*

The scenario considered for the sensitivity analysis consists in a continuous SSPHF bioreactor with a constant dilution rate equal to 0.12 h^{-1}. The initial conditions for the simulation were $X=1$ gL^{-1}, $S=120$ gL^{-1}, $P=15$ g $L^{-1}$and $M=50$ gL^{-1}. All these values are related to a specific operating point that will be justified later in chapter 5 and considered for the control strategy. The evolution of the different state variables with time is presented in figure 3.4. It shows transition behaviour of states in the bioreactor. The variables tend to reach their steady state after approximately 20 h.

Figure 3.5 represents the normalized sensitivity functions ($\theta_j (\partial x_i / \partial \theta_j)$) of the 7 parameters involved in the model equations. Only the parameter k_M has an effect on the maltose concentration as it can be expected due to its kinetics structure. Indeed, this state only depends on k_M, on its own concentration and on the dilution rate. All the studied parameters influence the biomass, glucose and lactic acid concentration variations at different grades. The parameters are ranked according to their influence on each state variable in table 3.3.
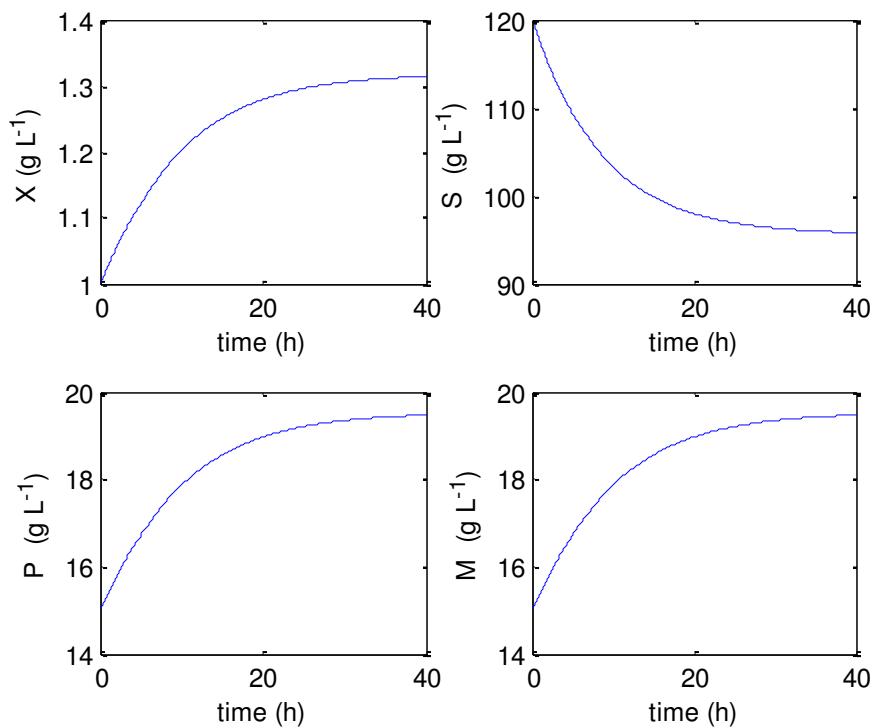
Figure 3.4 States evolution with time for sensitivity analysis of a continuous SSPHF bioreactor.

Constant dilution rate= 0.12 h^{-1}.
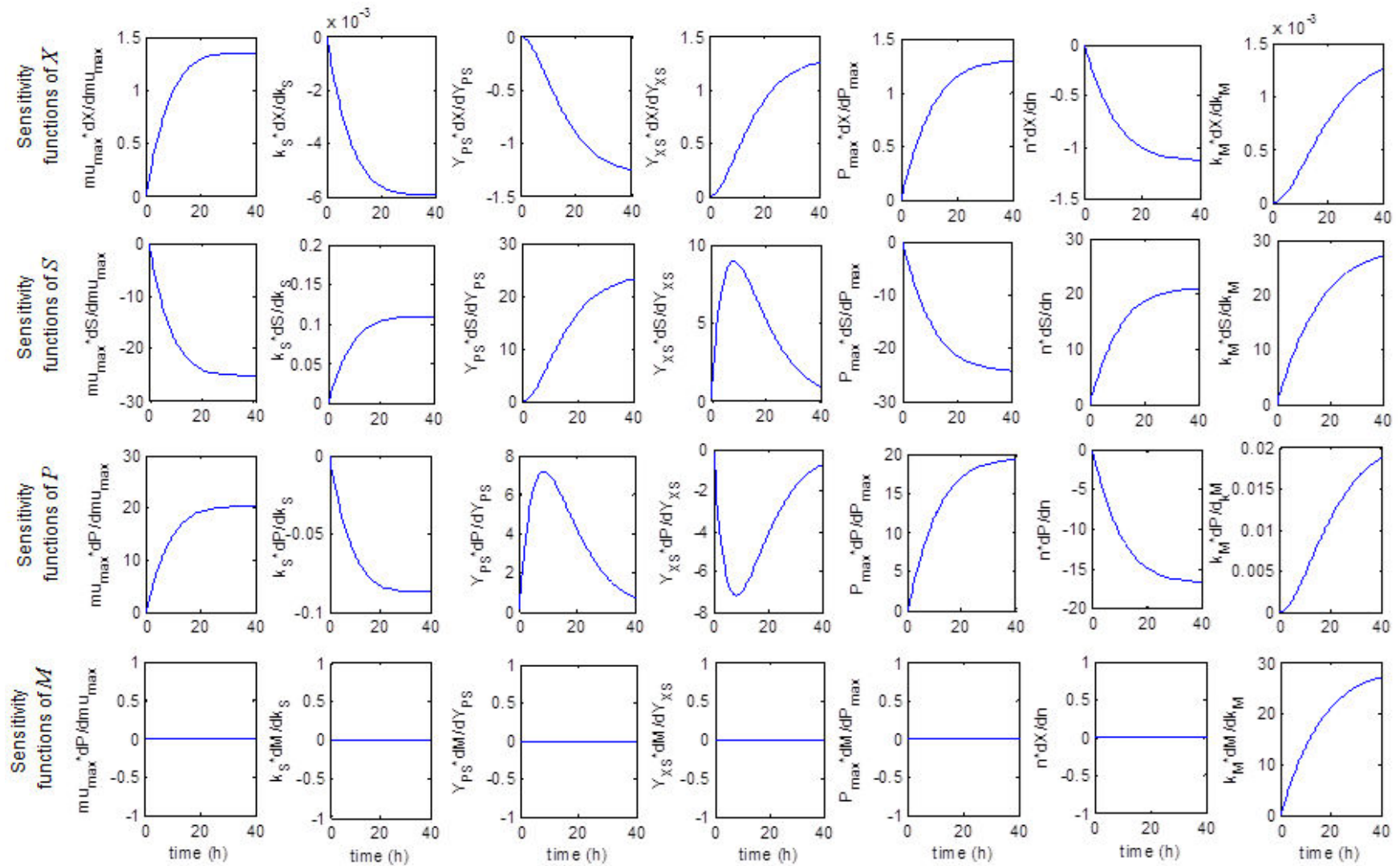
Figure 3.5 Normalized sensitivity functions of model parameters for each state variable. Continuous SSPHF bioreactor with $D=0.12$ h^{-1}.

Table 3.3 Parameters classification according to their influence on each state variable (from the most influential to the least influential). SSPHF continuous bioreactor with D=0.12 h^{-1}.

Influence on X	Influence on S	Influence on P	Influence on M
μ_{max}	k_M	μ_{max}	k_M
P_{max}	μ_{max}	P_{max}	-
Y_{PS}	P_{max}	n	-
Y_{XS}	Y_{PS}	Y_{PS}	-
n	n	Y_{XS}	-
k_S	Y_{XS}	k_S	-
k_M	k_S	k_M	-

The sensitivity functions of biomass with respect to the different parameters (first row in Figure 3.5) show that the most influential parameters on the biomass concentration are μ_{max}(its sensitivity function has the highest amplitude, 1.38) and P_{max} which has a sensitivity function with amplitude of 1.33. Both parameters are involved in the growth rate. It suggests that these parameters must be identified from the growth rate dynamics equation. The product and biomass on glucose yields have an important influence on the biomass concentration. They have both sensitivity amplitudes of 1.25. The impact of toxic power of lactic acid (n) on growth is lower (sensitivity function amplitude= 1.1). The least influential parameters on X are k_S and k_M (each one with sensitivity function amplitude around 0.001). It can be explained by the high initial glucose concentration used for the simulation (which will be always the case in our work) and by the fact that maltose does not have a direct influence on the biomass dynamics so the k_M value is not relevant in cells dynamics (for the tested culture conditions).

Concerning the impact of parameters on S (second row in Figure 3.5), the most influential parameter is k_M (with sensitivity function amplitude of 28). It is not surprising considering the contribution of maltose hydrolysis on the glucose concentration. The influence of μ_{max} and P_{max} on the glucose concentration is high (with sensitivity function amplitudes around 25), so their accurate identification is important. The other parameters have relatively high influence on S at different levels in exception of k_S which has a very low influence (with sensitivity function amplitude equal to 0.105).

The most influent parameters on P (third row in Figure 3.5) are those related to the growth rate kinetics, μ_{max} ,P_{max} and n that have sensitivity function amplitudes around 20. The biomass and product on glucose yields have less impact on this variable (sensitivity function amplitudes around 7). As for the biomass, the least influent parameters on P are k_M and k_S (with sensitivity function amplitudes equal to 0.017 and 0.085, respectively).

The evaluation of the magnitude of the sensitivity functions allowed selecting the parameters that are influential on the model. In conclusion, the parameter k_S is not influent on any of the states (for the range of glucose concentrations used in this work). So, its identification will not be performed since it will lead to a result with a poor accuracy. Its value is then fixed to the mean of values reported in the literature and summarized in table 3.2. This value is 0.5 gL^{-1}.

The parameter identification of the toxic power (n) in the growth rate kinetics seems complex due to the equation structure; its value will be fixed to 3. This value was chosen taking into account its impact on the product inhibition term in the growth rate equation (see section 3.3.1.2) and values reported by other authors working on lactic acid fermentation (Akerberg, et al., 1998)(Kwon, et al., 2001), who found power toxic values of 2.06 and 2.68, respectively.

Summarizing, the parameters to be identified were reduced to five (μ_{max}, P_{max}, Y_{PS}, Y_{XS} and k_M). The strategy used for their identification is presented in the next section.

3.4.2.   Towards an identification strategy

The estimation of the set of parameter values is performed considering experimental data collected from experiments described later in the materials and methods section (3.5.1). The model parameters were determined by minimizing the following objective function.

$$RSE = \sum_{i=1}^{N} w_X \cdot (X_{i,\exp} - X_{i,cal})^2 + \sum_{i=1}^{N} w_P \cdot (P_{i,\exp} - P_{i,cal})^2$$
$$+ \sum_{i=1}^{N} w_S \cdot (S_{i,\exp} - S_{i,cal})^2 + \sum_{i=1}^{N} w_M \cdot (M_{i,\exp} - M_{i,cal})^2$$

(3.34)

In equation (3.34), RSE is the total residual sum of squares, the sum of squares of errors between the calculated model values ($X_{i,cal}$, $P_{i,cal}$, $S_{i,cal}$ and $M_{i,cal}$,) and experimental data ($X_{i,exp}$, $P_{i,exp}$, $S_{i,exp}$ and $M_{i,exp}$,). N is the number of observations. w_X ,w_P, w_S, w_M are weighting factors tuned to normalize all terms in equation (3.34), they were fixed at 100, 1, 1 and 1, respectively considering the order of magnitude of each variable.

The differential equations (3.29) based on biomass growth, substrate consumption and product formation are solved numerically (by fourth order Runge-Kutta method). The calculated data are then compared to the measured ones by computing the RSE. The parameter values that minimize RSE conduct to the best fitting of the experimental data. This can be achieved considering an approach leading to the global identification of all the parameters, using nonlinear least-square algorithms (e.g. Levenberg-Marquardt algorithm,(Fletcher, 1987)). MATLAB R2014 (MathWorks, US) was used to solve the optimization problem and to simulate the fermentation behaviour. The function 'lsqnonlin' was used for non-linear least square minimization of differences between experimental and calculated data.

The optimization problem presented in equation (3.34) is however hard to solve, since there are several sub-optimal solutions (either because of the measurements accuracy or because of model mismatch). The determined optimal solution highly depends on the initialization of the parameter values in the optimization algorithm. The initialization could be determined by literature data, but unfortunately very limited literature data are available for the considered

bacteria. Thus, in order to solve this optimization problem, a specific identification procedure is developed.

The proposed three-step identification procedure is summarized in figure 3.6. The main idea is to determine each parameter value independently, using each dynamics separately. In order to reduce the complexity of the identification procedure, the approach considered is to determine the parameters values in the transient state. Indeed, the identification of parameters at steady state seems difficult as the dynamic terms in equations (3.29) are cancelled. For this reason, the identification was performed in transient phase, in particular here for simplification, during batch operation phases where *D=0*. This approach is not new, the parameters identification in batch mode for further validation in continuous fermentation was also considered by Boonmee et al. (2003).
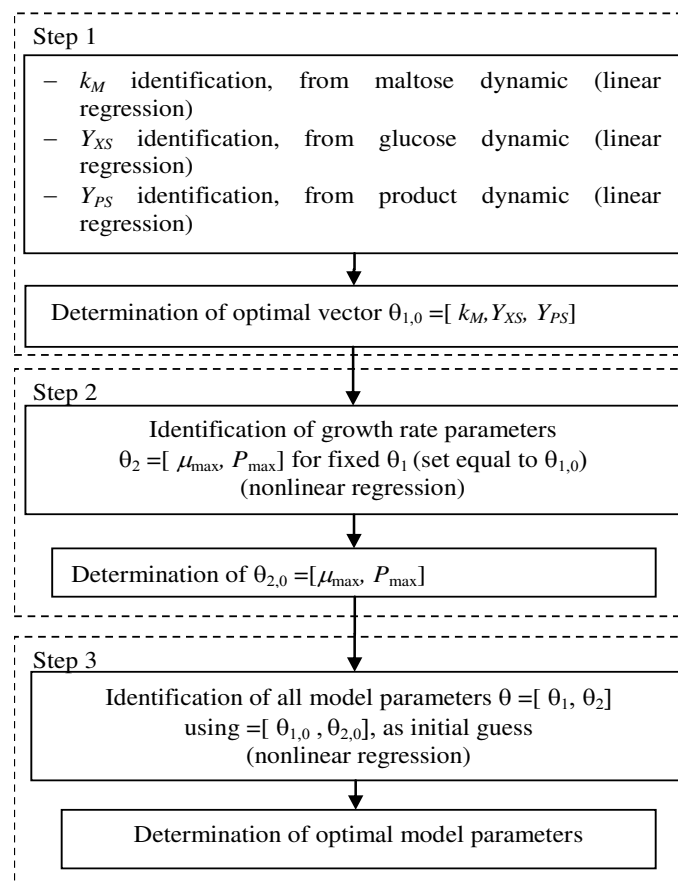
Figure 3.6 Identification procedure proposed to determine the model parameters.

The parameters involved in glucose, maltose and lactic acid dynamics (k_M, Y_{XS} and Y_{PS}) can be determined by linear regressions which do not need any initialization as it will be detailed later. Only the growth rate parameters have to be identified with a nonlinear least-square algorithm, leading to a non-convex optimization problem. In this case, the other parameters (k_M, Y_{XS} and Y_{PS}) are fixed to the values obtained from linear fitting. Finally, the global problem in equation (3.34) is solved using the obtained parameter values as initial guess. In the following each identification step is described.

3.4.2.1.   Step 1: Linear regression

The sensitivity analysis showed that only one parameter, the maltose degradation constant (k_M) has an effect on the maltose dynamics, It is easier to determine the value of this parameter for the batch phases, when $D=0$. With this approach, the mass balance of maltose is only represented by its first order kinetic as follows:

$$\frac{dM}{dt} = -k_M M \tag{3.35}$$

In equation (3.35), maltose dynamics only depends on its own concentration. k_M can be then determined by linear regression from maltose concentration measurements. The time derivative of maltose concentration is approached by a finite difference method (Euler method). The discretized equation is:

$$\frac{M_{k+1} - M_k}{\Delta t} = -k_M M_k \tag{3.36}$$

where k represents the time index, and $\Delta t = (t_{k+1} - t_k)$

In the same way, the biomass on glucose yield can be determined from the glucose batch dynamics (equation (3.28)) by approaching the state derivative by a finite difference method (for $D=0$). Since the parameter k_M is also involved in the substrate behaviour, it is eliminated by adding equations (3.27) and (3.28) leading to:

$$\frac{d(S+M)}{dt} = -\frac{1}{Y_{XS}} \frac{dX}{dt} \tag{3.37}$$

This procedure allows decreasing the effect of the uncertainty on k_M when determining the biomass on glucose yield coefficient. From equation (3.37) it can be noticed that Y_{XS} can still be derived by linear regression (by computing the derivative by a finite difference approach), based on biomass, glucose and maltose concentration measurements as follows:

$$\frac{S_{k+1} + M_{k+1} - (S_k + M_k)}{\Delta t} = -\frac{1}{Y_{XS}} \frac{X_{k+1} - X_k}{\Delta t} \tag{3.38}$$

with the same notation as in equation (3.36). The product on glucose yield Y_{PS} can be determined from equation (3.25) by linear regression, with the same method:

$$\frac{P_{k+1} - P_k}{\Delta t} = \frac{Y_{PS}}{Y_{XS}} \frac{X_{k+1} - X_k}{\Delta t} \tag{3.39}$$

with the same notations as in (3.36).

In the first step of the identification procedure, three parameters are already determined by linear regression and using all available experimental data, namely k_M, Y_{PS}, and Y_{XS}.

3.4.2.2.   Step 2: Growth parameters identification

The growth rate parameters, μ_{max} and P_{max}, are identified by nonlinear regression, solving the optimization problem (3.34) and fixing the other parameters values to those obtained in step 1. The initial values are chosen randomly in an interval based on typical values found in the literature (a large search domain is taken into account since very few data are available for the considered bacteria). These intervals were fixed at [0, 1] (h^{-1}) for μ_{max} and [0,120] (gL^{-1}) for P_{max}.

3.4.2.3.   Step 3: Global parameters identification

Finally, the optimization problem in equation (3.34) is solved starting from the model parameters determined in steps 1 and 2.

3.5.   EXPERIMENTAL VALIDATION

3.5.1.   Materials and methods
3.5.1.1.   Bioreactor description

The studied set-up consists in a continuous stirred tank reactor (CSTR) (Figure 3.7). This figure presents all bioreactor entries and outputs as well as the available offline and online measurements. The bioreactor is a 5L tank in stainless steel 316L (Roughness <0.8 µm mirror polished). There are five controlled variables: temperature, pH, culture broth level in the bioreactor, agitation and feed flow rate.

The temperature is controlled by a PID controller using a temperature sensor. When the temperature measured in the fermenter is higher than the setpoint, the controller opens a valve that allows cold water to flow in the exterior jacket of the bioreactor. In the other way, if the temperature is lower than the setpoint, the controller opens another valve to allow steam passing around the bioreactor.

The pH is also regulated by a PID controller. When the pH value is lower than the setpoint, the controller activates a peristaltic pump to add sodium hydroxide to the broth. Otherwise, if the measured pH is higher, the controller activates another peristaltic pump which allows the addition of sulfuric acid into the bioreactor.

The broth level in the reactor is controlled using a foam sensor situated just above the desired level. When the level of the broth reaches the foam sensor, this indicates a broth accumulation. The foam sensor sends a signal to a PID controller, which activates the peristaltic pump P2 (with constant flow) which controls the output flow (LC in Figure 3.7). In this way, the broth level is maintained constant, whether or not the input flow changes.

A mechanical overhead stirring device ensures the medium mixing and is regulated by a PID controller which adjsuts the motor speed of the agitator to a fixed setpoint value.

Finally the feed flow rate is regulated by a peristaltic pump with variable rotation speed.
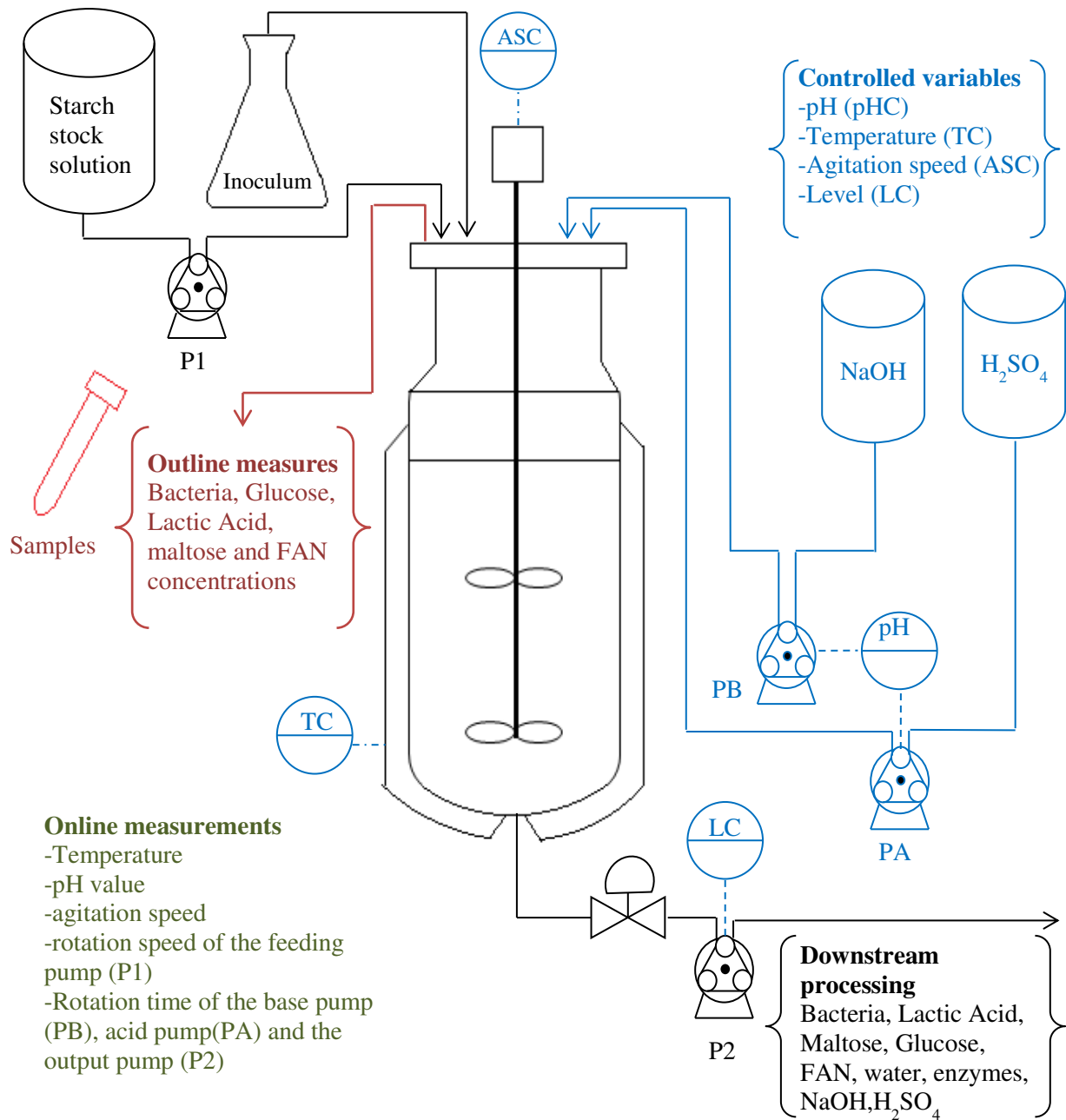
Figure 3.7 Scheme of the 5L bioractor used for the SSPHF step. In red the outline measurements, in blue the controlled variables and in black the feeding and output flows.

The online measurements available in the bioreactor, other than the ones used for the operation of the PID controllers described earlier, are related to the peristaltic pumps. The base, acid and output pumps (PB, PA and P2, respectively) work at a constant rotation speed (29 rpm). Their rotation speed cannot be modified, so in order to change the flow rate in these pumps, it is necessary to modify their rotation duration. They are designed to work in a control loop as described before. Consequently, they do not run all the time, depending on the

controller action. So in order to calculate the mean flow rate passing in the pumps, it is necessary to sum the running times over a certain period. The bioreactor software has a totalizer fonction which allows recoding the rotation times in a time basis and theses results are used to determine the flow rate in each pump.

The sole pump with variable flow in the set-up is the medium feeding pump (P1 in Figure 3.7). This pump runs at a rotation speed value assigned by the operator but it can also be part of a control loop. Its use will be discussed in chapter 5 when the control design will be presented.

3.5.1.2.   SSPHF Experiments description

In this work, the liquefaction and SSPH steps were perfomed in batch mode, whereas only the SSPHF step was performed in continuous mode. Two types of bioreactors are used, two 5 L bioreactors for the continuous experiments and a 12 L bioreactor to produce the wheat solution stock necessary to feed the continuous process (steps described afterwards). The SSPHF bioreactors are equipped with Baie inox controllers (Global Process Concept, La Rochelle France), in order to assure the control of temperature 30°C, pH 5.7, agitation 150 rpm, feed flow and liquid level. A schematic diagram of the bioreactors configuration is given in Figure 3.8. After batch liquefaction and SSPH, the stock solution is maintained at 12°C.
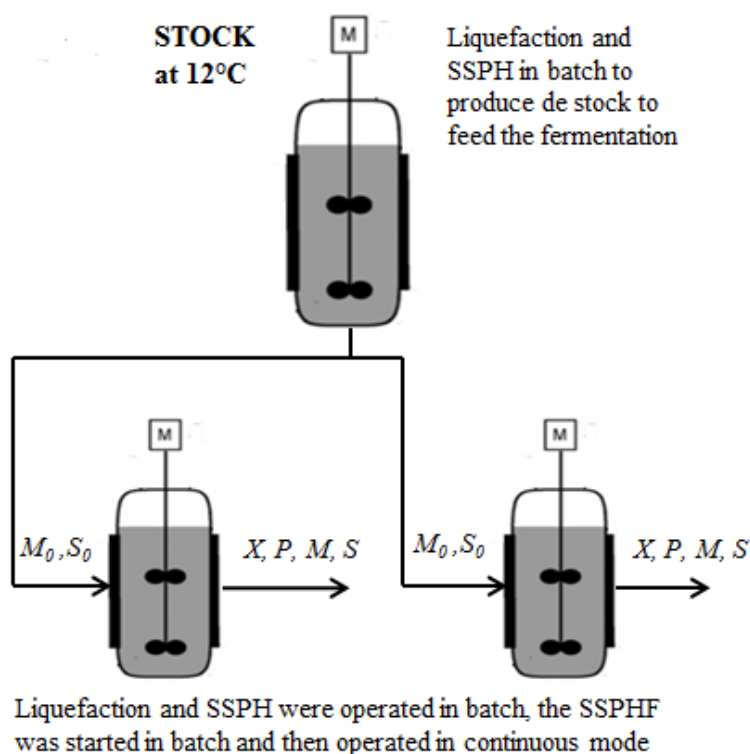
Figure 3.8 Bioreactors configuration to perform the continuous SSPHF.

The SSPHF is performed in two 5L bioreactors in parallel with the same conditions for duplication. The SSPHF step is started in batch mode and then operated continuously with the

stock solution as feed. In the following, a description of the steps performed in the continuous bioreactor (5 L) is presented.

Two experiments were performed in order to acquire experimental data in batch and continuous SSPHF, necessary for the parameters identification. In the first experiment, four dilution rates were tested: 0.05, 0.1, 0.15 and 0.31 h^{-1}. These dilution rates were chosen considering model parameters obtained in the batch modelling (see appendix B.3.) and a steady state analysis of the continuous model that will be further discussed in chapter 5. With this approach the optimal range of dilution rates obtained is comprised between 0.01 and 0.02 h^{-1}. We decided also to test dilution rates lower (0.05 h^{-1}) and higher (0.31 h^{-1}) than those obtained as the optimal ones. The interest of testing different dilution rate is to identify experimentally those which allow obtaining the highest productivities.

During the first 15 h, the bioreactor was operated in batch mode, then the first dilution rate (D_1=0.1 h^{-1}) was applied during 22 h. At 37 h the bioreactor was operated in batch mode again in order to increase the lactic acid concentration during 5 h. After the second batch period, a new dilution rate (D_2= 0.05 h^{-1}) was applied. After 60 h of culture, a higher dilution rate was tested (D_3=0.31 h^{-1}) in order to decrease the lactic acid concentration in the fermenters. Finally, at 63 h, the last dilution rate (D_4=0.15 h^{-1}) was applied.

In the second experiment, the continuous fermentation was performed with two dilution rates, 0.15 and 0.2 h^{-1}. The bioreactor was operated in batch mode for the first 10 h. Afterwards, the continuous operation was started with a dilution rate D_4 that equals 0.15 h^{-1}. At 18 h, a new dilution rate D_5=0.2 h^{-1} was applied. Finally, at 24 h, the fermenter contents were diluted three times with fresh medium and then the final batch sequence was performed during 6 h. The procedure is summarized in table 3.4.

Table 3.4 Flow rates tested in experiments 1 and 2.

	Step	Designation	Duration time (h)	Dilution rate (h^{-1})
Experiment 1	1	Batch phase 1=B1	15	0
	2	continuous phase 1= D1	22	0.1
	3	Batch phase 2=B2	5	0
	4	continuous phase 2= D2	21	0.05
	5	continuous phase 3= D3	3	0.31
	6	continuous phase 4=D4	4	0.15
Experiment 2	1	Batch phase 3=B3	10	0
	2	continuous phase 4=D4	8	0.15
	3	continuous phase 5=D5	7	0.2
	4	Batch phase 4=B4	6	0

Glucose and maltose concentrations feeding the bioreactor were different in each experiment. These conditions are summarized in table 3.5.

Table 3.5 Inlet glucose and maltose concentrations in each experiment

Values(gL^{-1})	S_0	M_0
Experiment 1	125	60
Experiment 2	115	70

3.5.1.3.   *Inoculum preparation*

Lactobacillus coryniformis subsp. *torquens* DSM 20004 stored at -80°C, was grown in a MRS medium in an incubator shaker MAXQ 4000 (Thermo Scientific). A first proliferation was performed at 30°C in 200 mL culture medium and agitated at 150 rpm during 24 h. For the second proliferation, the culture was transferred to a flask containing 500 mL fresh medium and agitated during 24 h. The cells were then harvested after centrifugation (3000 g, 3 min, 20°C), resuspended in 100 mL distilled water (corresponding to 3% of the total working volume of the fermenter). This suspension was then used for the fermenter inoculation.

3.5.1.4.   *Liquefactionand (SSPH)*

The preparation of the starch solution, liquefaction and SSPH are described in section 2.2.2.1.3.

3.5.1.5.   *Simultaneous saccharification and proteins hydrolysis (SSPH)*

Once the temperature attained 50°C in the bioreactor, pH was adjusted to 5.7 and the agitation set to 150 rpm. The experimental conditions were the same presented in section 2.1.2.1.

3.5.1.6.   *Hydrolyzed wheat stock*

To feed the 5L fermenters (GPC, La Rochelle, France), a wheat solution (260 gL^{-1}) was liquefied, then hydrolyzed in a 12 L bioreactor with the conditions described before. Once the SSPH step finished, the temperature in the fermenter was decreased to 12 °C in order to stop enzymes activities. This 12 L bioreactor (GPC, La Rochelle, France) fed the 5 L bioreactors (fermenters) in parallel and continuously, in order to guarantee the same feedstock for both fermenters.

3.5.1.7.   *Analyses*

The analyses performed to determine the FAN, biomass, glucose, lactic acid and maltose concentrations are described in section 2.2.2.1.7.

3.5.2.   *Experimental results*

3.5.2.1.   *Nitrogen substrate*

In order to determine if the nitrogen substrate was limiting during the SSPHF, measurements of the free acid nitrogen (FAN) concentration were performed during the experiments. Figure 3.9 shows the evolution of the FAN concentration with time throughout the fermentation. The first 9 hours of each experiment were devoted to liquefaction and SSPH steps (without the

presence of bacteria); during these phases, the Free Acid Nitrogen (FAN) concentration was increased almost 5 times of its initial value. For the first batch phase (B1) the FAN concentration remained constant during the SSPHF step, suggesting that in this step the amino acids production rate (from wheat proteins) was equal to the consumption rate (by the cells). In the continuous phases, the FAN concentration was stable.
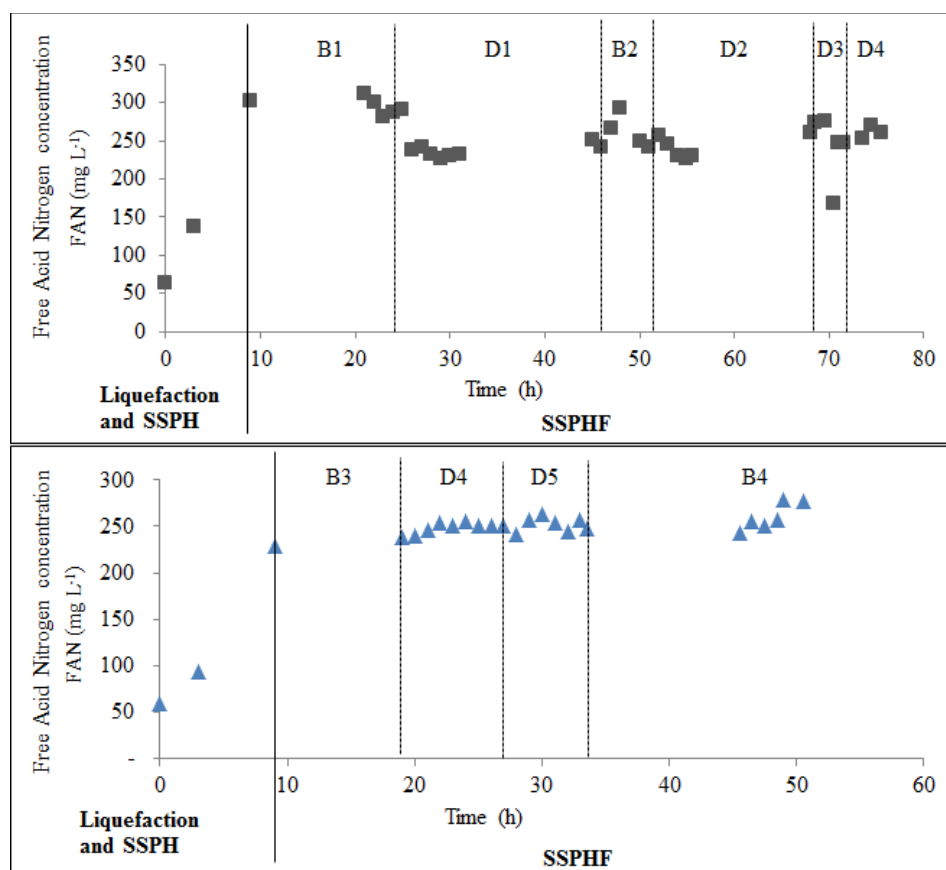
Figure 3.9 Free Acid Nitrogen concentration throughout Experiments 1(■) and 2(▲). Liquefaction and SSPH steps in the first 9 h and SSPHF step after time t=9h. Five dilution rates are tested:$D1= 0.1$ h^{-1}, $D2=0.05$h^{-1}, $D3=0.31$ h^{-1}, $D4=0.15$ h^{-1} and $D5=0.2$ h^{-1}.

3.5.2.2. Variables behaviour during experiments

The experimental results of SSPHF experiments described in the materials and methods section (see section 3.5.1.2.) are presented in figures 3.10 and 3.11.

As shown in figure 3.10 (experiment 1), the cell concentration increased during the first phase of batch operation mode B1. When the first dilution rate (D1=0.1 h^{-1}) was applied, the dilution effect slightly reduced the cell concentration; the system reached steady state after 22 h of continuous mode. The lactic acid concentration, being directly related to the bacteria growth, slightly decreased. The glucose concentration decreased at the beginning of the fermentation in the batch phase (B1) as a result of its consumption; in continuous mode its concentration remained almost constant thanks to its continuous introduction into the reactor by the feed solution and the enzymatic degradation of maltose. Maltose was consumed for glucose production during the batch period, so its concentration decreased; then in the

continuous operation, it was also fed into the reactor and its concentration increased indicating a slower consumption than its supply. The maltose concentration in the bioreactor approached the inlet maltose concentration.

At 42 h, after the second batch period (B2) where the biomass concentration increased, a new dilution rate (D2= 0.05 h^{-1}) was applied. The steady state was quickly reached and all the concentrations were constant until the end of this step. After 60 h of culture, a higher dilution rate was tested (D3=0.31 h^{-1}) in order to decrease the lactic acid concentration in the fermenters as shown in the figure. Finally, at 63 h, the last dilution rate (D=0.15 h^{-1}) was applied. The bioreactor seemed to quickly reach the steady state.

Figure 3.11 shows the experimental results for experiment 2. The bioreactor was operated in batch mode for the first 10 h of SSPHF. Then the continuous operation was started with the dilution rate D4=0.15 h^{-1}. After 8 h, the cell, lactic acid and glucose concentrations were stable. The maltose concentration slightly increased in this phase, due to its unbalanced supply to the reactor and consumption; steady state was not reached for maltose, but it seems to have no significant effect on cell, lactic acid and glucose behaviour. After 18 h of experiment, a new dilution rate D5=0.2 h^{-1} was applied; the steady state was reached fast. Finally, the final batch (B4) sequence was performed after dilution of the fermenters content with fresh medium.

The variables behaviour was as expected: in the batch phases, bacteria grew and produced lactic acid at high rates. In the continuous phases, lactic acid production rates values were higher than those obtained in previous batch experiments (see Chapter 2, section 2.2.4). It is because in the continuous operation it is possible to obtain higher productivities than in the batch one. In the experiments performed in continuous mode the production rate was around 2 g L^{-1} h^{-1}, compared to 1.0g L^{-1} h^{-1} for the previous batch experiments (see section 2.2.4). Indeed, in the latter experiments the end of the fermentation was performed in the stationary growth phase.

In the continuous phases, it was not possible to completely reach the steady state for all the tested dilution rates, and more specifically for the dilution rate D3=0.3 h^{-1} as attempted (the dilution rate was very high inducing a washout phenomenon). In this case, the exhaustion of the biomass concentration was not reached as this dilution rate was tested only during 3h and then its value was reduced (to stop the washout).

In summary, Glucose concentrations feeding the fermenter were high enough and no limitation by the substrate was observed in any experiment. The maltose concentration was high throughout the experiments. The maximal lactic acid concentration (around 30 g L^{-1}) was obtained with the lowest dilution rate tested (D2=0.05 h^{-1}) as expected.
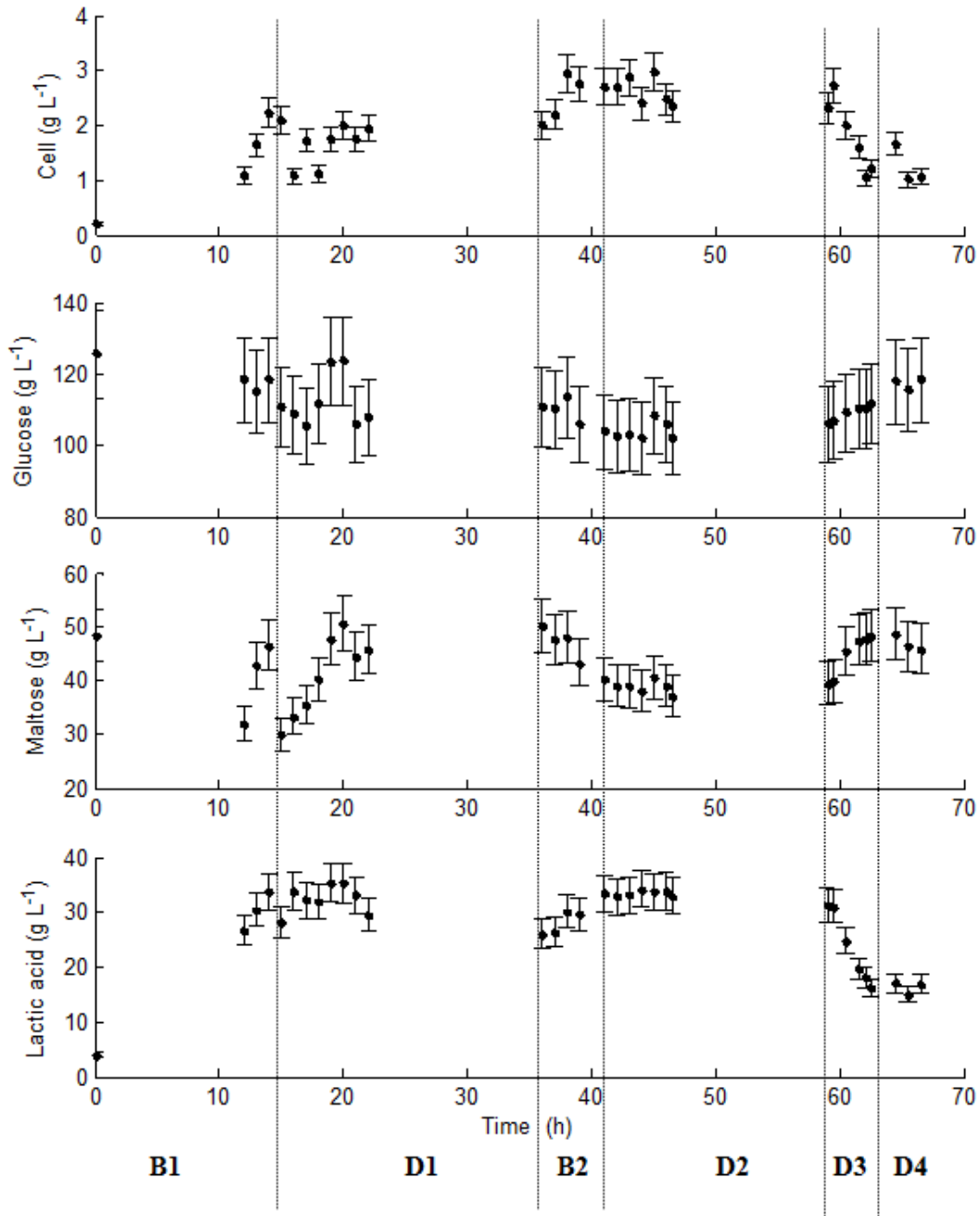
Figure 3.10 Experimental (●) cell, glucose, maltose and lactic acid concentrations for fermentation in batch and continuous operations for experiment 1. Four dilution rates are tested: D1= 0.1 h^{-1}, D2=0.05h^{-1}, D3=0.31 h^{-1} and D4=0.15 h^{-1}.
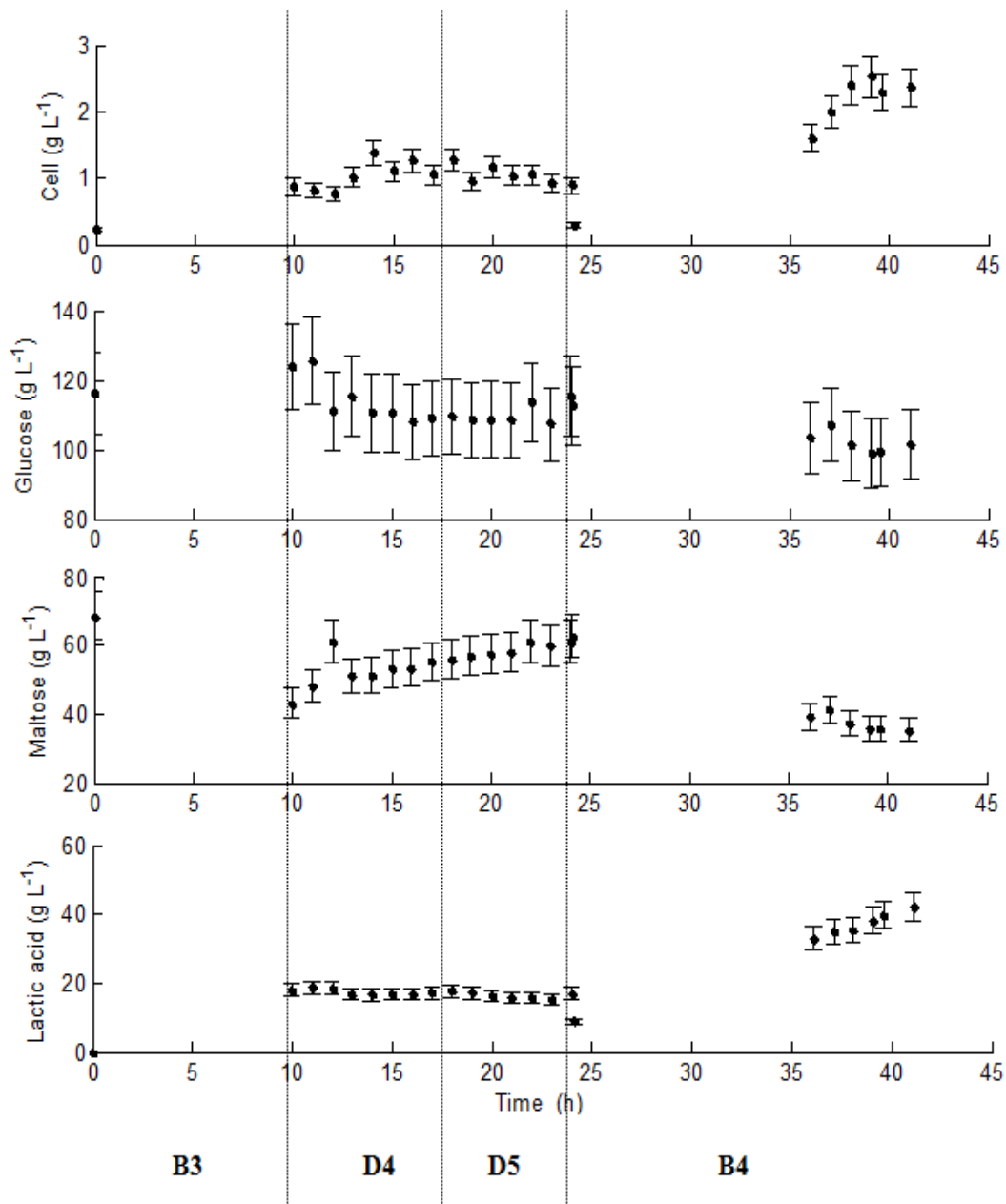
Figure 3.11 Experimental (●) cell, glucose, maltose and lactic acid concentrations for fermentation in batch and continuous operations for experiment 2. Two dilution rates tested D4= 0.15 h^{-1} and D5=0.2h^{-1}.

3.5.2.3.   *Comparison between the model and the experimental data*

The experimental data corresponding to the final batch phase of experiment 2, B4 (see table 3.4) were used to identify the model parameters. The parameters are presented in table 3.6. The identified value of μ_{max} is 0.28 h^{-1}. This value has the same order of magnitude than the one reported by Akerberg et al. (1998), 0.22 h^{-1}, obtained for another lactic acid bacteria strain but with the same substrate (whole-wheat flour). Our value is higher than the one (0.11 h^{-1}) reported by Anuradha et al.(1999) for *Lactobacillus delbrueckii* using potato starch. The μ_{max} value obtained in this work is nevertheless of the same order of magnitude.

The product inhibition effect in equation (3.10) is taken into account considering P_{max} and n, which in this work were: 98.6g L^{-1} and 3, respectively. The P_{max} value is relatively close to the results reported by Akerberg, et al., (1998) and by Kwon, et al.(Kwon, et al., 2001), who found P_{max}= 62.5 gL^{-1} and 114 gL^{-1}, respectively.

Concerning the yields obtained in this work: Y_{XS} = 0.053 g biomass g^{-1} glucose and Y_{PS} = 0.8 g product g^{-1} glucose, they are lower than those reported by (Pinelli, et al., 1997) for the same species of bacteria, but with enriched glucose media: Y_{XS} = 0.197 g biomass g^{-1} glucose and Y_{PS} = 0.990 g product g^{-1} glucose. The difference could be explained by the different composition of the culture media.

The model described satisfactorily the evolution of the variables concentrations with time for batch and continuous operations (Figures 3.12 and 3.13).

Concerning glucose concentration, the experimental data were slightly higher than the calculated values for several dilution rates, especially in experiment 2 (Figure 3.13). This could be explained by glucose production from sugars other than maltose, present in wheat, that were not taken into account in the model. Indeed, an additional experiment (data not shown) confirmed glucose production directly from starch. Therefore, our model underestimates the glucose concentrations.

The first order kinetic equation is sufficient to describe maltose dynamics, the modeled maltose concentrations are in good agreement with experimental data. The prediction of cell and lactic acid concentrations is rather good.

Table 3.6 Identified parameter values for a 5 L bioreactor with 9% death volume (Appendix B.1.)

Parameter	Identified Value
μ_{max} (h^{-1})	0.28
P_{max} (g L^{-1})	98.6
Y_{XS} (g Cell g^{-1} Glucose)	0.053
Y_{PS} (g Product g^{-1} Glucose)	0.8
k_M (h^{-1})	0.035
k_S (g L^{-1})	0.5 (fixed from literature)
n	3 (fixed after several trials)
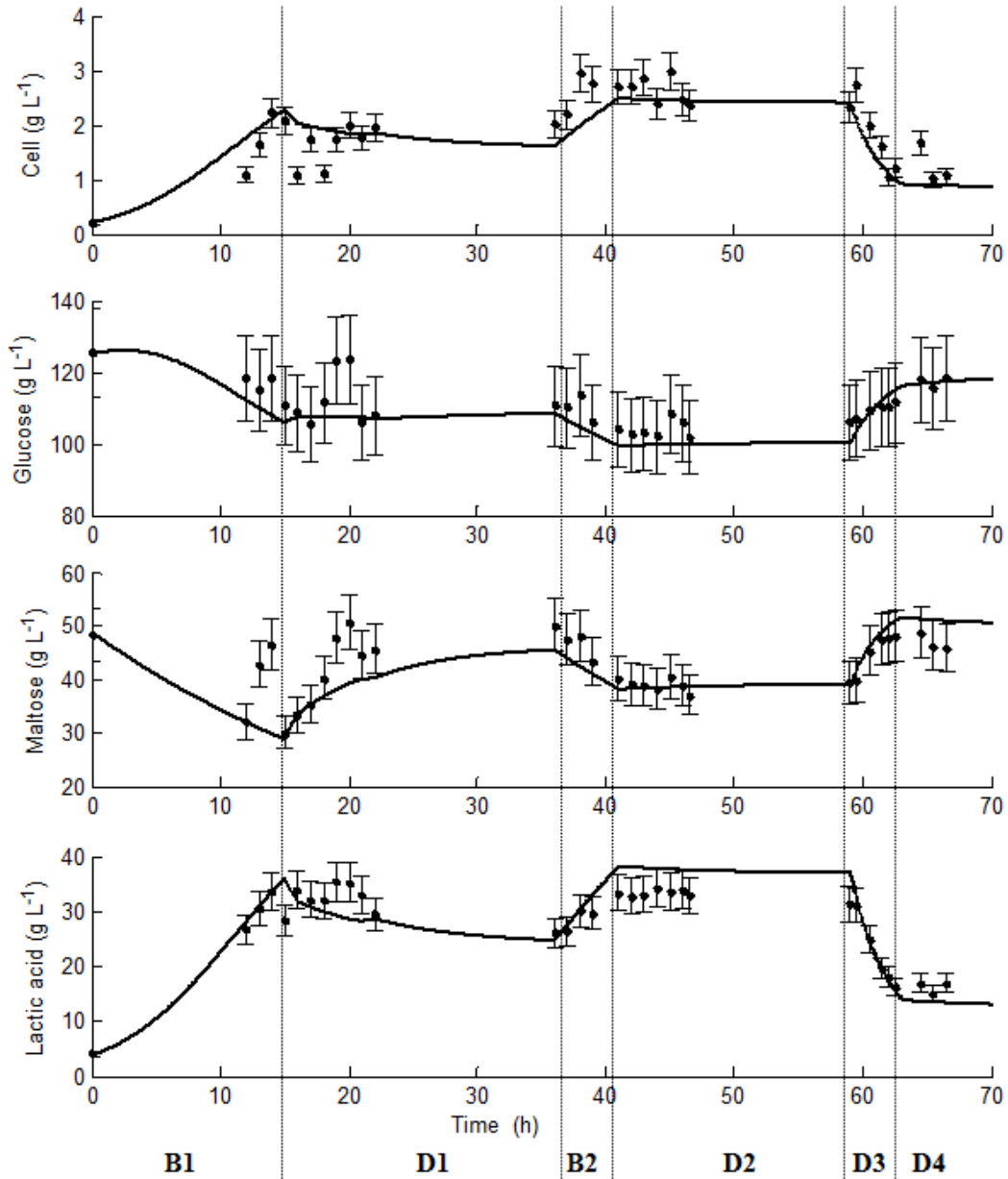
Figure 3.12 Experimental ($\bullet$) and simulated ($\longrightarrow$) cell, glucose, maltose and lactic acid concentrations for fermentation in batch and continuous operations for experiment 1. Four dilution rates are tested: D1= 0.1 h^{-1}, D2=0.05h^{-1}, D3=0.31 h^{-1} and D4=0.15 h^{-1}.
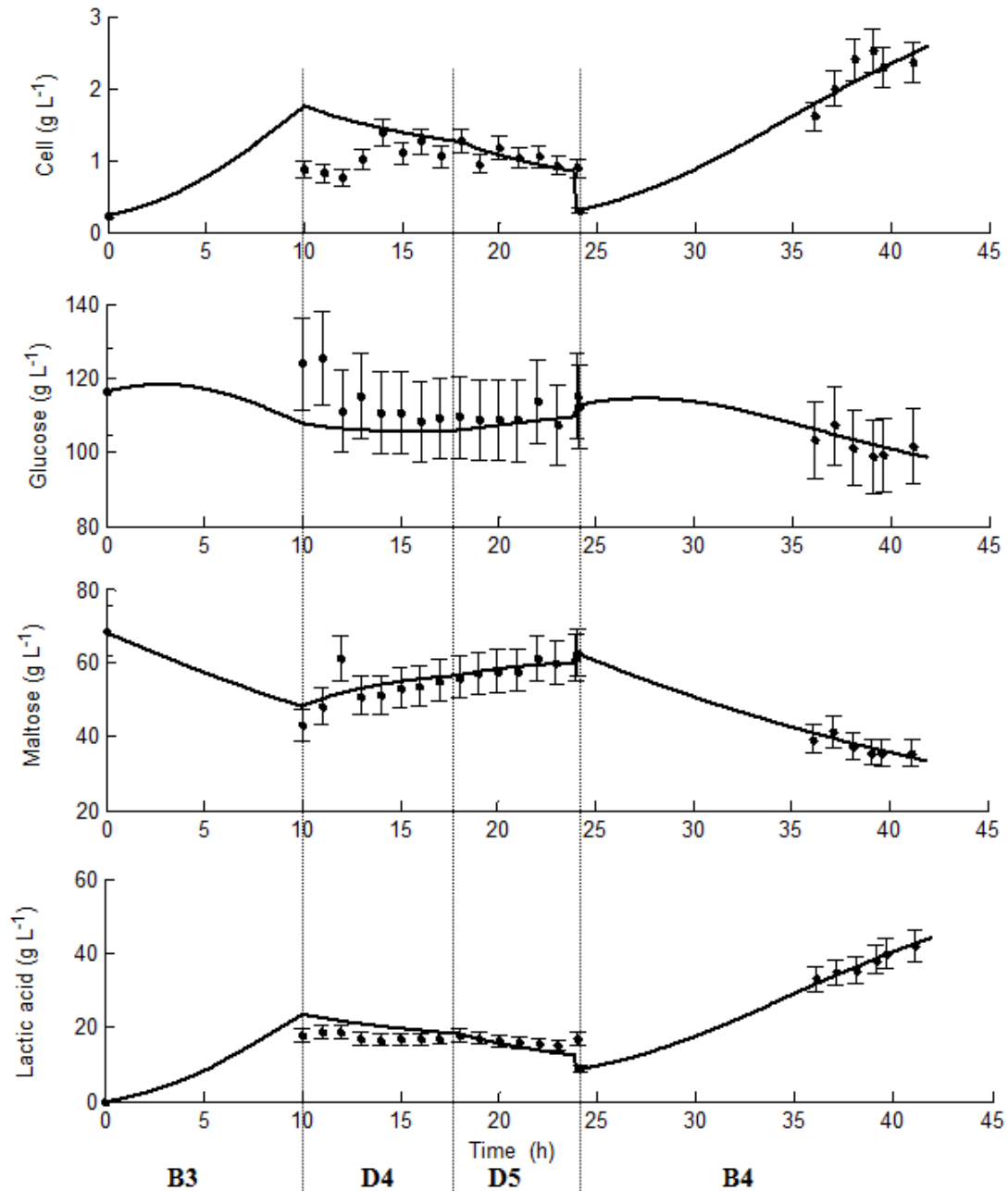
Figure 3.13 Experimental (●) and simulated (——) cell, glucose, maltose and lactic acid concentrations for fermentation in batch and continuous operations for experiment 2. Two dilution rates tested D4= 0.15 h^{-1} and D5=0.2h^{-1}.

The confidence in the prediction of the model compared to the experimental data was assessed by the determination of the root-mean-square error (RMSE) and the normalized-root-mean-square error (NRMSE). The RMSE is a measure of the differences between predicted values (by the model) and the real values (experimental data) and is defined by the following equation:

$$RMSE = \sqrt{\frac{\sum\limits_{i=1}^{N} (y_{i,\exp} - y_{i,cal})^2}{N}} \qquad (3.40)$$

where $y_{i,exp}$ is the experimental value, $y_{i,cal}$ the predicted value and N the number of experimental points. The NRMSE is defined as:

$$NRMSE = \frac{RMSE}{y_{\exp,\max} - y_{\exp,\min}} \qquad (3.41)$$

where $y_{exp,\max}$ is the maximal experimental value and $y_{exp,\min}$ is the minimal experimental value.

Both, RMSE and NRMSE values were determined for cell, glucose, maltose and lactic acid concentrations. Their values are reported in table 3.7.

The NRMSE values obtained in model validation with all experimental data remain in an acceptable range compared to those obtained with experimental data used for identification (B4). Calculated NRMSE values for cell and lactic acid concentrations are low. It proves the good agreement between experimental data and model predictions. Nevertheless, the calculated NRSME values for glucose concentration are high confirming that the glucose prediction is not so good. Concerning the NRMSE values for maltose concentration, the value obtained in experiment 1 is two times higher than the one obtained in experiment 2. It can be explained by the dispersion of experimental data obtained at the beginning of experiment 1 due to some experimental problems. For the first 3 experimental points in the phase D2 of experiment 1, it was not possible to assure a constant flow feeding the bioreactor.

Table 3.7 RMSE and NRMSE values for each experiment

Variable	B4 (Identification)		Experiment 1		Experiment 2	
	RMSE (g L^{-1})	NRMSE (%)	RMSE (g L^{-1})	NRMSE (%)	RMSE (g L^{-1})	NRMSE (%)
X	0.09	9.0	0.43	15.5	0.37	13.4
S	2.41	17.9	5.85	24.7	6.20	26.2
P	0.75	2.3	3.52	11.2	2.85	9.2
M	1.28	4.7	5.14	24.9	2.61	12.7

The model validation gave more satisfactory results for the experiment used to identify the parameters (experiment 2) than for the other. It can be explained by slight differences in in glucose and maltose feed concentrations.

Even so, the proposed model performs well. This model is therefore able to predict the experimental results for experiments conducted in batch and continuous modes.

3.6. CONCLUSIONS

In this chapter, the model development able to describe the variables behaviour in the SSPHF bioreactor was presented. First, a state-of-the-art on the available models for lactic acid was introduced. This allowed the establishment of the basis required for our model development. Batch experiments were performed to identify the inhibition and limitation phenomena on growth. Once the different phenomena having an impact on bacteria were identified, the model development for the continuous SSPHF bioreactor was performed.

The proposed model consists of four dynamical equations describing the bacteria growth, substrates consumption and product formation (3.29). Maltose was the sole sugar taken into account in the glucose dynamics. Parameter identification and validation were carried out using data from experiments performed in batch and continuous operation modes. Good agreement was found between the model and the experimental data.

This model can now be used to accomplish the next objective of this work: the bioprocess productivity optimization and the development of a control strategy to achieve this optimal operation condition.

CHAPTER 4: MONITORING

4.1. INTRODUCTION

After model validation, the main problem of biotechnological processes control is the lack of reliable and low cost physical sensors capable of measuring the different state variables online. It is often difficult, for economic or technological reasons, to measure all the variables required for the control of the bioreactor. An alternative solution is to estimate the unmeasured states through the synthesis of observers. The principle of these "software sensors" is the reconstruction of the non-online measurable states, based on a dynamical model of the system and on the online available measurements. It is also possible to estimate other important variables in the system, for example the kinetic rates of growth or production.

In this context, robust and reliable algorithms must be developed to estimate key variables and parameters both for process monitoring and control. The algorithms reported in the literature differ with respect to the measured and estimated variables, the known parameters, the type of observer convergence, the robustness issues, etc. (De Battista, et al., 2011). Asymptotic observers for state and parameter estimations in bioprocess were introduced for the first time by Aborhey and Williamson (1978). High-gain observers applied to bioreactors were studied by Farza et al. (1998); they were also treated in an adaptive approach by Bastin and Dochain (1986). More recently, hybrid state observers combining asymptotic and exponential approaches were developed (Bogaerts, et al., 2006). In order to deal with model uncertainties, sliding mode observers have also been described (Picó, et al., 2009)

In this chapter, a brief state-of-the-art of the different observers used in bioprocesses is first presented. Then, a software sensor to reconstruct, online, the lactic acid concentration is developed. Later, observers (Extended and Unscented Kalman filters), based on the Kalman filter approach, are proposed to estimate the state variables of the system (cell, glucose, maltose and lactic concentrations). They are then validated in simulation. Since the rate of lactic acid production is an important parameter to assess the bioprocess performance, observers to estimate the lactic acid production rate are developed. Their performance is validated through simulations. The experimental validation of proposed observers will be presented in Chapter 5.

4.2. STATE-OF-ART IN ESTIMATION TECHNIQUES

There are mainly two kinds of estimation techniques, both using online measurements, to estimate system states: the methods based on simple mass balances and the methods based on observers. A mathematical model of the system is required in the latter case. The observer to consider is strongly connected to the accuracy and the uncertainties of model and data. In the following some state estimation methods used in biotechnological processes are discussed.

4.2.1. Balance Equation-Based Methods

In this case, the estimation is based on theoretical and experimental relationships between the measured variables and the variables to be estimated. With this approach, by neglecting measurements errors, modelling uncertainties and instrument noises, only simple calculations are needed to estimate unmeasured variables. Different balance equation based methods have been proposed for bioprocesses.

The estimation of the biomass concentration and the growth rate from oxygen measurements was first reported (Zabriskie & Humphrey, 1978). Mou and Cooney (1983) calculated the same parameters in penicillin fermentation by means of overall and instantaneous carbon balance equations; the estimations were implemented in a feedback control strategy to regulate the growth rate. An online estimation of biomass concentration technique for the *Streptomyces avermitilis* fermentation was based on the oxygen uptake rate, calculated from oxygen concentration measurements (Gbewonyo, et al., 1989). The online estimation of biomass from maintenance equations was performed by Beluham, et al.,(1995) for a baker's yeast fermentation process and this estimation was used in a feedback control scheme. Finally in lactic acid fermentation, Lombardi (1996) proposed to estimate online the lactic acid concentration from the mass of base added to the bioreactor for pH regulation. This technique was also used in this work and will be discussed in section4.4.

The disadvantage of the mass balance methods compared to the other methods is that they do not include system uncertainties or noises. In order to consider these aspects, the observer based methods have been developed.

4.2.2. Observer Based Methods

Observers estimate state variables from the knowledge of the mathematical model of the bioprocess and from the available measurements. Figure 4.1 presents the observer principle. It is coupled to the system using the measured output, *y*. In this figure, *u* is the control variable, *x* the state and $\hat{x}$ the state estimate.
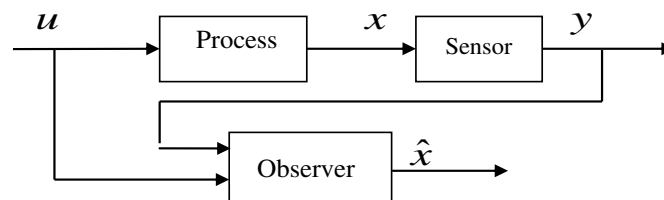
Figure 4.1 Observer principle

Observers can be designed and implemented as linear observers or nonlinear observers. Most real systems often include system uncertainties. Various bioprocess estimation methods based on observers have been proposed during the last 50 years, each having advantages and drawbacks according to: its ability to consider measurements error, the need of using an (accurate) model describing the bioprocess, if there are local approximations (linearization of

nonlinear models) or not (nonlinear theory) and its convergence rate which can be determined taking into account the cultures conditions, or arbitrarily fixed (Bogaerts & Vande Wouwer, 2003). Observers are classified in three types: exponential, asymptotic and hybrid observers. They are briefly presented hereafter.

Exponential Observers

The system state is reconstructed based on a process model and some available hardware sensor measurements. The system observability condition must be guaranteed in linear systems in order to design such observer. For nonlinear systems, at least the local observability condition (see appendix C.1) must be fulfilled (Kwakernaak & Sivan, 1972). The exponential observer uses a closed-loop structure; the measurements are used in a feedback path which drives the state estimates towards the true states of the process. Tuning parameters adjust the rate of convergence towards the true states. Nevertheless, this type of observer strongly depends on the model accuracy. Examples of exponential observers are: The extended Luenberger observer, the extended Kalman Filter, the receding horizon observer, and the high-gain observer (Bogaerts & Vande Wouwer, 2003).

Asymptotic Observers

Asymptotic observers are open-loop state estimation techniques using only a part of the process model and replacing the missing part by some available measurements assumed to be continuous in time and noise free. Therefore, the structure of the asymptotic observer does not have a correction term between the estimated output and its measurement. The main advantage of this kind of observer is the possibility to estimate the states without any *a priori* knowledge about the reaction kinetics. Nevertheless, the rate of convergence of the estimation towards the true states depends on the operation conditions (as the dilution rate)(Bastin & Dochain, 1990).

Hybrid observers

Hybrid observers combine the advantages of the exponential (adjustable convergence rate) and asymptotic (robust with respect to growth kinetics knowledge). This method considers the definition of a confidence level in the bioprocess model. According to this interval, the hybrid observer will oscillate between two extreme cases: it uses either an exponential observer structure when the model is assumed to be perfectly known or an asymptotic one in the opposite case (Bogaerts & Vande Wouwer, 2003). One example of this kind of observer is the interval observers which consist in an auxiliary dynamic system that provides guaranteed bounds of the state to be estimated. Interval observers incorporate uncertainty into the observer design, dealing with unknown dynamics, inputs and outputs. Nevertheless, know bounds on the uncertain terms are required (Rapaport & Dochain, 2005).

4.3.   KALMAN FILTER BASED METHODS

The Kalman filter has been used for the last 50 years but is still in use nowadays, due to its small computational requirement and its status as the best estimator for one-dimensional linear systems with Gaussian error statistics (Anderson & Moore , 2005). Kalman filter is

used to provide optimal estimates of unmeasured and measured states for time varying systems, in the presence of process and measurement noises, by using a mathematical model of the process. Its approach consists in minimizing the variance of the estimation error using an algorithm with two recursive steps. First, the process model is used to propagate the initial state estimates until a new measurement is available (prediction step). In the second step, the propagated model estimates are combined with the measurements to update or correct the estimates (Lewis, et al., 2008).

There are different kinds of Kalman filter, depending on the nature of system dynamics (continuous or discrete, linear or not) and measurements (discrete or continuous). In the case of bioprocesses, the measurements are usually available at large sampling periods, as in this work, leading to the consideration of discrete measurements. However the bioreactor dynamics are continuous, so considering Kalman filter for continuous dynamics is generally preferred. Nevertheless, in this work, since the system dynamics is slow in comparison to sensors characteristic times, it will be discretized, leading to an estimation problem for discrete time system with discrete time measurements. The Kalman filter equations for this kind of systems are presented in the following sections, considering the cases of linear and nonlinear dynamics, since these two versions of the filter will be used in this work. In the case of nonlinear systems, two Kalman strategies will be detailed and tested: the Extended Kalman filter (EKF) and the Unscented Kalman Filter (UKF).

4.3.1. Discrete Kalman Filter for linear systems

The Kalman filter addresses the general problem of estimating the state vector $x \in \Re^n$ of a discrete-time process that is governed by the linear stochastic recursive equation:

$$x_k = A_{k-1}x_{k-1} + B_{k-1}u_{k-1} + G_{k-1}w_{k-1} \tag{4.1}$$

with the measurement vector $y \in \Re^p$:

$$y_k = C_k x_k + v_k \tag{4.2}$$

where k is the time index and u the control input. The random variables w_k and v_k represent the process and measurement noise, respectively. They are assumed to be non-correlated, white and with normal probability distributions given by:

$$w \sim N(0, Q_k)$$
$$v \sim N(0, R_k) \tag{4.3}$$

where Q_k and R_k are the uncorrelated respective covariance matrices. They are used to model the confidence in the system model for the first one (w) and the measurement quality for the second one (v).

The nxn matrix A_k in equation (4.1) relates the state at time step k to the state $k+1$, in the absence of either a control input or process noise. The nxm matrix B_k relates the control input

$u \in \mathfrak{R}^m$ to the state x. The pxn matrix C_k in the measurement equation (4.2) relates the state to the measurement y_k.

Defining $\hat{x}_k^- \in \mathfrak{R}^n$ as the *a priori* state estimate at step k *(given knowledge of the process prior to step k)*, and $\hat{x}_k \in \mathfrak{R}^n$ the *a posteriori* state estimate at step k (given measurement y_k). It is then possible to define *a priori* and *a posteriori* estimate errors as (Welch & Bishop, 1995):

$$e_k^- \overset{\Delta}{=} x_k - \hat{x}_k^-,$$
$$e_k \overset{\Delta}{=} x_k - \hat{x}_k \tag{4.4}$$

The *a priori* estimation error covariance is defined as:

$$\mathbf{P}_k^- = E\left[e_k^- e_k^{-T} \right] \tag{4.5}$$

where E is the mathematical expectation. The *a posteriori* estimate error covariance is defined as:

$$\mathbf{P}_k = E\left[e_k e_k^T \right] \tag{4.6}$$

In the following the Kalman filter algorithm is described.

Algorithm
Initialization phase:

The initial estimated state vector is given by:

$$\hat{x}_0 = E[x_0], \ \mathbf{P}_0 = E\left[(x_0 - \hat{x}_0)(x_0 - \hat{x}_0)^T \right] \tag{4.7}$$

where $\mathbf{P}_0$ represents the covariance matrix of the estimation error, x_0 the state at the initial instant and $\hat{x}_0$ its estimate.

For $k=1,...,\infty$:

Step 1. Prediction phase (between instants k-1 and k):

In this step the *a priori* prediction of the state, $\hat{x}_k^-$,is calculated using the model and the covariance matrix of the prediction error $\mathbf{P}_k^-$:

$$\hat{x}_k^- = A_{k-1}\hat{x}_{k-1} + B_{k-1}u_{k-1} \tag{4.8}$$

$$\mathbf{P}_k^- = A_{k-1}\mathbf{P}_{k-1}A_{k-1}^T + Q_{k-1} \tag{4.9}$$

Step 2. Correction phase (at instant k, when a new measurement is available):

Update the prediction from the measurement y_k to obtain the *a posteriori* estimate $\hat{x}_k$ and the covariance matrix of the estimation error $\mathbf{P}_k$. The *a posteriori* estimate $\hat{x}_k$ is a linear combination of an *a priori* estimate $\hat{x}_k^-$ and a weighted difference between the actual measurement y_k and a measurement prediction $C_k\hat{x}_k^-$ as follows:

$$K_k = \mathbf{P}_k^- C_k^T (C_k \mathbf{P}_k^- C_k^T + R_k)^{-1}$$

(4.10)

$$\mathbf{P}_k = \mathbf{P}_k^- (I - K_k C_k)$$

(4.11)

$$\hat{x}_k = \hat{x}_k^- + K_k (y_k - C_k \hat{x}_k^-)$$

(4.12)

The difference $(y_k - C_k\hat{x}_k^-)$ in equation (4.12) is named the measurement *innovation* or the *residual*. It reflects the discrepancy between the predicted measurement $C_k\hat{x}_k^-$ and the actual measurement y_k. The *nxp* matrix K in equation (4.11) is the *gain* that minimizes the *a posteriori* error covariance presented in equation (4.10).

Step3. Repeat Steps 1 and 2 for the next sample. After each time and measurement update pair, the algorithm is repeated with the previous *a posteriori* estimates used to predict the new *a priori* estimates.

Filter Parameters and Tuning

The measurement noise R_k and the process noise Q_k covariance matrices described by equation (4.3) might be selected prior to operation of the filter. In the case of the measurement noise covariance R_k, it can be easily determined considering the nature of the measurement and sensor characteristics. In the case of Q_k, the choice is less obvious. Usually, this noise is added to represent the uncertainty on the process model. The filter performance in case of an uncertain model of the system can be improved by adding enough uncertainty via the selection of Q_k. In this case, reliable process measurements are preferred.

4.3.2. Extended Kalman Filter (EKF)

The Kalman filter approach described in the previous section (section 4.3.1) can be used for processes described by linear stochastic discrete equations. Nevertheless, most biochemical systems of practical interest are inherently nonlinear. In this case an Extended Kalman Filter (EKF) technique can be used. The estimation is performed by linearizing the nonlinear model equations around the current estimate and then by applying the Kalman filter strategy to the linearized equations. The EKF estimation technique has been reported for state estimation of several biotechnological processes. Pons et al. (1988) have applied EKF for the estimation of state variables of a biotechnological process operated in batch and fed-batch modes. The EKF method was also used in *Saccharomyces cerevisiae* fermentation for states estimation in (Zorzetto & Wilson, 1996). The control of glucose during yeast fed-batch cultivation was

performed combined to an EKF approach by Hitzmann et al. (2000). Tebbani et al. (2015) used an Extended Kalman Filter to estimate the biomass concentration in a nonlinear control approach for the *Prophyridium purpureum* process.

In the EKF strategy, the linearization of the estimation is performed around the current estimate using the partial derivatives of the process and measurement functions to compute estimates even if the system is represented by nonlinear equations. The EKF algorithm is detailed hereafter.

Let us consider a process with a state vector $x \in \Re^{\mathbf{n}}$, governed by nonlinear stochastic differential equations:

$$x_{k+1} = \mathbf{F}(x_k, u_k) + w_k \tag{4.13}$$

with measurements given by $y \in \Re^{\mathbf{p}}$:

$$y_k = \mathbf{H}(x_k) + v_k \tag{4.14}$$

The extended Kalman filter applied to the discrete system represented in equations (4.13) and (4.14) is an extension of the discrete Kalman filter in the linear case. It requires to linearize the equation around the estimated trajectories, and therefore to determine a discrete linear system, for which a linear discrete Kalman filter is applied.

The EKF algorithm is presented hereafter.

Algorithm
Initialization phase:

The initialization phase remains the same as presented in section 4.3.1 (see equation (4.7)).

For $k=1,...,\infty$:

Step 1. Prediction phase (between instants *k-1* and *k*):

A priori prediction of the state, $\hat{x}_k^-$

$$\hat{x}_k^- = \mathbf{F}(\hat{x}_{k-1}, u_{k-1}) \tag{4.15}$$

$$\mathbf{P}_k^- = A_{k-1}\mathbf{P}_{k-1}A_{k-1}^T + Q_{k-1} \tag{4.16}$$

where the matrix A_{k-1} is obtained by linearizing the dynamics around the actual estimation point $\hat{x}_{k-1}$:

$$A_{k-1} = \left.\frac{\partial \mathbf{F}(x,u)}{\partial x}\right|_{x=\hat{x}_{k-1}} \tag{4.17}$$

Step 2. Update phase at instant *k*:

Update the prediction from the measurement y_k to obtain the *a posteriori* estimate $\hat{x}_k$.

$$K_k = \mathbf{P}_k^- C_k^T (C_k \mathbf{P}_k^- C_k^T + R_k)^{-1}$$

(4.18)

$$\mathbf{P}_k = \mathbf{P}_k^- (I - K_k C_k)$$

(4.19)

$$\hat{x}_k = \hat{x}_k^- + K_k (y_k - C_k \hat{x}_k^-)$$

(4.20)

where the matrix C_k is obtained from:

(4.21)

$$C_k = \left. \frac{\partial \mathbf{H}(x,u)}{\partial x} \right|_{x=\hat{x}_k^-}$$

Step3. Repeat Steps 1 and 2 for the next sample.

As the EKF method is based on the linear approximation of the system at a given time instant, it may introduce errors in the state estimate, which may lead to divergence. In order to overcome these drawbacks, other nonlinear state estimators have been developed such as the Unscented Kalman filter (UKF) (Kandepu, et al., 2008). In the next section the implementation of the UKF estimator is presented.

4.3.3. Unscented Kalman Filter(UKF)

The UKF observer uses a similar approach as the EKF, avoiding the linearization procedure and leading to a better robustness and rate of convergence (Kandepu et al., 2008). As the system in the present work has strong nonlinearities and uncertainties, the derivative-free UKF method seems attractive. In this case, the state distribution is represented by means of a minimal set of carefully chosen sampling points, the so-called *sigma points*. Each of these points is propagated through the nonlinearities and then the state estimate is calculated as the average mean of these transformed points (Julier & Uhlmann, 1997). The UKF algorithm is detailed hereafter.

Consider the discrete-time nonlinear model described by equations (4.13) and (4.14) :

Algorithm

The UKF algorithm is given by:

Initialization (k=0):

The initialization phase remains the same as presented in section 4.3.1 (see equation (4.7)).

For *k=1,...,∞* :

Step 1. Sigma points (ξ_{k-1}) selection:

$$\left(\xi_{k-1}\right)_0 = \hat{x}_{k-1} \tag{4.22}$$

$$\left(\xi_{k-1}\right)_i = \hat{x}_{k-1} + \chi \cdot (\sqrt{\mathbf{P}_{k-1}})_i, i = 1,...,n, \tag{4.23}$$

$$\left(\xi_{k-1}\right)_i = \hat{x}_{k-1} - \chi \cdot (\sqrt{\mathbf{P}_{k-1}})_{i-n}, i = 1, n+1,...,2n, \tag{4.24}$$

where (ξ_{k-1}) has a dimension of 2*n+1, $\left(\sqrt{\mathbf{P}_{k-1}}\right)_i$ is the i-th column of the square root of the covariance matrix of the previous time step (calculated by Cholesky factorization). The χ parameter is the scaling factor used to move the position of the sigma points around the mean value and is given by $\chi = \sqrt{n+\lambda}$, with $\lambda = \phi^2(n+k_0) - n$ and (ϕ, k_0) tuning parameters to choose. Usually ϕ is small ($10^{-4} \leq \phi \leq 1$) and $k_0 \geq 0$ (generally k_0 is set to zero).

Step 2. Prediction. In this step, the sigma points (ξ_{k-1}) are propagated through the nonlinear dynamics and the state prediction is calculated:

$$\xi_{k|k-1} = \mathbf{F}[\xi_{k-1}, u_{k-1}] \tag{4.25}$$

$$\hat{x}_k^- = \sum_{i=0}^{2n} W_i^{(m)} \xi_{i,k|k-1} \tag{4.26}$$

where $W_i^{(m)}$ is a weighting factor given by:

$$W_0^{(m)} = \frac{\lambda}{n+\lambda} \tag{4.27}$$

$$W_i^{(m)} = \frac{1}{2(n+\lambda)} \tag{4.28}$$

The predicted covariance is computed using the following expression:

$$\mathbf{P}_k^- = \sum_{i=0}^{2n} W_i^{(c)} \left[\xi_{i,k|k-1} - \hat{x}_k^-\right]\left[\xi_{i,k|k-1} - \hat{x}_k^-\right]^T + Q_k \tag{4.29}$$

Where Q is the process noise covariance matrix and $W_i^{(c)}$ is a weighting factor given by

$$W_0^{(c)} = \frac{\lambda}{n+\lambda} + 1 - \phi^2 + \varepsilon \tag{4.30}$$

$$W_i^{(c)} = W_i^{(m)}, \quad i = 1, n+1,....,2n \tag{4.31}$$

where ε is a tuning parameter used to introduce prior knowledge of the distribution of the state (generally set to 2 for Gaussian distribution).

Step 3. Updating. Using the predicted sigma points (4.25) and covariance (4.26), a new set of sigma points is computed and projected through the observation model. The predicted measurements are described by:

$$Y_{k|k-1} = \mathbf{H}[\xi_{k-1}] \tag{4.32}$$

$$\hat{y}_k^- = \sum_{i=0}^{2n} W_i^{(m)} Y_{i,k|k-1} \tag{4.33}$$

The covariance of the innovation and the cross-covariance matrix are then given by:

$$\mathbf{P}_{\tilde{y}_k \tilde{y}_k} = \sum_{i=0}^{2n} W_i^{(c)} \left[Y_{i,k|k-1} - \hat{y}_k^- \right] \left[Y_{i,k|k-1} - \hat{y}_k^- \right]^T + R_k \tag{4.34}$$

$$\mathbf{P}_{y_k x_k} = \sum_{i=0}^{2n} W_i^{(c)} \left[\xi_{i,k|k-1} - \hat{x}_k^- \right] \left[Y_{i,k|k-1} - \hat{y}_k^- \right]^T \tag{4.35}$$

where R_k is the measurement noise covariance matrix.

The estimations are updated using the classical Kalman filter equations:

$$K_k = \mathbf{P}_{y_k x_k} \mathbf{P}_{y_k x_k}^{-1} \tag{4.36}$$

$$\hat{x}_k = \hat{x}_k^- + K_k (y_k - \hat{y}_k^-) \tag{4.37}$$

$$\mathbf{P}_k = \mathbf{P}_k^- - K_k \mathbf{P}_{\tilde{y}_k \tilde{y}_k} K_k^T \tag{4.38}$$

Step4. Repeat Steps 1 to 3 for the next sample.

It can be observed that in the UKF algorithm, Jacobian matrices are not needed as in the EKF one, making the UKF implementation easier. Indeed, with the UKF algorithm, it is not necessary to linearize the model to obtain the estimation of states, allowing changing the model (typically the specific growth rates) without any further developments. In section 4.5.2 the performances of both proposed Kalman filters are tested and compared in simulation.

4.4. ONLINE DETERMINATION OF THE LACTIC ACID CONCENTRATION

In this work, the key variables are biomass, glucose, lactic acid and maltose concentrations. For the development of the control law it is necessary to measure at least one of the key variables in the system. There are some sensors available in the market for the monitoring of the biomass and glucose concentrations. However, they are expensive and their implementation seems difficult considering the complex culture broth used in this work (wheat flour solution).

The aim of further developments is to reconstruct different states variables using online values of the lactic acid concentration. However, this cannot be measured online as mentioned previously. Thus, in this work, the lactic acid concentration is estimated by means of an online measured parameter, the mass of sodium hydroxide added to regulate the pH of the reactor. Lactic acid produced during the SSPHF step can be correlated to the mass of base

added to regulate pH at 5.7. Therefore, we developed a mathematical expression correlating these two variables, as presented in the following.

4.4.1. *Lactic acid concentration determination in the SSPHF bioreactor*

In the continuous SSPHF, the bioreactor actually has two inlet flows, the first one feeding the bioreactor with substrate and the second one adding the sodium hydroxide solution necessary to neutralize lactic acid. It is illustrated in figure 4.2.
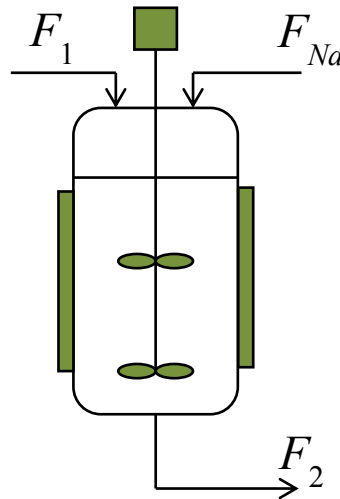
Figure 4.2 Feed flows and output flow in the SSPHF bioreactor

F_1 represents the substrate feed flow and F_2 the outlet flow. In fact, the latter is the sum of the substrate feed flow and the sodium hydroxide flow:

$$F_2 = F_1 + F_{Na}$$

(4.39)

In the experiments performed in continuous mode with pH control (see section 2.2.4) the sodium hydroxide flow is at least 35 times smaller than the substrate inlet flow. Consequently, F_1 is assumed to be equal to F_2 as previously mentioned in chapter 3. The lactic acid concentration mass balance is then the one described by equation (3.25) and recalled here:

$$\frac{dP}{dt} = \frac{Y_{PS}}{Y_{XS}} \mu X - DP$$

(3.25)

where P is the lactic acid concentration at t, D the dilution rate at t, X the biomass concentration at t (g L^{-1}), Y_{PS} and Y_{XS} the yields of transformation of substrate into lactic acid and biomass respectively (in g g^{-1}) and μ the specific growth rate (h^{-1}).

The aim is then to consider this mass balance and the lactic acid neutralization by the sodium hydroxide to develop a technique for the determination of the lactic acid concentration. In the following, the development of a mathematical expression correlating the lactic acid concentration to the sodium hydroxide inlet flow is presented.

143

4.4.2. Weak Acids and Bases

The following equation represents the acid-base equilibrium of an acid HA:

$$HA + H_2O \Leftrightarrow A^- + H_3O^+ \tag{4.40}$$
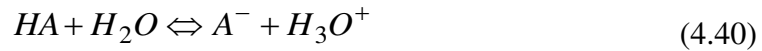
The acid is strong if the acid dissociation is complete, it means that no more HA molecules are present in the solution. If the dissociation is not complete (weak acid), as for lactic acid, it is possible to consider the equilibrium

$$K_A = \frac{\left[A^-\right]\left[H_3O^+\right]}{\left[HA\right]} \tag{4.41}$$

where K_A is the equilibrium constant called "acidity constant" and which only depends on the temperature. It is also possible to define:

$$pK_A = -\log K_A \tag{4.42}$$

From equations (4.41) and (4.42), the smaller the pK_A value of the acid, the stronger it is.

4.4.3. Lactic acid concentration determination from sodium hydroxide inlet flow

In the studied SSPHF bioreactor, the acid-base reaction to be considered is the neutralization of a weak acid (lactic acid) by a strong base, sodium hydroxide.

The acidity constant of lactic acid at the temperature in the bioreactor (30°C) is pK_A= 3.88 and sodium hydroxide as a strong base is totally dissociated. The water constant at the same temperature is pK_W=13.83.

The chemical reactions to be considered are then:

$$\underset{Lacticacid}{CH_3CHOHCOOH} + H_2O \Leftrightarrow \underset{lactate}{CH_3CHOHCOO^-} + H_3O^+, \ K_A = 10^{-3.88} \tag{4.43}$$

$$\underset{Sodiumhydroxyde}{NaOH} \Rightarrow Na^+ + OH^- \tag{4.44}$$

$$2H_2O \Leftrightarrow OH^- + H_3O^+ \qquad K_W = 10^{-13.83} \tag{4.45}$$

The whole equation is then represented by:

$$CH_3CHOHCOOH + OH^- \Leftrightarrow CH_3CHOHCOO^- + H_2O \tag{4.46}$$

By representing lactic acid by HA and lactate by A^-, the following equations are obtained:

$$10^{-3.88} = \frac{[A^-]_{eq}[H_3O^+]_{eq}}{[HA]_{eq}} \tag{4.47}$$

$$10^{-13.83}[OH^-]_{eq} = [H_3O^+]_{eq} \tag{4.48}$$

where the brackets $[]_{eq}$ indicates the concentrations of each compound in the bioreactor at the equilibrium. As the bioreactor is regulated at pH= 5.7, from the pH definition, it is possible to determine the concentration of each dissociated ion by:

$$[H_3O^+] = 10^{-5.7} \tag{4.49}$$

$$[OH^-] = 10^{-(13.83+5.7)} = 10^{-8.13} \tag{4.50}$$

From equations (4.47) and (4.50), it is possible to determine the ratio lactate/lactic acid:

$$\frac{[A^-]_{eq}}{[HA]_{eq}} = 10^{1.82} \tag{4.51}$$

Then the ratio lactate/lactic acid is equal to 66. The total concentration of produced lactic acid is:

$$\left[A^-\right] + \left[HA\right] = \left(1 + \frac{1}{66}\right)\left[A^-\right] = 1.015\left[A^-\right] \tag{4.52}$$

The neutralization is then quantitative.

From the reaction represented by equation (4.46), one mole of NaOH reacts with one mole of lactic acid, the quantity (mol) of produced lactic acid is then equal to the quantity (mol) of sodium hydroxide added.

The lactic acid production rate in g L^{-1} h^{-1} (defined as γ) at time t in the bioreactor can then be expressed as a function of the sodium hydroxide inlet flow by the following expression:

$$\gamma = \frac{Y_{PS}}{Y_{XS}}\mu X = \frac{F_{Na}C_{Na}M_{LA}}{V} \tag{4.53}$$

where V is the culture broth volume (L), F_{Na} the sodium hydroxide flowrate added into the bioreactor for lactate neutralization (L h^{-1}) at t, C_{Na} the sodium hydroxide concentration in its inlet flow (mol L^{-1}) and M_{LA} the lactic acid molecular weight (g mol^{-1}).

Replacing the definition of lactic acid productivity obtained in equation (4.53) in terms of sodium hydroxide inlet flow in the lactic acid mas balance (equation (3.25)) the following expression is obtained:

$$\frac{dP}{dt} = F_{Na}\frac{C_{Na}M_{LA}}{V} - DP \tag{4.54}$$

Discretizing the equation (4.54), the lactic acid concentration at each instant k is given by:

$$P_{k+1} = \left(F_{Na,k} \frac{C_{Na} M_{LA}}{V} - D_k P_k \right)(t_{k+1} - t_k) + P_k \qquad (4.55)$$

Equation (4.55) allows the determination of the lactic acid concentration in a continuous bioreactor at instant $k+1$ from the inlet sodium hydroxide flow, the dilution rate and the lactic acid concentration at instant k and the constants C_{Na}, M_{LA}, V. The lactic acid concentration is updated each sampling time from the online measured variables $F_{Na,k}$ and D_k.

The method was experimentally validated and is presented in appendix C.2. Hereafter, the acid lactic concentration will be considered online available through its calculation from added NaOH measurements.

4.5. STATE VARIABLES ESTIMATION

In this section observers are proposed to estimate key variables that are not measured online from the available ones, namely lactic acid concentration. First, an observability analysis is performed to determine the feasibility of the construction of estimators for biomass, glucose and maltose concentrations using the online determined lactic acid concentration.

4.5.1. Observability analysis

From the observability definition presented in appendix C.1, the observability of the system was checked. Considering the system (equations (3.29)) in the following representation

$$\begin{aligned} \dot{x}(t) &= \mathbf{F}(x(t), u(t)) \\ y(t) &= \mathbf{H}(x(t)) \end{aligned} \qquad (4.56)$$

with $x = (X, S, M, P)^T$, $u = D$, $y = P$ and $\mathbf{F}$ and $\mathbf{H}$ defined as:

$$\mathbf{F} = \begin{bmatrix} \mu_{max} \dfrac{S}{k_S + S} X \left(1 - \dfrac{P}{P_{max}} \right)^n - DX \\[4mm] -\dfrac{1}{Y_{XS}} \mu_{max} \dfrac{S}{k_S + S} X \left(1 - \dfrac{P}{P_{max}} \right)^n + k_M M + D(S_0 - S) \\[4mm] -k_M M + D(M_0 - M) \\[4mm] \dfrac{Y_{PS}}{Y_{XS}} \mu_{max} \dfrac{S}{k_S + S} X \left(1 - \dfrac{P}{P_{max}} \right)^n - DP \end{bmatrix}$$

$$(4.57)$$

$$\mathbf{H} = \begin{bmatrix} 0 & 0 & 0 & 1 \end{bmatrix} \qquad (4.58)$$

As x has dimension 4, it is necessary to calculate the first four Lie derivatives (defined in appendix C.1) as follows:

$$L_{\mathbf{F}}^0 \mathbf{H}(x) = P \tag{4.59}$$

$$L_{\mathbf{F}}^1 \mathbf{H}(x) = \sum_{i=1}^n \frac{\partial L_{\mathbf{F}}^0 \mathbf{H}(x)}{\partial x_i} \mathbf{F}_i(x) = \dot{P} \tag{4.60}$$

$$L_{\mathbf{F}}^2 \mathbf{H}(x) = \sum_{i=1}^n \frac{\partial L_{\mathbf{F}}^1 \mathbf{H}(x)}{\partial x_i} \mathbf{F}_i(x) = \frac{\partial \dot{P}}{\partial X}\dot{X} + \frac{\partial \dot{P}}{\partial S}\dot{S} + \frac{\partial \dot{P}}{\partial M}\dot{M} + \frac{\partial \dot{P}}{\partial P}\dot{P} \tag{4.61}$$

$$L_{\mathbf{F}}^3 \mathbf{H}(x) = \sum_{i=1}^n \frac{\partial L_{\mathbf{F}}^2 \mathbf{H}(x)}{\partial x_i} \mathbf{F}_i(x) = \frac{\partial L_{\mathbf{F}}^2 \mathbf{H}(x)}{\partial X}\dot{X} + \frac{\partial L_{\mathbf{F}}^2 \mathbf{H}(x)}{\partial S}\dot{S} + \frac{\partial L_{\mathbf{F}}^2 \mathbf{H}(x)}{\partial M}\dot{M} + \frac{\partial L_{\mathbf{F}}^2 \mathbf{H}(x)}{\partial P}\dot{P} \tag{4.62}$$

The observation space Ω is then defined by:

$$\Omega = \mathbf{span} \left\{ \mathbf{H}(x), L_{\mathbf{F}}^1 \mathbf{H}(x), L_{\mathbf{F}}^2 \mathbf{H}(x), L_{\mathbf{F}}^3 \mathbf{H}(x) \right\} \tag{4.63}$$

From equation (4.63), the observability distribution to collect the "gradient" vector of every component in Ω is then defined as follows:

$$d\Omega = \begin{bmatrix} \dfrac{\partial \Omega}{\partial X} \\ \dfrac{\partial \Omega}{\partial S} \\ \dfrac{\partial \Omega}{\partial M} \\ \dfrac{\partial \Omega}{\partial P} \end{bmatrix} \tag{4.64}$$

Using the dynamics equations of the states in equation (4.57), it was possible to demonstrate that $d\Omega$ has rank=4. The rank conditions state that the system is observable. Observers to estimate the state variables can then be constructed for the studied system. The observability analysis will be further studied in chapter 5 considering the optimal operating point (see section 5.5.3). In the following the development of these observers is presented.

4.5.2. EKF and UKF applied to the studied system

The studied system is characterized by nonlinear differential equations. As previously mentioned, the evolution of state variables with time is slow making the system discretization possible. Moreover, there is only one variable available online, the lactic acid concentration with a sampling period denoted by T_s. The continuous system (equations (3.29)) can be discretized by the Euler method considering that the evolution of the system dynamics is slow enough in comparison to T_s. The discretized representation of the system with a sampling period T_s is governed by the following equations:

$$\begin{cases} X_{k+1} = X_k + T_s(\mu_k X_k - D_k X_k) \\ S_{k+1} = S_k(-D_k T_s + 1) + T_s\left(-\dfrac{1}{Y_{XS}}\mu_k X_k + D_k S_0 + k_M M\right) \\ M_{k+1} = M_k(-D_k T_s - k_M T_s + 1) + T_s(D_k M_0) \\ P_{k+1} = P_k(-D_k T_s + 1) + T_s\left(\dfrac{Y_{PS}}{Y_{XS}}\mu_k X_k\right) \end{cases} \tag{4.65}$$

with

$$\mu_k = \mu_{max}\frac{S_k}{k_S + S_k}\left(1 - \frac{P_k}{P_{max}}\right)^n \tag{4.66}$$

The EKF and UKF strategies can then be applied to the system, by adding fictitious state and measurement noises to the system equations (4.65) as in equations (4.13) and (4.14). The obtained observers' structure is resumed in Figure 4.3.
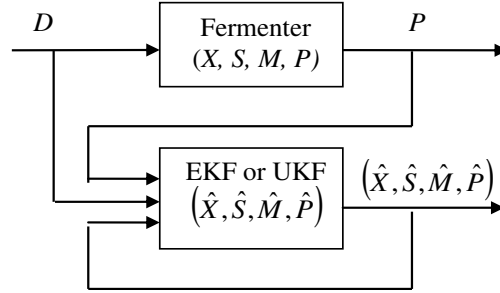
Figure 4.3 Extended Kalman Filter Structure

where $\hat{X}$, $\hat{S}$, $\hat{M}$ and $\hat{P}$ are the estimated biomass, glucose, maltose and lactic acid concentrations values. In order to simplify the observers' implementation, the state and measurement noises are supposed to be stationary. Their variance matrices are then constant over time:

$$\begin{aligned} Q_k &= Q\ \forall k \\ R_k &= R\ \forall k \end{aligned} \tag{4.67}$$

The Kalman Filters may have convergence problems, according to the values given to the matrices Q and R. Therefore, they will be empirically chosen (by trial/error) in order to ensure an acceptable rate of convergence and the stability of the filter. The covariance matrix of the prediction error is initialized according to the accuracy of the initial variables concentrations and the uncertainty on the lactic acid concentration determination.

4.5.3. *Kalman filters performances in simulation*

The EKF and UKF performances are analyzed in simulation. The parameters and experimental conditions used for simulations are the same for both filters and are those presented in table 3.6 (see section 3.5.2.3). The initial conditions are summarized in table 4.1.

Table 4.1 Initial conditions for simulations

Parameter	Value
$X(0)$ (g L^{-1})	0.2
$S(0)$ (g L^{-1})	120
$M(0)$(g L^{-1})	50
$P(0)$(g L^{-1})	0

The Lactic acid concentration is determined from online measurement of added NaOH. This technique leads to a low noise in the calculated lactic acid concentration. A centered Gaussian white noise is then applied to the latter with a standard deviation of 1%.

The choice of covariance matrices Q and R is performed empirically in order to obtain a good compromise between convergence rate, accuracy and stability. The best simulation results were obtained with the following matrices values:

$$Q = \begin{bmatrix} 0.01 & 0 & 0 & 0 \\ 0 & 4 & 0 & 0 \\ 0 & 0 & 4 & 0 \\ 0 & 0 & 0 & 0.2 \end{bmatrix} \tag{4.68}$$

$$R = 1$$

In equation (4.68), Q was chosen considering the order of magnitude of each state variable. The covariance matrix of the initial prediction error $\mathbf{P_0}$, which represents the threshold in the state initialization, has been chosen as the following diagonal matrix:

$$\mathbf{P_0} = \begin{bmatrix} 0.01 & 0 & 0 & 0 \\ 0 & 10 & 0 & 0 \\ 0 & 0 & 5 & 0 \\ 0 & 0 & 0 & 0.01 \end{bmatrix} \tag{4.69}$$

In the same way than for the Q choice, $\mathbf{P_0}$ was determined considering the order of magnitude of the state variables.

The UKF tuning parameters are chosen as follows: $\varepsilon = 2$, $\phi = 0.25$, k_0=0. These values were determined either from literature or from a trial-and-error technique. The observer performance for the system will be analyzed using two approaches. First, a state initialization error is considered without any model uncertainty. Secondly, a robustness study of the observer performance is carried out, considering uncertainties on the model parameters.

4.5.3.1. Observers simulation in the nominal case

The EKF and UKF strategies convergence is analyzed for an initialization error in biomass, glucose, maltose and lactic acid concentrations. No model parameter mismatch was considered in this first study (i.e. the model parameters considered in EKF and UKF algorithms are the same as those of the real system or simulated reference). Simulations are performed with the conditions presented in table 4.1. The performances of both estimators (EKF and UKF) are compared in figure 4.4. It illustrates biomass, glucose and maltose concentration estimations from the lactic acid concentration available online using the two observers. Simulations are performed during 60 h. The first 20 h of simulations represent the bioreactor behaviour in batch mode, with a dilution rate, $D=0$. After that, a $D=0.1$ h^{-1} was imposed. Both estimators allow estimating the cell, glucose and maltose concentrations from lactic acid concentration available online. Moreover, the estimations are not affected by the modification in the dilution rate at 20 h. It is important to notice that the filter convergence time could be improved by increasing values in matrices Q and R. Nevertheless it can impact the filter stability.
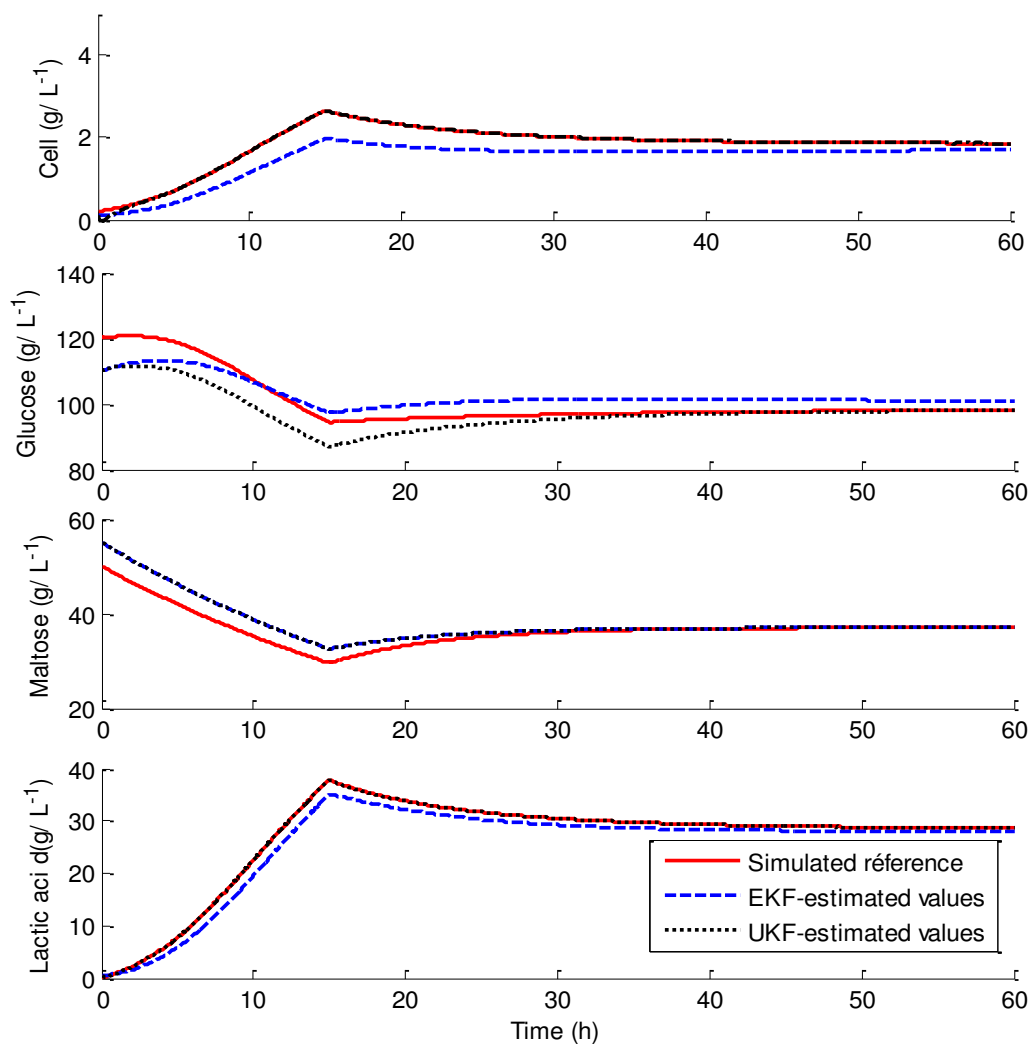
Figure 4.4 Extended Kalman filter and Unscented Kalman filter comparison. Estimation of cell, glucose, maltose and lactic acid concentrations with initialization error in the nominal case.

150

When comparing estimations by EKF and by UKF, estimated values are similar in the nominal case. Nevertheless, the UKF estimations perform better and converge to the real values faster than the EKF estimations in the case of glucose concentration.

4.5.3.2. *Observers robustness analysis*

In order to test the Kalman filters robustness with respect to model uncertainties, a 20% non-correlated parameters mismatch is applied to the real system (i.e. parameters of the real process are different by 20% from those used in the model considered in the observer). Values of the covariance matrices Q and in R are the same as those considered in the nominal case. The initialization error was also maintained. The performances of both filters are illustrated in figure 4.5. As it is shown, observers do not converge to the real system values at the end of the simulation (60 h).
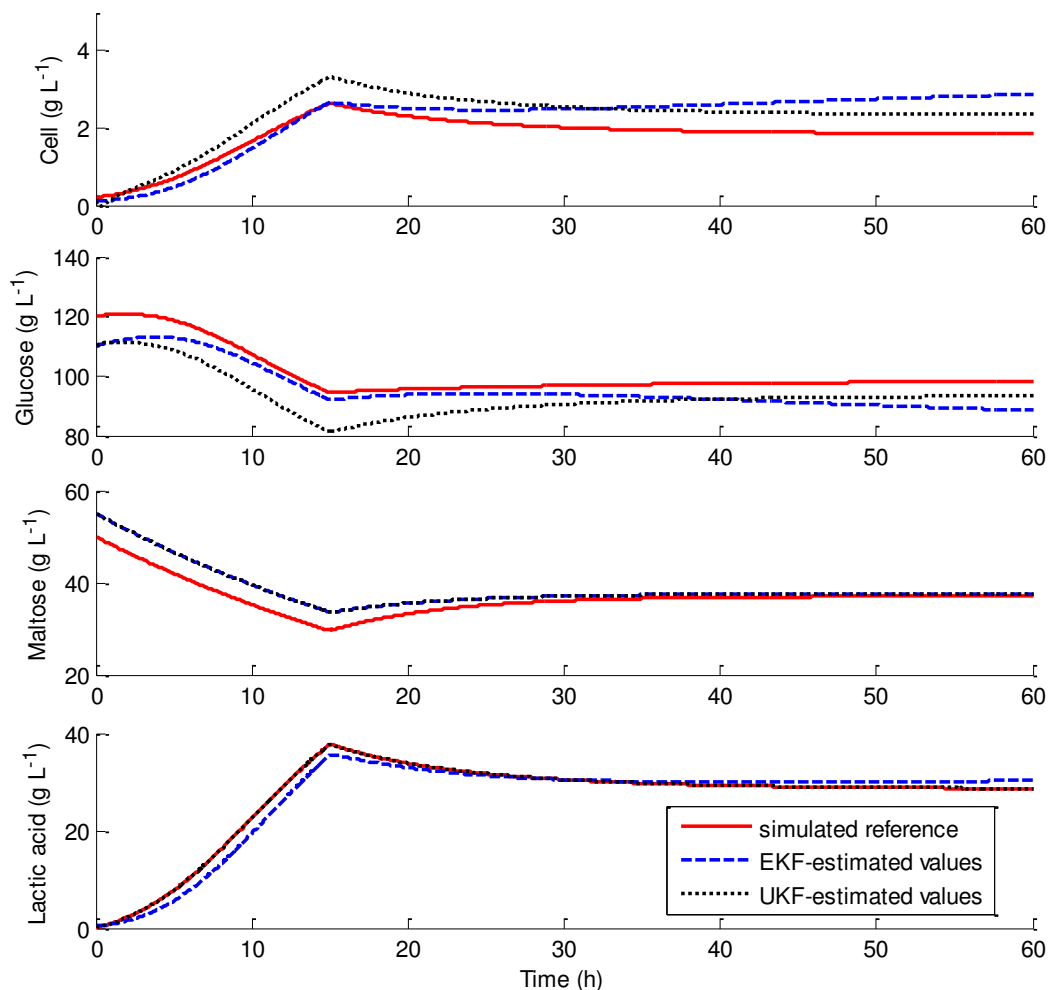

Figure 4.5 Extended Kalman filter and Unscented Kalman filter comparison. Estimation of cell, glucose, maltose and lactic acid concentrations with initialization error. 20% parameter mismatch between the real system model and the model used by EKF and UKF. 1% centred Gaussian white noise applied to *P*.

Simulation results prove that the quality of the estimation by the Kalman filters tested highly depends on the quality of the model. This limitation is the main drawback of exponential observers, and specifically of the Kalman filter. Indeed, chosen values in the covariance matrix Q representing the model accuracy are low and then the filter tends to trust the model. The solution is then to increase the value of Q. However, it is difficult to guarantee the filters stability with high values of Q. Indeed, tuning the covariance process noise matrix, Q, while guarantying the filter stability can be a difficult task. Simulation results in appendix C.2 prove that high values in the Q matrix leads to stability problems in the Filters.

It can be noticed that the UKF estimated values are closer to the real values than EKF estimated values. As the EKF method is based on the linear approximation of the system at a given time instant, it may introduce errors in the state estimation (Figure 4.5). The UKF performs better than the EKF but estimation remains dependent on the model quality. Model parameters must be accurately known in order to ensure the performance of the estimators. From this simulation study, it can be concluded that the Unscented Kalman filter is preferred since its implementation is easier (there is no need of model linearization) Moreover, a better performance compared with the Extended Kalman Filter was shown.

Nevertheless, both estimators remain dependent on the model accuracy and it can be a drawback for further control design. The estimation of the lactic acid production rate is then proposed in this work given that its estimation can potentially reduce the complexity of the control design and because it is an important variable of the system.

4.6. PRODUCTION RATE ESTIMATION

This section focusses on the development of an estimator for the lactic acid production rate. The motivation is that the objective of this PhD work is to optimize the lactic acid production process. Thus, one measurement of the effectiveness and good performance of the process is the production rate defined, for a continuous operation mode, as the product between the dilution rate and the product (lactic acid) concentration. The production rate estimation approach was chosen considering the online determined lactic acid concentration. In the next sections different observers are proposed to estimate the production rate.

The lactic acid production rate (denoted by γ, ing$L^{-1}h^{-1}$) is defined as:

$$\gamma = \frac{Y_{PS}}{Y_{XS}} \mu X \tag{4.70}$$

In the system model, the production rate is directly linked to the product concentration by:

$$\frac{dP}{dt} = \gamma - DP \tag{4.71}$$

Thus, the product concentration dynamics will be used to develop an estimate of γ.

It should be mentioned that due to restriction in the software for experimental validation, only observers with simple structures can be considered and developed. Three estimation strategies are therefore developed and will be presented hereafter.

4.6.1. Numerical differentiation

From the lactic acid concentration dynamics (equation (4.71)), a simple way to calculate an estimation of γ, denoted $\hat{\gamma}$ is to use the product concentration and its first order derivative:

$$\hat{\gamma} = \dot{P} + DP \qquad (4.72)$$

The first derivative $\dot{P}$ can be calculated by a backward differentiation technique. However, in case of noisy measurements of P, this approach can lead to a very bad estimation. A classical approach to avoid this phenomenon consists in filtering the noisy signal. In this work, the technique proposed in (Fliess, et al., 2008) was considered. It uses a moving horizon time-integration of the noisy signal in order to reconstruct its first derivative.

The first derivative of the product concentration is then calculated by:

$$\hat{\dot{P}} = -\frac{3!}{T^3} \int_0^T (T - 2t)P(t)dt . \qquad (4.73)$$

where [0,T] is a moving "short" time window.

4.6.2. The Kalman filter

In this section the linear Kalman filter principle presented in section 4.3.1 is considered in order to construct a linear estimator of the production rate. This approach is applied in two cases: constant and linear production rate models. These two cases are presented hereafter. Indeed, the production rate is constant at the steady state, and can be modeled by a linear model in the batch mode. Consequently, these two models are good candidates to model the real behaviour of the production rate. In addition, these models are among the simplest ones.

4.6.2.1. Constant production rate model

First, the production rate is assumed to be constant. The system to be considered for the estimation problem is as follows:

$$\begin{cases} \dot{P} = \gamma - DP \\ \dot{\gamma} = 0 \end{cases} \qquad (4.74)$$

where $\dot{\gamma}$ is the derivative of the production rate. The observability analysis (see appendix C.1) was performed for the system represented by equations (4.74). The system is then represented by equation (4.56) with $x=(P,\gamma)^T$, $u=D$, $y=P$ and **F** and **H** defined as:

$$\mathbf{F} = \begin{bmatrix} \gamma - DP \\ 0 \end{bmatrix} \qquad (4.75)$$

$$\mathbf{H} = \begin{bmatrix} 1 & 0 \end{bmatrix}$$

(4.76)

As x has dimension 2, it is necessary to calculate the first two Lie derivatives as follows:

$$L_{\mathbf{F}}^0 \mathbf{H}(x) = P$$

(4.77)

$$L_{\mathbf{F}}^1 \mathbf{H}(x) = \sum_{i=1}^{n} \frac{\partial L_{\mathbf{F}}^0 \mathbf{H}(x)}{\partial x_i} \mathbf{F}_i(x) = \dot{P}$$

(4.78)

the observation space Ω is then defined by:

$$\Omega = \mathbf{span} \left\{ \mathbf{H}(x), L_{\mathbf{F}}^1 \mathbf{H}(x) \right\}$$

(4.79)

From equation (4.79), the observability distribution to collect the "gradient" vector of every component in Ω is then defined as follows:

$$d\Omega = \begin{bmatrix} \dfrac{\partial \Omega}{\partial P} \\ \dfrac{\partial \Omega}{\partial \gamma} \end{bmatrix}$$

(4.80)

Using the dynamics equations of the states in equation (4.74), it was possible to determine that $d\Omega$ has rank=2. The rank conditions state that this new system is then observable. In order to develop the Kalman observer, this model (equation (4.74)) is first discretized. Indeed, the control and estimation strategies will be implemented online in a discrete form. As previously mentioned, the system dynamics are slow enough in comparison to the chosen sampling time, so that the Euler discretization scheme can be considered. Stochastic signals are further included in the model to take into account model uncertainties:

$$\begin{bmatrix} P_{k+1} \\ \gamma_{k+1} \end{bmatrix} = \begin{bmatrix} -D_k T_s & T_s \\ 0 & 1 \end{bmatrix} \begin{bmatrix} P_k \\ \gamma_k \end{bmatrix} + \begin{bmatrix} v_{1,k} \\ v_{2,k} \end{bmatrix}$$

(4.81)

$$P_k = \begin{bmatrix} 1 & 0 \end{bmatrix} \begin{bmatrix} P_k \\ \gamma_k \end{bmatrix} + w_k$$

(4.82)

where T_s is the sampling time, P is the lactic acid concentration, γ is the production rate, k in subscript represents the discrete time index, the dilution rate is discretized. v and w are the process and measurement noises respectively. They are assumed to be centered Gaussian white noises with constants covariance matrices Q and R respectively.

The discrete Kalman filter algorithm is applied to the system (equations (4.81) and (4.82) to reconstruct the product concentration and production rate from the product concentration available online. The observer structure is illustrated in figure 4.6.
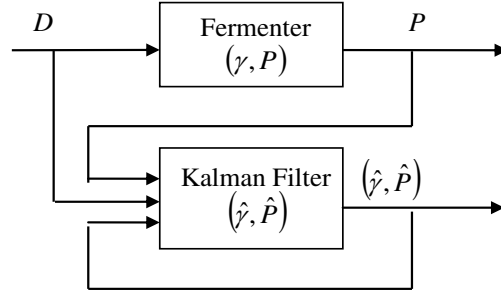
Figure 4.6 Kalman Filter structure for production rate estimation (constant model for γ).

4.6.2.2. *Linear production rate model*

Another possibility to model the evolution of the production rate with time is to consider a linear behaviour. This assumption is more accurate in case of a batch culture or during transient phase of a continuous culture. The model is in this case given by:

$$\begin{cases} \dot{P} = \gamma - DP \\ \ddot{\gamma} = 0 \end{cases} \tag{4.83}$$

where $\ddot{\gamma}$ is the second derivative of the estimated production rate. The observability analysis (see appendix C.1) was also performed for the system represented by equations (4.83). The system is then represented by equation (4.56) with $x=(P ,\gamma ,\dot{\gamma})^T$, $u=D$, $y=P$ and **F** and **H** defined as:

$$\mathbf{F} = \begin{bmatrix} \gamma - DP \\ \dot{\gamma} \\ 0 \end{bmatrix} \tag{4.84}$$

$$\mathbf{H} = \begin{bmatrix} 1 & 0 & 0 \end{bmatrix} \tag{4.85}$$

As x has dimension 3, it is necessary to calculate the first three Lie derivatives as follows:

$$L_{\mathbf{F}}^0 \mathbf{H}(x) = P \tag{4.86}$$

$$L_{\mathbf{F}}^1 \mathbf{H}(x) = \sum_{i=1}^{n} \frac{\partial L_{\mathbf{F}}^0 \mathbf{H}(x)}{\partial x_i} \mathbf{F}_i(x) = \dot{P} \tag{4.87}$$

$$L_{\mathbf{F}}^2 \mathbf{H}(x) = \sum_{i=1}^{n} \frac{\partial L_{\mathbf{F}}^1 \mathbf{H}(x)}{\partial x_i} \mathbf{F}_i(x) = \frac{\partial \dot{P}}{\partial X} \dot{P} + \frac{\partial \dot{P}}{\partial S} \dot{\gamma} + \frac{\partial \dot{P}}{\partial M} \ddot{\gamma} \tag{4.88}$$

the observation space Ω is then defined by:

$$\Omega = \mathbf{span} \left\{ \mathbf{H}(x), L_{\mathbf{F}}^1 \mathbf{H}(x), L_{\mathbf{F}}^2 \mathbf{H}(x) \right\} \tag{4.89}$$

From equation (4.89), the observability distribution to collect the "gradient" vector of every component in Ω is then defined as follows:

$$d\Omega = \begin{bmatrix} \dfrac{\partial \Omega}{\partial P} \\ \dfrac{\partial \Omega}{\partial \gamma} \\ \dfrac{\partial \Omega}{\partial \dot{\gamma}} \end{bmatrix} \qquad (4.90)$$

Using the dynamics equations of the states in equation (4.83), it was possible to determine that $d\Omega$ has rank=3. The rank conditions state that this new system is also observable.

As in the previous case, the model is discretized and additive noise signals are included to model uncertainties:

$$\begin{bmatrix} P_{k+1} \\ \gamma_{k+1} \\ \dot{\gamma}_{k+1} \end{bmatrix} = \begin{bmatrix} -D_k T_s + 1 & T_s & 0 \\ 0 & 1 & T_s \\ 0 & 0 & 1 \end{bmatrix} \begin{bmatrix} P_k \\ \gamma_k \\ \dot{\gamma}_k \end{bmatrix} + \begin{bmatrix} v_{1,k} \\ v_{2,k} \\ v_{3,k} \end{bmatrix} \qquad (4.91)$$

$$P_k = \begin{bmatrix} 1 & 0 & 0 \end{bmatrix} \begin{bmatrix} P_k \\ \gamma_k \\ \dot{\gamma}_k \end{bmatrix} + w_k \qquad (4.92)$$

In this case, the state to be estimated includes also the first derivative of the production rate. A discrete Kalman filter is used for the estimations in the system represented by equations (4.91) and (4.92). The observer structure is illustrated in figure 4.7.
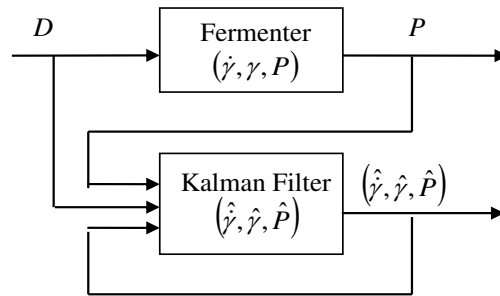
Figure 4.7 Kalman Filter structure for production rate estimation (linear model for γ).

4.6.3. *Validation of observers performance in simulation*

In this section, the production rate estimation strategies are validated in simulation. Model parameters and initial conditions used for simulation are those presented in table 4.1. Simulations lasted 30 hours, with a sampling time T_s= 5 min. Two cases were considered: a constant (figures 4.8 and 4.9) and a time varying (Figure 4.10) dilution rate.

Results obtained with the numerical differentiation approach, the Kalman filter with a constant model for γ (referred to as Kalman 1 hereafter) and the Kalman filter with a linear model for γ (referred to as Kalman 2) are presented in Figure 4.8. A Gaussian white noise is applied to the lactic acid concentration, P, with a standard deviation of 1% (as in previous sections). The simulation started in batch mode ($D = 0$) and at 15 h and onwards, a dilution rate of 0.1 h^{-1} was applied. The initial value of γ is calculated from the considered growth rate model (equation (3.29)). The covariance matrices Q and R for Kalman filter are chosen diagonal as follows. Kalman filter 1: Q=diag([0.01; 0.01]), R=0.01. Kalman filter 2: Q=diag([0.01; 0.01; 0.01]), R=0.01. These values were chosen considering the order of magnitude of variables in the system. The window for numerical differentiation is chosen equal to $20T_s$ (by a trial-and-error technique).
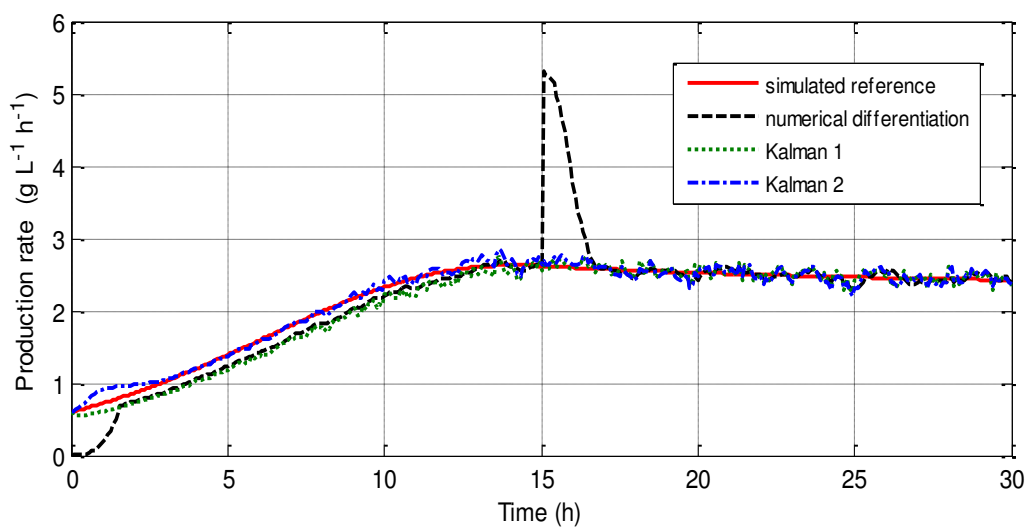
Figure 4.8 Observer (production rate) performances for piecewise constant dilution rate
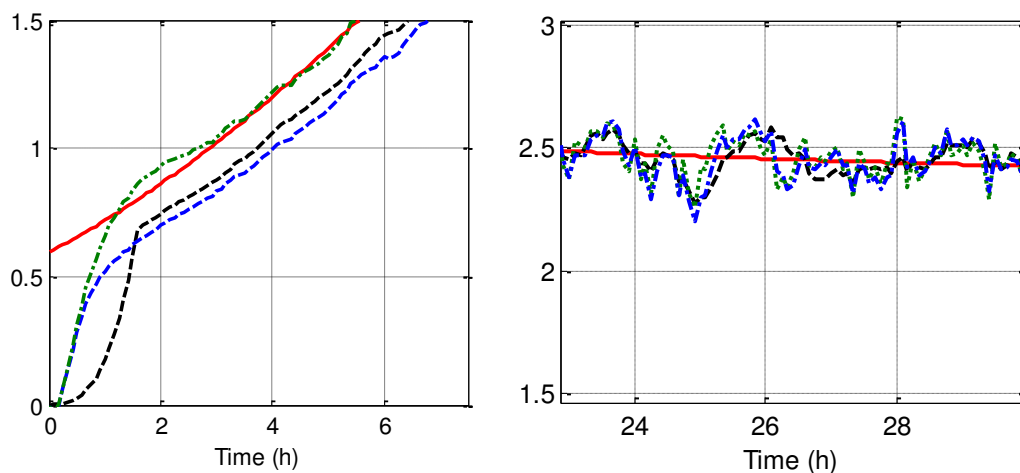
Figure 4.9 Zoom on production rate estimation during the first 5 hours (on the left) and at steady state (on the right).

157

With the numerical differentiation method, a discontinuity is observed when the dilution rate changes. The two Kalman filters present better performance than the numerical differentiation. The zoom on the production rate (Figure 4.9) shows that the Kalman filter 1 performs well when the dilution rate is not zero, but an offset is present when $D = 0$. In the case of the Kalman filter 2, an overestimation of the production rate occurs for the first 2 hours of fermentation. Then, the estimated value of γ is very close to the real one. In steady-state both filters lead to quite similar performances.

Secondly, a sinusoidal time varying dilution rate is considered (Figure 4.10) in order to test the performance of the three estimation strategies, even if this kind of variations is not necessarily realistic from the point of view of real operating conditions. In this case, no measurement noise was included to focus the study on the performance with respect to the dilution rate evolution. In addition, the estimators were initialized at 0 in order to study their performance with respect to initialization error. From Figure 4.10, it can be noticed the bad performance of the numerical differentiation strategy. This behaviour is mainly due to the choice of the sampling time which is not small enough in comparison to the variation of D. Consequently, the finite difference presents a poor accuracy. Another simulation was performed with a variation in the dilution rate less important than the considered in Figure 4.10. The obtained results are presented in Figure 4.11.
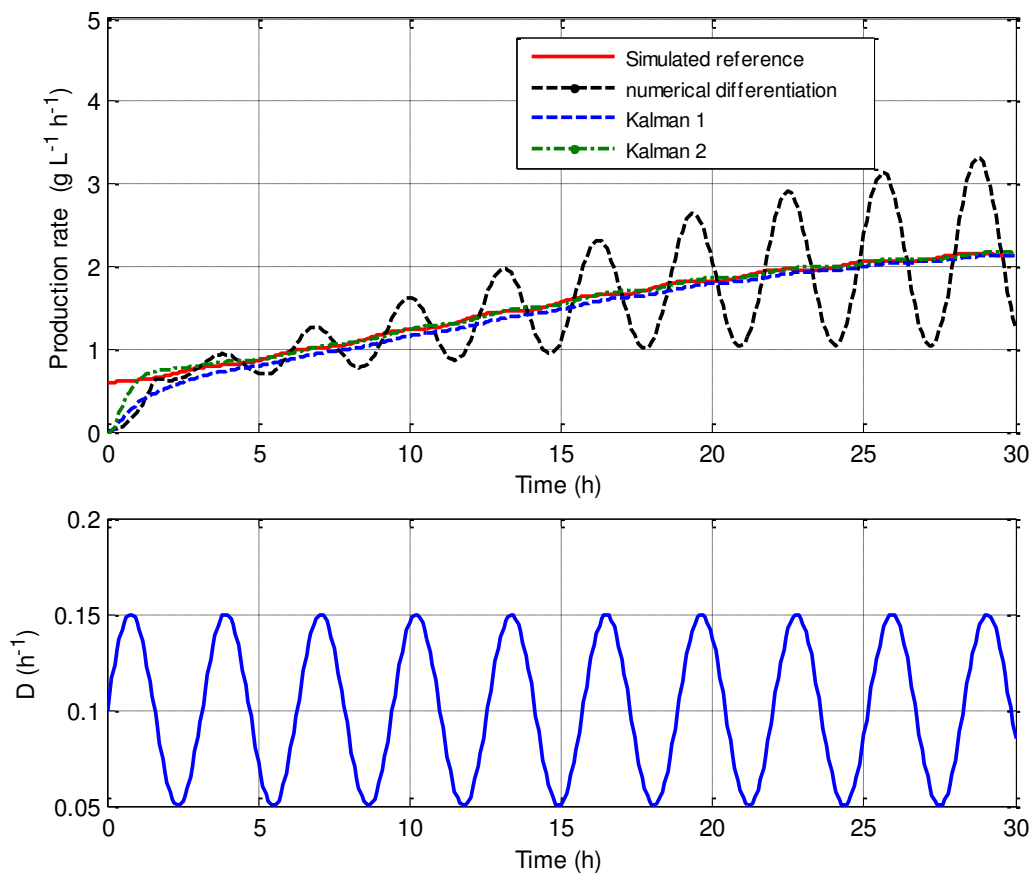
Figure 4.10 Observer (production rate) performances for sinusoidal dilution rate.
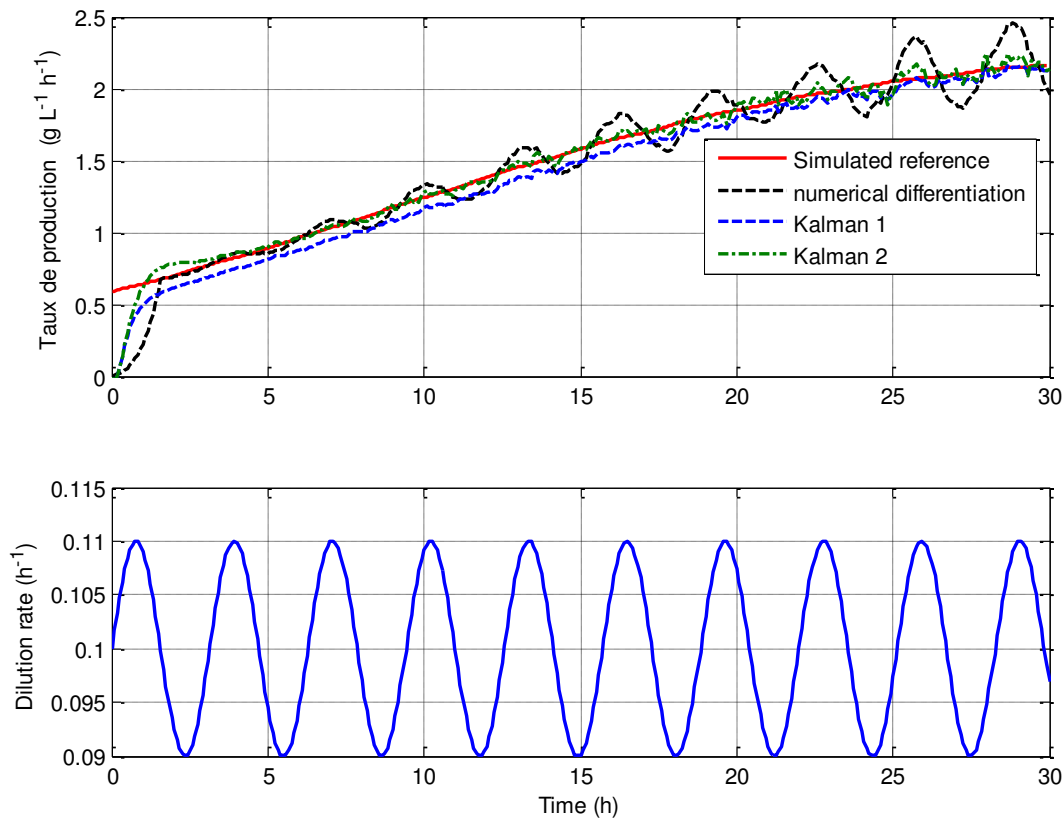
Figure 4.11 Observer (production rate) performances for sinusoidal dilution rate. Lower dilution rate variation.

As it is proved in Figure 4.11, the estimation by the numerical differentiation technique performs better with lower variations in the dilution rate. Nevertheless, its performance is rather bad compared to the performances of the Kalman filters.

The two Kalman filters reconstruct the production rate with a good accuracy. An error is however present but it remains small and bounded.

From this simulation study, the estimation of the production rate from the lactic acid concentration is possible using a Kalman filter. Both, linear and constant models of production rate lead to good performances, with a slight superiority of the linear model. Nevertheless, the Kalman based on a constant production rate model provides the best compromise between performance and simplicity of implementation.

4.7.   CONCLUSIONS

In this chapter the design of estimation strategies to reconstruct the state variables (glucose, biomass, maltose and lactic acid concentrations) of the SSPHF bioreactor was presented. First, the online calculation of the lactic acid concentration was developed based on the added

sodium hydroxide for pH regulation. Indeed, as the pH value in the bioreactor decreases with the increasing lactic acid concentration, the former must be regulated at constant value by adding sodium hydroxide. The considered approach exploits the online measurement of the sodium hydroxide inlet flow to obtain an online estimate of the lactic acid concentration. This approach allowed determining accurately the real lactic acid concentration in the bioreactor.

For the online estimation of the other not measured state variables, two observers were proposed: the Extended Kalman Filter (EKF) and the Unscented Kalman filter (UKF). The latter exhibited better results in simulation as it does not require any linearization approximation approach. Nevertheless, both estimators are very depending on the model quality.

Considering the importance of assessing the rate of lactic acid production during the fermentation process, the estimation of this variable from the calculated online lactic acid concentration was studied. Three different approaches were considered: a numerical differentiation method and two Kalman filters. The first Kalman filter approach considers a constant model for the production rate dynamics while the second one deals with a linear model. Simulations showed the accuracy and robustness of the proposed observers. The numerical differentiation method did not perform satisfactory, mainly in case of input discontinuities, whereas both Kalman filters performed well. The Kalman filter based on a constant production rate model provides the best compromise between performance and simplicity of implementation. It will be further implemented on the real system in chapter 5, combined to the control law.

CHAPTER 5: CONTROL STRATEGY

5.1. INTRODUCTION

Due to the expanding use of lactic acid the first monomer for the PLA (Poly Lactic Acid) production, more efficient and reliable processes to optimize its production are required. The process control becomes a must when trying to improve the process production operation. The main goals when applying control methods to this type of biotechnological processes are to improve operational stability and production efficiency (Ben Youssef, et al., 2005). Nevertheless, three main obstacles have hampered the development of modern control strategies in biotechnological processes: First, since bioprocesses involve living organisms, their dynamics are often poorly understood, strongly nonlinear and non-stationary; in addition, the replicability of experimental results is not guaranteed. Secondly, the microorganisms can suffer metabolic variations and physiological modifications over long operation periods resulting in a change in the model parameters values over time. Finally reliable sensors for real time monitoring of key variables are often lacking (Bastin & Dochain, 1990).

Despite these difficulties, several reference books and articles have been published during the last three decades. Proposed control techniques have been applied to various biotechnological processes such as biomass production, fermentations, anaerobic digestion, yeast production, penicillin production, microalgae cultures, etc. ((Pons, 1991);(Roux, et al., 1996);(Saha, et al., 1999);(Hilgert, et al., 2004);(Mailleret, et al., 2004) ;(Marcos, et al., 2004); (Ramaswamy, et al., 2005); (Jenzch, et al., 2006);(Selişteanu, et al., 2007) ;(Becerra Celis, 2009)).

In the case of lactic acid production, only few control strategies have been reported in the literature. Most of them concern fed batch cultures (Choi, et al., 2014) while other deal with continuous cultures using glucose as raw material. An adaptive on-line optimizing control strategy for maximizing lactic acid productivity from glucose has been proposed in (Shi, et al., 1990): two variables were measured online, the product and biomass concentrations.

More generally, an adaptive predictive control strategy for regulating the biomass concentration in continuous fermentation processes was proposed by (Dahhou, et al., 1991). This predictive control scheme calculates the dilution rate from the on-line estimation of the specific growth rate (considered as a time varying parameter). Simulations were performed to demonstrate the efficiency of the control strategy.

Lombardi (1996) proposed the regulation of lactic acid concentration in a bioprocess that used glucose as substrate. In this approach, the bioreactor is fed by two different inlet flows, one containing glucose, and other containing lactic acid. The control strategy consists in limiting bacteria growth by adding lactic acid at a low concentration while the glucose inlet flow is

maintained constant. The operational point of the bioreactor is determined to guarantee that the quantities of lactic acid introduced in the reactor are small. This approach was not experimentally validated.

A system with two bioreactors in cascade developed to maximize lactic acid production was proposed in (Ben Youssef, et al., 2000) using glucose as substrate. The control approach considered the substrate regulation using an adaptive predictive control structure and online measurements of the substrate concentration. The specific rates in the model (growth and production rates), required for the control law, were estimated online using an asymptotic observer. This approach was not validated experimentally, but simulations were encouraging. Petre et al. (2011) further studied the previous system and proposed an indirect adaptive controller based on a dynamical neural network. The effectiveness of this control approach was proved by simulations.

Considering the control methods for lactic acid production from wheat flour, no work has been reported in the literature. Nevertheless, some works concerning control strategies for ethanol fermentation from starch materials can be found. A control strategy for the fed-batch Simultaneous Saccharification Fermentation process from Starch to Ethanol (SSFSE) was proposed in (Ochoa, et al., 2008). The control objective was to maintain the glucose concentration at a quasi-equilibrium state by feeding starch into the process. An adaptive approach was considered estimating the glucose consumption and ethanol production rates in the bioreactor from starch and glucose concentrations, the latter were supposed to be measured. This approach was not experimentally validated due to the lack of online sensors to determine sugars concentrations.

In conclusion, most works in control strategies applied to the lactic acid production have not been experimentally validated due to the lack of reliable sensors. It is then interesting to study these aspects. This chapter focuses on the development of control strategies for lactic acid production from wheat flour, and their validation by experiments. After a brief control system description, a steady state analysis is performed in order to determine the optimal operation point which maximizes the lactic acid production rate. Then a linearizing control strategy is proposed in order to maintain the process operating at the desired optimal operation point. Later, an adaptive control approach is proposed in order to reduce complexity in the control design and improve its robustness. Finally, the experimental validation of the best control strategy for the process concludes the chapter.

5.2. CONTROL SYSTEM DESCRIPTION

In the first place it is important to describe the different components of the control system:

- The SSPHF (simultaneous saccharification, proteins hydrolysis and fermentation) bioreactor, represented by equations (3.29) is the system that we want to control.
- The output variable is the lactic acid concentration, online estimated through the measurement of the sodium hydroxide inlet flow (see section 4.4).

- The input or control variable is the dilution rate whose manipulation affects the output variable and therefore makes its control possible.
- The control objective is to regulate the lactic acid concentration at a desired value by modifying the dilution rate. The goal is to attain the best performances in lactic acid production rate, determined from a steady state analysis further described in the following sections.

Considering these statements, the next step in the development of a control law is to determine the optimal operation point which leads to the highest lactic acid production rates.

5.3. STATE SPACE REPRESENTATION OF THE SYSTEM

In order to facilitate the reading and understanding of this chapter the dynamical, system will be represented in the state space formalism. The dynamical model of the bioreactor is recalled here:

$$\frac{dX}{dt} = \mu X - DX \tag{5.1}$$

$$\frac{dP}{dt} = \frac{Y_{PS}}{Y_{XS}} \mu X - DP \tag{5.2}$$

$$\frac{dS}{dt} = -\frac{1}{Y_{XS}} \mu X + k_M M + D(S_0 - S) \tag{5.3}$$

$$\frac{dM}{dt} = -k_M M + D(M_0 - M) \tag{5.4}$$

$$\mu = \mu_{max} \frac{S}{k_S + S} \left(1 - \frac{P}{P_{max}}\right)^n \tag{5.5}$$

The set of state equations (5.1) to (5.5) will be rewritten in the state-space formalism, as a continuous time nonlinear dynamic system, described in the general case by:

$$\dot{x}(t) = f(x) + g(x)u$$
$$y(t) = h(x) \tag{5.6}$$

where $x(t) \in \mathfrak{R}^n$ is the state vector, $u(t) \in \mathfrak{R}^m$ is the control vector, $y(t) \in \mathfrak{R}^p$ is the output vector, $f=(f_1,f_2,...f_n)^T$ is a vector field of $\mathfrak{R}^n \rightarrow \mathfrak{R}^n$ and $h=(h_1,h_2,...,h_p)^T$ is a nonlinear vector on $\mathfrak{R}^p$. Equations (5.6) are the evolution and the observation equations, respectively. Indeed, the proposed continuous model for the SSPHF step is an affine in control system and can be represented in the simplified form in equations (5.6) with $\dot{x} = dx/dt$, $x=(X, S,M,P)^T$, $u=D$, $y=P$. g and f are given by:

$$g = \begin{bmatrix} -X \\ -(S - S_0) \\ -(M - M_0) \\ -P \end{bmatrix} \qquad (5.7)$$

$$f = \begin{bmatrix} \mu_{max} \dfrac{S}{k_S + S}\left(1 - \dfrac{P}{P_{max}}\right)^n \\[3mm] -\dfrac{\mu}{Y_{XS}} \mu_{max} \dfrac{S}{k_S + S}\left(1 - \dfrac{P}{P_{max}}\right)^n + k_M M \\[3mm] -k_M M \\[3mm] \dfrac{Y_{PS}}{Y_{XS}} \mu_{max} \dfrac{S}{k_S + S}\left(1 - \dfrac{P}{P_{max}}\right)^n X \end{bmatrix} \qquad (5.8)$$

The system represented by the equations (5.7) and (5.8) will be used for the mathematic developments in this chapter.

5.4. OPTIMAL CONTINUOUS OPERATION

5.4.1. Determination of steady state variables

In order to calculate the optimal operational point of the bioreactor, first, the state variables at steady state must be determined. In this approach, they are expressed as function of the dilution rate, the control variable. Indeed, as the manipulation of this variable will lead to the control of the bioreactor, it is important to determine the behaviour of state variables if a change in the dilution rate is applied.

In steady state conditions, the dilution rate equals the growth rate defined by equation (5.5) leading to:

$$\bar{D} = \bar{\mu} = \mu_{max} \frac{\bar{S}}{k_S + \bar{S}}\left(1 - \frac{\bar{P}}{P_{max}}\right)^n \qquad (5.9)$$

where $\bar{D}$, $\bar{S}$ and $\bar{P}$ are the dilution rate, glucose and lactic acid concentrations at steady state, respectively. As in this work high substrate concentrations (100 g/L) are used, the Monod term is equal to 1; indeed, the k_S value in equation (5.9) is generally very low (close to 1 g L^{-1}) according to several works (Akerberg, et al., 1998)(Ben Youssef, et al., 2000). The simplified equation (5.10) will then be used:

$$\overline{D} = \mu \approx \mu_{max}\left(1 - \frac{\overline{P}}{P_{max}}\right)^n \qquad (5.10)$$

The lactic acid concentration at steady state from (5.10) can then be represented by:

$$\overline{P} = \left(-\frac{\overline{D}^{1/n}}{\mu_{max}^{1/n}} + 1\right)P_{max} \qquad (5.11)$$

To determine the biomass concentration at steady state, the derivative in equation (5.2) is cancelled giving to:

$$\overline{P} = \frac{Y_{PX}}{Y_{XS}}\frac{\overline{\mu}}{D}\overline{X} \qquad (5.12)$$

where $\overline{X}$ is the biomass concentration at steady state. As $\overline{\mu} = \overline{D}$, the biomass concentration at steady state can be represented as a function of the dilution rate by combining equations (5.11) and (5.12) as follows:

$$\overline{X} = \frac{Y_{XS}}{Y_{PS}}\left(-\frac{\overline{D}^{1/n}}{\mu_{max}^{1/n}} + 1\right)P_{max} \qquad (5.13)$$

After cancelling the dynamic term in equation (5.3), the glucose concentration at steady state can be obtained:

$$\overline{S} = \frac{K_M \overline{M}}{\overline{D}} + S_0 - \frac{\overline{X}}{Y_{XS}} \qquad (5.14)$$

where $\overline{M}$ is the maltose concentration at steady state. Equation (5.14), shows that $\overline{S}$ does not only depend on the biomass concentration but also on the maltose concentration and on the dilution rate. From equation (5.4), it is possible to determine the maltose concentration at steady state:

$$\overline{M} = \frac{\overline{D}M_0}{\overline{D} + K_M} \qquad (5.15)$$

By combining equations(5.15) and(5.14) the following expression is obtained:

$$\overline{S} = \frac{K_M M_0}{(\overline{D} + K_M)} + S_0 - \frac{\overline{X}}{Y_{XS}} \qquad (5.16)$$

Finally, from equations (5.13) and (5.16), the glucose concentration at steady state becomes:

$$\overline{S} = \frac{K_M M_0}{(\overline{D} + K_M)} + S_0 - \frac{1}{Y_P}\left(-\frac{\overline{D}^{1/n}}{\mu_{max}^{1/n}} + 1\right)P_{max} \qquad (5.17)$$

From equations (5.11),(5.13), (5.15) and (5.17), all variables at steady state are expressed only as functions of the dilution rate. This result is important as it reduces the number of experiments necessary to obtain the optimal operational conditions of the bioreactor.

The experimental results obtained in the continuous experiments presented in chapter 3 (see section 3.5) were used to validate the steady state concentrations predicted by the model. Figure 5.1 shows the comparison of the model and experimental results at steady state. The prediction is rather accurate for biomass, lactic acid and maltose concentrations. The agreement for glucose concentration at steady state is less satisfactory due to its production from other sugars (than maltose) which was not taken into account in the model.

Each point in Figure 5.1 represents an operation point; the aim is then to determine the one which makes the process more performant in terms of lactic acid productivity. In the following the determination of this optimal operation point is presented.
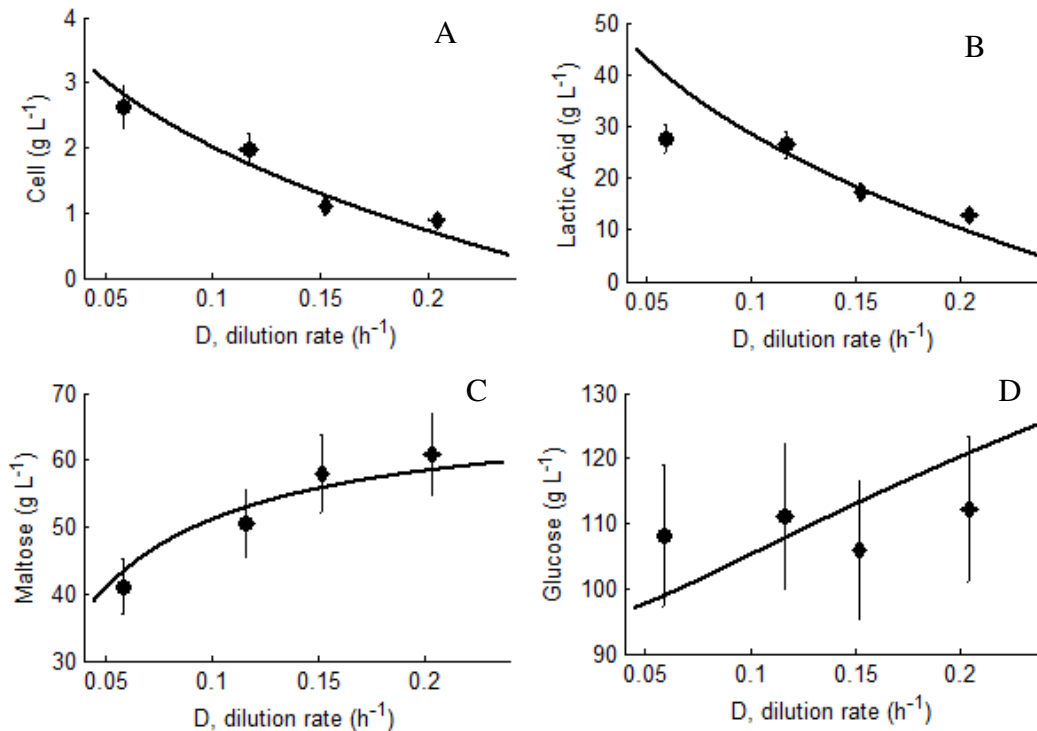
Figure 5.1 Modelling the SSPHF step at steady state. Comparison between experimental values at steady state for experiment 1 (●) and experiment 2 (◆) with the steady state model (——). (A) Cell concentration, (B) Maltose concentration, (C) Lactic Acid concentration (D) Glucose concentration.

5.4.2. *Optimal operation point*

The experimental lactic acid production rate (in g L^{-1} h^{-1}) at steady state (parameter to be maximized), defined as $\overline{P} * \overline{D}$ was calculated for each experiment described in chapter 3 (section 3.5.1.2) and estimated by the model (equations (5.11),(5.13), (5.15)) and (5.17)) for the range of dilution rates between [0.04 0.24] h^{-1} (Figure 5.2). This model predicts that the

productivity function is concave and has only one maximal value. It is due to the product inhibition effect. Indeed, for high lactic acid concentrations, the production rate decreases. The aim is to operate the process around this maximal productivity. Experimentally, it was not possible to find accurately the maximal productivity for two reasons: there are only few experimental points and for some points the perfect steady state conditions were not ensured. There is a large range of dilution rates (0.1 to 0.2 h^{-1}) ensuring an important lactic acid production rate around 2.7 g L^{-1}h^{-1}. Considering the parabolic shape of the steady state production rate as a function of $\overline{D}$, experimental data were fitted to an inverse parabola (Figure 5.2.) in order to facilitate the determination of the maximal productivity.
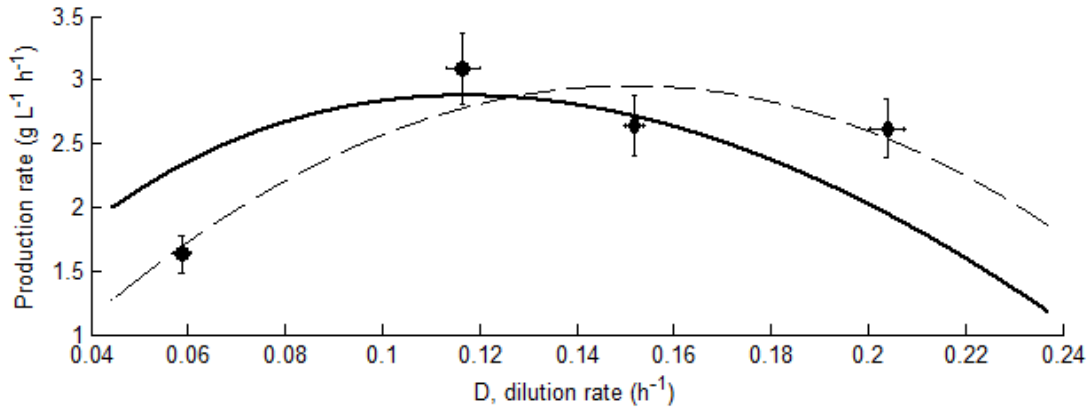
Figure 5.2 Modelling the SSPHF step at steady state. Comparison between experimental production rate values and model at steady state for experiment 1 (●) and experiment 2 (◆). (——)steady state model (– – -) Polynomial fitting of experimental production rates.

In the following, two approaches are considered in order to determine more accurately the optimal operation point from experimental data and model predicted values.

5.4.2.1.   Polynomial interpolation of experimental data

The optimal dilution rate can be determined by fitting experimental production rates to an inverse parabola and by estimating the maximum of the parabolic function:

$$\overline{\gamma} = -148.13\overline{D}^2 + 44.69\overline{D} - 0.42 \qquad (5.18)$$

where $\overline{\gamma} = \overline{P}\overline{D}$ is the production rate at steady state defined in the dilution range [0.04 to 0.24] h^{-1}. The obtained parabola (– –) is presented in Figure 5.2. The maximum value of $\overline{\gamma}$ can be determined by cancelling its derivative with respect to $\overline{D}$ as in the following equation:

$$\frac{d\overline{\gamma}}{d\overline{D}} = 0 = -2*148.13\overline{D} + 44.69 \qquad (5.19)$$

Optimal values of dilution rate and production rate at steady state obtained using equation (5.19) were 0.15 h^{-1} and 2.95 g L^{-1} h^{-1}, respectively.

5.4.2.2.   Using the developed model

In this approach the steady state point for the system ((5.11),(5.13), (5.15) and (5.17)) is determined so that the lactic acid productivity is maximized. This problem is formulated as a single-variable constrained optimization problem as follows:

$$\overline{D}^* = \arg\max \overline{D} \cdot \overline{P}$$
$$\text{s.t. Equations (5.11),(5.13), (5.15) and (5.17)} \qquad (5.20)$$
$$0 \leq \overline{D} \leq D_{max}$$

where D_{max} is the maximal dilution rate allowed by the experimental setup. The solution of this problem was determined numerically with a golden section search algorithm (Fletcher, 1987). Then, from the optimal value of $\overline{D}$ (denoted $\overline{D}^*$), the optimal setpoint ($\overline{X}^*$, $\overline{S}^*$, $\overline{P}^*$, $\overline{M}^*$, $\overline{D}^*$) can be determined from equations(5.11),(5.13), (5.15) and (5.17).The optimal solution obtained with this approach is $\overline{D}^* = 0.12\,h^{-1}$ and $\overline{\gamma}^* = 2.87$ g L^{-1} h^{-1}.

The optimal operational point values obtained by both approaches (polynomial interpolation and optimization problem formulation, see table 5.1) are similar and the lactic acid concentration mean value is then considered in the control law implementation. From these results, the control objective is to regulate the lactic acid concentration at the optimal value, 21 gL^{-1}.

In the following the development of control strategies to maintain the SSPHF bioreactor at the optimal operation point is described.

Table 5.1 Optimal operation point in the SSPHF bioreactor.

Steady State Variable	Polynomial Interpolation	Optimization problem formulation	Mean Values
$\overline{D}^*$	0. 15 h^{-1}	0. 12 h^{-1}	0.13 h^{-1}
$\overline{X}^*$	1.3gL^{-1}	1.7 gL^{-1}	1.5 gL^{-1}
$\overline{S}^*$	113 gL^{-1}	107.91 gL^{-1}	110gL^{-1}
$\overline{P}^*$	18 gL^{-1}	24.61 gL^{-1}	21gL^{-1}
$\overline{M}^*$	56 g L^{-1}	53 gL^{-1}	54 gL^{-1}
$\overline{\gamma}^*$	2.95 g L^{-1}h^{-1}	2.87g L^{-1}h^{-1}	2.9 g L^{-1}h^{-1}

5.5. DEVELOPMENT OF A FEEDBACK LINEARIZING CONTROL STRATEGY

For the control law development and its experimental validation, constraints related to the software capacity of the SSPHF bioreactor were taken into account. The bioreactor is equipped with a C-BIO software (Global Process Concept, La Rochelle France). This software has a calculation interface which can be used for the implementation of a control law. Nevertheless, due to restriction in the software (it only works with simple algorithms), only a simple control strategy must be designed.

Various conventional control techniques such as PID control law are proposed in the industry for the regulation of bioreactors. Nonetheless, these techniques are based on linear tangent model approximations or even on linear "black box models" (Bastin & Dochain, 1990). As we have prior knowledge of the nonlinear dynamics of the system, improved control performances can be designed. It can be done by the exploitation of the nonlinear structure of the model to solve the control design problem. In a first approach, the Feedback Linearizing Control will be used. Its development is presented in the next section.

5.5.1. Feedback Linearizing Control

Feedback linearization is an approach for nonlinear control design that has gained a lot of attention in recent years. The main idea is to algebraically transform nonlinear dynamic systems into (fully or partially) linear ones, so that linear control techniques can be further applied. In conventional control, one first calculates a linearized approximation of the model and then the control design is achieved using a linear controller for the approximate model. However, the closed loop remains nonlinear and its global stability is difficult to assess, maybe only valid around the linearizing point. The feedback linearization control differs from conventional (Jacobian) linearization because it is achieved by exact state transformation and feedback, rather than by linear approximations of the dynamics. In this approach a nonlinear controller is obtained and designed to achieve a linear closed loop model which is unconditionally stable. The basic idea is to simplify the form of a system by choosing a different state representation (Hedrick & Girard, 2010).
Let us introduce the feedback linearizing principle for a control affine system as the one represented by equation (5.6) and recalled here:

$$\dot{x}(t) = f(x) + g\big(x(t)\big)u(t)$$
$$y(t) = h(x(t))$$

(5.21)

Note that u appears linearly in equation (5.21). The controller design procedure for this kind of system is restricted to control affine systems. To ensure that the control law can be determined, it is usually assumed that the vector functions, $f(x)$ and $g(x)$, and the scalar function $h(x)$ are of class C^∞ (i.e. have continuous derivatives of all orders).

In order to calculate the linearizing control law some definitions and mathematical tools are recalled in the following:

Lie derivative for the control affine system

Consider the derivative of the output *y* with respect to time:

$$\dot{y} = \frac{\partial h}{\partial x}\dot{x} = \frac{\partial h}{\partial x}\left[f(x) + g(x)u\right] \tag{5.22}$$

Equation (5.22) can also be rewritten as:

$$\dot{y} = L_f h(x) + L_g h(x) \tag{5.23}$$

with

$$L_f h(x) = \frac{\partial h}{\partial x} f(x) \tag{5.24}$$

$$L_g h(x) = \frac{\partial h}{\partial x} g(x) \tag{5.25}$$

The Lie derivative function, $L_f h(x)$ corresponds to the derivative of the function $h(x)$ along the trajectories of the system $\dot{x} = f(x)$. In the same way, $L_g h(x)$ is called Lie derivative of $h(x)$ with respect to $g(x)$.

Relative degree of a nonlinear system

The relative degree of a system represents the number of times the output *y* has to be differentiated (with respect to time) until the control input *u* appears explicitly. It is defined as:

$$r \stackrel{\Delta}{=} \min\left\{k : L_g L_g^{k-1} h(x) \neq 0\right\} \tag{5.26}$$

If the system has a well-defined relative degree, the first *r* time derivatives of *y* can be represented as:

$$y^{(k)} = L_f^k h(x) \ k=0, 1, \dots ,r\text{-}1 \tag{5.27}$$

$$y^{(r)} = L_f^r h(x) + L_g L_f^{r-1} h(x)u \tag{5.28}$$

It can be shown that the nonlinear functions in equation (5.26) are linearly independent. If the system has a relative degree *r=n*, then it can be totally linearized and will be equivalent to *n* integrators (where *n* is the dimension of the state vector). This new linear model has a new input $\hat{u}$ and the output *y*. The state feedback control law is chosen as in (Isodori, 1989):

$$u = \frac{\hat{u} - L_f^r h(x_r)}{L_g L_f^{r-1} h(x_r)} \tag{5.29}$$

In the case where $r<n$, the system will be partially linearizable and will be equivalent to r integrators, using the relation (5.29).

5.5.2. *Application of the feedback linearizing control principle to our system*

First the relative degree of the system must be determined. The relative degree of the system is 1 as it is necessary to differentiate only once the output, $y=P$, with respect to time to obtain the input $u=D$ explicitly:

$$\dot{P} = \frac{Y_{PS}}{Y_{XS}} \mu X - DP \tag{5.30}$$

As $r=1$, only the product concentration dynamics can be linearized. The Lie derivatives necessary for the determination of the control law are calculated using equations (5.24),(5.25) and (5.28):

$$L_f h(x) = \frac{Y_{PS}}{Y_{XS}} \mu X \tag{5.31}$$

$$L_g L_f^0 h(x) = L_g h(x) = \frac{\partial h}{\partial x} g(x) = -P \tag{5.32}$$

Replacing equations (5.31) and (5.32) in equation (5.29) it is possible to obtain the control law for the system:

$$D = -\frac{1}{P}\left[\hat{D} - \frac{Y_{PS}}{Y_{XS}} \mu X\right] \tag{5.33}$$

The linearized system in equation (5.33) is equivalent to a simple integrator as r=1. In order to correct slight model/process mismatches and to reject disturbances, the control signal $\hat{D}$ will be delivered by an outer-loop by means of a Proportional controller:

$$\hat{D} = G(P - P_{ref}) \tag{5.34}$$

where G is the controller gain and P_{ref} is the reference product concentration. The controller gain is tuned to provide a desired closed-loop time response

The control law in equations (5.33) and (5.34) allows tracking the reference setpoint, P_{ref}, coming from the signal $\hat{D}$. The control law obtained is illustrated in figure 5.3.
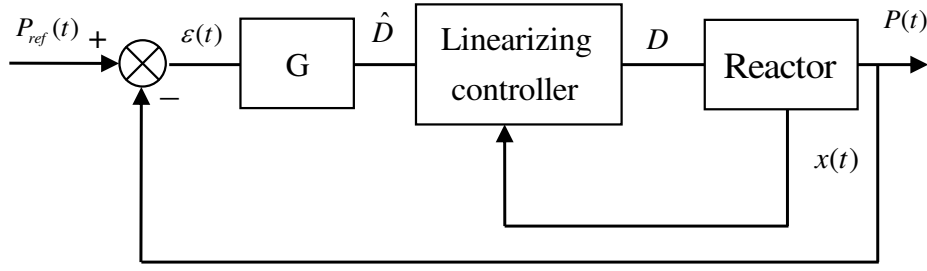
Figure 5.3 Feedback linearizing control architecture.

To implement the control strategy illustrated on figure 5.3, all states variables must be known online by measurement or by estimation. Since only the lactic acid concentration is available online, the other states must be estimated. The states observers developed in chapter 4 (see section 4.5), Extended Kalman filter and Unscented Kalman filter, were used to estimate the biomass, glucose and maltose concentrations from the lactic acid concentration.

5.5.3. *Feedback linearizing control performance in simulation*

As stated before, the aim of the control law is to regulate the lactic acid concentration to its optimal value P_{ref}=21 g L^{-1}.This value was chosen considering the optimal operation points summarized in table 5.1.To test the observability at this operation point, the determinant of the observability matrix($d\Omega$)was determined (see 4.5.1). This was possible as $d\Omega$ for the present system is a square matrix:

$$dΩ = \begin{bmatrix} \dfrac{\partial\Omega}{\partial X} \\ \dfrac{\partial\Omega}{\partial S} \\ \dfrac{\partial\Omega}{\partial M} \\ \dfrac{\partial\Omega}{\partial P} \end{bmatrix}$$

where the observation space Ω was defined by equation (4.63) and recalled here:

$$\Omega = \left\{ \mathbf{H}(x), L^1_{\mathbf{F}}\mathbf{H}(x), L^2_{\mathbf{F}}\mathbf{H}(x), L^3_{\mathbf{F}}\mathbf{H}(x) \right\}$$

The system is non-observable if det($d\Omega$)=0. Moreover, small values of det($d\Omega$) imply weak observability since the observability matrix is close to singularity (Magni et al., 2009). The observability is then considered along predicted trajectories for $\overline{X}$, $\overline{M}$, $\overline{S}$, $\overline{P}$ and $\overline{D}$. The model parameters obtained in chapter 3 (see Table 4.1) were used to determine the determinant of the observability matrix. At the optimal equilibrium point, det($d\Omega$) is found equal to 2.25×10^{-11}, very close to zero. The same test was done for various equilibrium points and parameter values. The det($d\Omega$) value was always as low as the value obtained with the optimal operation point. It means that even if the system is completely observable, it is

weakly observable. Thus, observers of state variables from P values available online can be not very accurate, depending in the considered operating conditions. Nevertheless, the performance of both developed state estimators coupled to the control loop was tested in simulation.

Three control laws were tested and compared. The first one considers the classical feedback linearizing controller given by equations(5.33)and (5.34)(referred to as Ideal), where all state variables are assumed to be measured online. It is important to notice that even if all states are measured online, the control law in equations(5.33)and (5.34) depends on values of parameters Y_{PS}, Y_{XS} and $\mu_{\max}$. Then, a prior knowledge of these parameters is required for the determination of the control law. In the second control law, the feedback linearizing controller is coupled to the EKF referred to as control EKF (see section 4.3.2). In the last control strategy, the state estimation is performed using the UKF estimation, referred to as control UKF (see section 4.3.3).

Initial values considered for the real system differ from those used in the EKF and UKF estimators in order to highlight the estimator robustness with respect to initialization errors. Simulations consider a random 20% non-correlated parameter mismatch in the real system (parameters of the real process differ from those used in both estimators and in the control law). This helps to test the robustness of the estimation and control law with respect to model mismatch.A Gaussian white noise is added to the output, the lactic acid concentration P, with a standard deviation of 1%.

The EKF and UKF tuning parameters are those chosen for the observers performance simulations (see section 4.5.3). Model parameters and initial conditions were presented in tables 3.6 and 4.1. The maximal dilution rate, D_{max},was fixed to 0.4 h^{-1} and the proportional controller gain was chosen as G=6h^{-1}. This gain value was chosen considering that the feedback linearized control law is equivalent to an integrator (leading to a closed-loop system with transfer function that equals $1/(1+s/G)$, where s is the Laplace transform); and that the desired response time was chosen equal to 0.5 h (leading to $3/G$=0.5).

Obtained results when applying the three control laws are presented in figure 5.4. When the fermentation starts, the bioreactor operates in batch mode in order to increase the lactic acid concentration. Once this concentration is close to the desired set point, a feed is introduced in the bioreactor in order to dilute the product concentration and maintain its value at the desired optimal point. The set point is reached after about 10 h with good transient behaviour. It can be noticed that the noise on the lactic acid estimation leads to some fluctuations on the control input. This phenomena could be reduced by filtering the output.

The comparison of the "ideal" trajectory (obtained with the Ideal control) with those obtained with the controller coupled with EKF and UKF shows that the three trajectories are very close. In all cases, the control law leads to a slight steady error (see zoom in figure 5.4). This is due to the parameter mismatch. It is important to highlight that even in the "control ideal" approach, an offset due to the error in the parameters used in the control law (equation (5.33)) is observed. This offset can be corrected by the implementation of an integral controller in the

outer-loop of the control strategy.Generally, in this case an anti-windup device is also necessary because of control input saturation (Gonzalez, et al., 2014). This has not been reported here since this strategy, as mentioned later, has not been implemented in the bioreactor. Nevertheless, good performances were obtained with the proposed control laws including EKF or UKF. In the case of EKF, an offset of 0.2 g L^{-1}in the set point tracking is observed, while the control law using the UKF provides an offset of only 0.004g L^{-1}.
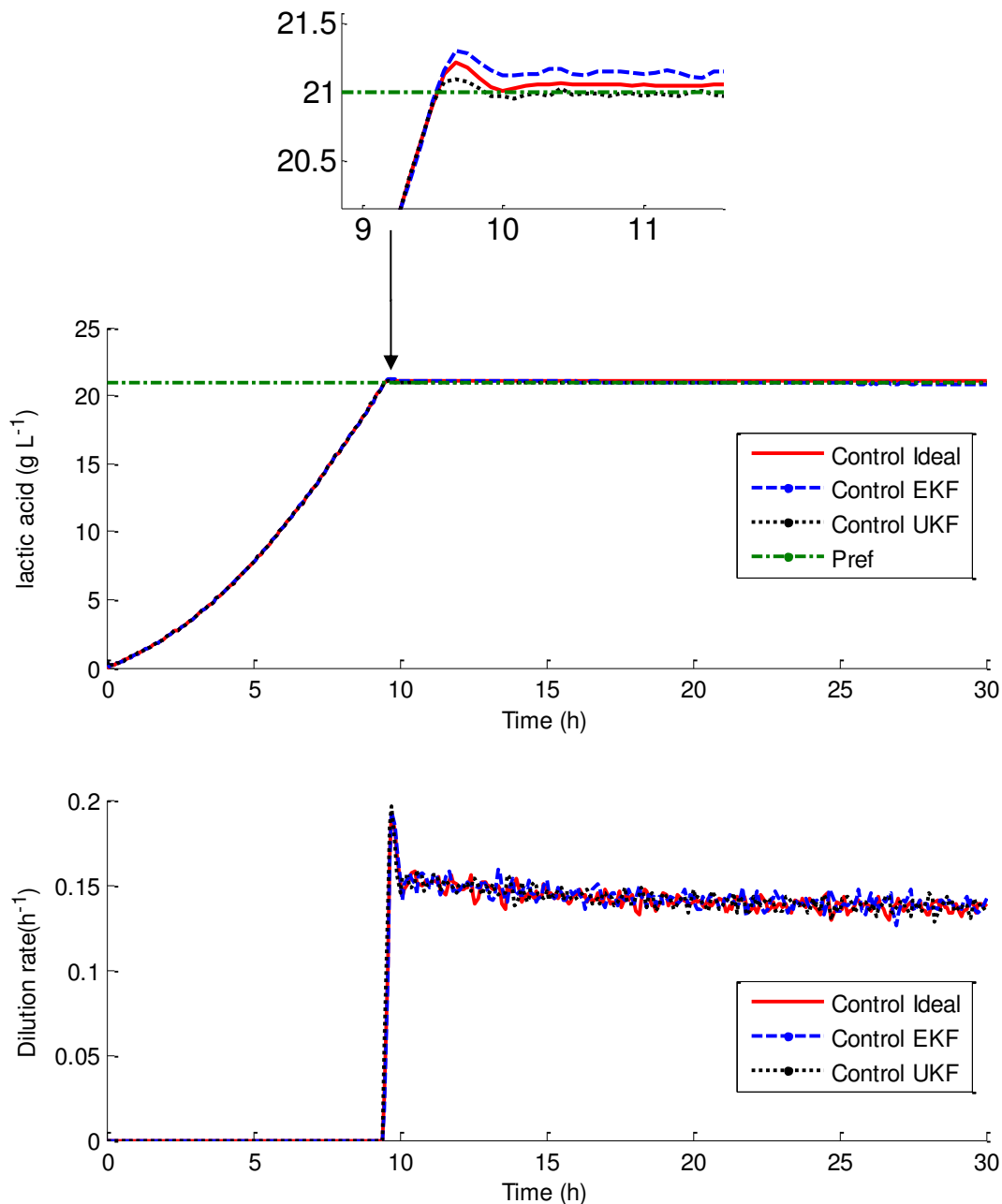
Figure 5.4 Control law performances for reference tracking. Feedback linearizing control. Product concentration and dilution rateversus time.

The state variables predicted by the real model (without parameter mistmach) and their estimated values obtained from the EKF and UKF estimators are compared in figure 5.5. The UKF better estimates the biomass concentration than the EKF one. The EKF biomass concentration estimate diverges at the end of the simulation. The glucose concentration estimations by UKF are closer to the real values than those obtained by EKF. The estimations of maltose concentration by both approaches are good and converge to the real value. It should be noticed that even if some of the state variables are not well estimated by the observers, the regulation of the lactic acid concentration is rather good with both estimators.

In conclusion, the control loop with the UKF filter shows better performances than the control law with EKF. Nevertheless considering the complexity of the UKF algorithm and as the bioreactor software for experimental validation is limited, the development of a simple control strategy is desired. In the next section the control approach is modified considering the experimental validation device and its capacities.
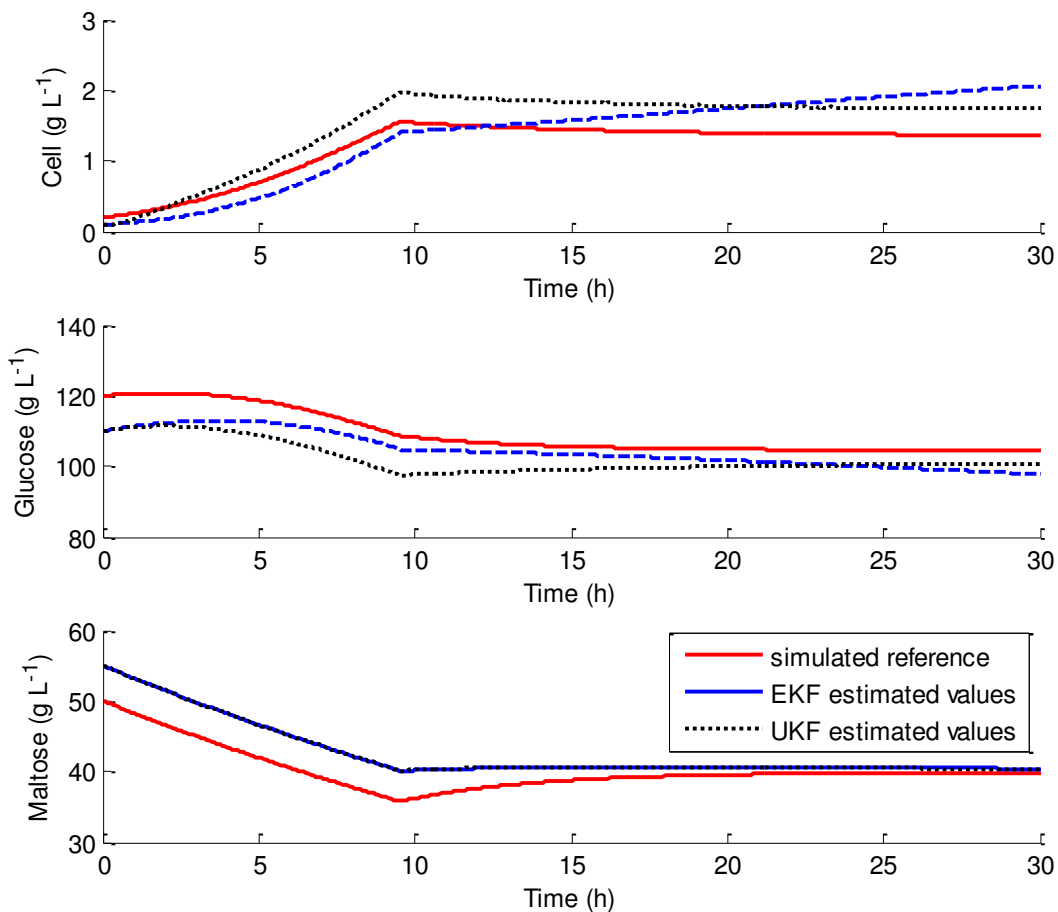
Figure 5.5 State variables evolution with time. Model and initial state values mismatches between the real system and the considered model.

5.6. ADAPTIVE CONTROL STRATEGY

As it was presented in the feedback linearizing control development in section5.5, the control design problem was solved by algebraic manipulations of the general dynamical model of the system. Nevertheless, the design was carried out assuming that the kinetics were known exactly which is not the case in this work. Moreover, in order to implement the feedback linearizing control, online estimators of the non-measured states were developed. However, in the state estimation, the quality of the estimate is not only related to the assumptions on uncertainty in the model and the parameters, but also to the convergence rate of the observers (Picó, et al., 2009). The simulation results showed that the observers proposed for the states estimation are very dependent on the model (see figure 5.5). Moreover as the system is weakly observable, this means that it is difficult to assure the good performance of the observers and consequently of the linearizing feedback control law.

To improve this, it is possible to consider other types of potential variables to be estimated, in particular kinetic rates. When this approach is considered in the control loop, the controller obtained is called an adaptive controller because it has the potential to adapt itself to variations in the kinetics (Bastin & Dochain, 1990). Considering the production rate estimators developed in chapter 4 (see section 4.6), an adaptive control strategy including this estimator is proposed to track the reference set point. This approach can reduce estimator errors and allows obtaining a controller less sensitive to model accuracy. The control design considering this approach is presented in the following section.

5.6.1. Adaptive control design

In order to reduce the control dependency on the model quality, an adaptive control strategy, where only the production rate is online estimated, is proposed. By introducing γ (defined by (4.70)) in equation (5.33), and replacing γ by its estimate $\hat{\gamma}$, the control law leads to:

$$D = -\frac{1}{P}\left[\hat{D} - \hat{\gamma}\right] \qquad (5.35)$$

where $\hat{D}$ is the control signal and is still given by(5.34), $\hat{\gamma}$ is the estimated production rate. The production rate was previously defined by equation (4.70) and is recalled here:

$$\gamma = \frac{Y_{PS}}{Y_{XS}}\mu X$$

For the estimation of the production rate, $\hat{\gamma}$, two Kalman filter showed good performances in simulation (see section 4.6.3). In the first Kalman filter approach, the estimation of the production rate was assumed to be constant:

$$\begin{cases} \dot{P} = \gamma - DP \\ \dot{\gamma} = 0 \end{cases}$$

where $\dot{\gamma}$ is the derivative of the production rate. In the second Kalman filter, the evolution of the production rate with time was considered to be linear. The model is in this case given by:

$$\begin{cases} \dot{P} = \gamma - DP \\ \dot{\gamma} = 0 \end{cases}$$

The advantage of the obtained adaptive controller (coupled to one of these Kalman filters) is that the estimation algorithm is simplified, and the controller (5.35) does not involve any growth model, leading to a more robust control strategy than the feedback linearizing control law (5.33). Moreover, the stability of the resulting closed-loop system can be proved as detailed hereafter:

The demonstration of the stability of the control loop(Gonzalez, et al., 2001)was performed with the following assumptions:

- All concentrations have finite values.

- Only the lactic acid concentration is available online.

- The functions for the model coefficients are bounded and unknown.

- The observer used for the estimation of the production rate leads to a bounded estimation error.

- The stability analysis is performed for the continuous operation, $D > 0$.

From equations (5.34) and (5.35) the linearizing controller is:

$$D = -\frac{1}{P}\left[G(P_{ref} - P) - \hat{\gamma}\right] \tag{5.36}$$

Renaming the regulation error as:

$$\widetilde{P} = (P - P_{ref}) \tag{5.37}$$

From equations (5.2)and (5.36), the dynamics for the regulation error is then:

$$\dot{\widetilde{P}} = -G\widetilde{P} + \widetilde{\gamma} \tag{5.38}$$

where $\widetilde{\gamma}$ is the estimation error of the production rate($\widetilde{\gamma} = \gamma - \hat{\gamma}$) and $\dot{\widetilde{P}}$ is the derivative of the regulation error. Solving(5.38)leads to:

$$\widetilde{P}(t) = \widetilde{P}(0)\exp(-Gt) + \int_0^t \exp(G(\sigma - t))\widetilde{\gamma}(\sigma)d\sigma \tag{5.39}$$

where $\widetilde{P}(0)$ is the initial condition for $\widetilde{P}(t)$.

Taking the absolute value of (5.39) we obtain:

$$\left|\widetilde{P}(t)\right| \le \left|\widetilde{P}(0)\right|\exp(-Gt) + \int_0^t \exp(G(\sigma - t))\left|\widetilde{\gamma}(\sigma)\right|d\sigma \tag{5.40}$$

And when $t \to \infty$:

$$\lim_{t \to \infty} \left| \tilde{P}(t) \right| \leq \lim_{t \to \infty} \int_0^t \exp(G(\sigma - t)) \left| \tilde{\gamma}(\sigma) \right| d\sigma \tag{5.41}$$

Let $\tilde{\gamma}_m = \max \left\{ \left| \tilde{\gamma}(\sigma) \right| \right\}$ be the maximum value of $\left| \tilde{\gamma}(\sigma) \right|$ (this maximum value exists from the bounded estimation error assumption), then:

$$\lim_{t \to \infty} \int_0^t \exp(G(\sigma - t)) \left| \tilde{\gamma}(\sigma) \right| d\sigma \leq \tilde{\gamma}_m \lim_{t \to \infty} \int_0^t \exp(G(\sigma - t)) d\sigma \tag{5.42}$$

leading to:

$$\lim_{t \to \infty} \left| \tilde{P}(t) \right| d\sigma \leq \frac{\tilde{\gamma}_m}{G} \tag{5.43}$$

Thus, the steady error of the proposed controller is bounded. This error could be reduced by increasing the value of G.

The estimation error of both production rate Kalman filters (proposed in chapter 4, section 4.6) is bounded in our case. Thus, if any of these observers is implemented in the control loop, it leads to a stable controller. In the following, their performances in the control loop are tested in simulation.

5.6.2. *Adaptive control law performance in simulation*

Considering the good performance of the two Kalman filters proposed in chapter 4 (see section4.6.3) to estimate the production rate from the lactic acid concentration available online, they were chosen to be implemented in the adaptive control loop. The control strategy (5.36) is then studied in simulation. Performances of this strategy with both estimators are compared to those obtained by the classical state feedback control strategy given by (5.33) and (5.35), referred to as Control Ideal. In this case, the state variables are assumed to be available online. The control loops coupled with the Kalman filters are referred to as Kalman 1 for the Kalman filter with the constant γ model and Kalman 2 for the Kalman filter with linear model for γ. The control objective is the regulation of the lactic acid concentration at its optimal value. For simulations, the optimal operation point was chosen considering the optimal values presented in table 5.1. The lactic acid concentration was then regulated at 21 g L^{-1}. In order to test the robustness of the control laws with respect to model mismatch, a 30% non-correlated parameters mismatch is applied to the real system (parameters of the real process are different by 30% from those used in the model considered in the control law). The performances of the control laws are illustrated on figure 5.6. The simulation parameters are the same asthose previously presented(see tables 3.6 and 4.1).The maximal dilution rate, D_{max},was fixed to 0.4 h^{-1} and the proportional controller gain was chosen as G=6 h^{-1}. A Gaussian white noise is applied to the lactic acid concentration, P, with a standard deviation of 1%.

In all cases, at the beginning of the fermentation, the dilution rate is null: the fermenter operates in open-loop which corresponds to a batch operation. Once the product concentration reaches its reference value, the dilution rate is increased in order to maintain the lactic acid concentration constant and equal to its reference value.
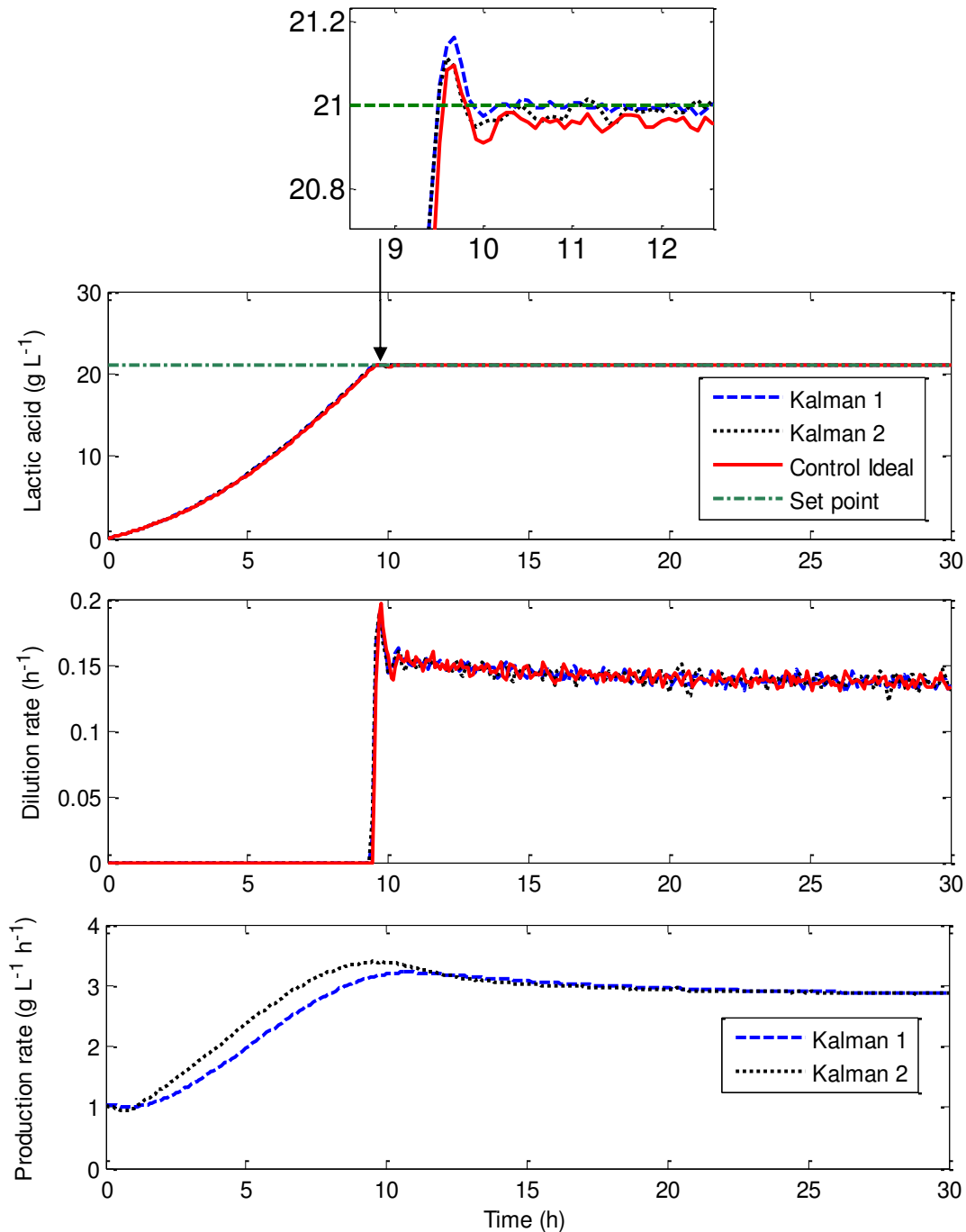
Figure 5.6 Adaptive control law performances for reference tracking. Product concentration, dilution rate and production rate versus time

179

The set point is reached after 10 h of fermentation with a good transient behaviour. As shown in Figure 5.6, a steady state error is noticed using the control strategy "Control Ideal". It is due to the parameter mismatch. Indeed a prior knowledge of model parameters is necessary to determine the control law (see equation (5.33)). Again, this steady error could have been corrected by the implementation of an integral action in the outer-loop (Gonzalez, et al., 2014). The performance of both adaptive controllers (Kalman 1 and Kalman 2) is satisfactory. There is no steady error using the adaptive control strategy. It should be pointed out that these controllers are robust with respect to model mismatch since they do not use the growth model. As the adaptive controller performances are similar by using the constant γ model (Kalman 1) or the linear model (Kalman 2), the former is preferred as its practical implementation for experimental validation is easier and its performance in the control loop is slightly better.

Globally, the proposed adaptive controller shows equivalent (in the nominal case) or better performances than the feedback linearizing control with all states supposed to be measured since the uncertain variable γ involved in the linearizing law is online estimated. In addition, including the estimation of state variables in the ideal control could lead to worse performances, as it was observed in the section (5.5.3). The proposed control strategy presents a good transient response with good accuracy and robustness.
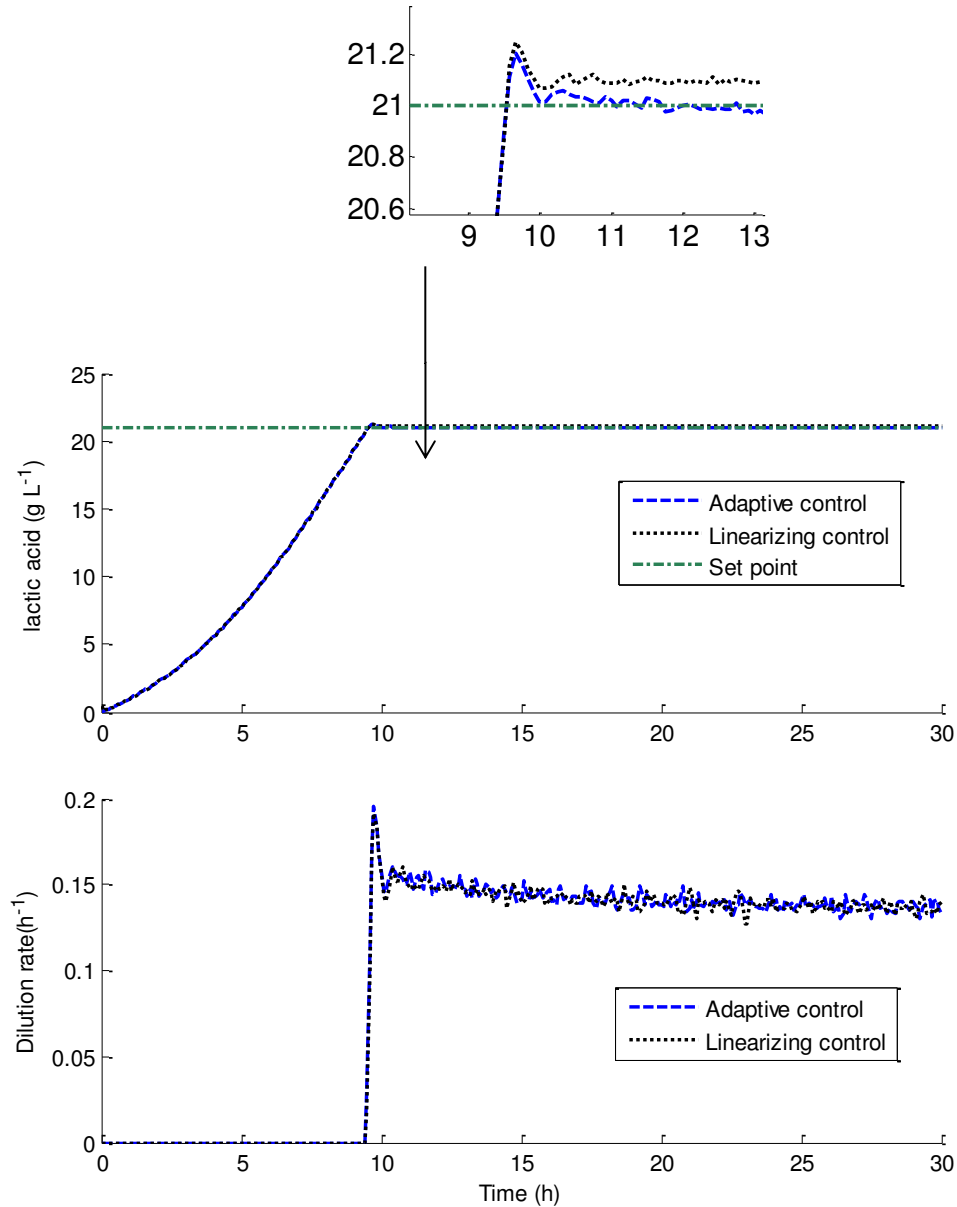
5.7.   COMPARISON OF THE CONTROL STRATEGIES

In this section, estimators with the best performance in each control strategy are compared. In the feedback linearizing control approach, the control loop coupled to the Unscented Kalman filter estimating the state variables showed the best performances. Moreover its implementation is easier than the EKF one as there is no need of model linearization. In the adaptive linearizing control approach, the two developed strategies (with different model for the production rate dynamics) showed similar performances. Nevertheless, the Kalman filter with the constant model for γ is preferred to the linear model approach, as its implementation is easier. The next step is to compare the performance of each control strategy to choose the one which will be experimentally validated. The simulation conditions are the ones presented in tables 3.6 and 4.1.In order to test the robustness of the control laws a 30% non-correlated parameter mismatch was considered between parameters used to simulate the real system and those used by the control laws. Figure 5.7 shows the performance of both control strategies.

The adaptive control law leads to a better tracking of the set point. The set point value is reached with a good transient behaviour and without steady error. This controller is robust with respect to model mismatch. The controller with the linearizing control loop coupled to UKF leads to an offset with respect to the set point. It proves its dependency on the model as this control law uses the growth model to determine the control. However, the offset observed is low and bounded. The advantage of the feedback linearizing controller where all states are estimated with respect to the adaptive controller is that it allows determining the state variables values online. It is important for the process monitoring. Nevertheless, the state estimation needs an accurate model to give good estimates of state variables. In the

perspective of experimental implementation, given the simplicity of the adaptive control law structure, and as it showed better performance for reference tracking, it was chosen for experimental validation in the bioreactor. In the following section the experiments performed to validate the control law are described.

Figure 5.7 Control laws performances for reference tracking. Product concentration and dilution rate versus time.

5.8.   EXPERIMENTAL VALIDATION OF THE CONTROL LAW

The experimental validation of the adaptive control strategy was performed in the 5 L bioreactor described in section 3.5.1.1. For the implementation of the control law, the C-BIO software (Global Process Concept, La Rochelle France) was used as detailed later. The control objective is to regulate the lactic acid concentration to its optimal value. The performance and robustness of the adaptive control strategy are evaluated in a SSPHF

experiment in continuous mode. In order to simulate a real process (starting in batch operation) the initial lactic acid concentration was chosen as null. Only ascending changes in the set point were considered. The control performance is evaluated comparing the online calculation of lactic acid concentration with offline lactic acid concentration measurements. In the following a description of the validation experiments is presented.

5.8.1. Control law implementation

For the control validation, the C-BIO software (Global Process Concept, La Rochelle France) was used.The feature used for the control implementation is the calculation module (see appendix D.2. for further information) which performs calculations using the values recorded by the system as well as constant values. The calculations can only be constructed using operators and functions similar to those found in Microsoft Excel. Due to this restriction, a simple control law is more convinient for implementation in the software. Thus, the adaptive control strategy with the constant γ model was implemented as detailed in appendix D.2. After the implementation of the control law, the experiment described in the following section was performed.

5.8.2. Experiment description

The materials and methods concerning the inoculum preparation, liquefaction, SSPH, SSPHF, wheat stock and analyses are those presented in chapter 3 (see section 3.5.1). The liquefaction and SSPHsteps are performed in batch mode. After inoculation, the control is activated in order to regulate the lactic acid concentration.A 12 L bioreactor was used to produce the wheat stock solution necessary to feed the continuous process. The regulation of temperature, pH, agitation, feed flow and liquid level was assured by Baie inox controllers. Two set points for the lactic acid concentration were tested during the experiment, the first one at 20 g $L^{-1}$and the second one at 27 g L^{-1}; they were chosen after the optimal lactic acid concentration obtained by modelling and by experimental fitting (21 g L^{-1}) (see table 5.1). At the end of the experiment, a temperature perturbation was applied to the system in order to test the robustness of the control law.

5.8.3. Experimental results

5.8.3.1. Adaptive control law performance

A 56 h experiment was performed in order to validate experimentally the adaptive control law for two different set points of lactic acid concentration (20 and 27 g L^{-1}). The control is activated after inoculation; this means that all calculations started immediately after addition of cells to the fermenter. Experimental results are presented in figure 5.8.
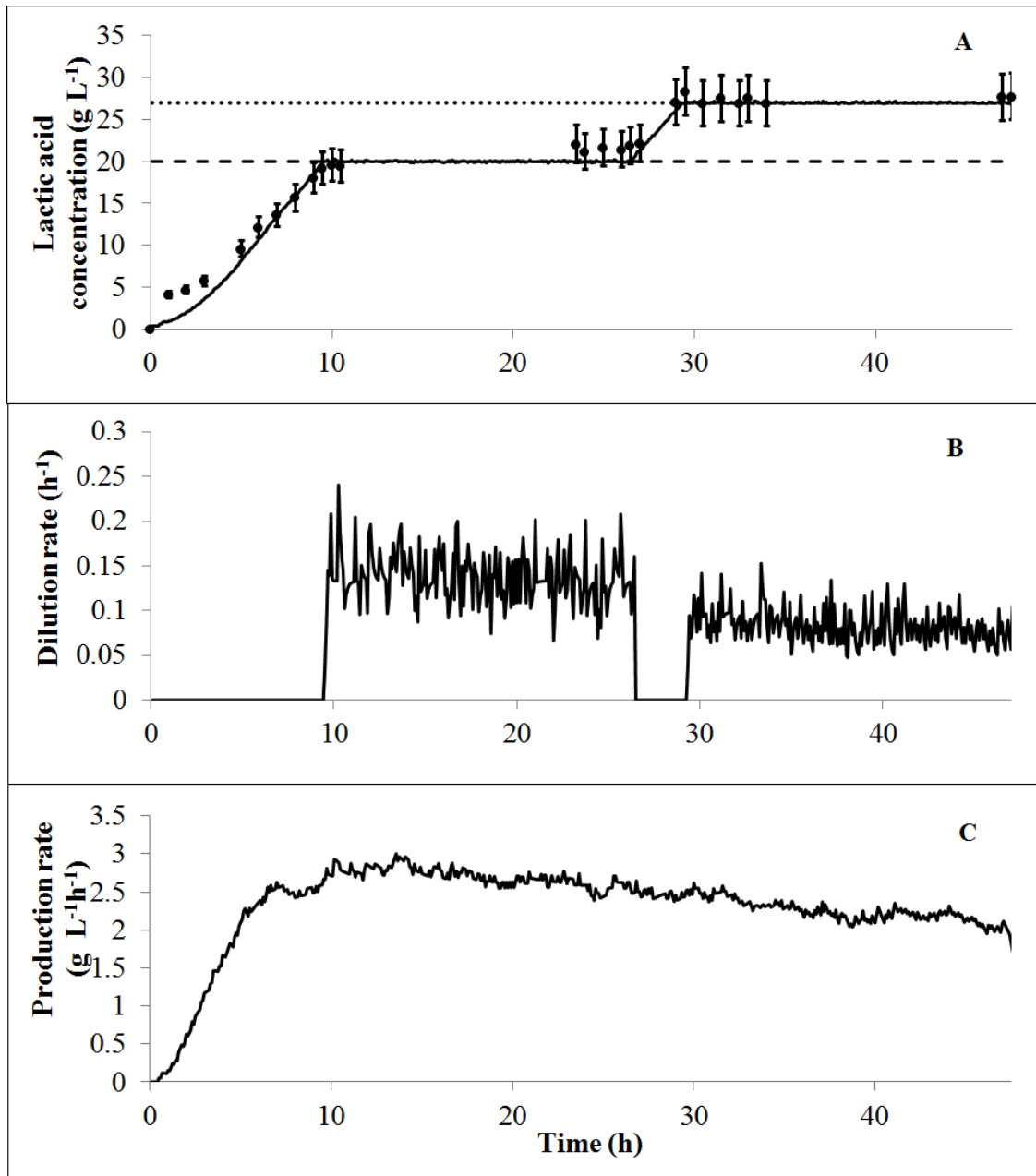
Figure 5.8. Adaptive control law experimental validation. **A** Lactic acid concentration evolution with time. Pref 1= 20g L^{-1}(– –), Pref 2= 27 g L^{-1} (·····), lactic acid concentration available (——) and lactic acid offline measurement (●). **B** Dilution rate evolution with time. **C** Estimated production rate.

The first setpoint was fixed to 20 g L^{-1}. After inoculation, the control law behaviour is to operate in batch mode to increase the lactic acid concentration. The set point is reached after 10 h then the reactor starts to operate continuously (the dilution rate is increased) in order to maintain the lactic acid concentration constant and equal to 20 g L^{-1}. No overshoot of the set point is observed. It can be noticed that the noise on the lactic acid concentration available online is higher than the one predicted in simulation. This leads to fluctuations on the dilution rate (control input). This phenomenon could be reduced by filtering the output, as proposed in the section Conclusions and Perspectives. The offline lactic acid concentration measurements are in good agreement with those calculated online, proving a good performance of the lactic acid estimation from the sodium hydroxide flow.

At 26 h the setpoint was changed from 20 g L^{-1} to 27 g L^{-1}. Then, the reactor operates in batch mode in order to concentrate lactic acid. Once the lactic acid concentration reaches the new setpoint, the dilution rate is increased. This time, the mean of dilution rates calculated by the control law are lower than those calculated during the first phase with a setpoint of 20 g L^{-1}. Concerning the production rate, in the first phase (setpoint =20 g L^{-1}) it is around2.6 g L^{-1}h^{-1}. In the second phase (setpoint= 27g L^{-1}), it slightly decreases and at the end is equal to 2.1 g L^{-1}h^{-1}. It proves that the optimal lactic acid concentration is closer to 20 g L^{-1}than to 27 g L^{-1}.

5.8.3.2. *Adaptive control law robustness analysis*

In this section, the robustness study of the adaptive control law with respect to disturbances is presented. Experimental results are summarized in Figure 5.9. At *t*=17 h, for a setpoint equal to 27 g L^{-1},a temperature disturbance was applied. The temperature in the fermenter was modified from 30°C to 20°C until the end of the experiment. The study of the effect of the temperature on lactic acid production is presented in appendix D.2. These experimental results show that the lactic acid productivity at 20°C is four times lower than the one obtained at 30°C. Figure 5.9 shows that the control law is robust with respect to this important temperature reduction. Despite the disturbance, the control law regulates and stabilizes the lactic acid concentration at its reference value reducing the dilution rate. From figure 5.9, the online calculation of lactic acid concentration slightly decreases after the disturbance moment. The control acts immediately to maintain the lactic concentration at the desired value and after that, both lactic acid concentration and dilution rate stabilize. On the other hand, the lactic acid production rate decreases considerably after the disturbance proving that this temperature reduction affects significantly the lactic acid production, as expected. In conclusion, the developed adaptive control strategy performs satisfactory with respect to changes in the set point as well as to temperature disturbances. Results prove that this control strategy allows regulating the lactic acid concentration at the desired value. Moreover the online estimation of the lactic acid production rate is possible.

From experimental results (Figure 5.8) it was found that the optimal operation point is around 20 g L^{-1}, leading to a lactic acid production rate of 2.6 g L^{-1} h^{-1}.
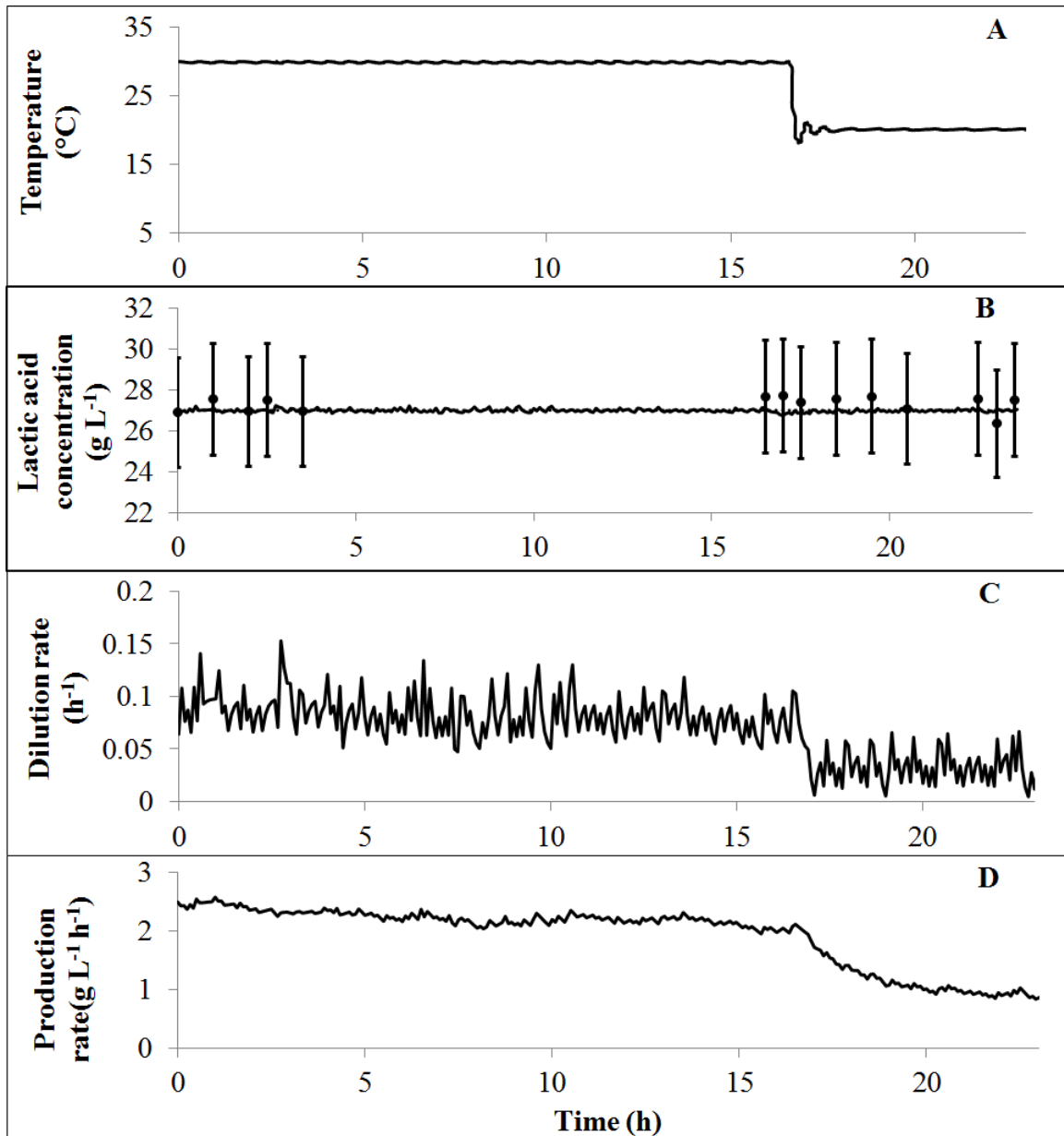
Figure 5.9 Adaptive control lawrobustness study. **A** Temperature disturbance. **B** Lactic acid concentration evolution with time. Pref 2= 27g L^{-1} (······), lactic acid concentration available online (──) and lactic acid offline measurement (●). **C** Dilution rate evolution with time. **D** Estimated production rate.

5.8.3.3. *Validation of the bioprocess monitoring*

Experimental results obtained with the validation experiment of the adaptive control law were used to validate the biomass, glucose and maltose concentration estimators, EKF and UKF. Indeed, knowing the variables concentrations can be relevant for the process monitoring. Two estimation approaches were studied in section 4.5.3, the Extended Kalman Filter and the Unscented Kalman Filter. In this section, the observers performance is evaluated comparing the state variables estimations from the lactic acid concentration available online with offline biomass, glucose and maltose concentrations measurements. Results are presented in figure

5.10.The filters parameters were those used for simulation tests (see section 4.5.3). This results show that the biomass concentration is not accurately estimated by any of the estimators. At the beginning, UKF shows better performance but in the last 5 h, there is a significant offset between experimental and estimated values. On the other hand, the EKF estimated values are closer to the real ones at the end of the simulation. These results prove once again that the estimators tested are dependent on the model. Concerning the glucose concentration, estimations by both approaches are rather good considering that the model is not accurate (it does not consider the glucose produced from other sugars than maltose). The UKF estimations of glucose concentration are closer to the real values than the EKF estimates. The maltose concentration is more accurately estimated by UKF than EKF. In conclusion, considering the complexity of the model considered in this work, the estimations of the key variables of the process are rather good, especially by the UKF approach. Further work remains necessary to improve the state variables estimation.
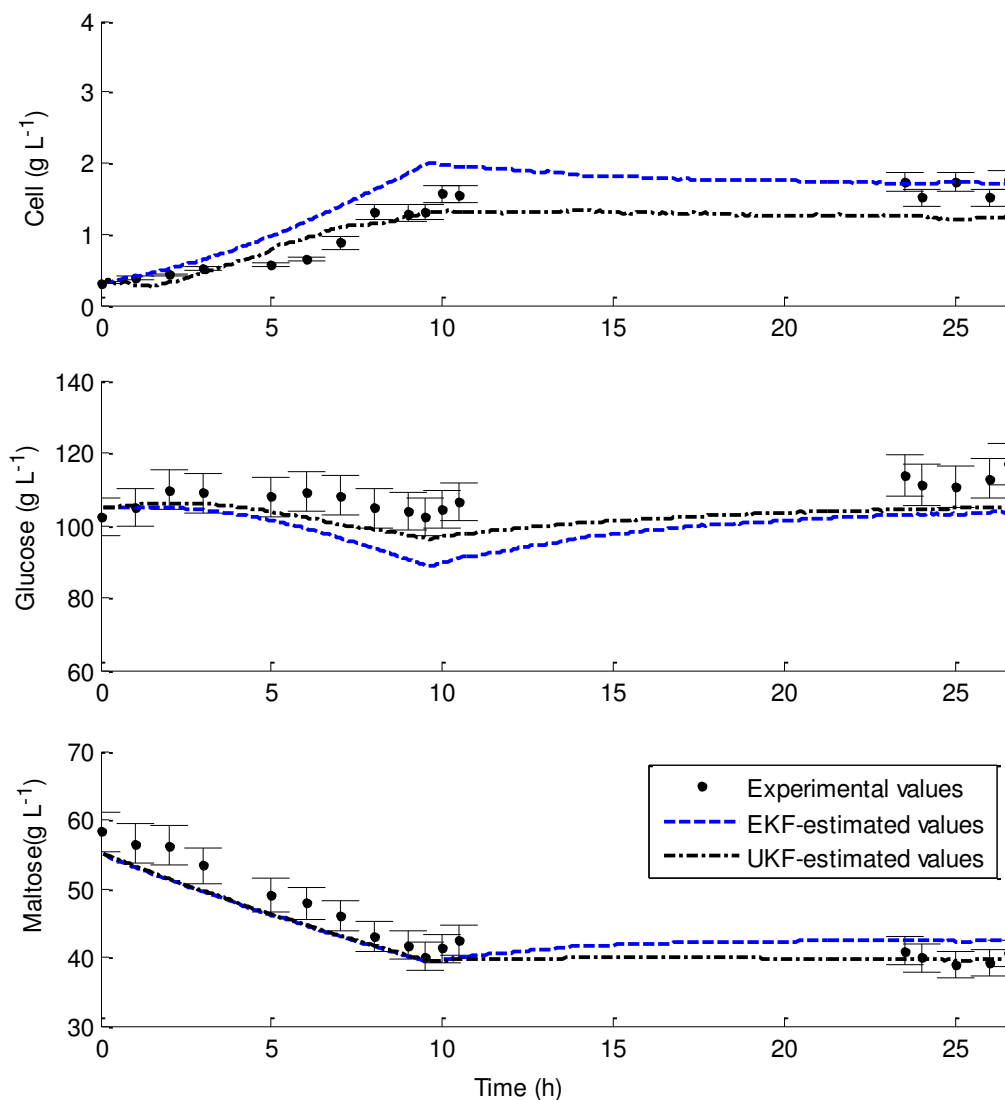
Figure 5.10 Estimators experimental validation from lactic acid concentration available online. Comparison with experimental data from adaptive control law experiment.

5.9. CONCLUSION

In this chapter the development of control strategies for the SSPHF continuous process was described. The following considerations were taken into account to design the control strategy: the dilution rate was chosen as the control variable; the lactic acid concentration was the output variable which was available online; the final goal of the control law was to optimize the bioprocess by maximizing its productivity. Therefore, the lactic acid concentration was regulated to an optimal value which maximizes the lactic acid productivity.

For the determination of this optimal value, corresponding to an optimal operation point, first, a steady state analysis of the system was performed. System variables at steady state were then expressed as a function of the control variable (dilution rate), Then, the optimal operation point was determined from experimental data and using the steady state study of the process.

The next step was to develop control strategies to regulate the lactic acid concentration at the desired value. In the first approach, a feedback linearizing controller was proposed to track the reference set point, requiring the online measurement or estimation of all state values. A proportional controller was added in the outer loop in order to obtain a desired closed-loop time response. The estimation of state variables not measured online was tested using two observers proposed in chapter 4: the Extended Kalman Filter (EKF) and the Unscented Kalman filter (UKF). This latter exhibited better results in simulation as it does not require the linearization approximation approach considered by the EKF. Nevertheless, both estimators are very dependent on the model quality. Thus, in order to avoid the model dependency and reduce the control law complexity, a second approach was considered.

In the second control strategy an adaptive controller was developed including only the estimation of the lactic acid production rate. Two Kalman filters estimating the lactic acid production rate were implemented in the control law. The first one considers a constant model for the production rate dynamics and the second one a linear model. Simulations showed the accuracy and robustness of the proposed control strategy. Both Kalman filters performed well but the former was preferred as its implementation in the bioreactor software was easier.

Performances of the feedback linearizing controller with UKF and the adaptive controller were compared. Simulations considered a 30% non-correlated parameter mismatch between parameters used to simulate the real system and those used by the controllers. An offset with respect to the set point was noticed with the feedback linearizing controller with UKF while the adaptive controller tracked accurately the reference set point as it was not impacted by the model parameter mismatch. The adaptive controller was then chosen to be experimentally validated due to its good performance and easier implementation.

The adaptive control strategy was then experimentally validated in a continuous SSPHF bioreactor. Results proved the good performance of the adaptive control strategy. The lactic acid concentration was regulated at two different set points with accuracy, good transient behaviour and without overshoot. The robustness of the control law was proved when a temperature disturbance was introduced in the system. Finally, the EKF and UKF estimations

were also experimentally validated using lactic acid concentration available online. The UKF performance was rather good considering that this estimator is very dependent on the model and that the system is weakly observable. However, further work is required to improve the estimator performance.

CONCLUSIONS AND PERSPECTIVES

CONCLUSIONS

This work aimed at maximizing the lactic acid production from wheat flour by a *Lactobacillus* strain in order to meet the SouffletGroup goal of optimizing this bioprocess. According to Soufflet industrial policy, involving the use of cereal-based ingredients to replace chemical-based ones in the production of value-added products, wheat flour was chosen thanks to its low cost and its potential ability to bring all the nutrient needs for the cell growth and lactic production. The maximization of the productivity was successfully accomplished if we compare the lactic acid productivities obtained by the process used by Soufflet at the beginning of this PhD work and those obtained by the process and control strategy developed here. Indeed, the productivity was increased two fold.

This work was performed in three main steps: First, the optimization of the lactic acid production process (medium and reactor's operation mode) was considered. The second step concerns the development of a mathematical model to better understand the dynamics taking place in the bioreactor. In the last step, a control strategy to regulate the lactic acid concentration at its optimal value was developed. In the following the main conclusions obtained for each step are summarized.

Process optimization (Chapters 1 and 2)

Wheat flour transformation to lactic acid involves enzymatic reactions that make available the nutrients for the microorganisms. In the conventional process, the starch contained in wheat flour is first transformed into oligosaccharides (mainly maltose) in a liquefaction step followed by saccharification where maltose is transformed into glucose; in the last step, glucose is fermented to lactic acid.

The process optimization of this work started from the lactic acid production process proposed by the Soufflet Group which comprises three steps: Liquefaction, pre-saccharification and simultaneous saccharification and fermentation. The considered aspects were the ability of wheat flour to meet the needs of bacteria (especially the nitrogen ones) without further supplementation and the possibility to minimize the number of the process steps.

A first study confirmed the capacity of the culture broth to fulfill all the nitrogen needs of lactic acid bacteria, by hydrolysis of the insoluble protein fraction of wheat (gluten) into amino acids. It led to the choice of Prolyve NP among several industrial proteases.

189

In conclusion, an innovative process was proposed consisting of two major steps following the classical liquefaction one giving mainly maltose:

- A simultaneous saccharification and proteins hydrolysis (SSPH), in which maltose and gluten are only partially hydrolyzed into glucose and amino acids respectively; experiments in a 5 L bioreactor attested the feasibility of the operation and lead to the choice of its reaction time (6 h).
- A simultaneous saccharification, proteins hydrolysis and fermentation (SSPHF) in which the remaining maltose and gluten were hydrolyzed simultaneously with the fermentation; the feasibility of this step was also confirmed by experiments performed in a pilot bioreactor. This step was identified as the limiting step of the process

In addition a literature survey allowed choosing the best operation mode for the process, the continuous mode, due to its greater industrial feasibility, improved productivity and its potential for the control design. The modelling and control development were thus devoted to the SSPHF step as it was the limiting step in the process and operating in continuous mode.

Modelling (Chapter 3)

The modelling approach to describe the microbial behaviour was based on an unstructured model that by definition, does not involve any physiological characterization of the cells. Thus only the total cell concentration was considered. First, a literature survey on modelling of lactic acid production was used to establish the basis for the model development. Then the main phenomena affecting cell metabolism (growth and lactic acid production)were studied in batch experiments.

Later the SSPHF continuous model was developed. The model considers four dynamical equations describing bacteria growth, glucose and maltose consumption and lactic acid production. For modelling, the amino acids dynamics was not taken into account. In the equation used to describe the growth kinetics, glucose was considered as the limiting substrate. Moreover, an inhibition factor associated to lactic acid was also included in this kinetics. The enzymatic transformation of maltose into glucose was also introduced in the modeling approach. Although glucose may be produced by various sugars presented in the wheat, maltose was the sole sugar taken into account in the glucose dynamics. The model describes then the variables (maltose, glucose, lactic acid and biomass) behaviour in the SSPHF bioreactor.

Due to the model complexity and strong nonlinearities, an identification strategy was developed in order to determine the model parameters. First, the most influential parameters were determined through a sensitivity analysis. Then some model parameters particularly difficult to identify were fixed at values found in the literature or given by simulation tests. Finally, a well-structured identification strategy was proposed. The parameters involved in cell growth, substrate consumption and product formation were determined and ultimately

validated via experimental data obtained in continuous SSPHF experiments. A good agreement was found between the model and the experimental data.

Monitoring (Chapter 4)

Due to the lack of reliable sensors to measure online the key variables in the system, estimators were developed as they would be necessary for a further control design. In a first step, an online sensor to determine the lactic acid concentration was developed. This estimator calculates the lactic acid concentration from the online measurement of the sodium hydroxide inlet flow (necessary to regulate pH at a constant value). This approach allowed accurately determining the lactic acid concentration in the bioreactor in real time.

The other key variables of the system (biomass, glucose and maltose concentrations) that cannot be measured and are required for the process monitoring were estimated online by two observers based on the Kalman Filter principle: The Extended Kalman Filter (EKF) and the Unscented Kalman filter (UKF). The latter does not require the linearization approximation approach considered by EKF. As a result UKF exhibited better results in simulation. Nevertheless, both estimators are very depending on the model quality.

The lactic acid production rate was estimated from the lactic acid concentration available online as it is indeed a measure of the process productivity. For lactic acid production rate estimations, three different approaches were considered: a numerical differentiation method and two Kalman filters. The first Kalman filter approach considers that the production rate dynamics is constant and the second one considers a linear behaviour. The numerical differentiation method did not give good results estimating the production rate. In contrast, both Kalman filters showed good performances.

Control strategy (Chapter 5)

The main objective in developing a control method for the SSPHF continuous bioreactor was to improve operational stability and efficiency of lactic acid production. Minimal prior modelling and on-line estimation were the basis of the development of control strategies. The first step to construct a control law was to determine the optimal operation point which maximizes the lactic acid productivity; the control objective would then be to operate the process around this point. The optimal operation point was determined using experimental data and the model developed in chapter 3.

The next step in the development of the control strategy was to establish the control objective. As the process purpose is to produce lactic acid with high productivity, the control was conceived to regulate the lactic acid concentration at its optimal value by modifying the dilution rate. Based on the control affine property of the system, a feedback linearizing controller was considered in the first place. This approach requires the online measurement or estimation of all state variables. Observers developed in chapter 4 for state variable estimation (EKF and UKF) were implemented in the feedback linearizing control law. Their

performances (in the state variables estimation) were rather good, at least in simulation. Finally, due to the dependency of both estimators on the model quality another approach was considered as an alternative strategy.

An adaptive controller with the lactic acid production rate as the sole estimation was considered in the second step. This adaptive control strategy showed better performances in simulation than the feedback linearizing control approach. Moreover, the adaptive controller is robust with respect to model mismatches and its implementation in the bioreactor software is easier. This adaptive controller was then chosen to be experimentally validated in the continuous SSPHF bioreactor. Ascending steps tests proved the efficiency and accuracy of the control law. The lactic acid concentration was well regulated at two different set points. The set points were reached with good transient behaviour and without overshoot.

The robustness of the control strategy was studied with respect to temperature perturbations. Results proved that the control can adapt itself to variations in the production rate after a perturbation. Finally experimental data obtained with these final control validation experiments were useful to validate the state variables estimators EKF and UKF. The UKF showed the best performances. Nevertheless, a further study on the parameters tuning must be performed in order to obtain better estimates of the state variables.

PERSPECTIVES

The results presented in this PhD work reveal many interesting perspectives. They are summarized in the following sections.

Medium optimization

Concerning the medium optimization, various approaches can be considered to maximize the lactic acid productivity.

The wheat concentrations used in this work are significant leading to high initial glucose concentrations at the end of the SSPH step, in order to avoid glucose exhaustion during the SSPHF step. This approach allowed the identification of some phenomena as lactic acid inhibition effect on growth. Nevertheless, considering that the optimal lactic acid concentration is around 20 gL^{-1}, with the conditions considered in this work, the glucose concentration in the output flow is very high as only a small part of glucose is transformed into lactic acid. Moreover, the glucose is consumed and produced at the same time in the bioreactor, thus its output concentration is similar to its concentration in the inlet flow (around 100 g L^{-1}). If not reused, the substrate, highly concentrated in the output flow of the reactor, is wasted. This may negatively impact the economy of the process. It is then important to try to reduce its concentration in this flow. To do so, a study of the wheat concentration in the culture medium can then be performed. It should be pointed out that the diminution of wheat charge in the broth solution must be performed carefully. Indeed, the proteins hydrolysis study was performed for a culture medium containing high levels of wheat, thus the diminution of the wheat charge can lead to lower performance in the hydrolysis of gluten. A

more detailed kinetic study of the SSPH and SSPHF steps must then be performed in order to find a good compromise between a low wheat concentration (leading to a lower initial glucose concentration) without altering considerably the availability of nitrogen substrates in the medium.

Another disadvantage of a very concentrated wheat solution is related to hydrodynamic problems. The residence time distribution study showed that the bioreactor operating in continuous mode has a dead volume of 9%. It is due to the high wheat concentration in the culture medium leading to a significant viscosity and to the reduced agitation speed. Thus decreasing the wheat concentration in the culture medium will reduce its viscosity and improve mixing, which will be especially useful for larger fermenters. Moreover, the dead volume in the fermenter can be reduced by increasing agitation inside the vessel, but resulting in the same time in an increase of energy consumption.

Modelling

Further experiments could be planned in order to improve the identification strategy of the model parameters. Indeed more data must be available in order to identify limiting or inhibition phenomena on growth, other than those taken into account. Experimental results showed that the glucose production from other sugars than maltose is almost 10% of the total glucose quantity, thus it can be interesting to introduce a term considering this phenomenon in the glucose dynamics.

The identification of K_S and n growth parameters can be considered using a more rigorous approach. To do so, the improvement of the biomass concentration measurement must be considered. Indeed the cell count technique leads to high uncertainty and highly depends on the experimental procedure used for the measurement (i.e. samples dilution, person counting, etc). Moreover this technique is time consuming and often provides an overestimate of the number of cells due to their unequal distribution in the medium or the presence of damaged or non-cultivable cells. Some techniques to measure the biomass concentration online are available. They include biomass probes based on near infrared (NIR) light absorption or dielectric spectroscopy (Kiviharju, et al., 2007). Nevertheless, considering the complex culture medium used in this work, only the dielectric spectroscopy probe seems convenient. The implementation and improvement of this type of technique should be further studied.

It will be interesting to test the developed model with other microorganisms and substrates as corn flour. Further experiments must be performed in order to identify the model parameters

A detailed kinetic study of starch liquefaction (in the liquefaction step) and maltose saccharification (in the SSPH step) is important for modelling the whole starch transformation process. It could be further useful to develop a control strategy for the three bioreactors in cascade.

Monitoring and Control

For the process monitoring, the estimators of the biomass, glucose and maltose concentrations must be improved. Observers developed for the state variables estimation are dependent on

the model accuracy. As there are some modelling mismatches in the developed model, the state estimations by these observers lead to an estimation of some state variables that can be improved. As an alternative, The Unscented Kalman filter can be considered using a Monte Carlo approach leading to better estimations of the state variables.

Asymptotic observers, which consider a state transformation in order to avoid using the kinetic model, can also be developed. Nevertheless, these observers have a convergence rate imposed by the process dilution rate. An interesting approach for state variables estimation is the implementation of a hybrid observer as proposed by (Hulhoven, et al., 2006). This approach combines the advantage of exponential and asymptotic observers estimating a level of confidence in the process model. According to this confidence level the hybrid observer evolves between two limit cases: model perfectly known or kinetic model unknown. The development of a hybrid observer can be considered for the studied system.

Concerning the control strategy, results proved the performance of the adaptive control loop for the lactic acid concentration regulation. Nevertheless, high fluctuations in the control variable were observed due to the measurement noises. In order to reduce these phenomena, these noises can be filtered. A possible technique to filter the noisy measured signal is the one proposed in (Fliess, et al., 2008), which can be further studied.

Since the aim of the control strategy is to maximize the lactic acid process productivity, one interesting approach considers the regulation of the lactic acid production rate instead of its concentration. This approach is mainly justified as the location of the optimum operation point can change during the fermentation. Indeed bacteria are inherently unpredictable and disturbances, such as changes in feed concentration or drifts caused by enzymatic deactivation or environmental changes, can lead to modify the optimum operation point significantly. In these cases the system will work under suboptimal conditions. Consequently, an on-line optimization strategy could be integrated in the control algorithm to track the changing optimum point.

For our application, an optimizing nonlinear model predictive control strategy can be developed, considering the on-line lactic acid production rate optimization. This approach allows determining online the optimum production rate (γ) which can be then determined at intervals larger than the sampling time. Then, the control objective would be the regulation of the lactic acid production rate at the optimal value γ_{ref} obtained from the online optimization approach, (e.g. by means of a nonlinear predictive control (NMPC) strategy).

Finally, a global control strategy for the process (liquefaction-SSPH-SSPHF) can be developed in order to optimize the whole process. To do so, it is necessary to develop mass balance models for each bioreactor and to measure at least one of the key variables in each one. In a first instance, we propose the development of a control law for the two last steps (SSPH and SSPHF). In the case of the SSPH bioreactor, if only the maltose saccharification kinetics is considered for modelling, one can define two key variables, the glucose and maltose concentrations. The maltose kinetics (representing the SSPH) differs from the one presented in this work for the SSPHF (see equation (3.27)) on the k_M value (maltose

degradation constant). Indeed, this parameter depends on the temperature which is not the same in both bioreactors.

It is also necessary to measure one of the key variables in the SSPH bioreactor. We propose to measure online the glucose concentration. To do so, a YSI immobilized enzyme biosensor (YSI (UK) Ltd., United Kingdom) can be used. This equipment is already available at Soufflet to perform off-line measurements; nevertheless, it can be used to provide online measurements of glucose concentration by automatic sampling and treatment. A special device (proposed by the YSI biosensor provider) must be acquired in order to implement the automatic sampling. This online glucose concentration measurement is not only necessary for the control design of the SSPH bioreactor, but also can improve the process monitoring and the control strategy for the SSPHF.

Industrial perspectives

The whole three steps process of wheat transformation into lactic acid should be implemented in an industrial bioreactor system in order to make the process industrially exploitable. Modelling and control approaches must be developed for the implementation in a real industrial system.

Concerning the presented adaptive control strategy, it can be used for other industrial process where the product of interest is measured online.

BIBLIOGRAPHY

Abdel-Rahman, M., Tahiro, Y. & Sonomoto, K., 2011. Lactic acid production from lingocellulose derived sugars using lactic acid bacteria: overview an limits. *Journal of Biotechnology,* Volume 156, pp. 286-301.

Abdel-Rahman, M., Tashiro, Y. & Sonomoto, K., 2013. Recent advances in lactic acid production by microbial fermentation processes. *Biotechnology Advances,* Volume 31, pp. 877-902.

Aborhey, S. & Williamson, D., 1978. State and parameter estimation of microbial growth processes. *Automatica,* Volume 14, pp. 493-498.

Aborhey, S. & Williamson, D., 1997. Modeling of lactic acid production by *Streptococcus cremoris* HP. *The Journal of General and Applied Microbiology,* Volume 23, pp. 7-21.

Adler-Nissen, J., 1986. *Enzymatic hydrolysis of food proteins.* New York: Elsevier.

Akerberg, C., Hofvendahl, K., Zacchi, C. & Hahn-Hagerdal, B., 1998. Modelling the influence of pH, temperature, glucose and lactic acid concentrations on the kinetics of lactic acid production by *Lactococcus lactis* ssp. *lactis* ATCC 19435 in whole-wheat flour. *Applied Microbiology and Biotechnology,* Volume 49, pp. 682-690.

Allison, G. E. & Klaenhammer, T. K., 1998. Phage resistance mechanisms in lactic acid bacteria. *International Dairy Journal,* Volume 8, pp. 207-216.

Altiok, D., Tokalti, F. & Harsa, S., 2006. Kinetic modeling of lactic acid production from whey by *lactobacillus casei* (NRRL B-441). *Journal of Chemical Technology and Biotechnology,* Volume 81, pp. 1190-1197.

Amrane, A. & Prigent, Y., 1994. Lactic acid production from lactose in batch culture: Analysis of the data with the help of a mathematical model; Relevance for nitrogen source and pre-culture assessment. *Applied Microbiology and Biotechnology,* Volume 40, pp. 644-649.

Anderson, B. D. O. & Moore , J. B., 2005. *Optimal Filtering.* New York: Dover.

Anguelova, 2007. *Observability and identifiability of nonlinear systems with applications in biology.*Göteborg, Sweden: PhD thesis. Chalmers University of Technology and Göteborg University.

Anuradha, R., Suresh, A. K. & Ventkatesh, K. V., 1999. Simultaneous saccharification and fermentation of starch to lactic acid. *Process Biochemistry,* Volume 35, pp. 367-375.

Auras, R., Lim, L. T., Selke, S. E. M. & Tsuji, H., 2010. *Poly (Lactic Acid) synthesis, structures, properties, processing, and Applications.* New Yersey: Wiley.

Bibliography

Babiker, E. F., Fujisawa, N., Matsudomi, N. & Kato, A., 1996. Improvement in the functional properties of gluten by protease digestion or acid hydrolysis followed by microbial transglutaminase treatment. *Journal of Agricultural and Food Chemistry,* Volume 44, pp. 3746-3750.

Bailey, J. E. & Ollis , D. F., 1986. *Biochemical engineering fundamentals.* New York: McGraw-Hill.

Bastin, G. & Dochain, D., 1986. On-line estimation of microbial specific growth rates. *Automatica ,* Volume 22, pp. 705-709.

Bastin, G. & Dochain, D., 1990. *Online estimation and adaptive control of bioreactors, Process measurement and Control.* Amsterdam: Elsevier.

Bath, S. M. & Srivastava, S. K., 2008. Lactic acid production from cane molasses by *Lactobacillus delbruecki* NCIM 2025 in submerged condition: optimization of medium component by Taguchi DOE Methodology. *Food Biotechnology,* Volume 22, pp. 115-139.

Becerra Celis, G. P., 2009. *Proposition de stratégies de commande pour la culture de microalgues dans un photobioréacteur continu,* Châtenay-Malabry, France: PhD thesis, Ecole Centrale Paris.

Belhocine, D., 1987. *Lactose valorisation by lactic acid fermentation,,* Rennes, France: PhD thesis, University of Rennes.

Beluham, D., Gosak, D., Pavlovic, N. & Vampola, M., 1995. Biomass estimation and optimal control of the baker's yeast fermentation process. *Computers ands Chemical Engineering,* Volume 19, pp. 11-14.

Ben Youssef, C., Goma, G. & Olmos-Dichara, A., 2005. Kinectic modelling of l*actobacillus casei* ssp. *rhamnosus* growth and lactic acid production in batch cultures under various medium conditions. *Biotechnology Letters,* Volume 27, pp. 1785-1789.

Ben Youssef, C., Guillou, V. & Olmos-Dichara, A., 2000. Modelling and adaptive control strategy in a lactic fermentation process. *Control Engineering Practice,* Volume 8, pp.1297-1307.

Bogaerts, P., Hulhoven, X. & Vande Wouver, A., 2006. Hybrid extended luenberger-asymptotic observer for bioprocess state estimation. *Chemical Engineering Science,* Volume 21, pp. 7151-7160.

Bogaerts, P. & Vande Wouwer, A., 2003. Software sensors for bioprocesses. *ISA Transactions,* Volume 42, pp. 547-558.

Boonmee, M., Leksawasdi, N., Bridge, W. & Rogers, P., 2003. Batch and continuous culture of *Lactococcus lactis* NZ133: experimental data and model development. *Biochemical Engineering Journal,* Volume 14, pp. 127-135.

Bouguettoucha, A., Balannec, B. & Amrane, A., 2008. Unstructured generalized models for the analysis of the inhibitory and the nutritional limitation effects on *Lactobacillus helveticus* growth-Models validation. *Biochemical Engineering Journal,* Volume 39, pp. 566-574.

Bouguettoucha, A., Balannec, B. & Amrane, A., 2011. Unstructured models for latic acid fermentation- A review. *Food Technology and Biotechnology.*

Bouguettoucha, A., Nacef, S., Balannec, B. & Amrane, A., 2009. Unstructured models for growth and lactic acid production during two-stage continuous cultures of *Lactobacillus helveticus.Process Biochemistry,* Volume 44, pp. 742-748.

Brandam, C., Meyer, X. M., Proth, J., Strehaiano, P. & Pingaud, H., 2003. An original kinetic model for the enzymatic hydrolysis of starch during mashing. *Biochemical Engineering Journal,* Volume 13, pp. 43-52.

Bustos, G., de la Torre, N., Moldes, A. B., Cruz, J. M. & Dominguez, J. M., 2007. Revalorization of hemicellulosic trimming vine shoots hydrolyzates trough continuous production of lactic acid and biosurfactants by *L. pentosus*. *Journal of Food Engineering,* Volume 78, pp. 405-412.

Charalampopoulos, D., Pandiella, S. S., Wang, R & Webb, C., 2002. Application of cereals and cereal components in functional foods: A review. *International Journal of Food Microbiology,* Volume 79, pp. 131-141.

Choi, M., Al-Zahrani, S. M. & Lee, S. Y., 2014. Kinetic model-base feed-forward controlled fed-batch fermentation of *Lactobacillus rhamnosus* for the production of lactic acid from Arabic data juice. *Bioprocess and Biosystems Engineering,* Volume 37, pp. 1007-1015.

Dahhou, B., Chamilothoris, G. & Roux, G., 1991. Adaptive predictive control of a continuous fermentation process. *International Journal of Adaptive Control and Signal Processing,* Volume 5, pp. 351-362.

De Battista, H., Picó, J., Garelli, F. & Vignoni, A., 2011. Specific growth rate estimation in (fed)batch bioreactors using second-order sliding observers. *Journal of Process Control,* Volume 21, pp. 1049-1055.

Diaz, C., Lelong, P., Dieu, P., Feuillerat, C. & Salomé, M., 1999. On-line analysis and modelling of microbial growth using a hybrid system approach. *Process Biochemistry,* Volume 34, pp. 39-47.

Ding, S. & Tan, T., 2006. Lactic acid production by *lactobacillus casei* fermentation using different fed-batch feeding strategies. *Process Biochemistry,* Volume 41, pp. 1451-1454.

Djidel, A., 2007. *Production d'acide lactique par Lactobacillus casei subsp. rhamnosus sur jus de datte: Cinétique et optimisation en cultures discontinues, semicontinues et continues.,* France: PhD thesis, Institut National Polytechnique de Lorraine.

Dochain, D., 2008. *Automatic Control of bioprocesses.* 1st ed.,Wiley.

Ducat, D. C., Way, J. C. & Silver , P. A., 2011. Engineering cyanobacteria to generate high-value products. *Trends in biotechnology,* Volume 29, pp. 95-103.

Farza, M., Busawon, K. & Hammouri, H., 1998. Simple nonlinear observers for on-line estimation of kinetic rates in bioreactors. *Automatica,* Vol 34(3), pp. 301-318.

Fletcher, R., 1987. *Practical methods of optimization.* 1st edition, John Wiley & Sons.

Fliess, M., Join , C. & Sira-Ramirez, H., 2008. Non-linear estimation is easy. *International Journal of Modelling, Identification and Control,* Volume 4, pp. 12-27.

Friedman, M., 2004. Applications of the ninhydrin reaction for analysis of amino acids, peptides and proteins to agricultural and biomedical sciences. *Journal of Agricultural and Food Chemistry,* Volume 52, pp. 385-406.

Gadjil, C. & Venkatesh, K. V., 1997. Structured model for batch culture growth of *lactobacillus bulgaricus. Journal of Chemical Technology and Biotechnology,* Volume 68, pp. 89-93.

Garrigues, C., Mercade, M., Loubière, P., Lindley, N. C. & Cocaign-Bousquet, M., 1998. Comportement métabolique de *Lactococcus lactic* en réponse à l'environnement. *Lait,* Volume 78, pp. 145-155.

Gbewonyo, K., Jain, D., Hunt, G., Drew, S. W. & Buckland, B. C., 1989. On-line analysis of Avermectin fermentation cell growth kinetics in an industrial pilot plant. *Biotechnology and Bioengineering,* Volume 34, pp. 234-241.

Ghaffar, T., Irshad, M., Anwar, Z., Aqil, T., Zulifqar, Z., Tariq, A., Kamran, M., Ehsan, N. & Mehmood, S., 2004. Recent trends in lactic acid biotechnology: A brief review on production to purification. *Journal of Radiation Research and Applied Sciences,* Volume 7, pp. 222-229.

Gonzalez, J., Fernandez, G., Aguilar, R., Barron, M. & Alvarez-Ramirez, J., 2001. Sliding mode observer-based control for a class of biorectors. *Chemical Engineering Journal,* Volume 83, pp. 25-32.

Gonzalez, K., Tebbani, S., Dumur, D., Pareau, D., Lopes, F., Givry, S., Entzmann, F., 2013. Modeling and parameter identification of the batch lactic acid production process from wheat flour. *In Proceedings of 17th International Conference on System Theory, Control and Computing -* ICSTCC 2013, Romania, pp. 238-243.

Gonzalez, K., Tebbani, S., Dumur, D., Pareau, D., Lopes, F., Givry, S., Entzmann, F., 2014. Control strategy for continuous lactic acid production from wheat flour. *In proceedings of 2nd International Conferencee on Control, Decision and Information Technologies,* Metz, France,pp. 465-470.

Bibliography

Grand-View-Research, 2015. *Grand View Research.* [Online]. Available at: http://www.grandviewresearch.com/industry-analysis/lactic-acid-and-poly-lactic-acid-market.2014.[Accessed 16 march 2015].

Hafidi, G., 2008. *Application de la commande prédictive non-linéaire à la commande de culture de bactéries Escherichia coli ,* Orsay, France: PhD thesis. Automatic. Université Paris Sud- Paris XI.

Hedrick, J. K. & Girard, A., 2010. *www.me.berkeley.edu.* [Online] Available at: http://www.me.berkeley.edu/ME237/ControlOfNonlinearDynamicSystems.pdf. [Accessed 17 March 2015].

Henrissat, B., 1991. A classification of glycosyl hydrolases based on amino acid sequence similarities. *Biochemical Journal,* Volume 280, pp. 309-316.

Henson, M. A. & Seborg, D. E., 1992. Nonlinear control strategies for continuous fermenters. *Chemical Engineering Science,* Volume 4, pp. 821-835.

Hermann, R. & Krener, A. J., 1977. Nonlinear controllability and observability. *IEEE Transactions on Automatic Control,* Volume 22, pp. 728-740.

Hetényi, K., Németh, A. & Sevella, B., 2010. First steps in the development of a wheat flour based lactic acid fermentation technology. Culture medium optimization. *Chemical and Biochemical Engineering Quarterly,* Volume 24, pp. 195-201.

Hilgert, N., Harmand, J., Steyer, J. P. & Vila, J. P., 2004. Non parametric identification and adaptive control of an anaerobic fluidized bed digester. *Control Engineering Practice,* Volume 8, pp. 264-272.

Hirayama , S. & Ueda, R., 2004. Production of optically pure D-lactic acid by *Nannochlorum* sp.26A4. *Applied Biochemistry and Biotechnology,* Volume 119, pp. 71-76.

Hirt, G., Tanner, W. & Kandler, O., 1971. Effect of light on the rate of glycolysis in *Scenedesmus Obliquus*. *Plant Physiology,* Volume 47, pp. 841-843.

Hitzmann, B., Broxtermann, O., Cha, Y. L., Sobieh, O., Stärk, E. & Scheper, T., 2000. The control of glucose concentration during yeast fed-batch cultivation using a fast measurement complemented by an extended Kalman filter. *Bioprocess Engineering,* Volume 23, pp. 337-341.

Hofvendahl, K. & Hahn-Hligerdal, B., 1997. L-lactic acid production from whole wheat flour hydrolysate using strains of *Lactobacilli* and *Lactococci*. *Enzyme and Microbial Technology,* Volume 20, pp. 301-307.

Hofvendahl, K. & Hahn-Hligerdal, B., 2000. Factors affecting the fermentative lactic acid production process from renewables sources. *Enzyme and Microbial Technology,* Volume 26, pp. 87-107.

Ho, K. L., Pometto III, A. L. & Hinz, P. N., 1997. Optimization of L-(+)-lactic acid production by ring and disc plastic composite supports through repetaed batch biofilm fermentation. *Applied and Environmental Microbiology,* Volume 63, pp. 2533-2542.

Huang, Y. Y. H., 2007. The use of sensitivity analysis in on-line aquifer parameter estimation. *Journal of Hydrology,* Volume 335, pp. 406-418.

Hujanen, M. & Linko, Y. Y., 1996. Effect of temperature and various nitrogen resources on L(+)-lactic acid production by *Lactobacillys casei.Applied Microbiology and Biotechnology,* Volume 45, pp. 307-313.

Hulhoven, X., Vande Wouwer, A. & Bogaerts, P., 2006. Hybrid extended Luenberger-asymptotic observer for bioprocess state estimation. *Chemical Engineering Science,* 61(21), pp. 7151-7160.

Ilmén, M., Koivuranta, K., Ruohonen, L., Rajgarhia, V., Suominen, P. & Penttilä, M., 2013. Production of L-lactic acid by the yeast *Candida sonorensis* expressing heterologous bacterial and fungal lactate dehydrogenases. *Microbial Cell Factories,* Volume 12, pp. 1-15.

Jenzch, M., Simutis, R. & Luebbert, A., 2006. Generic model control of the specific growth rate in recombinant *Escherichia coli* cultivations. *Journal of Biotechnology,* Volume 122, pp. 483-493.

Jin, B., Van Leeuwen, H. J., Patel, B., Doelle, H. W. & Yu, Q., 1999. Production of fungal protein and glucoamylase by *Rhizopus oligosporus* from starch processing wastewater. *Process Biochemistry,* Volume 34, pp. 59-65.

John, R. P., Anisha, G. S., Nampoothiri, K. M. & Pandey, A., 2009. Direct lactic acid fermentation: focus on simultaneous saccharification an lactic acid production. *Biotechnology Advances,* Volume 27, pp. 145-152.

John, R. P., Nanpoothiri, K. M. & Pandey , A., 2007. Fermentative production of lactic acid from biomass: an overview on process developments and future perspectives. *Applied Microbiology and Biotechnology,* Volume 74, pp. 524-534.

Julier, S. J. & Uhlmann, J. K., 1997. A new extension of the Kalman filter to nonlinear systems. *In Proceedings of International Symp. Aerospace/Defense sensing, Simul. and Controls,* pp. 182-193.

Kamm, B., 2015. *Microorganisms in Biorefineries.* 1st ed. Teltow, Germany: Springer.

Kandepu, R., Foss, B. & Imsland, L., 2008. Applying the Unscented Kalman filter for nonlinear state estimation. *Journal of Process Control,* Volume 18, pp. 753-768.

Keller, A. K. & Gerhardt, P., 1975. Continuous lactic acid fermentation of whey to produce a ruminant feed supplement high in crude protein. *Biotechnology Bioengineering,* Volume 17, pp. 977-1018.

Bibliography

Kheir, N., 1996. *Systems Modeling and Computer Simulations.* Second ed. New York: Marcel Dekker, Inc..

Kiviharju, K., Salonen, K., Moilanen, U., Meskanen, E., Leisola, M. & Eerikäinen, T., 2007. On-line biomass measurements in bioreactor cultivations: comparison study of two on-line probes. *Journal of Industrial Microbiology and Biotechnology,* Volume 34, pp. 561-566.

Kong, X., Zhou, H. & Qian, H., 2007. Enzymatic hydrolysis of wheat gluten by proteases and properties of the resulting hydrolysates. *Food Chemistry,* Volume 102, pp. 759-763.

König, H., Unden, G. & Fröhlich, J., 2009. *Biology of Microorganisms on Grapes, in Must and in Wine.* Berlin: Springer.

Kosseva, M. R., Panesar, P. S., Kaur, G. & Kennedy, J. F., 2009. Use of immobilised biocatalysts in the processing of cheese whey. *International Journal of Biological Macromolecules,* Volume 45, pp. 437-447.

Kumar Dutta, S., Mukherjee, A. & Chakraborty, P., 1996. Effect of product inhibition on lactic acid fermentation: Simulation and modelling. *Applied Microbiology and Biotechnology,* Volume 46, pp. 410-413.

Kwakernaak, H. & Sivan, R., 1972. *Linear Optimal Control Systems.* New York: John Wiley & Sons.

Kwon, S., Yoo, I. K., Lee, W. G., Chang, H. N. & Chang, Y. K., 2001. High-rate continuous production of lactic acid by l*actobacillus rhamnosus* in a two-stage membrane cell-recycle bioreactor. *Biotechnology and Bioengineering,* Volume 73, pp. 25-34.

Leh, M. B. & Charles, M., 1989. The effect of whey protein hydrolyzate average molecular weight on the lactic acid fermentation. *Journal of Industrial Microbiology and Biotechnology,* Volume 4, pp. 77-80.

Lewis, F. L., Xie, L. & Popa, D., 2008. *Optimal and Robust Estimation: With an Introduction to Stochastic Control Theory, Automation and control engineering.* Second ed. Boca Raton: CRS Press, FL.

Liu, S., 2013. *Bioprocess Engineering: Kinetics, Biosystems, Sustainability, and Reactor Design.* 1st ed. Amsterdam: Elsevier.

Lombardi, M., 1996. *Modélisation, observation et commande pour le bioprocédés: Application à la fermentation lactique,* Lyon, France: PhD thesis. Université de Lyon 1.

Luedeking, R. & Piret, E. L., 1959. Transient and steady states in continuous fermentation: Theory and experiments. *Journal of Biochemical and Microbiological Technology and Engineering,* Volume 459, p. 431.

Bibliography

Lyddon, C., 2013. *world-grain.com.* [Online] Available at: http://www.world-grain.com/Departments/Country%20Focus/Country%20Focus%20Home/Focus%20on%20France.aspx. [Accessed 16 March 2015].

Madigan, M. T., Martinko, J. M. & Parker, J., 2000. *Brock Biology of Microorganisms.* 9th ed. New Jersey: Prentice Hall.

Mailleret, L., Bernard, O. & Steyer, J. P., 2004. Nonlinear adaptive control for bioreactor with unknown kinetics. *Automatica,* Volume 40, pp. 1397-1385.

Marcos, N. I., Guay, M. & Dochain, D., 2004. Output feedback adaptive extremum seeking control of a continuous stirred tank bioreactor with Monod's kinetics. *Journal of Process Control,* Volume 14, pp. 807-818.

marketsandmarkets.com, 2015. *Markets and Markets.* [Online] Available at: http://www.marketsandmarkets.com/Market-Reports/polylacticacid-387.html.2014. [Accessed 16 March 2015].

Marshal, V. M. & Law, B. A., 1984. *"The Physiology and growth of dairy lactic acid bacteria" Advances in the Microbiology and Biochemistry of Cheese and Fermented Milk.* London: Elsevier.

McNeil, B. & Harvey, L. M., 1990. *Fermentation: A practical Approach.* Oxford: Oxford University, Press.

Miura, S., Arimura, T., Itoda, N., Dwiarti, L., Beng Feng, J., Hong Bin, C. & Okabe M., 2004. Production of L-lactic acid from corncob. *Journal of Bioscience Bioengineering,* Volume 97, pp. 153-157.

Moldes, A. B., Alonso, J. L. & Parajo, J. C., 1999. Cogeneration of cellobiose and glucose from pretreated wood and bioconversion to lactic acid: A kinetic study. *Journal of Bioscience and Bioengineering,* Volume 87, pp. 787-792.

Monnet, V., Le Bars, D., Neviani, E. & Gripon, J. C., 1987. Partial characterization and comparison of cell wall proteinases from 5 strains of *Streptococcus lactis.* *Le lait,* Volume 67, pp. 51-61.

Monteagudo, J. M., Rodriguez, L., Rincon, J. & Fuertes, J., 1997. Kinetics of lactic acid fermentation by *lactobacillus delbrueckii* on beet molasses. *Journal of Chemical Technology and Biotechnology,* Volume 87, pp. 787-792.

Mou, D. G. & Cooney, C. L., 1983. Growth monitoring and control in complex medium: A case study employing fed-batch penicillin fermentation and computer-aided on-line mass balancing. *Biotechnology and bioengineering,* Volume 26, pp. 257-269.

Nancib, A., 2007. *Lactic acid production by Lactobacillus casei subsp. rhamnosus growing on date juice: Batch, fed-batch and continuous culture kinetics and optimization,* Nancy, France: PhD thesis, University of Nancy.

Nandasana, A. D. & Kumar, S., 2008. Kinetics modeling of lactic acid production from molasses using *Enterococus faecelis* RKY1. *Biochemical Engineering Journal,* Volume 38, pp. 277-284.

Narayanan, N., Roychoudhury, P. & Srivastava, A., 2004. L (+) lactic acid fermentation and its product polymerization. *Journal of Biotechnology,* Volume 7, pp. 167-178.

Narita, J., Nakahara, S., Fukuda, H. & Kondo, A., 2004. Efficient production of L-(+)-lactic acid from raw starch by *Streptococcus bovis* 148. *Journal of Bioscience and Bioengineering,* Volume 97, pp. 423-425.

Niemelä, S., Keskus, M. 2002. Uncertainty of Quantitative Determinations Derived by Cultivation of Microorganisms. Centre for Metrology and Accreditation, Finland.

Nielsen , J., Nikolaisen, K. & Villadsen, J., 1991. Structured modelling of a microbial system: A theorical study of lactic acid fermentation. *Biotechnology and Bioengineering ,* Volume 38, pp. 1-10.

Nigam, P. & Singh, D., 1995. Enzyme and microbial systems involved in starch processing. *Enzyme and Microbial Technology,* Volume 17, pp. 770-778.

Ochoa, S., Lyubenova, V., Repke, J, Ignatova, M. & Wozny G., 2008. Adaptive control of the simultaneous saccharification-fermentation process from starch to ethanol. *Computer Aided Chemical Engineering,* Volume 25, pp. 489-494.

Ohara, H., Hiyama, K. & Yoshida, T., 1992. Non-competitive product inhibition in lactic acid fermentation from glucose. *Applied Microbiology and Biotechnology,* Volume 36, pp. 773-776.

Panesar, P. S., Kennedy, J. F., Gandhi, D. M. & Bunko, K., 2007. Bioutilisation of whey for lactic acid production. *Food Chemistry,* Volume 105, pp. 1-14.

Peeva, L. & Peev, G., 1997. A new method for pH stabilization of the lactoacid fermentation. *Enzyme and Microbial Technology,* Volume 21, pp. 176-181.

Petre, E., Selişteanu, D. & Şendrescu, D., 2011. Neural networks based adaptive control of a fermentation bioprocess for lactic acid production. *Proceedings of the 3rd International Conference on Intelligent Decision Technologies, SIST 10,* pp. 201-212.

Picó, J., De Battista, H. & Garelli, F., 2009. Smooth sliding-mode observers for specific growth rate and substrate from biomass measurement. *Journal of Process Control,* 19(8), pp. 1314-1323.

Pinelli, D., Gonzalez-Vara, A. R., Matteuzzi, D. & Magelli, F., 1997. Assesment of kinetic models for the production of L-and D- lactic acid isomers by *lactobacillus casei* DMS 20011 and *Lactobacillus coryniformis* DMS20004 in continous fermentation. *Journal of Fermentation and Bioengineering,* Volume 83, pp. 209-212.

Bibliography

Pons, M. N., 1991. *Bioprocess monitoring and control.* Munich: Hanser Publishers.

Pons, M. N., Rajab, A., Flaus, J. M. & Engasser, J. M., 1988. Comparison of estimation methods for biotechnological processes. *Chemical Engineering Science,* Volume 43, pp. 1909-1914.

Ramaswamy, S., Cutright, T. J. & Qammar, H. K., 2005. Control of a continuous bioreactor using model predictive control. *Process Biochemistry,* Volume 40, pp. 2763-2770.

Rapaport, A. & Dochain, D., 2005. Interval observers for biochemical processes with uncertain kinetics and inputs. *Mathematical Biosciences,* Volume 193, pp. 235-253.

Rashid, R., 2008. *Optimization and modeling of lactic acid production from pineapple waste. Technical Report, VOT 74263,* Malasya: Faculty of Chemical and Naturan Engineering, Universiti Teknologi Malasia.

Rojan, P. J., Nampoothiri, K. M. & Pandey, A., 2006. Simulaneous saccharification and L-(+)-lactic acid fermentation of protease-treated wheat bran using mixed culture of *lactobacilli. Biotechnology Letters,* Volume 28, pp. 1823-1826.

Roux, G., Dahhou, B. & Queinnec, I., 1996. Modelling and estimation aspects of adaptive predictive control in a fermentation process. *Control Engineering Practice,* Volume 4, pp. 55-66.

Saha, P., Patwardhan, S. C. & Ramachandra Rao, V. S., 1999. Maximizing productivity of a continuous fermenter using nonlinear adaptive optimizing control. *Bioprocess engineering,* Volume 20, pp. 15-21.

Selişteanu, D., Petre, E. & Răsvan, V. B., 2007. Sliding mode and adaptive sliding-mode control of a class of nonlinear bioprocesses. *International Journal of Adaptive Control and Signal Processing,* Volume 21, pp. 795-822.

Serban, R. & Hindmarsh, A. C., 2005. CVodes, the sensitivity-enabled ode solver in SUNDIALS. *ASME 2005 International Design Engineering Technical Conferences and Computers and Information in Engineering Conference,* Volume 6, pp. 257-269.

Shibata, K., Flores, D. M., Kobayashi, G. & Sonomoto, K., 2007. Direct L-lactic acid fermentation with sago starch by a novel amylolytic lactic acid bacterium, *Enterococcus faecium.Enzyme and Microbial Technology,* Volume 41, pp. 149-155.

Shi, Z., Shimizu, K., Lijima, S., Morisue, T. & Kobayashi, T., 1990. Adaptive on-line optimizing control for lactic acid fermentaiton. *Journal of Fermentation and Bioengineering,* Volume 70, pp. 415-419.

Sinclair, C. G. & Kristiansen, B., 1987. *Fermentation Kinetics and Modelling.* Milton Keynes: Open University Press.

Bibliography

Tebbani, S., Lopes, F. & Becerra Celis, G., 2015. Nonlinear control of continuous cultures of *Porphridium pupureum* in a photobioreactor. *Chemical Engineering Science,* Volume 123, pp. 207-219.

Trontel, A., Baršić, V., Slavica, A., Šantek., B. & Novak, S., 2010. Modelling the effect of different substrates and temperature on the growth and lactic acid production by *lactobacillus amylovorus* DSM 20531 in batch Process. *Food Technology and Biotechnology,*Volume48, pp. 352-361.

Van der Maarel, M., Van der Veen, B., Uitdehaag, J. C., Leemhuis, H. & Dijkhuizen, L., 2002. Properties and applications of starch-convergint enzymes of the α-amylase family. *Journal of Biotechnology,* Volume 94, pp. 137-155.

Varadarajan, S. & Miller, D., 1999. Catalytic Upgrading of Fermentation-Derived Organic Acids. *Biotechnology Progress,* Volume 15, pp. 845-854.

Vick Roy, T. B., 1985. *Lactic acid, In Comprehensive biotechnology: the principles, applications and regulations of biotechnology in industry, agriculture and medicine.* 2nd ed. New York: Pergamon Press.

Vos, P. ,Garrity, G., Jones, D., Krieg, N. R., Ludwig, W., Rainey, F. A., Schleifer, K. H. & Whtiman, W., 2011. *Bergey's Manual of Systematic Bacteriology: Volume 3: The Firmicutes.* Springer Science & Business Media.

Wee, Y., Kim, J. & Ryu, H., 2006. Biotechnological Production of Lactic Acid and Its Recent Applications. *Food Technology and Biotechnology,* Volume 44, pp. 163-172.

Welch, G. & Bishop, G., 1995. *An introduction to the Kalman Filter,* Chapel Hill, USA: University of North Carolina.

Willems, J. L., 1970. *Stability theory of dynamical systems.* London: Nelson.

Wood, B. J. & Holzapfel, W. H., 1995. *The Genera of lactic Acid Bacteria.* volume 2. London: Champlan & Hall.

Yin, P., Nishina, N., Kosakai, Y., Yahiro, K., Pakr, Y. & Okabe M., 1997. Enhanced production of L(+) lactic acid from corn starch in a culture of *Rhizopus oryzae* using an air lift bioreactor. *Journal of Fermentation and Bioengineering,* Volume 84, pp. 249-253.

Yumoto, I. & Ikeda, K., 1995. Direct fermentation of starch to L-(+)-lactic acid using *Lactobacillus amylophilus*. *Biotechnology Letters,* Volume 17, pp. 543-546.

Zabriskie, D. W. & Humphrey, A. E., 1978. Real-time estimation of aerobic batch fermentation biomass concentration by component balancing. *Aiche Journal ,* Volume 24, pp. 138-146.

Bibliography

Zhang, B., He, P. J., Ye, N. F. & Shao, L. M., 2008. Enhanced isomer purity of lactic acid from the non-sterile fermentation of kitchen wastes. *Bioresources Technology,* Volume 99, pp. 855-862.

Zhang, W., Chen, L. & Zhang, Y., 2009. Surprising shape-memory effect of polylactide resulted from toughening by polyamide elastomer. *Polymer,* Volume 50, pp. 1311-1315.

Zhao, B., Wang, L., Li, F., Hua, D., Ma, C., Ma, Y. & Xu, P., 2010. Kinetics of D-lactic acid production by *Sporolactobacillus* sp. strain CASD using repeated batch fermentation. *Bioresourche Technology,* Volume 101, pp. 499-505.

Zhou, Y. Dominguez, J. M., Cao, N., Du, J. & Tsao, G. T., 2003. Optimization of L-lactic acid production from glucose by *Rhysopus oryzae* ATCC 52311. *Applied Biochemistry and Biotechnology,* Volume 78, pp. 401-407.

Zorzetto, L. F. M. & Wilson, J. A., 1996. Monitoring bioprocesses using hybrid models and an extended Kalman Filter. *Computers & Chemical Engineering,* Volume 20, pp. 689-694.
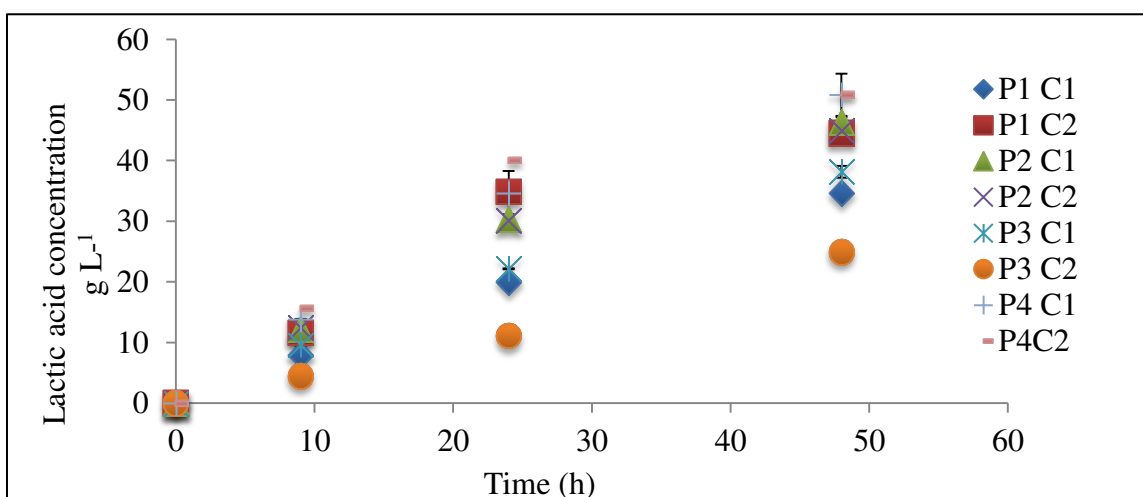
APPENDIXES

APPENDIX A.1 Protease study (complement)

In this section, all the results of the protease choice experiments are presented including both concentrations tested. The concentration 200 mg Kg^{-1}is presented as C1 and the concentration 1400 mg Kg^{-1} is referredas to C2. Figure A.2.1 shows the free acid nitrogen concentration (FAN) during the SSPHF. Figure A.2.2 is presented in order to show the impact of the FAN on lactic acid production.
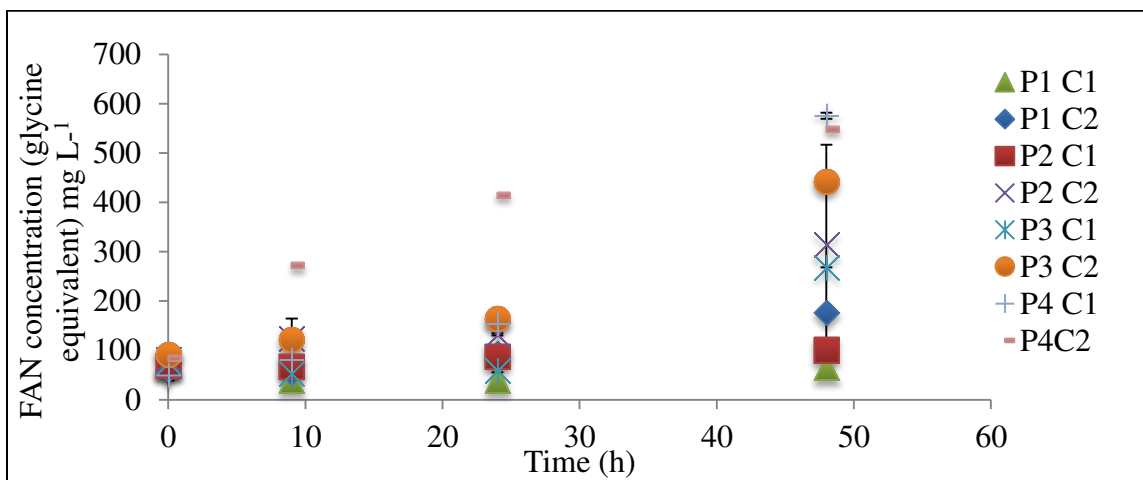
Figure A.2.1. Free Acid Nitrogen (FAN) concentration during the fermentation. P1= Prolyve PAC, P2= Prolyve BS, P3= Prolyve 4000 and P4= Prolyve NP. C1= 200g Kg^{-1}, C2=1400 gKg^{-1}. Fermentation conditions: 30°C and pH 5.7.

Figure A.2.2. lactic acid concentration during the fermentation. P1= Prolyve PAC, P2= Prolyve BS, P3= Prolyve 4000 and P4= Prolyve NP. C1= 200g Kg^{-1}, C2=1400 g Kg^{-1}. Fermentation conditions: 30°C and pH 5.7.

The protease concentration effect on lactic acid productivity was not important for almost all proteases tested. Only a small effect was detected using the protease P3. Nevertheless, this protease showed the worst performance. Only a small concentration effect on FAN production was detected for the protease Prolyve NP (P4) from comparison of obtained results with each concentration (P4C1 and P4C2) in figure A.2.1. Nevertheless, as the experiment P4C2 (Prolyve Np at 1400 g Kg^{-1}) did not have a replica, the experimental FAN measurements obtained for this condition can be questionable. Moreover, it is possible to see that the experiments performed with P4 had the highest lactic acid concentrations regardless of the protease concentration used. For this reason, the lowest concentration was chosen as the optimal one for the process.

APPENDIX A.2 Data Sheet of Prolyve NP

Fungal neutral protease

DESCRIPTION

PROLYVE NP CONC is a neutral protease obtained from a selected strain of *Aspergillus oryzae*.

PROLYVE NP CONC contains some side activities like amylases and hemicellulases.

PROPERTIES

PROLYVE NP CONC has a wide pH range with an optimum at pH 7.0 (see graph 1) the optimum temperature is 50°C (graph 2).

PROLYVE NP CONC is stable at 30°C for 60 minutes from pH 6.0 to 10.0.
PROLYVE NP CONC contains endo and exo peptidases activities.

Effect of pH on the activity

Effect of temperature on the activity
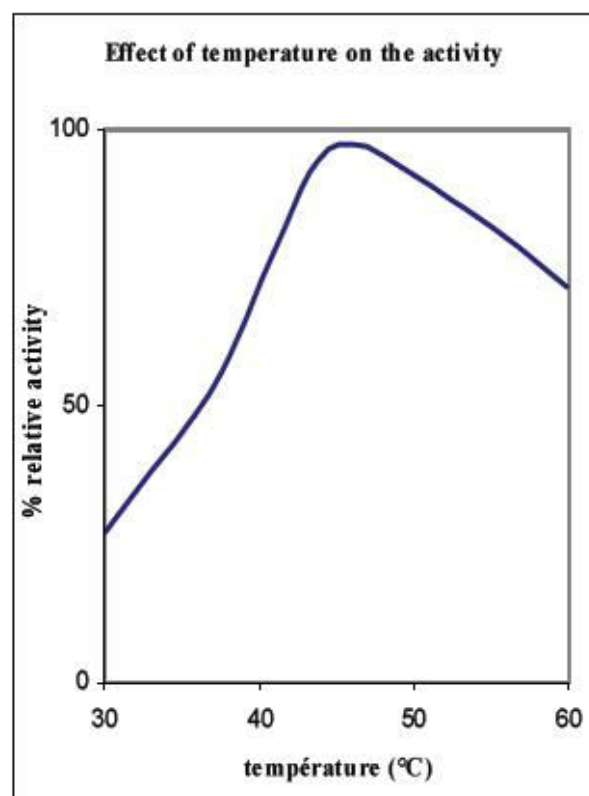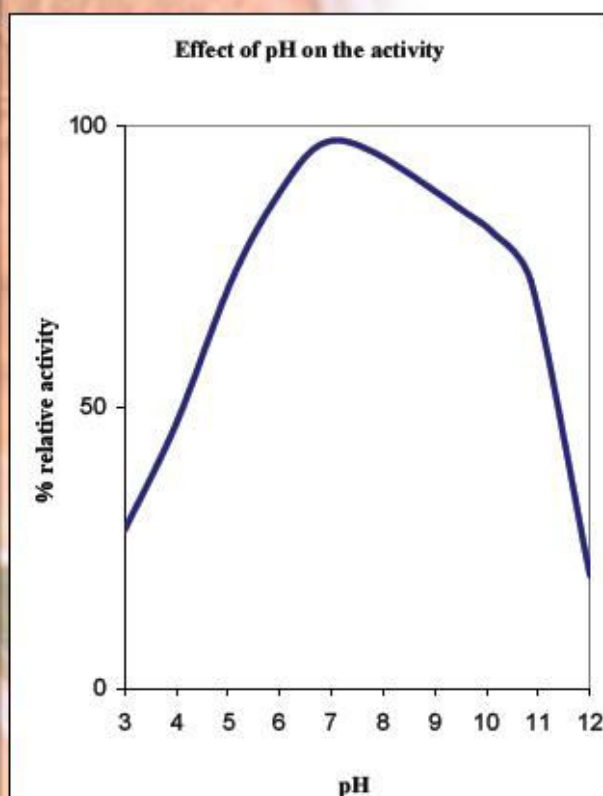
APPLICATION

PROLYVE NP CONC can be used in very different fields of applications : baking, manufacture of seasonings, gluten hydrolysis etc...

PROLYVE NP CONC is generally more active on heat denatured proteins.

Mn and Ca ions enhance the enzymatic activity.

FORMULATION

PROLYVE NP CONC is a slightly brownish powder soluble in water.
PROLYVE NP CONC in standardised at 3000 PNU/g following LYVEN assay method (available on request).

PRACTICAL INFORMATION

Presentation and packaging :	**PROLYVE NP CONC** is supplied in powder form and packaged in 20 kg cardboard box.
Precautions in use :	In case of contact with the skin or the eyes, rinse thoroughly with water. The spraying of **PROLYVE NP CONC** can lead to pulmonary reactions.
Conformity to standards :	**PROLYVE NP CONC** conforms to the relevant French and international standards. France : Arrêté 19/10/2006 International : Specifications agreed by FAO, WHO, JECFA and FCC specifications.
Storage :	When stored at temperature below 20 °C and in a dry place, **PROLYVE NP CONC** shows non significant loss in activity over a period of two years.

LYVEN YOUR PARTNER,

Due to its diverse structure and great flexibility, LYVEN can provide special formulations adapted to your needs. Do not hesitate to contact us.

*APPENDIX B.1Residence time distribution*

As the culture broth is very complex (wheat flour) and has a significant viscosity compared to water, the ideal behaviour of the bioreactor must be checked. Indeed the proposed modelling approach is based on mass balance for a perfectly stirred tank bioreactor. In order to characterize the mixing in the bioreactor, the residence time distribution (RTD) was performed.

Experiment Description

The residence time distribution (RTD) was studied in the 5 L bioreactor used for the continuous SSPHF. For the RTD determination a solution of NaCl at 2.8 M was used as tracer and the conductivity was the variable measured over time.

The broth was the liquefied wheat flour that fed the fermentation reactor. No bacteria or enzymes were added in the broth in order to reduce the biological reactions and the possible interferences on conductivity.

First of all, experiments aiming at determining the conductivity of the broth for different NaCl concentrationswere carried out (figure B.1.1). Accordingly, there is a perfect linearity between the parameters showing that conductivity is a good measurement of NaCl concentration in the considered medium.

y = 1 006,07x + 1,49
R² = 1,00
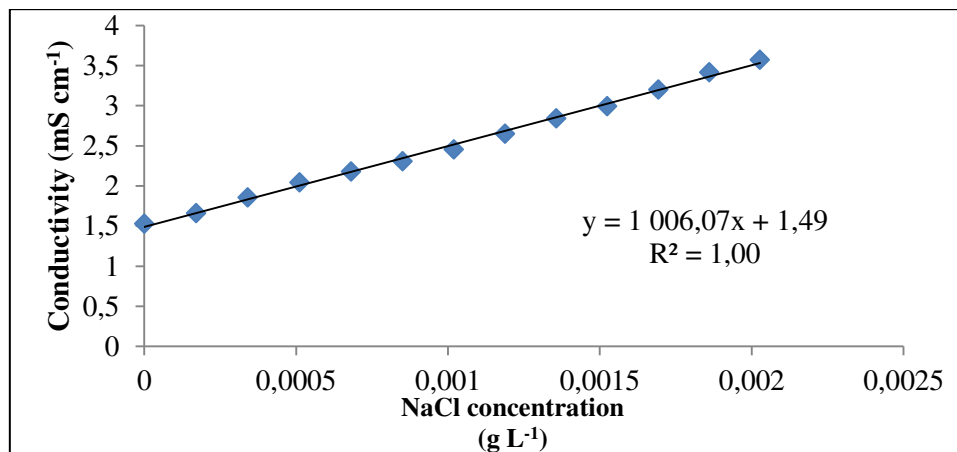
Figure B.1.1 Correlation between the conductivity and the NaCl concentration

The RTD was determined experimentally by injecting 35mL of the NaCl solution into the tank at time zero and collecting samples at 5 minutes intervals for conductivity measurements. Two flow rates were tested: 0.35 Lh^{-1} and 0.7 L h $^{-1}$, with replicates (corresponding to dilutions rates with ideal mixing equal to 0.11 and 0.22 h^{-1}, respectively).

Results and analysis

Assuming a well-mixed reactor, a mass balance on NaCl was done:

$$\frac{dC_{NaCl}}{dt} = -\frac{F}{V}C_{NaCl_0} \tag{B.1.1}$$

where C_{NaCl} is the concentration of NaCl at time t, C_{NaCl_0} is the concentration of NaCl in the fermenter at the beginning of the assay, F is the output flow, V is the effective volume of the bioreactor and t is the time.

The integration of the equation B.1.1 leads to:

$$\frac{C_{NaCl}}{C_{NaCl_0}} = \exp\left(-\frac{F}{V}t\right) \tag{B.1.2}$$

In the case of the pulse assay performed here, the concentration increases in the first minutes reaching a maximum concentration, then it decreases (equation B.1.2.). There is then a gap between the time of tracer injection and the time of the concentration peak, the difference between these two instants was named t_1.

In order to take into account this lag time, the theoretical relation was modified leading to:

$$-\ln\left(\frac{C_{NaCl}}{C_{NaCl_0}}\right) = \frac{F}{V}(t - t_1) \tag{B.1.3}$$

The effective dilution rate imposed in the reactor is determined then by the slope of the curve of $-\ln(C_{NaCl}/C_{NaCl_0})$ versus $(t-t_1)$.
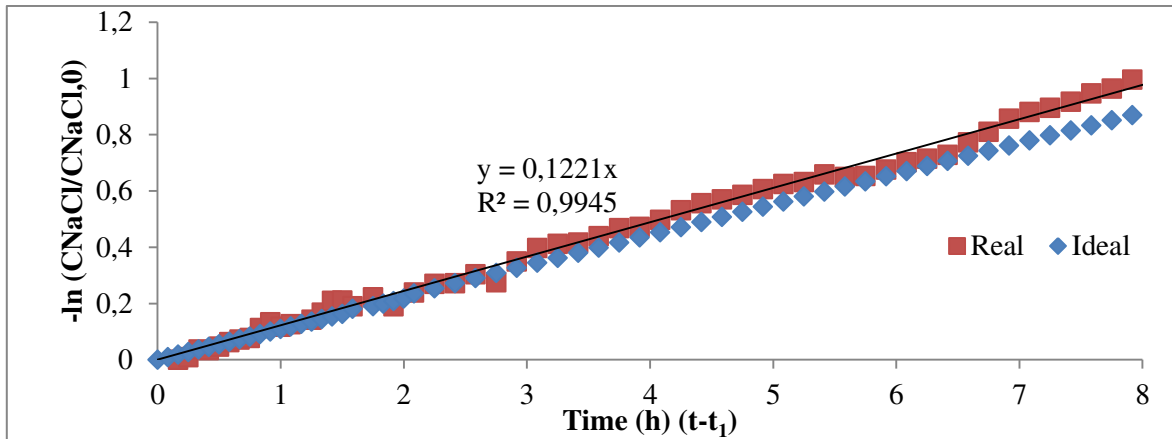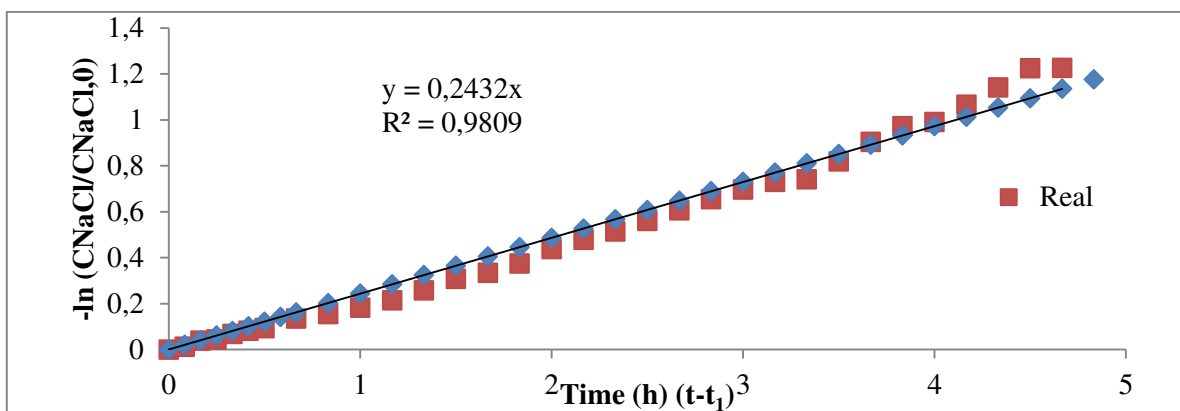
Results are presented in figures B.1.2 to B.1.5.
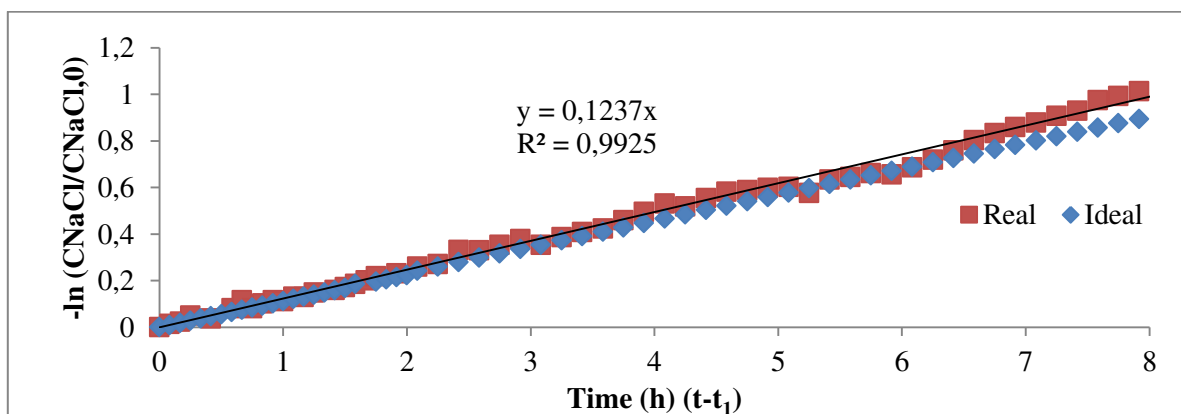
Figure B.1.2 Comparison between the real and the ideal behaviour of the bioreactor with a flow rate equal to 0.35 L h^{-1} (Ideal dilution rate=0.1 h^{-1}). Replicate 1.
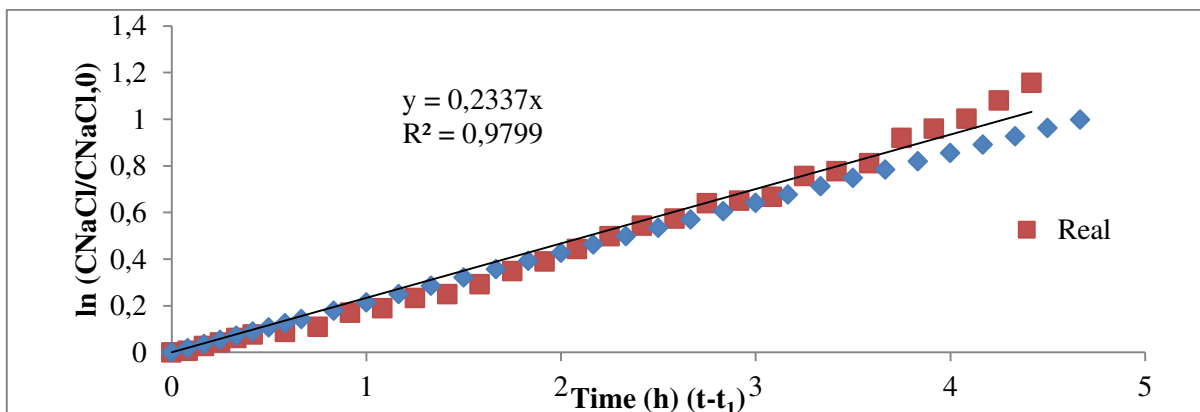
214

Figure B.1.3 Comparison between the real and the ideal behaviour of the bioreactor with a flow rate equal to 0.35 L h^{-1}. (Ideal dilution rate=0.1 h^{-1}). Replicate 2.

Figure B.1.4 Comparison between the real and the ideal behaviour of the bioreactor with a flow rate of 0.7 L h^{-1}. (Ideal dilution rate=0.2 h^{-1}). Replicate 1.

Figure B.1.5 Comparison between the real and the ideal behaviour of the bioreactor with a flow rate of 0.7 L h^{-1}. (Ideal dilution rate=0.2 h^{-1}). Replicate 2.

From these results it is possible to conclude that there is a dead volume in the bioreactor. The residence time is lower than the ideal one (Table B.1.1). The elements passing through the bioreactor stay less time in the bioreactor because of the dead volume.

Table B.1.1 Comparison between the real and ideal residence times and volumes for each experiment

Assay	Flow rate (Lh^{-1})	Ideal τ (h)	real τ (h)	Ideal Volume(L)	real volume (L)	% effective volume
Assay 1 F1	0.36	8.94	8.08	3.20	2.89	90.39
Assay 1 F2	0.35	9.20	8.19	3.20	2.85	89.01
Assay 2 F1	0.72	4.42	4.11	3.20	2.98	93.03
Assay 2 F2	0.68	4.68	4.28	3.20	2.93	91.49
					Deviation Average (%)	90.98

The average deviation between the real volume and the ideal one is 90.1%. In order to take into account this non ideal behaviour,it is necessary to introduce a coefficient in the dilution rate determination (in modelling and control). This coefficient will be introduced by equation B.1.4:

$$D = F / V_{real} \text{ where } V_{real} = 0.91 * V_{culturemedium} \qquad \text{(B.1.4)}$$

APPENDIX B.2 Substrate effects on growth and lactic acid production

The aim of this study was to determine the impact of the initial glucose concentration on bacteria growth and lactic acid production kinetics.

In this work, usually the carbon source is provided by the liquefaction and further saccharification of starch to maltose and glucose. Nevertheless, in order to control the carbon source supplied at the beginning of the experiment, the carbon substrate was provided by commercial glucose added to the wheat flour solution at different initial concentrations. The nitrogen source was provided by the wheat proteins hydrolysis using the enzyme Prolyve NP. In this case, the proteins hydrolysis started simultaneously with the fermentation. The FAN (Free Acid Nitrogen), biomass, glucose, maltose and biomass concentrations were measured during the experiments.

Materials and methods

Experiments description

Two experimental campains were carried out. In the first one, the initial glucose concentrations tested were: 33, 43, 53 and 70 g L^{-1}. Two repicates were performed for each concentration tested. In the second experimental campain, the initial glucose concentrations tested were: 12 and 22 g L^{-1}, each one with two replicates. The experiments were performed in 200 mL flasks with 100 ml of wheat flour solution. The proteins hydrolysis was performed simultaneously with the fermentation.

Inoculum preparation

Lactobacillus coryniformis subsp. *torquens* DSM 20005 stored at -80°C, was grown in MRS. The strain was cultured in an incubator shaker MAXQ 4000 (Thermo Scientific) in a 100 mL flask at 30°C. This culture was used to inoculate all the flasks tested.

Preparation of starch solution: Liquefaction

The liquefaction step was carried out in the Soufflet Laboratory in a 5 L reactor as described in section 2.2.2.1.3.

Preparation of flasks

1.5 L of the liquefied starch solution was thawed at 60°C in a water bath during 30 minutes. Then it was diluted with distilled water to get a final wheat concentration of 130 g L^{-1}. MnSO$_4$ was added at 0.05 g L^{-1} to the wheat solution and pH was adjusted to 5.7 with the addition of NaOH (7N) or H$_2$SO$_4$ (2.5 N). This solution was distributed in flasks. The wheat solution volume in each flask was 100 mL. Glucose was added to each flask in order to obtain the target initial glucose concentration. Calcium carbonate was then added to each flask at a concentration of 30 g L^{-1} in order to buffer the wheat solution and to reduce the pH decrease due to lactic acid production. Flasks were then sterilized for 20 min at 120°C.

Simultaneous proteins hydrolysis and fermentation (SPHF)

The solution containing the protease Prolyve NP (Lyven, Colombelles, France) was diluted tenfold in a sodium acetate buffer solution (0.1 M, pH 5.7). The SPHF step started with the addition of the protease Prolyve NP (200 mg of enzyme Kg^{-1} of wheat) and the inoculation in each flask. The initial biomass concentration was 10^9 cellsmL^{-1}. In the first campaign, the SPHF step was performed during 48 h at 30°C and with an agitation 150 rpm. In the second campaign the step was performed during 48 h as well but only results concerning the first 24 h are presentedas flasks were contaminated at the last phase of the experiment.

Analyses

In order to measure the cell, substrates (maltose and glucose) and lactic acid concentrations, samples were withdrawn from each flask at various time intervals. Analyses performed to determine biomass, glucose, maltose and lactic acid concentrations are further detailed in section2.2.2.1.7.

Results and discussion

The evolution of the Free Acid Nitrogen (FAN) concentration with time is presented on figure B.2.1. A similar trend is obtained for all tested conditions. Cell concentration with time was also similar in all flasks (figure B.2.2). Cells reached the stationary growth phase after approximately 24 h.

Concerning maltose (figure B.2.3), its concentration remained almost constant with time in all flasks suggesting that no starch saccharification occurred during the experiments. On the other hand the glucose consumption rate was similar in all flasks (Figure B.2.4) and its exhaustion occurred after 48 h for the smallest initial glucose concentration tested (34g L^{-1}). Similar lactic acid production was observed in the different conditions (figure B.2.5). During the stationary growth phase cells continued to produce lactic acid at a similar rate than in the exponential growth phase.
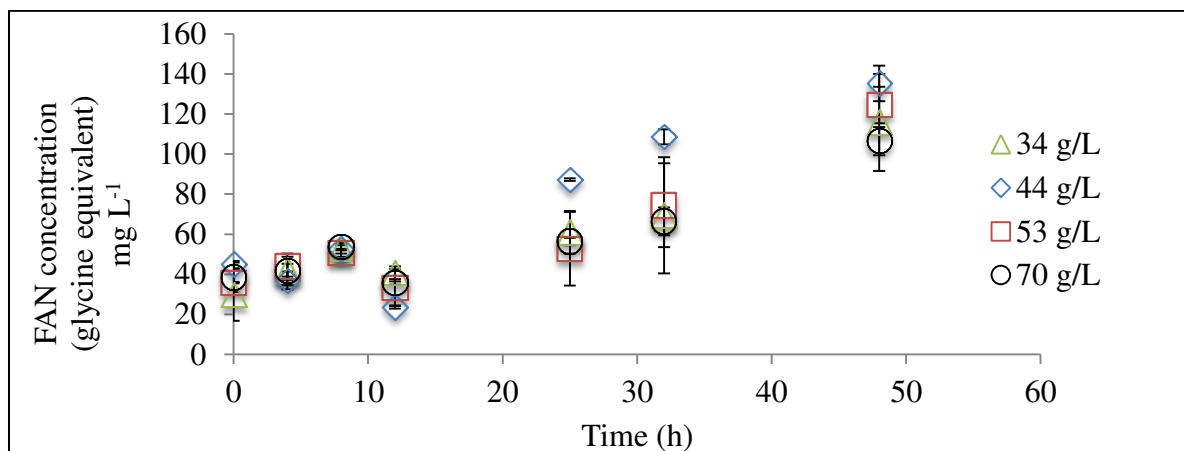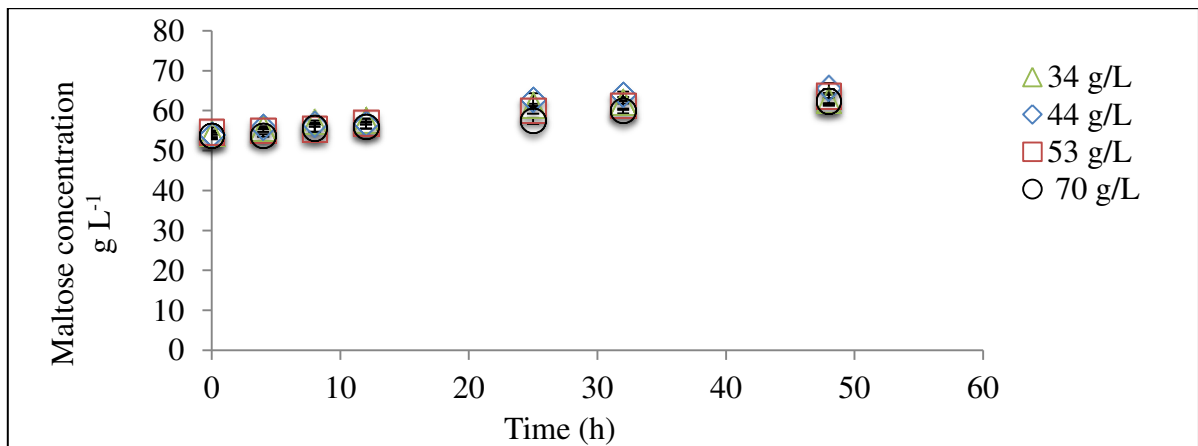

Figure B.2.1. Free Acid Nitrogen (FAN) concentration during the SPHF for different initial glucose concentration values: 33, 43, 53 and 70 g L^{-1}Conditions: 30°C and pH 5.7.
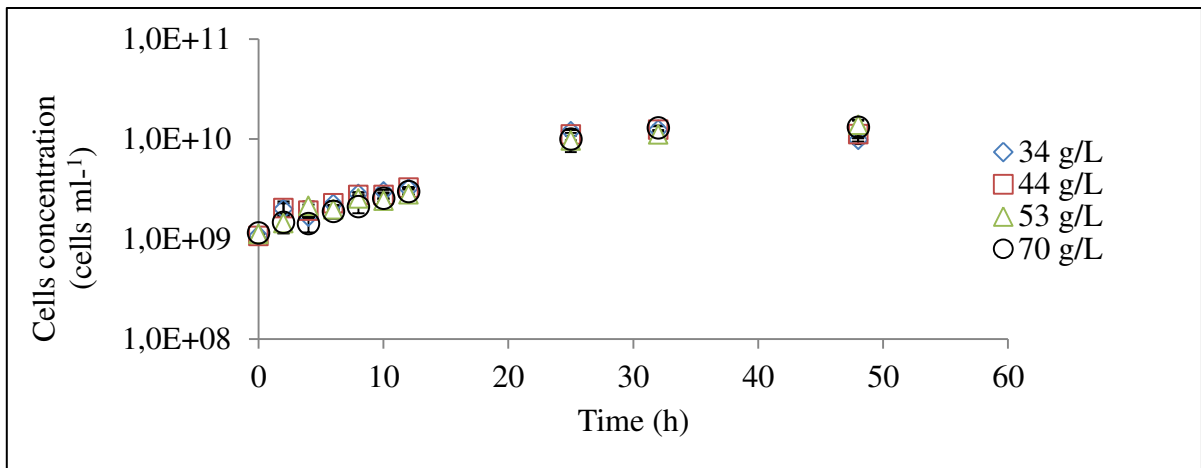
Figure B.2.2. Biomass concentration during the SPHF for different initial glucose concentration values: 33, 43, 53 and 70 g L^{-1}Conditions: 30°C and pH 5.7.

Figure B.2.3. Maltose concentration during the SPHF for different initial glucose concentration values: 33, 43, 53 and 70 g L^{-1}Conditions: 30°C and pH 5.7.

Figure B.2.4. Glucose concentration during the SPHF for different initial glucose concentration values: 33, 43, 53 and 70 g L^{-1}Conditions: 30°C and pH 5.7.

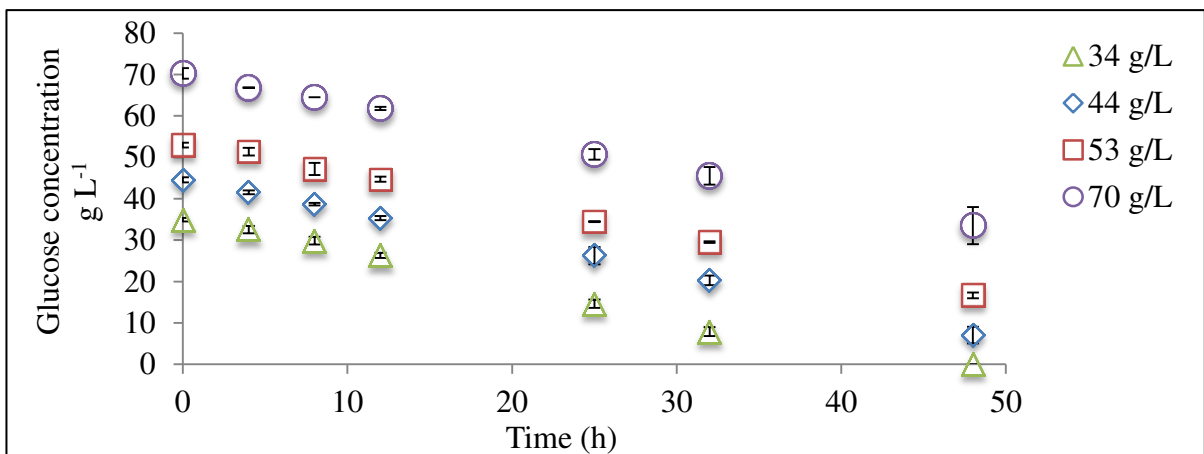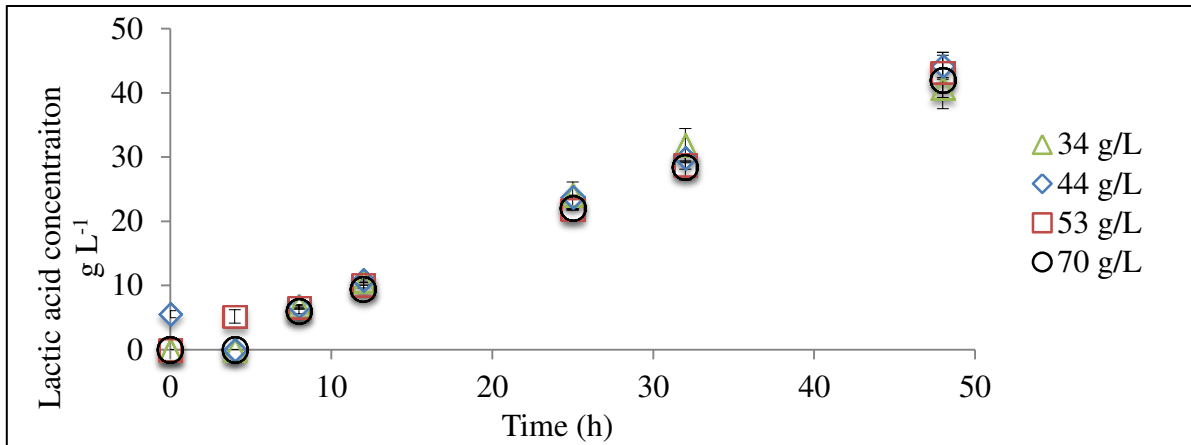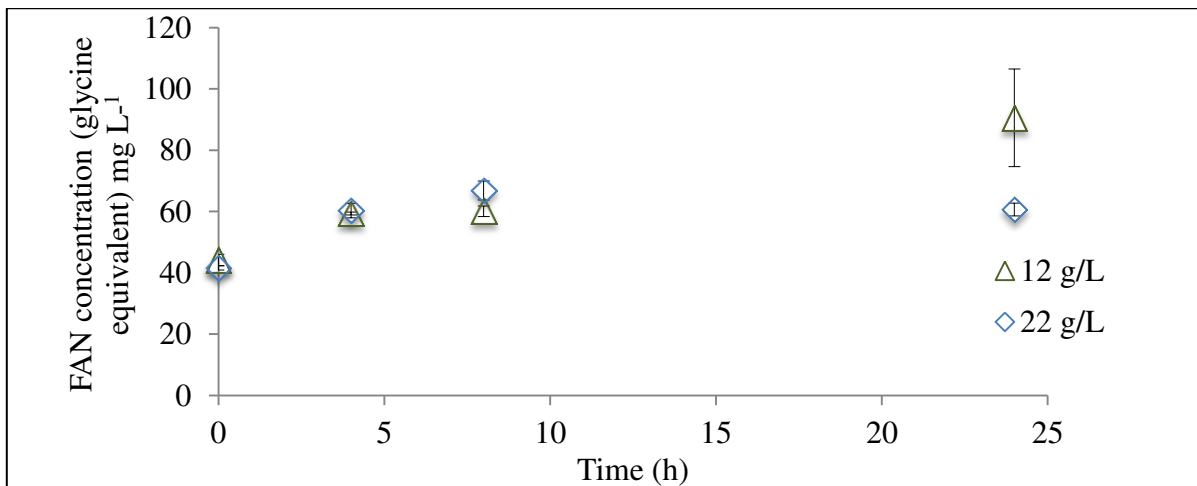**Figure B.2.5.** Lactic acid concentration during the SPHF for different initial glucose concentration values: 33, 43, 53 and 70 g L^{-1} Conditions: 30°C and pH 5.7.

According to the results, the growth rate (0.1 h^{-1}) was not limited by glucose in the range of concentrations tested. Additionally, no effect of the initial glucose concentration on lactic acid production rate (1.1 g L-^{1} h^{-1}) was observed.

Lower initial glucose concentrations were then tested in a new campaign (12 g L^{-1}and 22 g L^{-1}). Results from this second experimental campaign are presented in the following figures:

Figure B.2.6. Free Acid Nitrogen (FAN) concentration during the SPHF for different initial glucose concentration values: 12 and 22 g L^{-1}Conditions: 30°C and pH 5.7.

Figure B.2.7. Biomass concentration during the SPHF for different initial glucose concentration values: 12 and 22 g L^{-1} Conditions: 30°C and pH 5.7.

Figure B.2.8. Maltose concentration during the SPHF for different initial glucose concentration values: 12 and 22 g L^{-1} Conditions: 30°C and pH 5.7.
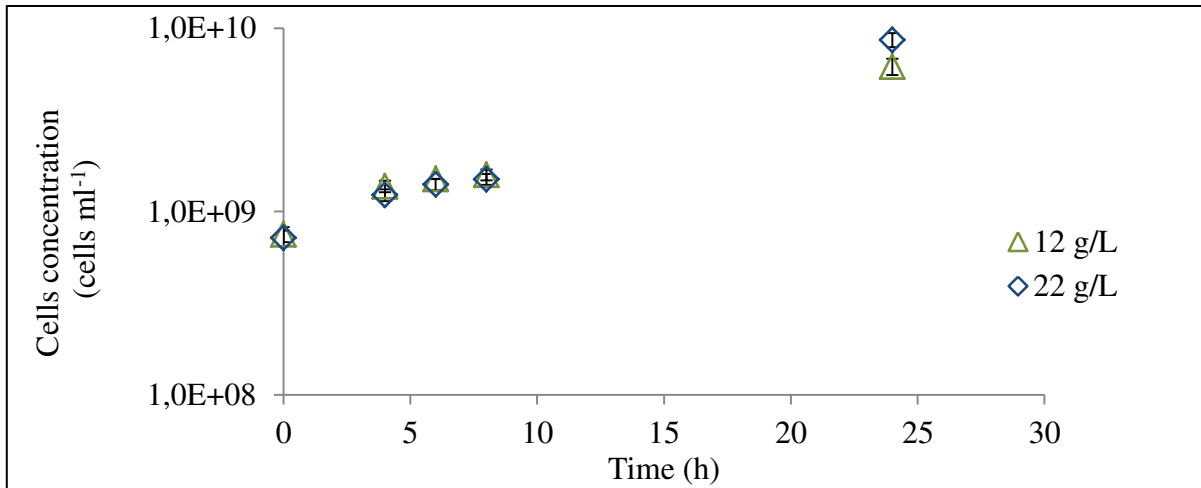

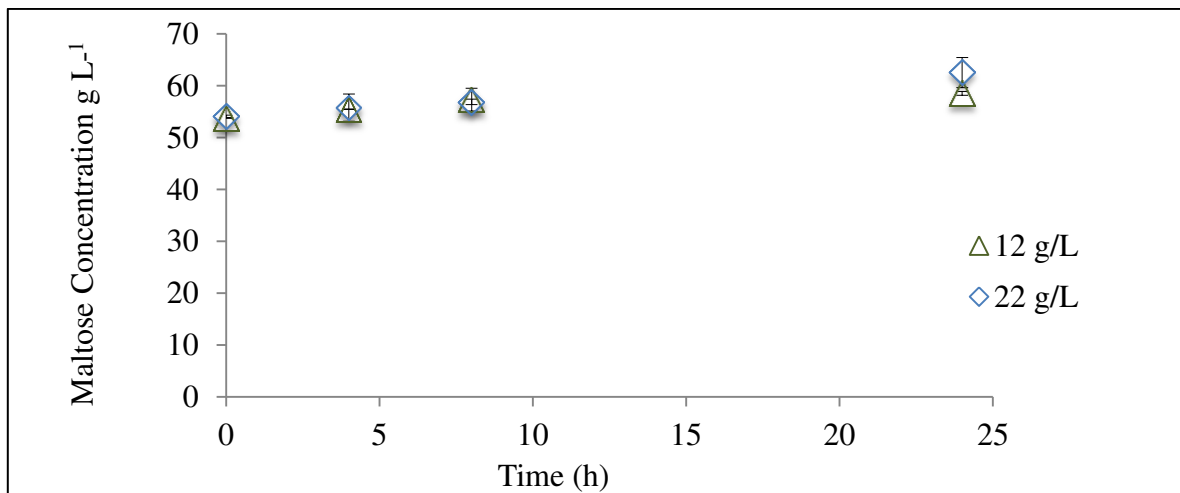**Figure B.2.8.** Glucose concentration during the SPHF for different initial glucose concentration values: 12 and 22 g L^{-1} Conditions: 30°C and pH 5.7.

Figure B.2.9. Lactic acid concentration during the SPHF for different initial glucose concentration values: 12 and 22 g L^{-1}Conditions: 30°C and pH 5.7.

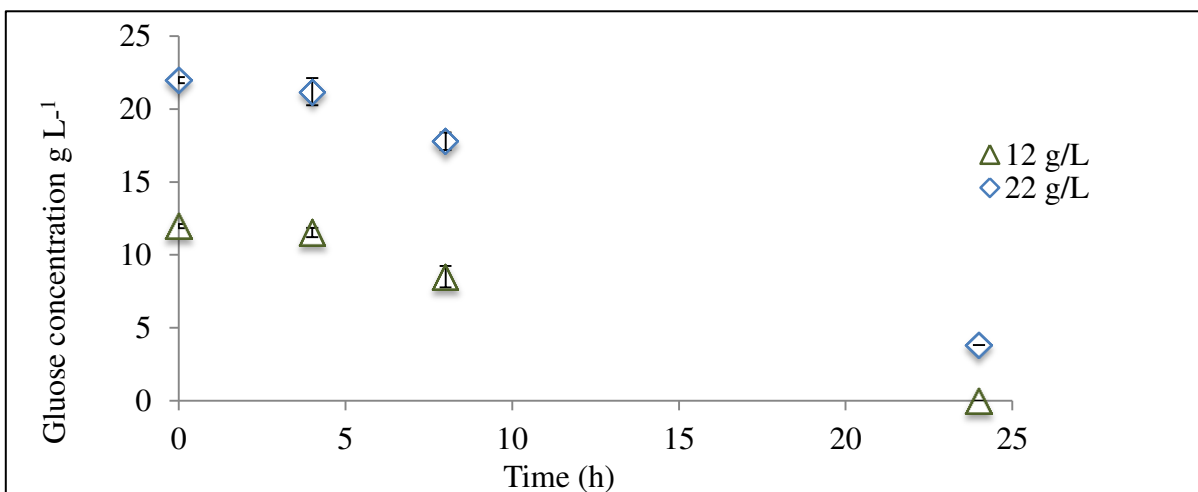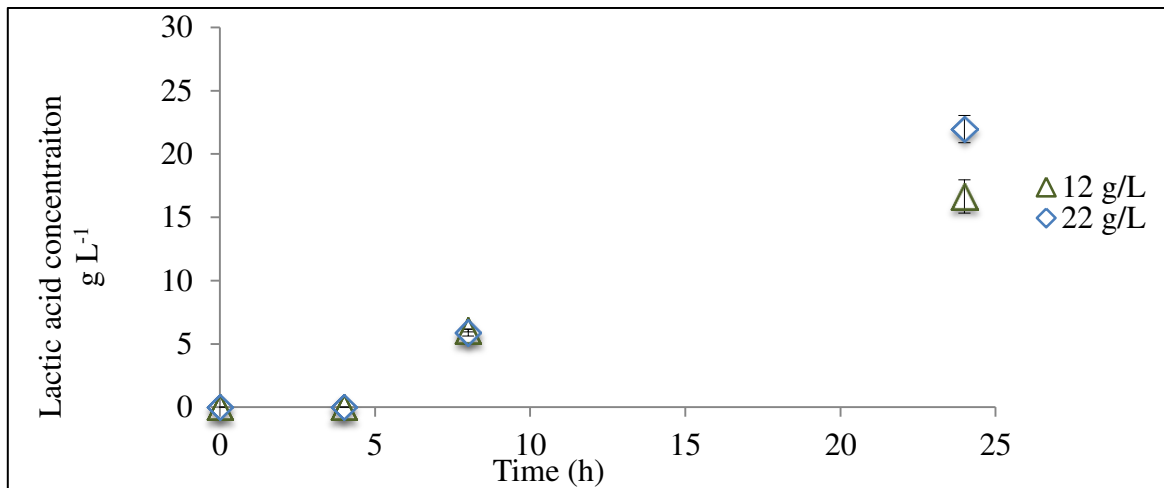The stationary growth phase was not reached for this experimental campaign. Concerning the maltose concentration (figure B.2.7), its concentration remained the same and almost constant in all flasks. The evolution of the glucose concentration during the SPHF is presented in figure B.2.8. The glucose consumption rate was similar in all flasks and its exhaustion was only obtained in flasks with an initial glucose concentration of 12 g L^{-1}after 24 h. The lactic acid concentration at the end of the experiment was higher at 24 g L^{-1}than at 12 g L^{-1} of glucose concentration (figure B.2.9).

It proves that when the glucose is exhausted (as in the case of flasks with an initial glucose concentration of 12 g L^{-1}), the production rate is affected significantly. In this experiment, the production rate obtained at 24 h was 0.9 g L^{-1}h^{-1} in flasks with an initial glucose concentration equal to 24 g L^{-1}compared to 0.6g L^{-1}h^{-1}for the lower initial glucose concentration (12 g L^{-1}) . It is then important to ensure that glucose will not be exhausted during the fermentation in order to get high lactic acid production rates.

In conclusion, no inhibition or limitation effects on growth were detected in the range of initial glucose concentration tested. A limitation effect by the glucose on lactic acid production was observed in experiments with an initial glucose concentration equal to 12 gL^{-}$_{1}$.

APPENDIX B.3 Batch modelling

For the batch modelling, it is important to model the different phases as the lag, exponential, stationary and death phases occurring successively, unlike the continuous modelling, where growth cannot be segregated into phases. In consequence, the batch model must take into account phenomena in all growth phases, particularly the lactic acid production in the stationary growth phase.

In the following, the model developed for the bioprocess operated in batch mode is described. As previously presented, a significant lactic acid production is observed during the stationary growth phase (see section2.2.4). Thus, in our approach, lactic acid production in exponential and stationary growth phases is considered and represented by the Luedeking and Piret (1959) model.

Summarizing, the batch model of the SSPHF process is described by the following four differential equations:

$$\frac{dX}{dt} = \mu X \tag{B.3.1}$$

$$\frac{dP}{dt} = \alpha\mu X + \beta X \tag{B.3.2}$$

$$\frac{dS}{dt} = -\frac{1}{Y_{PS}}(\alpha\mu X + \beta X) + k_M M \tag{B.3.3}$$

$$\frac{dM}{dt} = -k_M M \tag{B.3.4}$$

with

$$\mu = \mu_{max} \frac{S}{k_S + S}\left(1 - \frac{P}{P_{max}}\right)^n \tag{B.3.5}$$

where μ is the specific growth rate (in h^{-1}),α is the growth associated production coefficient (in g g^{-1}),β is the non-growth associated coefficient (in g $g^{-1}h^{-1}$), $Y_{PS}$is the product yieldwith respect to glucose (in g g^{-1}), k_M is the maltose degradation constant (in h^{-1}), μ_{max} the maximal specific growth rate (in h^{-1}), k_S is the half saturation constant (g L^{-1}), n the lactic acid inhibitor power and P_{max} themaximal lactic acid concentration above which bacteria do not grow (in g L^{-1}). The first term in equation (B.3.5) represents the growth limitation by the substrate according to the Monod model. The second term refers growth inhibition by the product (i.e. for high product concentration, the growth rate decreases).

The production rate in equation (B.3.2) is associated to the growth rate by means of the α coefficient and to the cell concentration by the βcoefficient. Unlike the continuous model
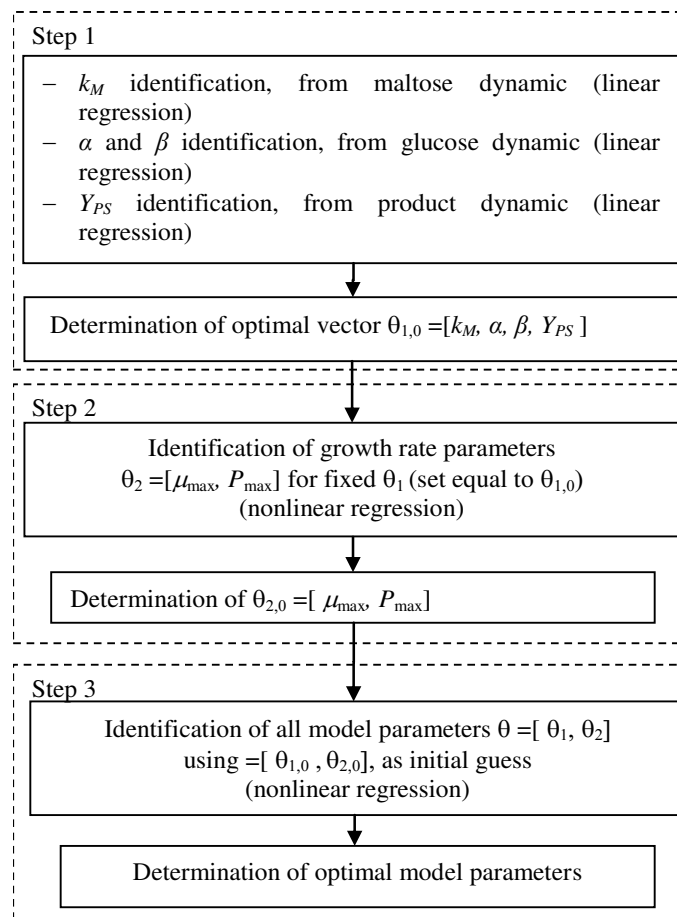
where the glucose consumption was linked to bacteria growth, in the batch case the glucose consumption was directly linked to the lactic acid production rate. With this approach, lactic acid production in the stationary growth phase is considered in all dynamics.

Identification strategy

In order to determine the evolution of biomass, product, substrate and maltose concentrations with time, thefollowing parameters must be identified: the coefficients involved in the specific growth rate (μ_{max}, k_S, P_{max}, and$n$), and coefficients α, β, k_M, Y_{PS}. The experimental data used to identify the model parameters are those obtained from hydrolysis time experiments (see section 2.2.4).

The identification strategy was the one developed in Gonzalez et al. (2013) and adapted to the final proposed batch model (equations (B.3.1) to (B.3.5)).The three-step identification procedure is summarized in figure B.3.1. The main idea is to determine each parameter value independently, using each state measurement separately. As presented in chapter 3,$k_S$and$n$ were fixed to 0.5 g L^{-1}and 3, respectively.

Step 1
- k_M identification, from maltose dynamic (linear regression)
- α and β identification, from glucose dynamic (linear regression)
- Y_{PS} identification, from product dynamic (linear regression)

Determination of optimal vector $\theta_{1,0}$ =[k_M, α, β, Y_{PS}]

Step 2
Identification of growth rate parameters
θ_2 =[μ_{max}, P_{max}] for fixed θ_1 (set equal to $\theta_{1,0}$)
(nonlinear regression)

Determination of $\theta_{2,0}$ =[μ_{max}, P_{max}]

Step 3
Identification of all model parameters θ =[θ_1, θ_2]
using =[$\theta_{1,0}$, $\theta_{2,0}$], as initial guess
(nonlinear regression)

Determination of optimal model parameters

Figure B.3.1 Identification strategy for batch modelling.

Results and discussion

The parameters were identified using experimental data of the bioreactor experiment performed with a hydrolysis time of 6 h and validated on experimental data of experiment with a hydrolysis time of 1.5 h (section 2.2.4). The set of parameters obtained is presented in table B.3.1.

Table B.3.1 Identified model parameters for batch operation

Parameter	Identified Value
μ_{max} (h^{-1})	0.28
P_{max} (g L^{-1})	101.75
β (g Productg^{-1} Cell h^{-1})	0.12
α (g Product g^{-1} Cell)	19.75
$1/Y_{PS}$ (g Product g^{-1}Glucose)	1.40
k_M (h^{-1})	0.02
k_S (gL^{-1})	0.5 (fixed from literature)
n	3 (fixed after several trials)

The fermentations used for parameters identification and validation were performed under the same operating conditions, only the initial maltose and glucose concentrations changed. Experimental and simulated data from both fermentations are presented in figures B.3.2 and B.3.3. From the collected data, it can be noticed that there is a small lag phase at the beginning of the fermentation that is not modeled and can affect the model performance. There was a significant period of non-growth associated lactic acid production in both experiments.

Moreover, glucose was exhausted in the experiment with 1.5 h hydrolysis (Figure B.3.3.) after 23 h. Nevertheless we suspect that bacteria continued lactic acid production using maltose as a substrate. Concerning the product evolution with time, it is accurately predicted by the model.Predicted maltose concentrations are very close to the measured ones, showing a good model accuracy. Glucose prediction by the model is notsatisfactory; This is certainly due to glucose production by other sugars than maltose that is not modeled and also to measurement uncertainties.

The identified model is validated considering the 1.5 h experiment. Obtained results are given on Figure B.3.3. In general, a good agreement between calculated and measured data is observed. This model is useful to predict the variables behaviour in a batch bioreactor under the SSPHF conditions used in this work.
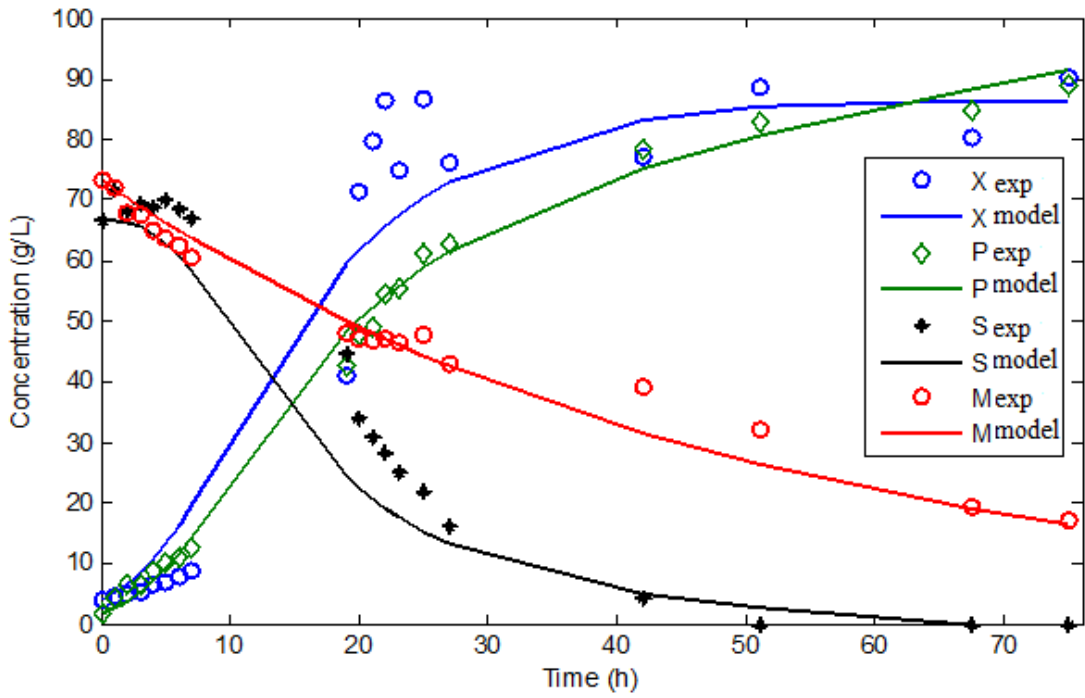
Figure B.3.2 Model parameters identification with experimental data from 6 h hydrolysis experiment

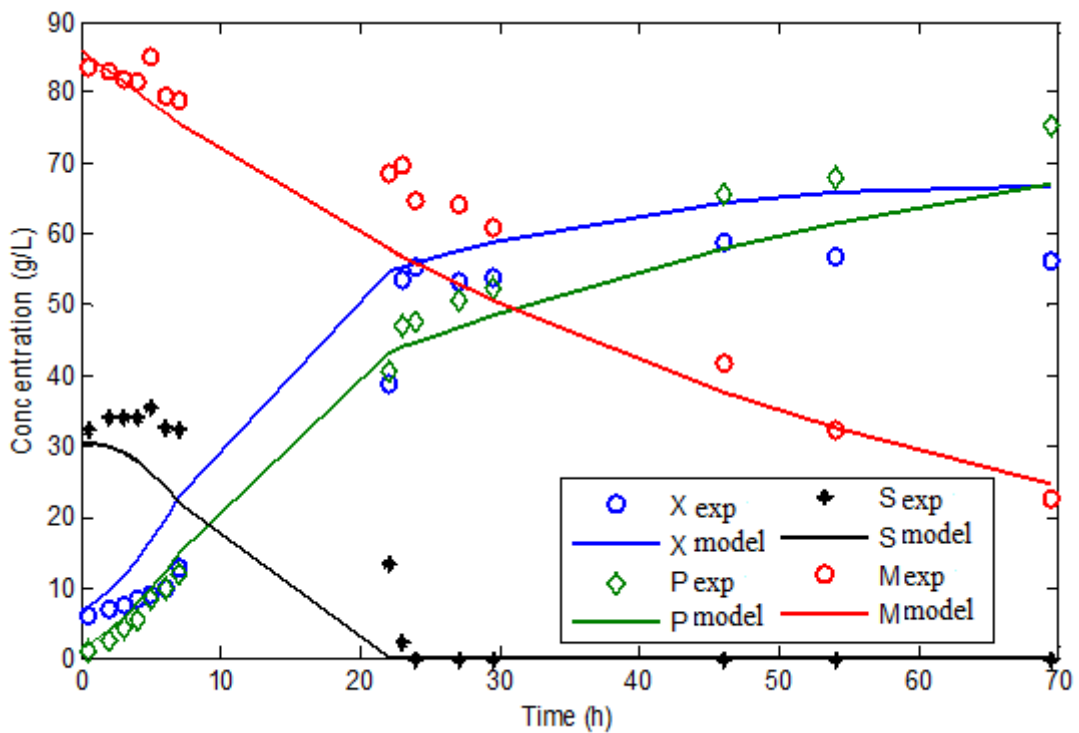**Figure B.3.3** Model parameters validation on experimental data from 1.5 h hydrolysis experiment.

226

Appendixes

APPENDIX C.1 Observability analysis

Consider the system in the form:

$$\dot{x}(t) = \mathbf{F}(x(t), u(t))$$
$$y(t) = \mathbf{H}((x(t))$$

$$(C.1.1)$$

We assume that $x \in N$ where N is an open subset of $\mathfrak{R}^{\mathbf{n}}$, $u \in \mathfrak{R}^{\mathbf{m}}$, $y \in \mathfrak{R}^{\mathbf{p}}$. It is also necessary to assume that the system is complete, it means that for every bounded measurable input u and every $x \in N$ it exists a solution $\dot{x}(t) = \mathbf{F}(x(t), u(t))$ such that $x(0) = x_0$ and $x(t) \in N$ for all $y \in \mathfrak{R}^{\mathbf{p}}$.

$y(t, x_0, t_0, u)$ is defined as the output of the system in equation (C.1.1) related to the initial condition at the instant $t = t_0$ and to the input $u(t)$.

In general, the inputs do not describe all the space $\mathfrak{R}^{\mathbf{m}}$ but just one part W of $\mathfrak{R}^{\mathbf{m}}$. This constraint is imposed by the physical process. The entries in question are called eligible entries; their evolution space is denoted *W*.

Some definitions related to the observability are given hereafter (Anguelova, 2007)

Definition 4.1

A pair of points x_0 and x_1 in N are *W-distinguishable* if it exists a measurable bounded input $u(t)$ defined on the interval $[0,T]$ that generates solutions $x_0(t)$ and $x_1(t)$ of $\dot{x}(t) = \mathbf{F}(x(t), u(t))$ satisfying $x_i(0) = x_i$ such that $x(t)_i \in W$ for all $t \in [0,T]$ and $\mathbf{H}(x_0(t)) \neq \mathbf{H}(x_1(t))$ for some $t \in [0,T]$. We denote by $I(x_0, W)$ all points $x_1 \in W$ that are not *W-distinguishable* from x_0.

Definition 4.2

The system in equation (C.1.1) is *W-observable* or just observable if there are no pairs of distinct points that are indistinguishable. This means that if a system is observable, thesystem output measurement corresponds to a unique value for each state variable at a given time.

Definition 4.3

The system in equation (C.1.1) is *observable* at $x_0 \in N$ if $I(x_0, N) = x_0$.

Definition 4.4

The system in equation (C.1.1) is *locally observable* at $x_0 \in N$ if for every open neighborhood W of x_0, $I(x_0, N) = x_0$.

Both observability definitions ensure that a point at $x_0 \in N$ can be distinguished from every other point in N. In practice, it is often enough to be able to distinguish between neighbors in *N*. It is then necessary to introduce two new definitions.

Definition 4.5

The system in equation (C.1.1) has the *distinguishability property* at $x_0 \in N$ if x_0 has an open neighborhood V such that $I(x_0, N) \cap V = x_0$.

For a system having the distinguishability property, any point x_0 can be distinguished from neighboring points but there could be arbitrarily large intervals of time $[0,T]$ in which the points cannot be distinguished. Another concept is presented in order to fix a limit on the time interval:

Definition 4.6

The system in equation (C.1.1) has the *local distinguishability property* at $x_0 \in N$ if x_0 has an open neighborhood V such that for every open neighborhood W of x_0, $I(x_0, N) \cap V = x_0$.

Local observability implies local distinguishability setting V equal to N. Therefore, if a system does not have the local distinguishability property at some x_0, it is not locally observable at the point either.

The observability rank condition (ORC)

In this section, the determination of the local distinguishability property of a system is presented using the "observability rank condition" (Hermann & Krener, 1977), first in the case of a linear system and then for a nonlinear one.

Condition for linear systems

Consider a stationary linear systemwith a linear output equation as the following:

$$\dot{x}(t) = Ax(t) + Bu(t), \qquad x(0) = x_0$$
$$y(t) = Cx(t) \tag{C.1.2}$$

where $A \in \Re^{n \times n}$ and $C \in \Re^{p \times n}$ are constant matrices with n the state vector dimension. The observability matrix is then defined by:

$$(\Omega) = \begin{pmatrix} C \\ CA \\ \vdots \\ CA^{n-1} \end{pmatrix} \tag{C.1.3}$$

The system is observable if the observability matrix Ω has rank n.

Condition for nonlinear Systems

In the case of the nonlinear system with a nonlinear equation given in (C.1.1), the observability criterion (C.1.3) cannot be applied. It is then necessary to use a more general criterion to determine the observability of this kind of systems. It can be done using the Lie algebra.

Let us introduce the Lie derivative, a directional derivative for a scalar field $\mathbf{H}(x)$, with $x(t) \in \Re^n$ along the direction of a n-dimensional vector field $\mathbf{F}(x)$. The mathematical expression is described by:

$$L_{\mathbf{F}}\mathbf{H}(x) = \sum_{i=1}^{n} \frac{\partial \mathbf{H}(x)}{\partial x_i} \mathbf{F}(x) \qquad (C.1.4)$$

As $\partial \mathbf{H}(x)/\partial x$ is a 1xn gradient vector of the scalar $\mathbf{H}(x)$, the norm of a gradient vector represents the maximum rate of function value changes, and the product of the gradient and the vector field $\mathbf{F}(x)$ in C.1.4 becomes the directional derivative of $\mathbf{H}(x)$ along $\mathbf{F}(x)$. Thus, the Lie derivative of a scalar field defined by C.1.4 is also a scalar field. If the operation in equation C.1.4 is repeated k times, it gives:

$$L_{\mathbf{F}}^k \mathbf{H}(x) = \frac{\partial(L_{\mathbf{F}}^{k-1}\mathbf{H})}{\partial x} \mathbf{F} \text{ for } k \geq 1 \qquad (C.1.5)$$

with

$$L_{\mathbf{F}}^0 \mathbf{H}(x) = \mathbf{H}(x) \qquad (C.1.6)$$

If each component of a vector field $\mathbf{H}(x) \in \Re^p$ is considered to take a Lie derivative along $\mathbf{F}(x) \in \Re^n$, then all components can be replaced on concurrently and the result is a vector field that has the same dimension as $\mathbf{H}(x)$; its ith element is the Lie derivative of the ith component of $\mathbf{H}(x)$. Namely, if $\mathbf{H}(x) = \left(\mathbf{H}_1(x)...\mathbf{H}_p(x)\right)^T$ and each component $\mathbf{H}_i(x)$ is a scalar field, then the Lie derivative of the vector field $\mathbf{H}(x)$ is defined as(Anguelova, 2007):

$$L_{\mathbf{F}}\mathbf{H}(x) = \begin{pmatrix} L_{\mathbf{F}}\mathbf{H}_1(x) \\ \vdots \\ L_{\mathbf{F}}\mathbf{H}_p(x) \end{pmatrix} \qquad (C.1.7)$$

With the Lie derivative concept, it is possible to define an observation space Ω over $\Re^p$ as the set of all linear combinations formed from the derivatives of the Lie function of $\mathbf{H}(x)$:

$$\Omega = \mathbf{span}\left\{\mathbf{H}(x), L_{\mathbf{F}}\mathbf{H}(x),..., L_{\mathbf{F}}^{n-1}\mathbf{H}(x)\right\} \qquad (C.1.8)$$

This space is spanned by all up to (n -1) order Lie derivatives of the output function $\mathbf{H}(x)$. It is also necessary to define an observability distribution, denoted by $d\Omega$, which collects the "gradient" vector of every component in Ω:

$$d\Omega = \left\{d\mathbf{H}(x), dL_{\mathbf{F}}\mathbf{H}(x),..., dL_{\mathbf{F}}^{n-1}\mathbf{H}(x)\right\} \qquad (C.1.9)$$

With these definitions, the following theorem is proposed for testing the observability of the system (Kheir, 1996).

Theorem 4.1

The system (C.1.1) is observable if and only if dim ($d\Omega$)= n. It is locally observable at some point x_i if $d\Omega(x_i, u)$ has full rank at this point for all u .
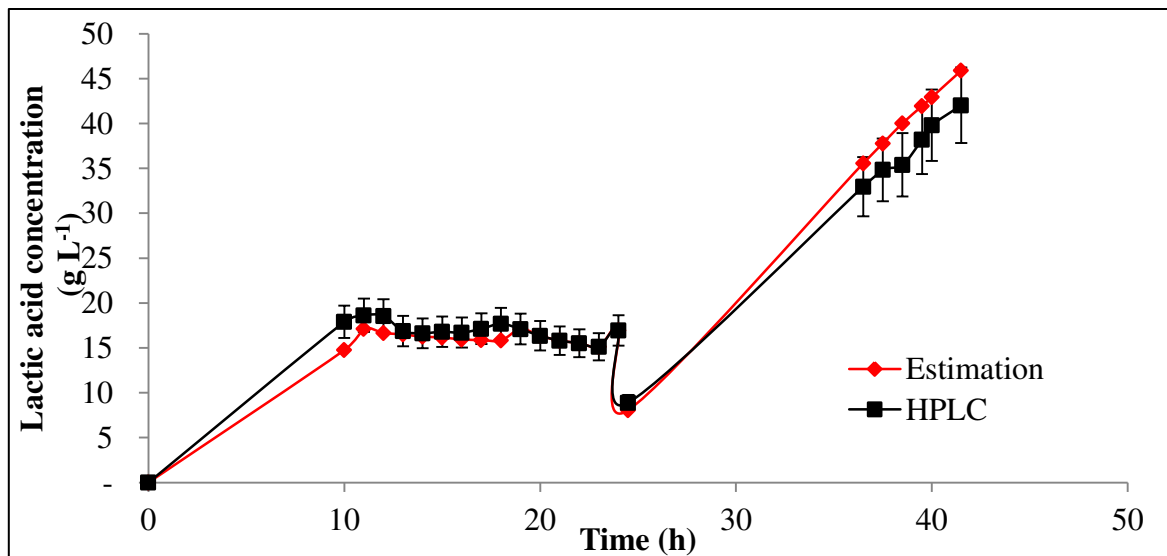
APPENDIX C.2 Experimental validation of the lactic acid concentration determination from sodium hydroxide

In this appendix, the method to estimate the lactic acid concentration from sodium hydroxide flow added to the bioreactor is experimentally validated. In this case, experimental results obtained with experiment 2 in chapter 3 (see section 3.5.2) were used to validated the method. The lactic acid concentration at each instant *k* is given by:

$$P_{k+1} = \left(F_{Na,k} \frac{C_{Na} M_{LA}}{V} - D_k P_k \right)(t_{k+1} - t_k) + P_k \tag{C.2.1}$$

Equation (C.2.1.)(4.55) was used to determine the lactic acid concentration at instant *k+1* from the sodium hydroxide inlet flow measured each hour during the experiment and from the known dilution rates. Figure C.2.1. shows the comparison between offline lactic acid concentration measurement using HPLC (High performance liquid chromatography) and the online determination using the sodium hydroxide inlet flow at a sampling time of 1 hour.

Figure C.2.1. Comparison between the lactic acid concentration offline measurements with the online lactic acid concentration determination from sodium hydroxide inlet flow. (♦) Online determination of lactic acid concentration, ■) Offline measurements of lactic acid concentration by HPLC. Results of experiment 2 (modelling experimental validation, section 3.5.2).

As it is shown in figure C.2.1, the lactic acid concentration is well determined from the sodium hydroxide inlet flow when comparing to the offline measurements. It should be pointed out that the sampling time was considerably high (1 hour). The accuracy of the lactic acid concentration determination can be improved by reducing the sampling time. For the next experiments this sampling time was reduced until 5 minutes.

APPENDIX C.3 Influence of the process noise covariance matrix.

Simulations using higher values in the Q matrix than those used in Figure 4.5 were performed and are presented hereafter. Values in the Q matrix were chosen as diag ([10; 100; 100; 10]).
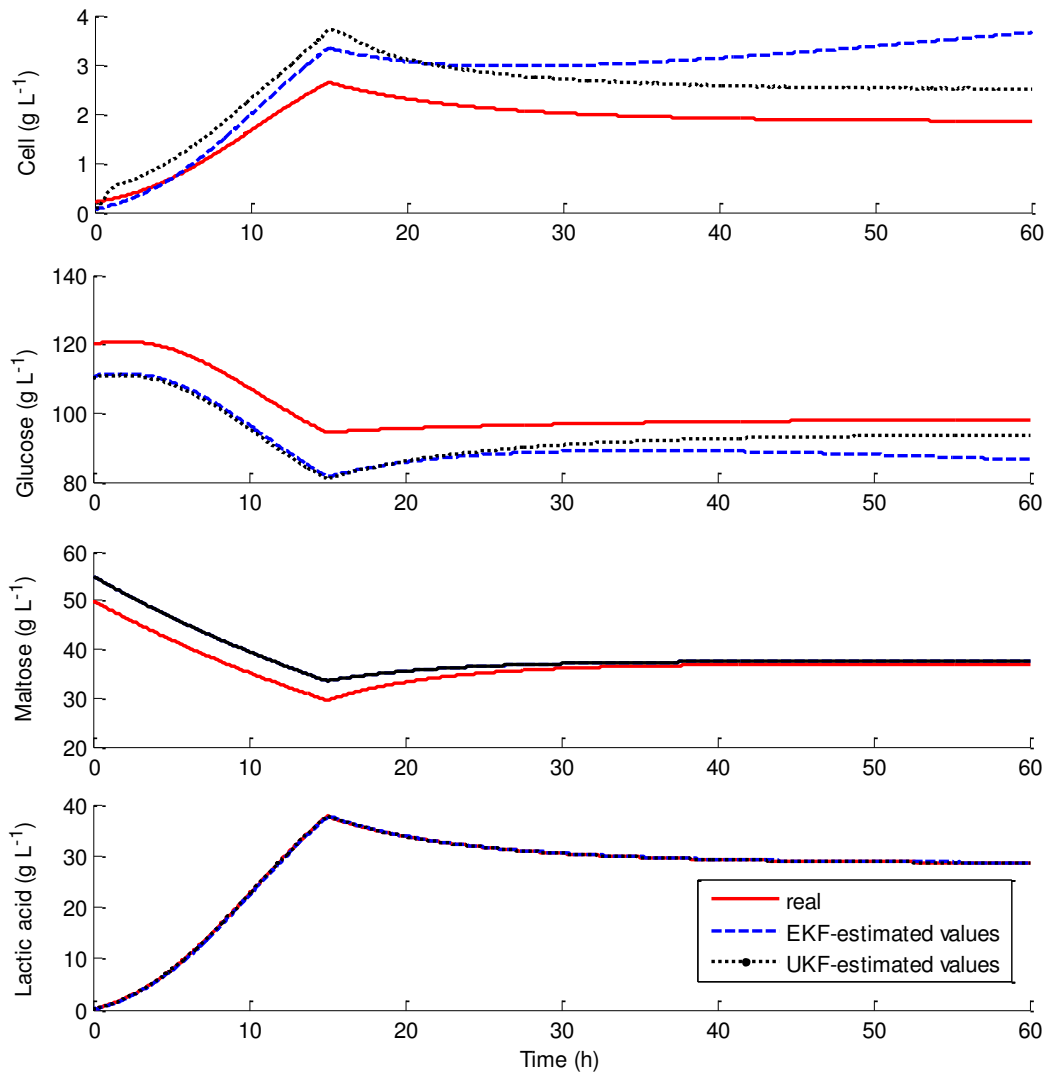
Figure C.3.1. Extended Kalman filter and Unscented Kalman filter comparison. Estimation of cell, glucose, maltose and lactic acid concentrations with initialization error. 20% parameter mismatch between the real system model and the model used by EKF and UKF. 1% centred Gaussian white noise applied to P. Higher values in the Q matrix.

The performance of both estimators is worst in figure C.3.1. than in figure 4.5, where values in the Q matrix were smaller. The EKF diverges at the end of the simulation proving that the filter stability is not guaranteed with high values in the Q matrix. Concerning the UKF performance, its prediction is less accurate but the filter remains still stable. Thetuning of the Q matrix must be then performed carefully in order to obtain the best performances.

APPENDIX D.1 Control law implementation in the C-BIO software

For the control validation, the C-BIO software was used.The feature used for the control implementation is the calculation module (Figure D.2.1). This module allows creating calculations using the values recorded by the system and constant values. The calculations are constructed using operators and functions similar to those found in Microsoft Excel. These calculations can be used to represent a sensor input allowing the user to buil a "virtual" regulator.

The adaptive control strategy with the constant γ model was implemented in the C-BIO software as shown in figure D.2.1. The first column represent the online measurements of the bioreactor and the next two columns their past and actual values. The fourth column has all the constant values that can be modified by the user. The fifth column shows the formulas; all the control law equations are implemented here. Their current values are presented in the seventh column. This module allows then the calculation of the control variable (D) to regulate the lactic acid concentration at the reference value (P_{ref}). In the following the procedure performed to implement the control law is presented.
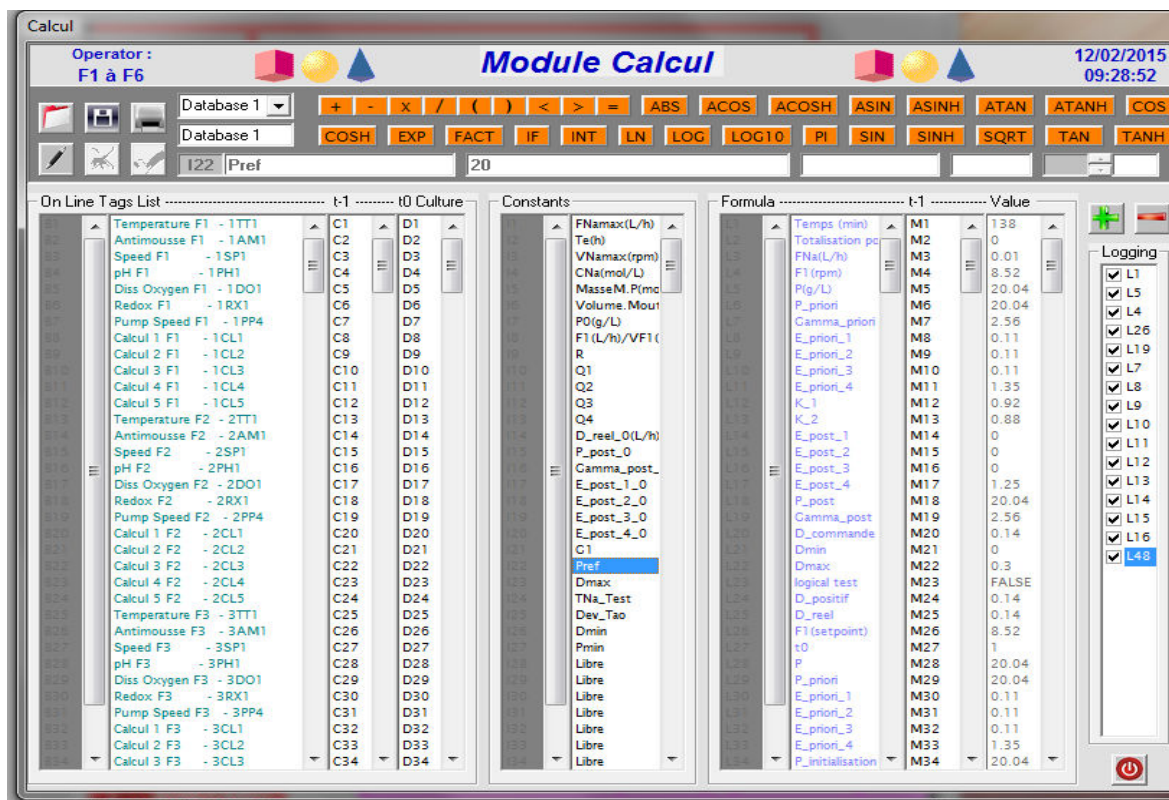

Figure D.2.1. Control law impplementation in the C-BIO software.

Procedure and control law algorithm

In chapter 4 (section 4.4) a method to estimate online the lactic acid concentration from the sodium hydroxide inlet flow was presented. Nevertheless, the bioreactor system does not provide directly the sodium hydroxide inlet flow F_{Na}. Thus,this must be determined from one of the system online measurements. As previously mentioned (see section 3.5.1.1), the bioreactor software has a totalizer fonction for each peristaltic pump (with fixed rotation speed) which registers the time of rotation of the corresponding pump in a time basis (sampling time, T_s). The totalizer (T_{Na}) of the sodium hydroxide pump or PB (Figure 3.7) (h) can then be used to determine the sodium hydroxide inlet flow, F_{Na}. Then this information is used for the online calculation of the lactic acid concentration, the estimation of production rateand the determination of the control law.

For the implementation of the control law in the C-BIO software, all equations necessary for the control law were transformed into simple calculations. Thus, the matricial equations presented in sections 4.3.1 and 4.6.2.1 for the estimation of the production rate were developed leading to a set of equations. The whole calculation algorithm is represented in tables D.2.1 and D.2.2. Each calculation is updated at each sampling time, T_s (5 min). All equations presented in these tables were implemented in the C-BIO software as Microsoft Excel functions.As it is shown in table D.2.2 after the calculation of all equations of the control law, the control variable is in fact the rotation speed of the feeding pump, P1 (Figure 3.7).

Table D.2.1. Algorithm for the determination of the control law in the C-BIO software of the bioreactor.

Step	Equation or description	variables
Sensor (rotation time of base pump)	Acquired magnitude. A/D. Converter of the continuous signal in a discrete signal at instant k (rotation time of base pump)	T_{Na} = totalizer base pump (h) k= time index (h)
F_{Na} **determination from** T_{Na}	$$F_{Na,k} = \frac{(T_{Na,k} - T_{Na,k-1})*72}{\rho_{Na}T_s}$$	ρ_{Na} = sodium hydroxyde density (g mL^{-1}) T_s = sampling time (h) F_{Na} =Sodium hydroxide inlet flow (L h^{-1}) 72 represents the correlation between the base pump totalizer and F_{Na}
P **determination from** F_{Na}	$$P_{k+1} = \left(\frac{F_{Na,k}C_{Na}M_{LA} - F_k P_k}{V_{real}} \right) T_s + P_k$$	C_{Na} = Sodium hydroxide concentration mol L^{-1} V_{real} = effective volume of the bioreactor (L) P = lactic acid concentration (g L^{-1}) M_{LA}= lactic acid molecular weight (g mol^{-1}) F= Feed flow rate(h^{-1})
Kalman filter algorithm	**Initialization step :** **Variables** **Constants** $\hat{P}_0 = 0$ $Q_1 = 0.1$ $\hat{\gamma}_0 = 0$ $Q_2 = 0$ $\mathbf{P}_{1,0} = 0.1$ $Q_3 = 0$ $\mathbf{P}_{2,0} = 0$ $Q_4 = 0.1$ $\mathbf{P}_{3,0} = 0$ $R = 0.01$ $\mathbf{P}_{4,0} = 0.1$ **Prediction step :** $\hat{P}_k^- = \hat{P}_k \left(-D_k T_s + 1 \right) + \hat{\gamma}_k$ $\hat{\gamma}_k^- = \hat{\gamma}_k$ $\mathbf{P}_{1,k}^- = \mathbf{P}_{1,k} \left(-D_k T_s + 1 \right)^2 + T_s \left(\mathbf{P}_{2,k} + \mathbf{P}_{3,k} \right)(-D_k T_s + 1) + \mathbf{P}_{4,k} T_s^2 + Q_1$ $\mathbf{P}_{2,k}^- = \mathbf{P}_{2,k} \left(-D_k T_s + 1 \right) + T_s \mathbf{P}_{4,k} + Q_2$ $\mathbf{P}_{3,k}^- = \mathbf{P}_{3,k} \left(-D_k T_s + 1 \right) + T_s \mathbf{P}_{4,k} + Q_3$ $\mathbf{P}_{4,k}^- = \mathbf{P}_{4,k} + Q_4$	$\hat{P}_0$ = initial lactic acid concentration (h^{-1}) $\hat{\gamma}_0$ = initial production rate (h^{-1}) $\mathbf{P}_{1,0}, \mathbf{P}_{2,0}, \mathbf{P}_{3,0}, \mathbf{P}_{4,0}$ are the first, second, third and fourth components of the initialization error covariance matrix, respectively. Q_1, Q_2, Q_3, Q_4 are the first, second, third and fourth components of the process noise error covariance matrix, respectively. $\hat{P}^-$ = lactic acid predicted value (g L^{-1}) $\hat{\gamma}^-$ = production rate predicted value (g L^{-1} h^{-1}) $\mathbf{P}_1^-, \mathbf{P}_2^-, \mathbf{P}_3^-, \mathbf{P}_4^-$ are the first, second, third and fourth components of the error covariance matrix prediction, respectively. D= dilution rate (F/V_{real})h^{-1}

Table D.2.2 Algorithm for the determination of the control law in the C-BIO software of the bioreactor (continuation)

Step	Equation or description	variables
Kalman filter algorithm	**Correction step** $$K_{1,k} = \mathbf{P}^-_{1,k} / \left(R + \mathbf{P}^-_{1,k}\right)$$ $$K_{2,k} = \mathbf{P}^-_{3,k} / \left(R + \mathbf{P}^-_{1,k}\right)$$ $$\hat{P}_k = \hat{P}^-_k + K_1\left(P_k - \hat{P}^-_k\right)$$ $$\hat{\gamma}_k = \hat{\gamma}^-_k + K_2(P_k - \hat{P}^-_k)$$ $$\mathbf{P}_{1,k} = \mathbf{P}^-_{1,k}\left(1 - K_{1,k}\right)$$ $$\mathbf{P}_{2,k} = \mathbf{P}^-_{2,k}\left(1 - K_{1,k}\right)$$ $$\mathbf{P}_{3,k} = K_{2,k}\mathbf{P}^-_{1,k} + \mathbf{P}^-_{3,k}$$ $$\mathbf{P}_{4,k} = K_{2,k}\mathbf{P}^-_{2,k} + \mathbf{P}^-_{4,k}$$	$K_1 = $ first component of the Kalman *gain* $K_2 = $ second component of the Kalman *gain* $\hat{P} = $ lactic acid updated value (g L^{-1}) $\hat{\gamma} = $ production rate updated value (g L^{-1} h^{-1}) $\mathbf{P}_1, \mathbf{P}_2, \mathbf{P}_3, \mathbf{P}_4$ are the first, second, third and fourth components of the updated error covariance matrix , respectively.
Error calculation	$Error_k = P_{ref} - P_k$	P_{ref}= Reference lactic acid concentration (g L^{-1})
Proportional action calculation	$\hat{D}_k = G(P_{ref} - P_k)$	$\hat{D} = $ proportioned signal by the proportional controller. $G = $ proportional regulator gain
Calculation of the linearized control law	$$D_k = -\frac{1}{P_k}\left[\hat{D}_k - \hat{\gamma}_k\right]$$ s.t. $$0 \leq D_k \leq 0.4$$	$\hat{\gamma} = $ production rate value estimated by the Kalman filter.
Determination of feed flow pump speed $\left(r_F\right)_{\textbf{(rpm)}}$	$$r_F = \frac{D_k * V_{real}}{0.053}$$	where 0.053is the correlation between the feed flow rate and the speed of its respective peristaltic pump
D/A converter	Converter of the discrete signal (rpm) in a continuous signal (action on the outlet flow pump)	

APPENDIX D.2 Determination of the temperature disturbance effect on lactic acid production

In the experimental validation of the adaptive control law, the system was subject to a temperature disturbance in order to test the robustness of the control strategy. In this appendix, the study of temperature reduction effect in the SSPHF process from 30°C to 20°C is presented. The aim is to determine if cells are inhibited by this disturbance and to quantify its impact on the lactic acid production rate.

Materials and Methods

The materials and Methods for wheat solution preparation, inoculum preparation, liquefaction, SSPH and analytical methods are those presented in the materials and methods description of experiments performed for the continuous SSPHF model validation (see section 3.5.1). The SSPHF was performed in batch operation in two 5 L bioreactor each one with 3.2 L of culture broth. The temperature in fermenter number 1 was fixed to 30°C during all the experiment and to 20°C in the fermenter number 2. The pH value in both fermenters was regulated to 5.7 by the addition of sodium hydroxide. The online determination of the lactic acid concentration was performed by its online calculation from the sodium hydroxide inlet flow. Biomass, glucose, maltose and lactic acid concentrations were measured offline using cell counting and HPLC at different time intervals.

Results

Lactic acid concentration online and offline values obtained in the two batch SSPHF experiments are summarized on figure D.2.1. This figure proves that lactic acid bacteria are strongly disturbed by changes in the temperature. The lactic acid concentration profiles are very different. The lactic acid concentrations obtained in the fermenter at 30°C are 4 times higher than those obtained in the fermenter at 20°C. For example at 17 h the lactic acid concentration in the fermenter at 30°C is around 27 g L^{-1} while in the fermenter at 20°C, it is just 6 g L^{-1}. It means that the production rate was of 1.8 g $L^{-1}h^{-1}$ in the first case and of 0.4 g $L^{-1}h^{-1}$ in the second case. There are some slight differences between the lactic acid concentration estimated online from the sodium hydroxide flow and the lactic acid concentration measured offline (by HPLC). These errors are acceptable considering the estimation error of the technique.

These results prove that a temperature disturbance in the SSPHF bioreactor (from 30°C to 20°C) reduces significantly the production rate. The control law must then adapt itself to this kind of disturbance in order to track the reference set point.
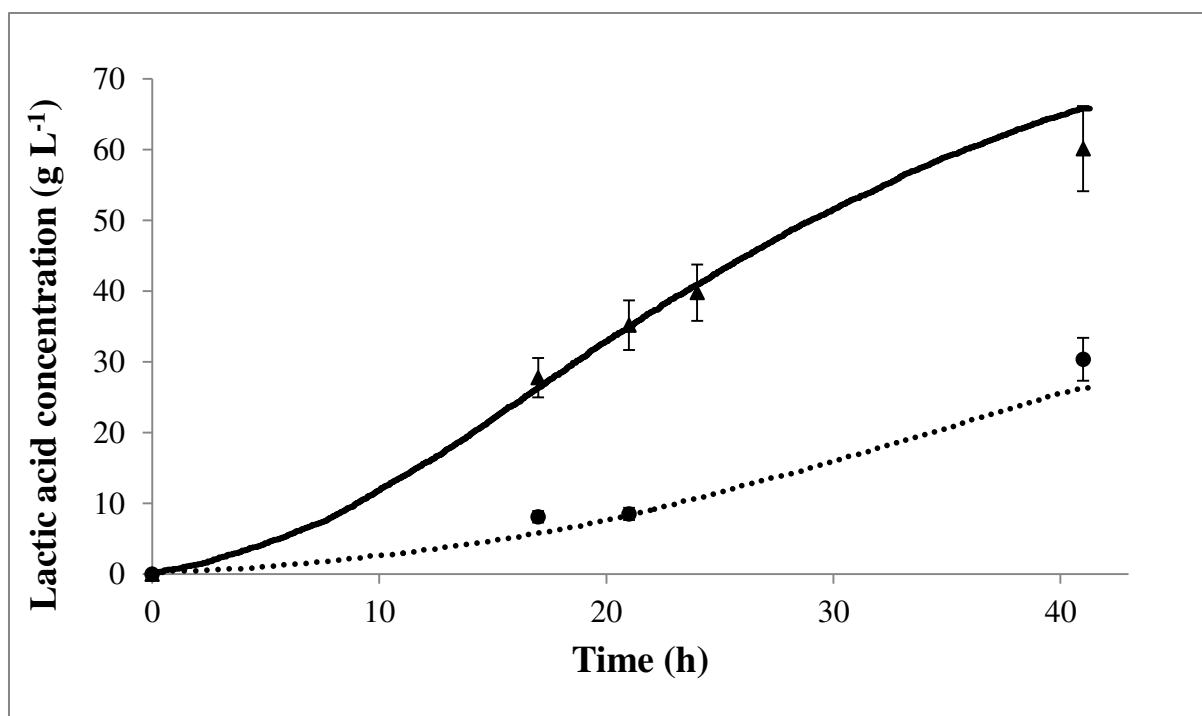
Figure D.2.1. Lactic acid evolution with time during SSPHF experiments at different temperatures: 20°C and 30°C. (●) Offline measurement of lactic acid at 20°C, (▲) Offline measurement of lactic acid at 30°C, (▬▬) Online measurement of lactic acid at 30°C, (······) Online measurement of lactic acid at 20°C.

APPENDIX D.3 Glossary

Name	Definition
Aerotolerant	Surviving and growing in small amounts of air; said of anaerobic microorganisms
Aerobe	An organism, especially a bacterium, that requires air or free oxygenfor life
Anaerobe	An organism that lives and grows in the absence of molecular oxygen
Anaerobiosis	Metabolic processes occurring in the absence of molecular oxygen
Amylolytic	Conversion of starch into sugar by the action of acids or enzymes such as amylase
Amylopectin	Soluble polysaccharide and highly branched polymer of glucose found in plants. It is one of the two components of starch, the other being amylose
Amylaceous	Pertaining to, or the nature of, starch
Bacteriocins	Proteinaceous toxins produced by bacteria to inhibit the growth of similar or closely related bacterial strain(s)
Bacteriophage	Virus that infects and replicates within a bacterium
Betabacterium	A genus or subgenus of heterofermentative lactobacilli
Biosorption	Physiochemical process that occurs naturally in certain biomass which allows it to passively concentrate and bind contaminants onto its cellular structure
Catalase negative	Bacteria that may be anaerobes, or they may be facultative anaerobes that only ferment and do not respire using oxygen as a terminal electron acceptor
Cell lysis	Refers to the breaking down of the membrane of a cell, often by viral, enzymatic, or osmotic mechanisms that compromise its integrity
Chirality (chemistry)	A molecule is considered chiral if there exists another molecule that is of identical composition, but which is arranged in a non-superposable mirror image
Chemoorganotroph	An organism that depends on organic chemicals for its energy and carbon
Cytosine	One of the four main bases found in DNA and RNA, along with adenine, guanine and thymine (uracil in RNA)
Enantiomers	Chiral molecules that are mirror images of one another. Furthermore, the molecules are non-superimposable on one another
endo-amylase	An enzyme acting on internal glycosidic bonds

exo-amylase	enzyme acting on a glycosidic bond near an end of the polysaccharide
hemeprotein	Metalloprotein containing a heme prostetic group- an organic compound that allows a proteinto carry out several functions that it cannot do alone
gelatinization of starch	Process of breaking down the intermolecular bonds of starch molecules in the presence of water and heat, allowing the hydrogen bonding sites (the hydroxyl hydrogen and oxygen) to engage more water
glycolysis	Metabolic pathway that converts glucose into pyruvate
Gram staining	Differentiates bacteria by the chemical and physical properties of their cell walls by detecting peptidoglycan, which is present in a thick layer in gram-positive bacteria
Heterofermentative	That undergoes fermentation to produce more than one product
Hexoses	Monosaccharide with six carbon atoms
Homofermentative	That undergoes fermentation to produce only one product
Hydrolysate	Refers to any product of hydrolysis
Hydrolysis	Reaction involving the breaking of a bond in a molecule using water. The reaction mainly occurs between an ion and water molecules and often changes the pH of a solution
Lignocellulosic biomass	Refers to plant dry matter
Mesophile	Organisms that grows best in moderate temperature, neither too hot nor too cold, typically between 20 and 45 °C
Monomer	Molecule that may bind chemically to other molecules to form a polymer
Oligomer	Molecular complex that consists of a few monomer units
Oligosaccharide	Saccharide polymer containing a small number (typically three to nine) of simple sugars
Pentose	Monosaccharide with five carbon atoms
PEP-phosphotransferase system	Sugar transport system that couples the transport of a sugar to its phosphorylation. The phosphate group is derived from phosphoenolpyruvate (PEP) and transferred via the general PTS proteins Enzyme I (EI) and HPr to the substrate-specific Enzymes II (EII) to the incoming sugars
Polycondensation	A chemical condensation leading to the formation of a polymer by the linking together of molecules of a monomer and the releasing of water or a similar simple substance
Phosphorylation	Addition of a phosphate (PO_4^{3-}) group to a protein or other organic molecule
Probiotics	Microorganisms that are believed to provide health benefits when consumed
Saccharification	Process of breaking a complex carbohydrate (as starch or cellulose) into its monosaccharide components

Saccharolityc	of breaking the glycosidic bonds in saccharides.
Steroisomer:	Isomeric molecules that have the same molecular formula and sequence of bonded atoms (constitution), but that differ only in the three-dimensional orientations of their atoms in space
Stereocomplex biopolymer	A stereoselective interaction between two complementing stereoregular polymers, that interlock and form a new composite, demonstrating altered physical properties in comparison to the parent polymers
Streptobacterium	A supposed variety of bacterium, consisting in reality of several bacteria linked together in the form of a chain.
Thermobacterium	Thermobacterium: Any of various thermoduric lactobacilli often considered to constitute a subgenus (*Thermobacterium*) of the genus *Lactobacillus*
Transferase	The general name for the class of enzymes that enact the transfer of specific functional groups (e.g. a methyl or glycosyl group) from one molecuel (called the donor) to another (called the acceptor)

Résumé en français :

Cette thèse de doctorat porte sur l'optimisation du bioprocédé de production d'acide lactique à partir de la farine de blé. L'acide lactique s'avère en effet de plus en plus attractif pour la production de PLA (acide poly lactique), un bio polymère, d'autant plus que différentes matières premières peu coûteuses comme la farine de blé sont désormais utilisées comme sources de carbone pour sa production. Cette thèse comprend trois parties principales. Une première partie propose pour l'optimisation du procédé de transformation du blé un schéma innovant composé de trois étapes successives : une liquéfaction, suivi d'une étape de saccharification et hydrolyse des protéines simultanées (SSPH) et une étape finale de saccharification, hydrolyse des protéines et fermentation simultanées (SSPHF). La deuxième partie s'intéresse à la modélisation de l'étape SSPHF (étape limitante) dans un bioréacteur continu. La détermination des paramètres du modèle ainsi que leur validation sont réalisées à l'aide de campagnes d'essais sur un bioréacteur de 5 L.

Enfin, la dernière partie développe la mise en œuvre de stratégies de commande permettant de maintenir le bioprocédé à son point optimal de fonctionnement. Pour ce faire, du fait de l'absence de capteurs pour la mesure en temps réel des concentrations des variables clé dans le bioréacteur, des estimateurs de ces concentrations ainsi que du taux de production en acide lactique sont tout d'abord élaborés. Des stratégies de commande régulant la concentration d'acide lactique à sa valeur optimale sont ensuite synthétisées et comparées en simulation. Une commande adaptative combinant une commande linéarisante par retour d'état et un estimateur du taux de production en acide lactique est finalement retenue et validée expérimentalement sur un réacteur instrumenté. Cette dernière s'est avérée robuste vis-à-vis des erreurs de modélisation et a permis lors des expériences de doubler la productivité de l'acide lactique.

Mots-clés : Bioprocédé, acide lactique, farine de blé, estimateur d'état, commande adaptative

Résumé en anglais:

This PhD thesis focuses on the optimization of the bioprocess of lactic acid production from wheat flour. Indeed, lactic acid has received much attention for the production of PLA (Poly Lactic Acid), a biopolymer, since different inexpensive raw material such as wheat flour are now used as carbon source for its production. This work was performed in three main steps. In the first step, an innovative wheat transformation process is proposed, whose main steps are the following: a liquefaction followed by a simultaneous saccharification, proteins hydrolysis (SSPH) and and a final simultaneous saccharification, proteins hydrolysis and fermentation (SSPHF). Secondly, the modeling of the SSPHF (limiting step) in a continuous bioreactor is considered. The determination and validation of model parameters is performed by means of experimental campaigns in a 5 L bioreactor.

In the last step, the development of control strategies to maintain the process at its optimal operating point is considered. To do so, due to the absence of sensors for real-time measurement of the concentrations of key variables of the bioreactor, estimators of these concentrations and of the lactic acid production rate are first developed. Then, control strategies for regulating the lactic acid concentration at its optimal value are designed and compared in simulation. An adaptive control combining a state feedback linearizing control and an estimator of the lactic acid production rate is finally chosen to be experimentally validated on an instrumented reactor. This strategy showed good robustness features with respect to modeling mismatches and was able during experiments to increase twice the lactic acid productivity.

Keywords: Bioprocess, lactic acid, wheat flour, state estimator, adaptive control.